



HAL
open science

Identification of the intrinsic energy performance of multi-family housing and tertiary sector buildings from in-situ measurements

Lorena de Carvalho Araujo

► **To cite this version:**

Lorena de Carvalho Araujo. Identification of the intrinsic energy performance of multi-family housing and tertiary sector buildings from in-situ measurements. Mechanics [physics]. Université de Bordeaux, 2022. English. NNT : 2022BORD0105 . tel-03864758

HAL Id: tel-03864758

<https://theses.hal.science/tel-03864758v1>

Submitted on 22 Nov 2022

HAL is a multi-disciplinary open access archive for the deposit and dissemination of scientific research documents, whether they are published or not. The documents may come from teaching and research institutions in France or abroad, or from public or private research centers.

L'archive ouverte pluridisciplinaire **HAL**, est destinée au dépôt et à la diffusion de documents scientifiques de niveau recherche, publiés ou non, émanant des établissements d'enseignement et de recherche français ou étrangers, des laboratoires publics ou privés.

Thèse présentée pour obtenir le grade de

**DOCTEUR
DE L'UNIVERSITÉ DE BORDEAUX**

ECOLE DOCTORALE SCIENCES PHYSIQUES ET DE L'INGENIEUR

MÉCANIQUE

Par **Lorena de Carvalho Araújo**

Identification de la performance énergétique intrinsèque des bâtiments collectifs et tertiaires à partir de mesures in-situ

Sous la direction de : **Frédéric Bos**
Laurent Mora
Co-encadrement : **Simon Thébault**
Thomas Recht

Soutenue le 23 mars 2022

Membres du jury :

Mme. Monika Woloszyn	Professeur	Université Savoie Mont Blanc	Rapporteuse
M. Stéphane Lassue	Professeur	Université d'Artois	Président du jury
M. Patrick Schalbart	Ingénieur de recherche	MINES ParisTech	Examineur
M. Simon Rouchier	Maître de conférences	Université Savoie Mont Blanc	Examineur
M. Frédéric Bos	Professeur	Université de Bordeaux	Directeur de thèse
M. Laurent Mora	Professeur	Université de Bordeaux	Directeur de thèse

Invités :

M. Thomas Recht	Maître de conférences	Université de Bordeaux	Encadrant de thèse
M. Simon Thébault	Docteur et ingénieur	CSTB	Encadrant de thèse

Titre

Identification de la performance énergétique intrinsèque des bâtiments collectifs et tertiaires à partir de mesures *in-situ*

Resumé

L'efficacité énergétique des bâtiments est un facteur clé pour réduire les émissions de CO₂. Les États membres de l'UE se sont engagés à améliorer celle-ci afin de répondre aux critères fixés par la directive sur la performance énergétique des bâtiments. Malgré l'adoption de réglementations dans le domaine, la performance énergétique réelle présente souvent un écart par rapport à celle prévue. Afin de combler cet écart, il est important de disposer d'indicateurs de performance réelle fiables permettant de vérifier et ainsi garantir la qualité des bâtiments. L'application de méthodes *in-situ* après les phases de construction ou de rénovation permet d'évaluer des indicateurs de performance, à l'instar du coefficient de déperditions global de chaleur (HLC) ou du coefficient de déperditions de chaleur par transmission (HTC). Différentes méthodes d'estimation de la performance énergétique des bâtiments sont aujourd'hui disponibles avec des protocoles, des principes mathématiques et des domaines d'application variés. Parmi ces méthodes, celles avec un protocole de mesure rapide ont été principalement conçues pour être appliquées aux maisons individuelles. Cependant, les logements collectifs et les bâtiments tertiaires représentent une part non négligeable du parc immobilier, ce qui leur confère un potentiel important d'économies d'énergie. Le présent travail étudie l'applicabilité d'une méthode de courte durée pour identifier le HTC et le HLC des bâtiments de grande taille.

Suite à la revue de la littérature sur les méthodes existantes pour l'évaluation de la performance thermique de l'enveloppe du bâtiment, il a été choisi d'adapter les méthodes ISABELE/SEREINE au contexte des grands bâtiments. Ces méthodes ont l'avantage de permettre un calcul de propagation d'incertitudes, mais elles ont été initialement conçues pour identifier la performance thermique de l'enveloppe de maisons individuelles. Le changement de taille des bâtiments implique de nouveaux défis d'un point de vue scientifique, technique et opérationnel. Le premier défi rencontré dans l'adaptation de ces méthodes est lié aux dimensions importantes des bâtiments collectifs et tertiaires. Pour faire face à ce problème, deux approches principales ont été envisagées : l'approche globale et l'approche par échantillonnage. La première consiste à appliquer le protocole à l'ensemble du bâtiment et le périmètre de l'espace testé coïncide avec l'enveloppe du bâtiment. Dans la deuxième, le protocole est appliqué à des parties du bâtiment et le périmètre du volume testé comprend des échantillons de l'enveloppe du bâtiment et des murs mitoyens. Les deux approches présentent des avantages

et des inconvénients, pour cette raison, le protocole et le processus d'estimation ont été adaptés à chacune d'elles. Le travail d'investigation a été effectué en simulation avec l'utilisation du logiciel Pléiades + COMFIE afin d'améliorer le protocole de la méthode et étudier ses limites. Par la suite, les deux approches ont été appliquées à des bâtiments réels afin d'améliorer la compréhension de leur faisabilité *in-situ*.

Les principales limites de l'approche globale sont liées à l'applicabilité du protocole, concernant l'instrumentation et l'occupation de l'ensemble du bâtiment. Le volume d'équipement nécessaire à la réalisation du protocole peut être une contrainte pour son application. Pour faire face à ce problème l'utilisation du système de chauffage local est une option pour des bâtiments collectifs et tertiaires de taille importante. Cette solution est toutefois conditionnée par les limites du système local et la contrainte d'immobilisation du bâtiment entier au cours de l'essai. Elle a été considérée comme possible dans les bâtiments dotés d'un système de chauffage centralisé avec distribution d'eau chaude, dans lesquels un calorimètre peut être utilisé pour mesurer la puissance délivrée pendant le test. Cela serait le cas de la moitié du parc immobilier français de logements collectifs, selon la base de données de l'Enquête Nationale Logement de 2013. L'approche serait applicable avec plus de difficulté pour des bâtiments dotés des systèmes de chauffage individuel électriques, ce qui représente un quart des bâtiments collectifs selon la même source.

L'approche globale a été appliquée à un modèle de bâtiment de quatre étages, en utilisant des variations de la puissance maximale du système de chauffage et des températures de test et de préchauffage. Les protocoles avec une faible différence de température entre le début et la fin du test ont présenté moins de dispersion de température entre les zones thermiques et de meilleurs résultats. L'approche globale a également été appliquée à un petit bâtiment collectif réel avec l'utilisation de plusieurs kits SEREINE, obtenant des résultats stables après deux jours et demi de test.

L'approche par échantillonnage est une alternative à l'approche globale, dans laquelle la performance thermique de l'enveloppe est vérifiée localement. Le principal défi de cette approche concerne les pertes thermiques à travers les murs mitoyens. Ces murs sont généralement moins isolés que les murs extérieurs, ce qui facilite le flux de chaleur pendant un test *in-situ* et peut générer un bruit dans les indicateurs HTC et HLC. Même si les flux mitoyens soient estimés pendant le test, une incertitude est associée à cette estimation, ce qui peut entraîner des incertitudes importantes sur le résultat final de la méthode selon les conditions de l'essai. Pour améliorer la qualité des résultats il est important de maximiser les flux vers l'extérieur par rapport aux flux mitoyens. Cela peut être fait en choisissant des échantillons avec une surface d'enveloppe maximale, comme dans les cas des logements d'angle au dernier

étage. Les différences de températures entre l'intérieur, l'extérieur et les espaces adjacents sont aussi des paramètres importants lors de l'application du protocole de mesure. Concernant la typologie des parois, les bâtiments neufs et rénovés sans isolation phonique dans les murs mitoyens, présentent les conditions les moins favorables au regard du rapport des flux, mais représentent également la typologie pour laquelle les tests *in situ* pour la détermination de la performance thermique serait majoritairement utilisées.

En plus de maximiser le rapport des flux extérieurs et mitoyens, il est important d'estimer le flux vers les espaces adjacents. Deux méthodes sont proposées à cette fin : la méthode indirecte et la méthode directe. Pour la méthode indirecte, le flux est estimé en considérant un régime stationnaire sur le mur mitoyen. Pour cela la différence de température entre les deux côtés du mur, l'U-value et la surface du mur mitoyen sont utilisées. Cette méthode implique l'installation de capteurs de température dans les espaces adjacents, ce qui peut être une contrainte pour l'application du protocole dans certains cas. La méthode directe est basée sur la mesure du flux de chaleur à travers le mur à l'aide des fluxmètres. D'un côté cela a le potentiel d'améliorer l'estimation des flux mitoyens en prenant en compte des effets dynamiques sur la paroi étudiée, et de l'autre cela implique l'utilisation de plus de capteurs et la complexification de l'installation du matériel pendant le test. Les deux méthodes présentent des limites et des avantages, pour cette raison, les deux ont été étudiées, développées avec des simulations virtuelles et appliquées *in situ*.

Les études numériques ont conclu que la méthode indirecte permet d'obtenir des résultats stables plus rapidement dans les bâtiments dont les murs sont isolés à l'intérieur et lorsque le bâtiment est préchauffé avant l'application du protocole. La méthode indirecte a donné de meilleurs résultats pour des différences de température plus élevées avec l'extérieur et plus faibles avec les espaces adjacents. Si aucun contrôle de la température des espaces voisins n'est réalisé, cette condition peut être atteinte pendant l'hiver. L'incertitude des résultats a été l'aspect le plus difficile pour obtenir des résultats acceptables en utilisant la méthode indirecte. Le critère de biais a été généralement atteint en hiver et en mi-saison, et pour certains des tests réalisés en été. La méthode indirecte est viable pendant les mois les plus froids de l'année et deux jours de test sont suffisants pour atteindre des résultats stables si le bâtiment est préchauffé. La méthode directe a présenté des niveaux élevés de convergence et d'interprétabilité lorsque de faibles niveaux d'incertitudes d'entrée sont associés aux mesures fluxmétriques. Cependant, si cette incertitude d'entrée est élevée, cette méthode n'est pas avantageuse par rapport à la méthode indirecte. Si les températures des espaces adjacents peuvent être contrôlées pendant l'essai, la méthode directe présente des résultats acceptables à partir d'une demi-journée d'essai et est applicable toute l'année. Les deux méthodes ont été appliquées *in situ* pour vérifier

leur comportement dans un scénario de cas réel et les résultats ont convergé vers une valeur similaire. Toujours dans une application réelle, la méthode directe présente des résultats stables plus rapidement, avec une demi-journée de test, contre deux jours pour la méthode directe.

Ce travail propose un cadre pour évaluer de manière fiable les coefficients HLC et HTC dans les typologies de grands bâtiments en se fondant sur la méthode ISABELE/SEREINE. Les conclusions finales de cette étude sont le produit des choix effectués pour faire face aux défis rencontrés lors de l'adaptation de cette méthode. En raison du large espace de possibilités à tester, concernant les méthodes, les caractéristiques des bâtiments et les conditions météorologiques, beaucoup d'entre elles n'ont pas été étudiées plus avant et font partie des perspectives de recherche. Néanmoins, un raisonnement similaire pourra être appliqué à l'adaptation d'autres méthodes à de grandes typologies de bâtiments. Le processus d'adaptation d'une méthode d'identification de la performance énergétique intrinsèque d'un bâtiment en dehors de ses limites initiales est donc la principale contribution du présent travail dans ce domaine.

Mots-clés : Performance énergétique intrinsèque des bâtiments, mesures *in-situ*, bâtiments collectifs, bâtiments tertiaires.

Title

Identification of the intrinsic energy performance of multi-family housing and tertiary sector buildings from *in-situ* measurements

Abstract

Building energy efficiency is a key factor in reducing CO₂ emissions and assuring the thermal comfort for inhabitants. EU member states are committed to increase building energy performance to meet the criteria set by the Energy Performance in Buildings Directive (EPBD). Despite the endorsement of building regulations, the as-built energy performance commonly presents a discrepancy with the predicted one, the so called energy performance gap. In order to close this gap, it is important to have reliable performance indicators to assure new building quality and to estimate the improvements achieved after renovation works. The application of *in-situ* methods after construction or retrofitting phases enables the measurement of performance indicators, as the whole heat loss coefficient (HLC) and the transmission heat transfer coefficient (HTC).

Different *in-situ* methods for estimating building energy performance are nowadays available with various protocols, mathematical principles and domains of applicability. Among them, the methods relying on fast duration protocol have been mainly conceived for applying in single-family houses. However, multi-family housings and tertiary sector building account for an important part of the building stock, presenting them a relevant potential for energy savings. The current work studies the applicability of a short duration test for identifying the HTC and HLC in large buildings and how to improve the method protocol. The ISABELE/SEREINE methods were chosen to be adapted to large building typologies. These methods were initially conceived to identify the envelope thermal performance of vacant single family houses. The first challenge encountered for achieving the adaptation objective is related to building dimensions, which hinders the protocol logistics. For facing this problem, two main approaches were considered. The first consists in applying the protocol to the whole building, using the local heating system. This approach is however limited to the conditions of the local system and impacts globally the building normal usage. The second approach is based on the protocol application to parts of the building, where samples of the building envelope have their thermal performance verified. In this case, the main difficulty is related to the heat flow passing through the shared walls. These walls are typically less insulated than the exterior walls, which facilitates the heat flow during an *in-situ* test and can potentially behave as a noise in the HTC and HLC indicators. Another challenge in this approach concerns the meaning of the final indicator, that is related to just part

of the building envelope. Both approaches present their advantages and drawbacks, reason why they have been further investigated to verify their potentials and limits. The investigation work was based on virtual simulation with the use of Pléiades + Comfie for improving the method protocol and studying its limits. Later, both approaches were applied to real buildings to enhance the comprehension of their feasibility *in-situ*.

This work proposes a framework for assessing reliable results of HLC and HTC in large building typologies, based on the ISABELE method. The final conclusions of this study are a product of the choices made to face the encountered challenges on adapting this method. As there is a wide space of possibilities to be tested concerning the methods, the building characteristics and weather conditions, many of them were not further studied and constitute part of the outlooks. Nevertheless, a similar reasoning could be applied to the adaptation of other methods to large building typologies. The process of adapting a method for the intrinsic building energy performance identification out of its original limits is therefore the main contribution of the present work to the field.

Keywords: Building envelope thermal performance, *in-situ* measurements, multi-family housing, tertiary sector buildings.

Acknowledgements

I had the chance to do a PhD in between two universes: the company CSTB and the University of Bordeaux. In the beginning, I was most of the time at CSTB where I learned lessons of professionalism. With the advancing of the thesis I could develop more my research skills at the University where my presence became integral.

Regarding the first context of work, I would like to thank CSTB for this opportunity and Stéphanie DEROUINEAU, for her global vision in the subject, that gave the guidelines of this work. I am also grateful for the data analysis courses they invested on me during the beginning of my thesis. When it comes to the work development, I am extremely thankful to my supervisor Simon THEBAULT, who supported me all the way. His empathy, commitment, knowledge and scientific curiosity taught me so much and made a pleasant atmosphere to develop my research in. He is someone I could always communicate with and count on for guidance and encouragement during all this time. Within the company other people also gave me advice and contributed to development of my work, such as Arnaud CHALLANSONNEX and Fadi LAHLOU. I am also grateful to the collaborators of SEREINE project, in special to those who feed this thesis with data: Michaël COHEN and Patrick SCHALBART with the virtual experimental plan and Arnaud JAY with in-situ study on flow meters. Thanks to my colleagues: Nico B., Nico D., Simon L., Toan, Islem and all colleagues from DEE department that made this time a pleasant experience with animated discussions, games and travels.

At the university, I had the chance to be mentored by brilliant people: Professor Laurent MORA, with his vast scientific knowledge of energy performance in buildings and commitment motivated and guided me greatly during this time. I am grateful for his advice, which has been precious for the development of this research. My thesis director Frédéric BOS that made this PhD thesis possible and encouraged me with his enthusiasm. Thomas RECHT with his scientific rigour and goodwill, helped to keep the project on track and to improve its quality. Who could say that my professor in China would become my thesis supervisor?! Special thanks to Alain SEMPEY that contributed with his vision to the subject during almost one year as an additional supervisor. I would also like to thank Tingting VOGT-WU and Ryad BOUZOUIDJA for the help with the heat flow measurements. I want to thank my friends at Bordeaux University: Tosin, Kanka, Shaolin, Yannick, Huynh, Enguerrand and Mathieu. All of you made these last months of the thesis a much nicer moment and were an important support for me! Also my former labmate, Clément, with all his bad jokes that have been defying my humor sense for about two years now.

All this work was only possible because, beyond these two universes, lovely people surrounded me. They were the source where I looked for inspiration, motivation, companionship. I want first to express my gratitude to Robin, for his immense support and love all this long, that were essential for me to complete this work. What a chance to be married to a smart Python and Git expert! Thanks for his understanding when I had to dedicate to my research, giving me space and help whenever I needed. In addition he gave me some gifts in France: my sweetest friend Adélie, that put all her heart to guarantee things were always going well, and revised my thesis! The second gift was my lovely family in law, that made me feel home in France. A special thanks to Stéphanie, always so present, who gave me a lot of motivation to dedicate to my goals.

Talking about lovely people, leads me to my family in Brazil. First, I would like to thank my mother Raquel and my sister Ana Luiza, who encouraged me all long. What a paradox to be always so close from so far?! Also Valéria, Eunira, Antônio Gerson, Lucas, Sandra, Adriano, thank you for always supporting me in my studies! Without you, none of this would have happened. Henrique, thank you very much for taking the time to read, give me feedback and encourage me for all this time.

I also need to mention my family from the heart in China. It was 张慧, with her infinite support, who first advised me to do a PhD. To my soul sister, 孙瑞泽, for who I wish a smooth and successful PhD completion. I just want us all to stay close, wherever we are.

Finally yet importantly, I want to acknowledge my family in the heaven. My grandmother Célia that showed me the importance of studying and working hard to make this world a better place.

I am delighted to see that at the end of this journey my luggage is full of new lessons, knowledge and tools to face the next challenges on my life. I can guarantee that each example and smile of yours have been essential to get here today. Thank you, *merci, obrigada, dhan'yabāda, cảm ơn, o seun, شكرا, 谢谢*.

Dedication

To Célia F. de Carvalho, who will always be my guiding star.

Favorite citation

"In my heart I feel you are all my brothers
Create a world with no fear
Together we cry happy tears
See the nations turn their swords into plowshares"

M. Jackson

Nomenclature

Latin letters

A_{wk}	Area of an exterior homogeneous wall	$[m^2]$
A_i	Transparent envelope element effective area	$[m^2]$
$b_{v,p}$	Ratio to adjust external air temperature	$[-]$
C	Air leakage coefficient	$[m^3/(h.Pa^n)]$
C_{air}	Air heat capacity	$[J/K]$
C_i	Effective heat capacity of the zone thermal mass	J/K
c_p	Specific heat capacity of the air	$[J/(kg.K)]$
g_i	G-value of a transparent envelope element	$[-]$
h	Global surface exchange coefficients	$[W/(m^2.K)]$
h_c	Convective heat transfer coefficient	$[W/(m^2.K)]$
H_{inf}	Thermal losses by air infiltration	$[W/K]$
h_r	Radiant heat transfer coefficient	$[W/(m^2.K)]$
HLC	Heat Loss Coefficient	$[W/K]$
HTC	Heat transfer coefficient	$[W/K]$
HTC_{ext}	Heat transfer coefficient of the sampled area envelope	$[W/K]$
HTC_{shar}	Heat transfer coefficient of the shared walls	$[W/K]$
HTC_{ref}	Reference envelope heat transfer coefficient	$[W/K]$
$I_{sol,i}$	Direct and diffuse solar irradiance	$[W/m^2]$
L_i	Length of a linear thermal bridge	$[m]$
n	Air flow exponent	$[-]$
P_{heat}	Total heat delivered during a test	$[W]$
P_{inf}	Heat flow due to infiltration	$[W]$
$Q4Pa$	Air permeability at 4 Pa	$[m^3/s]$
Q_{inf}	Air infiltration rate	$[m^3/s]$
$Q_{v,p}$	ventilation flow rates	$[m^3/s]$
R_e	Thermal resistance of a homogeneous wall	$[m^2.K/W]$
R_{inf}	Thermal resistance due to the air infiltration	$[K/W]$
S_{ext}	Surface of sampled area envelope	$[m^2]$
S_{shar}	Surface of sampled area shared walls	$[m^2]$
T	Temperatures	$[K \text{ or } ^\circ C]$
T_{adj}	Temperature of the spaces adjacent to the studied area	$[K \text{ or } ^\circ C]$
T_{int}	Temperature of the studied area	$[K \text{ or } ^\circ C]$
T_{em}	Equivalent external temperature	$[K \text{ or } ^\circ C]$
T_{ext}	External temperature	$[K \text{ or } ^\circ C]$
U_b	Thermal transmittance of building envelope	$[W/(m^2.K)]$
U_g	Thermal transmittance of the glazing	$[W/(m^2.K)]$
U-value	Thermal Transmittance	$[W/(m^2.K)]$
U_{wk}	Thermal transmittance of an exterior homogeneous wall	$[W/(m^2.K)]$

Greek letters

α_s	Absorptivity coefficient of the exterior wall	[-]
χ_j	Point thermal transmittance of a thermal bridge	[W/K]
$\Delta T_{beg-end}$	Temperature difference between the beginning and the end of a test	[K]
$\Delta T_{int-ext}$	Temperature difference between the interior and the exterior	[K]
$\Delta T_{int-adj}$	Temperature difference between the interior and the adjacent space	[K]
ϕ_h	Heat flow from heating systems	[W]
ϕ_{int}	Heat flow from internal gains	[W]
ϕ_{sol}	Heat flow from solar gains	[W]
ϕ_v	Heat flow due to ventilation	[W]
ϕ_{inf}	Heat flow due to infiltration through building envelope	[W]
ϕ_{tr}	Heat flow due to transmission through building envelope	[W]
$\phi_{h,sys}$	Power of the heating system	[W]
$\phi_{int,Occ}$	Heat flow from occupants	[W]
$\phi_{int,Ap\&Li}$	Heat flow from appliances and lightning	[W]
$\phi_{int,Wat}$	Heat flow related to hot water and sewage	[W]
ϕ_{shar}	Heat flow passing through the shared walls	[W]
φ_{shar}	Surface heat flow passing through a heat flow meter	[W/m ²]
$\Gamma_{\Delta T_{ext-adj}}$	Ratio between $\Delta T_{int-ext}$ and $\Delta T_{int-adj}$	[-]
$\Gamma_{\phi_{ext-shar}}$	Heat flow ratio between the exterior and shared walls	[-]
$\Gamma_{S_{ext-shar}}$	Surface ratio between the exterior and shared walls	[-]
$\eta_{h,sys}$	Overall system efficiency	[-]
λ	Thermal conductivity	[(W/(m.K))]
θ	Vector of a model parameters	[-]
ρ_{air}	Air density	[kg/m ³]
ψ	Linear thermal transmittance of a thermal bridge	[W/(m.K)]

Abbreviations and acronyms

ARMAX	Auto-regression moving average with extra inputs
ARX	Auto-regression with extra inputs
BAS	Building Automation System
BEP	Building Energy Performance
BETPA	Building Envelope Thermal Performance Assessment
BLC	Building Loss Coefficient
COP	Coefficient of Performance
CSTB	Centre Scientifique et Technique du Bâtiment
DHW	Domestic Hot Water
DPE	Diagnostic Performance Énergétique
EPILOG	Evaluation de la Performance Intrinsèque de Logements
EPBD	Energy Performance in Buildings Directive
EPC	Energy Performance Certificates
FDD	(System) Fault Detection and Diagnosis
GHG	Greenhouse Gases
HBM	(<i>Habitations à Bon Marché</i>) Low-cost housing
HFM	Heat Flow Meters
HVAC	Heating, Ventilation, and Air conditioning Technology
IEA	International Energy Agency
ISABELE	In Situ Assessment of Building Envelope Performances
M&V	Measurement and Verification
MFH	Multi-Family Housing
MPC	Model Predictive Control
OED	Occupancy Estimation and Detection
PACTE	Action Program for the Quality of Construction and Energy Transition
QUB	Quick U-value of Buildings
RC	Resistor-capacitor
SEREINE	<i>Solution d'Évaluation de la Performance Énergétique Intrinsèque</i> (Intrinsic Energy Performance Assessment Solution)
SFH	Single-Family Housing
TSB	Tertiary Sector Buildings

Table of contents

Résumé	i
Abstract	v
Nomenclature	xi
Table of contents	xv
List of Figures	xix
List of Tables	xxvii
1 Introduction	1
1.1 Motivation	2
1.2 Research objectives	3
1.3 Thesis structure	3
2 Context	5
2.1 Energy performance in buildings	5
2.1.1 Energy performance gap	8
2.2 Multi-family housing and tertiary sector buildings	10
2.2.1 Multi-family housings	10
2.2.2 Tertiary sector buildings	11
2.2.3 Energy consumption of MFH and TSB	11
2.3 Chapter conclusion	13
3 Building energy performance evaluation	15
3.1 A panorama on BEP evaluation	16
3.2 Basic concepts on BETPA	21
3.2.1 Analysis scale	21
3.2.2 Performance indicators	22
3.2.3 Heat balance in BETPA methods	24
3.2.4 Site conditions during protocol application	25
3.2.5 Inverse problems	28

3.3	Existent methods for BETPA	29
3.3.1	Averaging method	29
3.3.2	Linear regression	29
3.3.3	Dynamic methods	33
3.4	Applications in the MFH and TSB context	42
3.4.1	Application of linear regression methods	42
3.4.2	Application of average method	44
3.4.3	Application of state space methods	45
3.4.4	Overview	45
3.5	Chapter conclusion	45
4	Adapting ISABELE and SEREINE methods to MFH and TSB	49
4.1	A general BETPA method	51
4.1.1	Protocol of a BETPA method	52
4.1.2	Estimation process in a BETPA method	55
4.1.3	Limits of a BETPA method	58
4.2	ISABELE and SEREINE methods	60
4.2.1	Protocol	60
4.2.2	Estimation process	64
4.3	Challenges of testing MFH and TSB	74
4.3.1	The main challenges of the global approach	75
4.3.2	The main challenges of the sampling approach	83
4.4	Strategy for testing the approaches	93
4.4.1	Virtual experiments	94
4.4.2	In-situ experiments	98
4.5	Strategy for analysing the results	98
4.5.1	Result quality indicators	99
4.5.2	Method improvement process	102
4.6	Chapter conclusion	103
5	Global approach	105
5.1	Characteristics of local heating system	106
5.2	Dynamic thermal simulations	111
5.2.1	Reference indicator	112
5.2.2	Experimental plan	112
5.2.3	Results analysis	114

5.2.4	Discussion	122
5.3	In-situ test	122
5.3.1	Site description	122
5.3.2	Implementation of equipment in-situ	123
5.3.3	Estimation algorithm results	126
5.3.4	Discussion	131
5.4	Chapter conclusion	132
6	Sampling approach	135
6.1	Impact of neighbour heat flows	137
6.1.1	U_{eq} ratio	138
6.1.2	Surface ratio	138
6.1.3	Temperature difference ratio	140
6.2	Static method for exploring the sampling approach	142
6.2.1	Result uncertainty with the indirect method	144
6.2.2	Result uncertainty with the direct method	146
6.3	Indirect method for neighbours flow estimation	149
6.3.1	Ranges of U_{shar} uncertainty	149
6.3.2	Virtual experimental plan	150
6.4	Direct method for neighbours flow estimation	167
6.4.1	Ranges of φ_{shar} uncertainty.	168
6.4.2	Virtual experimental plan	180
6.5	In-situ test application	184
6.5.1	Building description	184
6.5.2	Experimental description test	187
6.5.3	Results and discussion	190
6.6	Chapter conclusion	192
7	Conclusion and perspectives	195
	Bibliography	199
	Annexes	223
A.	Input files from SEREINE method	223
B.	Building components of Pléiades Comfie model	228

List of Figures

2.1	General schema of the relation between the parameters used to calculate energy use in buildings - from various standards presented in the European Committee for Standardization and the Energy Performance of Buildings Directive [30] . . .	7
2.2	Example of a potential source of energy performance gap due to defaults in the construction phase: space between insulation boards leading to increased heat loss [51]	9
2.3	Distribution of the residential stock by housing typologies and by construction time in France (number of units). Adapted from [59].	10
2.4	Typology composition of residential building stock in different European countries: distribution of single and multi family housings [57]	11
2.5	Final energy consumption of the tertiary sector according to uses in France 2019 in % [62].	12
3.1	Scale of BEP characterization: (a) building component, (b) building envelope, (c) whole building energy characterization	21
3.2	What is investigated in forward and inverse problems	28
3.3	Example of co-heating data – power versus internal and external temperature difference (Delta-T) [145]	31
3.4	Energy Signature curve according to the outside temperature [147]	32
3.5	RC thermal network model for QUB method [170]	37
3.6	Model 4R3C: one of EPILOG RC thermal network models	38
3.7	a) ISABELE heating module, b) SENS sensors [176]	40
3.8	RC thermal network model used initially in ISABELE method [175]	40
3.9	Exemple of RC thermal network model from SEREINE method [176]	41
4.1	Decision matrix linking the methods to the quality of the input data and achievable accuracy of the outcome[195]	54
4.2	Relevant questions to define a protocol heating scenario in a BETPA method. . . .	54

4.3	Schema of a BETPA method with the main components of the estimation process.	56
4.4	Main mathematical frameworks used for BETPA methods	56
4.5	Representation of the pertinency domain of a BETPA method.	58
4.6	Intuition about the pertinency domain of a BETPA method developed for SFH, when applied to MFH and TSB and for three different weather conditions.	59
4.7	Modules in ISABELE/SEREINE kit. Adapted from [199].	61
4.8	Example of a heating scenario with stable temperature from ISABELE.	63
4.9	Example of a heating scenario with PSA power signal from SEREINE.	63
4.10	Overall schema on the data process of ISABELE and SEREINE methods. Adapted from [202]	65
4.11	Model M2_TmTi: a second order SEREINE RC thermal network model. Adapted from [122].	66
4.12	Simplified representation of the airflow network used in the EN 15242 without ventilation [177]	70
4.13	Schema of model selection in ISABELE method	71
4.14	Examples of measured signals with (a) purely stochastic error, (b) purely systematic error, and (c) a combination of stochastic and systematic errors [178].	72
4.15	Illustration of the uncertainty propagation procedure [178].	74
4.16	Vehicles with the whole equipment of ISABELE/SEREINE methods version 2020.	76
4.17	Examples of a potential multi-zone RC thermal network model for the global approach. Adapted from [208].	81
4.18	Example of the measured perimeter and the boundaries in a sampling approach method application. Adapted from [212].	84
4.19	Different possibilities for the tested areas in the sampling approach. Adapted from [218].	88
4.20	Example of a RC thermal network model with the addition of a power source ϕ_{shar} to represent the neighbour heat flow. Adapted from [219].	90
4.21	Axonometric view of the building model in Pleiades Modeller	96
4.22	The probability density of four different tests with the results bias and uncertainty	100
4.23	Representation of the interpretability indicator with cumulative distribution function and probability density function of the result [236]	101
4.24	Representation of the interpretability indicator with the cumulative distribution function and the probability density function of the result for the cases <i>a</i> and <i>b</i> . .	101
4.25	Representation of the interpretability indicator with the cumulative distribution function and the probability density function of the result for the cases <i>c</i> and <i>d</i> . .	102

4.26	General representation of a method improvement process based on model result quality	103
5.1	Distribution of generator types for centralized heating systems according to ENL database.	108
5.2	Distribution of generator types for decentralized heating systems according to ENL database.	108
5.3	Example of installation of the calorimeter sensors at the main building heating pipes [185].	110
5.4	Protocol feasibility of global approach using local system in French MFH building stock, according to ENL database.	111
5.5	Dispersion of HTC bias according to test duration	114
5.6	Dispersion of HTC bias according to maximum power for tests until 2 days (left) and tests longer than 2 days of duration (right).	115
5.7	Dispersion of HTC bias according to preheating for tests until 2 days (left) and tests longer than 2 days of duration (right).	116
5.8	Dispersion of HTC bias according to setpoint temperature for tests until 2 days (left) and tests longer than 2 days of duration (right).	116
5.9	Dispersion of HTC bias according to the $\Delta T_{beg-end}$ (K) of temperature for all duration	116
5.10	Dispersion of HTC bias according to the $\Delta T_{beg-end}$ (K) of temperature for tests until 2 days (left) and tests longer than 2 days of duration (right).	117
5.11	Histogram of HTC bias for tests longer than two days	117
5.12	Percentage of acceptable results per $\Delta T_{beg-end}$ for tests longer than two days	118
5.13	Heating power and temperature (variant: 50 kW and 30 K of $\Delta T_{beg-end}$)	119
5.14	HTC progression with test duration (test: 50 kW and 30 K of $\Delta T_{beg-end}$)	119
5.15	Heating power and temperature (test: 80 kW and 2 K of $\Delta T_{beg-end}$)	120
5.16	HTC progression with test duration (variant: 80 kW and 2 K of $\Delta T_{beg-end}$)	120
5.17	Percentage of acceptable results per delta of temperature and duration - lateral vision in the lefts and superior vision in the right	121
5.18	Pictures of the MFH building facades in Sallanches site	123
5.19	Location of the sensors during the measurement by global approach of the Sallanches site [208]	125
5.20	Pictures of some of the equipment installed outdoor and indoor at the Sallanches site [208]	125

5.21 Sallanches site progression of HLC results using ISABELE estimation algorithms and a time step of 1 hour	127
5.22 Sallanches site progression of HLC results using SEREINE estimation algorithms and a time step of 1 hour	127
5.23 Sallanches site progression of HLC results using ISABELE estimation algorithms and a time step of 5 min	128
5.24 Sallanches site progression of HLC results using SEREINE estimation algorithms and a time step of 5 min	128
5.25 Permeability indicators main measures for MFH in Sallanches [208]	129
5.26 Hypothesis on the blower door indicators to estimate the air infiltration losses during the test in Sallanches site with the global approach [219]	129
5.27 H_{inf} estimation based on hypothesis 1 and 2 during the test in Sallanches site with the global approach [219]	130
5.28 H_{inf} estimation of each apartment for hypothesis 2 during the test in Sallanches site with the global approach [219]	130
5.29 Sallanches site progression of HTC results using SEREINE estimation algorithms with a time step of 1 hour and the hypothesis 1 for the estimation of H_{inf}	131
5.30 Sallanches site progression of HTC results using SEREINE estimation algorithms with a time step of 1 hour and the hypothesis 2 for the estimation of H_{inf}	131
6.1 Separation of thermal transmission coefficients to the outside and to adjoining spaces [219]	137
6.2 Example of tested area location in a four-storey building with twenty-four apartments of 7 m x 7 m.	140
6.3 HTC uncertainty according to U-value and surface ratio using the indirect method considering 5 % of uncertainty in U_{shar}	145
6.4 HTC uncertainty according to U-value and surface ratio using the indirect method considering 20 % of uncertainty in U_{shar}	145
6.5 HTC uncertainty according to U-value and surface ratio using the indirect method considering 40 % of uncertainty in U_{shar}	145
6.6 HTC uncertainty according to the U-value and surface ratio using the direct method considering 0.01 W/m ² of uncertainty in the heat flow meter measurements.	147
6.7 HTC uncertainty according to the U-value and surface ratio using the direct method considering 1 W/m ² of uncertainty in the heat flow meter measurements.	147

6.8	HTC uncertainty according to the U-value and surface ratio using the direct method considering 2 W/m ² of uncertainty in the heat flow meter measurements.	147
6.9	HTC uncertainty according to the U-value and surface ratio using the direct method considering 4 W/m ² of uncertainty in the heat flow meter measurements.	148
6.10	Histogram of partition walls (left) and intermediate floor (right) U-value, obtained from the Monte-Carlo uncertainty propagation sample size of 10000	150
6.11	Internal view of the building model top floor in Pleiades Modeller with floor of apartment n° 15 in red.	151
6.12	RC thermal models of first order used in the estimation process of the numerical experiments.	152
6.13	Indoor and outdoor temperatures during the test	154
6.14	Results progression for the variant with heavy shared walls and internal wall insulation	154
6.15	Results progression for the variant with heavy shared walls and external wall insulation	155
6.16	Results progression for the variant with light shared walls and internal wall insulation	155
6.17	Results progression for the variant with light shared walls and external wall insulation	155
6.18	Solar radiation per facade (top) and outdoor and equivalent outdoor temperatures (down) during virtual protocol application of second experimental plan.	157
6.19	Results interpretability for different protocol setpoint temperature and preheating conditions for half day of test duration.	158
6.20	Results interpretability for different protocol setpoint temperature and preheating conditions for 1 day of test duration.	159
6.21	Results interpretability for different protocol setpoint temperature and preheating conditions for 2 days of test duration.	159
6.22	Results interpretability for different protocol setpoint temperature and preheating conditions for 3 days of test duration.	159
6.23	Results progression for the numerical test performed in February in La Rochelle with experimental plan B.	163
6.24	Bias and uncertainty of results according to the mean $\Delta T_{int-ext}$ and $\Delta T_{int-adj}$ for 2 days of test in experimental plans A, B and C.	165

6.25 Interpretability of results according to the mean $\Delta T_{int-ext}$ and $\Delta T_{int-adj}$ for 2 days of test in experimental plans A, B and C.	166
6.26 Location of heat flow meters in the Bordeaux IUT experiment (left) and detail on the sensor (right).	168
6.27 Temperature and heat flow measurements during IUT Bordeaux experiment.	169
6.28 Histogram of the difference between HFM measurements and mean value for each time step for IUT experiment.	170
6.29 Photo of the office with the equipment installed for CEA experiment Adapted from [246].	171
6.30 Temperature and heat flow measurements on the wall and floor for the scenario of low $\Delta T_{int-adj}$ from CEA experiment.	172
6.31 Histogram of the difference between HFM measurements and mean value for each time step for the scenario of low $\Delta T_{int-adj}$ of the concrete floor from CEA experiment.	173
6.32 Histogram of the difference between HFM measurements and mean value for each time step for the scenario of low $\Delta T_{int-adj}$ of the double concrete wall from CEA experiment.	174
6.33 Histogram of the difference between HFM measurements and mean value (without HFM_X06_Z04) for each time step for the scenario of low $\Delta T_{int-adj}$ of the double concrete wall from CEA experiment.	175
6.34 Temperature and heat flow measurements on the wall and floor for the scenario of high $\Delta T_{int-adj}$ from CEA experiment.	176
6.35 Histogram of the difference between HFM measurements and mean value for each time step for the scenario of high $\Delta T_{int-adj}$ of the concrete floor from CEA experiment.	177
6.36 Histogram of the difference between HFM measurements and mean value (without HFM_X24_Y18 and HFM_X29_Y01) for each time step for the scenario of high $\Delta T_{int-adj}$ of the concrete floor from CEA experiment.	177
6.37 Histogram of the difference between HFM measurements and mean value for each time step for the scenario of high $\Delta T_{int-adj}$ of the double concrete wall from CEA experiment.	178
6.38 Evolution of mean interpretability value with the test duration using the direct and indirect method with different input uncertainty levels.	181
6.39 Interpretability, bias and uncertainty of the results using the direct and indirect method with different input uncertainty levels.	182

6.40	Interpretability of the results using the direct and indirect method with different input uncertainty levels.	183
6.41	Progression of results for the test applied in July in Trappes city using the direct method with $\pm 2 \text{ W/m}^2$ of uncertainty associated to φ_{shar}	184
6.42	Google image of A11 building (left) and view of the tested office (in red) west facade from the central building area (right).	185
6.43	Blueprint of A11 building first floor, with the tested office marked in orange.	185
6.44	SEREINE Heating module placed in the tested office (left), SENS sensors placed outside the building in the footbridge in front of the entrance of the unheated space (right).	187
6.45	HFM location for each shared wall of the tested office in A11 building.	187
6.46	Heat flow passing through the shared walls (HFM measurements) and adjacent spaces temperature during the experiment in A11 building.	188
6.47	Heat power and temperatures during the experiment in A11 building.	189
6.48	Blower door setup in the office doorway (left) and the result of the four tests in the graph of air leakage versus pressure (right).	189
6.49	Progression of results for the test in the A11 building using the indirect method with $\pm 20 \%$ of uncertainty input in the U_{shar}	191
6.50	Progression of results for the test in the A11 building using the direct method with $\pm 3 \text{ W/m}^2$ of uncertainty input in the φ_{shar}	191
A.1	Description of the building: excel sheet tab of exterior walls.	223
A.2	Description of the building: excel sheet tab of shared walls.	224
A.3	Description of the building: excel sheet tab of windows	224
A.4	Description of the building: excel sheet tab of other information	224
A.5	Description of the experiment: json file.	225
A.6	Description of the estimation process: yml configuration file	226
A.7	Weather time series measurements: csv file.	227
A.8	Sensors time series measurements: csv file.	227

List of Tables

2.1	Estimation of energy consumption per building typology in France. Adapted from [50].	12
3.1	Comparison of main building energy performance evaluation methodologies [109]	20
3.2	Different indicators concerning building envelope. Adapted from [121, 122]. . .	23
3.3	Parallel between parameters from electrical and thermal RC networks	35
3.4	Different methods for BETPA on the context of MFH and TSB	46
4.1	The insulation performance level as a function of the envelope's average thermal transmission coefficient (U_{bat}). Adapted from [217].	87
4.2	Benefits and drawbacks of the methods for taking into account the neighbours heat flows. Adapted from [219].	93
4.3	Analysis of French MFH building stock in 2017 by building type and size category	95
4.4	Global characteristics of building model in Pleiades Modeller	95
4.5	Combined radiant and convective heat transfer coefficients for surfaces in COMFIE software [234]	98
5.1	Some of the possible technologies for the local heating system components	106
5.2	Distribution of heating system installation type in SFH and MFH (%) according to ENL database.	107
6.1	Ratio of exterior and shared walls for apartments located at different locations of the building	139
6.2	Ratio of exterior and shared walls for aggregated tested areas located at different parts of the building	139
6.3	HTC_{ext} reference value for the tested apartment in the building model in Pleiades Modeller	151
6.4	Setpoint temperatures for the scenario with variation in the neighbours temperature in P+C	153

6.5	Shared wall characteristics for the heavy and light variants	153
6.6	Preheating and setpoint temperatures of the experimental plan.	157
6.7	Statistical description of results interpretability according to acceptability and test duration.	158
6.8	Indoor temperatures (°C) for the experimental plans A, B, C.	162
6.9	Mean interpretability for tests with maximum duration of 7 days by results acceptability.	163
6.10	Interpretability and acceptability for 2 days of duration	164
6.11	Statistics on the mean $\bar{\varphi}_{shar}$ and $\Delta T_{int-adj}$ over the time for the IUT experiment.	170
6.12	Statistics on the mean $\bar{\varphi}_{shar}$ and $\Delta T_{int-adj}$ over the time for the scenario with low temperature difference with adjacent spaces in CEA experiment.	173
6.13	Statistics on the mean $\bar{\varphi}_{shar}$ and $\Delta T_{int-adj}$ over the time for the scenario with high $\Delta T_{int-adj}$ from CEA experiment.	176
6.14	φ_{shar} uncertainty range according to the tested scenarios.	180
6.15	Description of the composition and project U-values concerning the tested area of the A11 East wing.	186
B.1	Thermal resistance of walls of the building model in Pleiades Modeller	228
B.2	Heat capacity of the building model per component material in Pleiades Modeller	228
B.3	Thermal properties of thermal bridges of the building model in Pleiades Modeller	229
B.4	Thermal properties of openings of the building model in Pleiades Modeller	229

Chapter 1

Introduction

Contents

1.1 Motivation	2
1.2 Research objectives	3
1.3 Thesis structure	3

In the fight against climate change, the European Union is committed to decreasing its greenhouse gas emissions (GHG). In 2007, The European Council advised the EU member states to achieve at least 20% of reduction in GHG emissions and to increase the same amount for energy efficiency and the share of renewable energies by 2020 compared to 1990 [1]. These targets being partially met [2], they were tightened in the 2030 climate & energy framework to at least 32.5% improvement in energy efficiency and 40% in GHG emissions [3]. Energy efficiency is highlighted among the different climate policies implemented to achieve these goals, since it mitigates the final energy consumption, if the level of goods and services are kept constant, contributing then to reduce GHG emissions [4]. The building sector is responsible for about 40% of primary energy consumption in Europe, presenting then a relevant potential for energy savings [5]. For this reason, major investments should be led to achieve better energy performance in buildings by applying both high standards to new buildings and renovation actions to the existing building stock.

The European Energy Performance of Buildings Directive (EPBD), last updated in 2018 [6], applies minimum requirements to the energy performance of new buildings and existing buildings that are subject to major renovation. It also gives guidelines to minimum standards for building envelope elements with a significant impact on the energy performance when they are retrofitted or replaced [6]. To ensure the implementation of the European EPBD, the 27 member states developed thermal regulations and labels for buildings. Among them, France was one of the first countries to implement building thermal regulations, with its first dating of 1974 [7].

The present Environmental Regulation 2020 ("*Réglementation Environnementale 2020*") is the eighth legal act set out by the French government related to this EU directive.

Despite the endorsement of building regulations, the as-built energy performance does not always follow the anticipated one, the so called energy performance gap. Buildings that are less efficient than they were designed to be present higher final energy use during its operational phase than predicted. This phenomena has been broadly reported in the literature, with different ranges of variation from expected and actual performances [8, 9, 10, 11].

Assessing building's real energy performance contributes for reducing the performance gap. This is also an important lever for increasing building construction quality and consequently reducing energy consumption and minimizing the sector environmental impacts. Nonetheless, efforts should be taken to evaluate the entire set of building stock, going beyond single-family houses and also including multi-family housings and tertiary sector buildings.

1.1 Motivation

Maximizing buildings energy efficiency is essential for reducing the sector environmental impacts. Ensuring the as-built building energy performance (BEP) leads to better quality buildings helping to lower the final energy consumption levels.

Presently, there are different methods available for assessing real BEP, with various protocols and application domains. These methods can be divided into two main families: steady-state and dynamic methods [12]. In the first family the heat dynamics occurring in the building thermal mass are not taken into account. This is correct mainly when long time steps for the data collection and analysis are used. The time should be long enough so that the dynamics phenomena can be neglected. These methods are in overall mathematically simpler, but they present longer test duration than the dynamic methods.

The test duration is an important parameter of test protocol, depending on the impacts it has on normal building usage, as it disturbs occupancy and implies on financial impacts. Long duration methods are conceived to be applied into occupied buildings. However, occupancy brings complexity to the model, especially when it comes to estimating the envelope thermal performance. Dynamic methods have less constraints in the data time step and typically shorter test duration. This allows their application in both vacant and occupied buildings. The application of dynamic methods into vacant buildings are well studied from the research community, as by the Annex 58, "Reliable Building Energy Performance Characterisation Based on Full Scale Dynamic Measurements", from the International Energy Agency (IEA)[13]. Recent initiatives have been done to apply it to occupied buildings, and to model thermal phenomenon

associated with occupancy, such as solar and internal gains and ventilation losses, in Annex 71, "Building Energy Performance Assessment Based on In-situ Measurements", from IEA and related works [14, 15].

Although progress has been made in dynamic methods for BEP characterization, most of the efforts have been directed to Single-Family Housing (SFH), while Multi-Family Housing (MFH) and tertiary sector buildings (TSB) are commonly treated by steady-state methods. These buildings typologies represent an important part of building stock and deserve efforts to develop a reliable fast method to assess their real BEP. The motivation of the present work is to bring applicable solutions for assessing the building intrinsic energy performance through the use of dynamic methods to cover multi-family housings and tertiary sector buildings.

1.2 Research objectives

The ultimate goal of this work is to define strategies for assessing the envelope thermal performance of multi-family dwellings and office buildings using a dynamic method. For working in this direction, the following objectives were set:

- To adapt an existing method, conceived to assess the envelope thermal performance of single-family houses, to be applicable to multi-family housings and tertiary sector buildings.
- To define suitable protocol strategies for new and retrofitted large typology buildings.
- To delimit the pertinency domain for each explored strategy.
- To apply the developed protocols in-situ to verify their technical feasibility.

The baseline principle behind these goals is to achieve quality results, regarding bias and uncertainty, with a cost-effective and short-duration protocol. The immobilisation time during a protocol application is an important factor on practice, since the protocol application disturbs the building normal usage. However, an unduly short duration can lead to poor indicator results. The protocol should be fast enough to be applicable and operational for in-situ measurements, but long enough to ensure the results quality.

1.3 Thesis structure

Focusing on the main objective previously mentioned, we have designed the thesis to achieve a concrete and detailed protocol for assessing the energy performance of multi-family housings

and tertiary sector buildings envelope. Different tests conditions using a global and sampling approach, with simulations and the application in real buildings, have been analyzed. The thesis is divided into 7 chapters, as detailed below.

We start from the introduction, motivation and objectives in the current chapter. In **chapter 2** there is a discussion about BEP, where we also call attention to the energy consumption contributions from large typology buildings. In **chapter 3**, a brief state of the art on the methods for assessing real BEP is presented. Some methods that have been formerly applied to multi-family housings and tertiary sector buildings are then presented. Finally, the limits from the state of the art to assess energy performance in large buildings is discussed as an open door to the development of this thesis work.

The **chapter 4** presents the challenges on adapting existing methods for assessing the building envelope energy performance of SFH to MFH and TSB. The discussion is based on two different solution strategies: global and sampling approaches. The specific issues and possibilities concerning each of them are addressed for guiding the following study. In both approaches, virtual and real protocol applications were used to study the proposed methods. The quality criteria used to evaluate the test results are also covered by this chapter.

In chapters 5 and 6, we investigate different protocols to address the thesis problematic. **Chapter 5** is focused on a global approach protocol that consists in the whole building mobilisation. We go through the main challenges when applying this approach. Variants of a method protocol are tested to optimize the results accuracy and uncertainties, and to reduce test duration. In order to find suitable solutions for large typology buildings, a MFH model was used for virtual protocol application. Then, a real case test application in a French multi-family house is presented in the end of the chapter.

Chapter 6 addresses the sampling approach that mobilises only part of the building to investigate its envelope thermal performance. The main challenge of this approach is the thermal flux going through the shared walls. This parameter is evaluated with two different methods: the measurements with heat flow meters and estimation of the walls thermal properties. The effect of this parameter uncertainty on the results is addressed. The differences between both methods are investigated with the use of virtual and *in-situ* protocol applications. Finally, **Chapter 7** gives the general conclusions of this thesis and the possible future outlooks.

Chapter 2

Context

Contents

2.1 Energy performance in buildings	5
2.1.1 Energy performance gap	8
2.2 Multi-family housing and tertiary sector buildings	10
2.2.1 Multi-family housings	10
2.2.2 Tertiary sector buildings	11
2.2.3 Energy consumption of MFH and TSB	11
2.3 Chapter conclusion	13

In this chapter, the context that embraces this work is presented. Initially, the concept of energy performance in buildings is discussed along with the energy gap matter. After that, particularities about MFH and TSB are presented to show the relevance of assessing their real energy performance.

2.1 Energy performance in buildings

Behind the concept of building energy performance (BEP), there is always the notion of how well the building behaves regarding its energy consumption. However, it can have different interpretations according to which parts of the building are considered in the analysis and the context in which it is located. A report from the Department of Environmental Protection of Connecticut ([16]) gives a definition for it as "*a measure of the relative energy efficiency of a building, building equipment, or building components, as measured by the amount of energy required to provide building services. For building equipment and components, it means a relative measure of the impact of equipment or components on building energy usage*". The EPBD [17]

defines it as the amount of energy actually consumed or estimated to meet the different needs related to a standardized use of the building.

In the definitions above, the expressions "relative energy efficiency" and "standardized use" express the idea that BEP depends on climate, building situation and usage. The efficiency concept is related to providing a service wasting minimum resources [18]. When applied to BEP context, energy is the mentioned **resource**, however, the **results** can be in accordance with a variety of end-use activities with effects on energy consumption during building occupation. Space heating and cooling and domestic hot water (DHW) account for a large proportion of buildings energy consumption, depending not only on the systems energy efficiency and temperature control, but also on the envelope thermal efficiency of the buildings in which they operate [19].

In the European Union, it is the responsibility of the Member States to provide calculation guidelines and methods for determining energy efficiency at the national or local level. In most cases, software will be developed to perform these calculations. In France, the permit to build is granted only if the building project respects minimal criteria regarding BEP according to the current thermal regulation. In this case, before the start of the construction works, simplified energy dynamics simulation software are used to determine an expected level for the BEP and check its conformity with regulatory values. Other instruments that are often put in place by the Member States are the Energy Performance Certificates (EPC). They indicate the energy performance of a building or building unit, according to a methodology adopted respecting the EPBD. In France, the new Energy Performance Certificate (in French "Diagnostic Performance Énergétique" or DPE) from July 2021 takes into account 5 uses concerning BEP: heating, domestic hot water, cooling, lighting and auxiliaries (such as pumps for ventilation and heat distribution) [20]. The previous standards in France accounted just for the first three mentioned uses, which shows that there is not a unique and absolute approach to analyse BEP.

Figure 2.1 shows a general relationship from various standards in Europe to consider the energy use in buildings. We can see that the final energy use and CO₂ emissions of a building is an interaction of the different thermal phenomena taking place into it with building characteristics and usages.

In general, four main factors affect directly BEP: weather, occupancy, building envelope and systems [21]. Even though the first two factors have an important impact in building energy consumption [22], they are not related to building quality but to its context. The geographical location (latitude, longitude and altitude) and local thermal phenomena are going to define the weather and the micro-climate around a building. Its relevance can be seen by the amount of recent studies addressing the resiliency of building stock to global warming consequences

[23, 24, 25, 26, 27, 28]. The building and occupants might adapt to the local weather conditions to achieve an optimum energy performance. For instance, the same building in a tropical or temperate climate would not be rated with the same energy performance. In the first location, space cooling would be far more relevant than space heating. Once the energetic needs for the buildings are different, the strategies to meet them should also be adapted to achieve better performances [29].

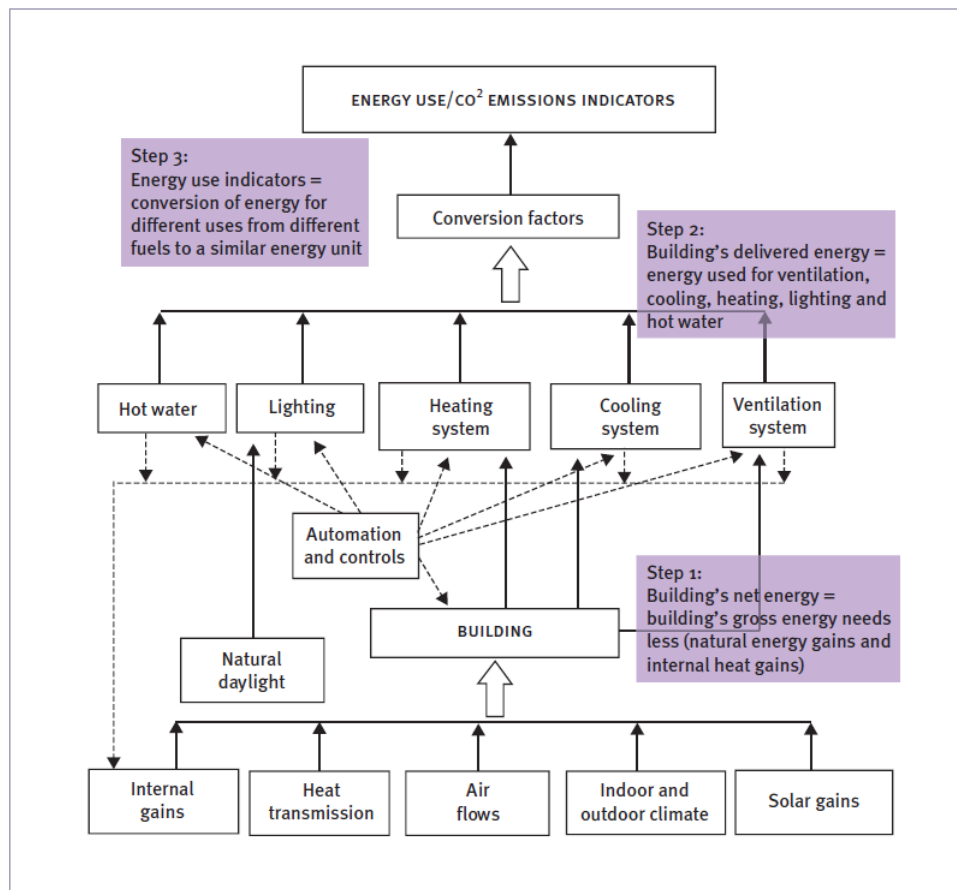


Figure 2.1 – General schema of the relation between the parameters used to calculate energy use in buildings - from various standards presented in the European Committee for Standardization and the Energy Performance of Buildings Directive [30]

Thermal comfort is a key concept behind BEP, since a significant amount of energy is spent to regulate the indoor temperature providing comfort in the building. Thermal comfort is related to climate conditions, building quality, but also to the occupants perception [31, 32] and it needs to be coherent with building context. The occupancy impacts the energy usage of a building through the activities taken in it that are motivated by the different needs and perceptions of occupants [33, 34, 35]. Improving behavior and adjusting human expectations and choices is not a simple task, but it can be encouraged by awareness campaigns and energy performance indicators.

The last two factors are related to building quality. Physical characteristics such as the

wall type of insulation, the window characteristics and the HVAC system are going to have a significant impact on energy savings. A lot of technologies has been developed to improve building elements energy performance. They can be separately rated by different indicators, such as the U-value of walls and windows, the boiler efficiency and the heating seasonal coefficient of performance of a heat pump. To achieve an overall performance quality, it is important to have a coherent combination of building elements. It is known that a triple glazed window will perform better in a cold climate than a single glazed one, as well as a thicker layer of insulation diminishes exterior wall heat losses and an efficient boiler consumes less energy for space heating. However, these elements alone do not solve the problem of energy losses. For this reason it is necessary to have an overall vision about building elements that play together an important role on BEP. The intrinsic BEP concerns the energy losses due to the building envelope, where HVAC systems efficiency and occupant behavior are not taken into account. It is directly related to the building envelope, which is the integrated elements of a building separating its interior from the outdoor environment. Due to the importance of intrinsic BEP, the new French EPC integrates an evaluation of the envelope thermal transmittance, U_{bat} , with a scale to emphasize the envelope thermal performance. The building envelope quality is the main focus of this work and it will be further discussed in the next chapter.

2.1.1 Energy performance gap

A difference between the predicted and actual building envelope performances, called energy performance gap, has been broadly presented in the literature [36, 37, 38, 39]. Its evaluation depends on how the predicted and actual performances are estimated, making it dependent on the context of observation [40]. Combined with the variety of building stock, this factor hinders a common sense on the expected ranges of the performance gap. Its magnitude varies from different sources. For instance, going up to 287 % for a specific building [41]. When coming to larger data sets of buildings, this discrepancy is in average lower, but still significant: in the order of 8 to 30 % lower efficiency in some studies [42, 43] or going up to 117 % [41].

The energy performance gap can be attributed to several factors that can take place during the design and simulation stage, construction and commissioning stage and operation stage [8]. During the design and simulation stage, it is generally related to theoretical deviations on input data for the energy dynamic simulations, as inaccuracy of weather data, occupant behaviour modelling and inaccuracy of inputs and assumptions on building modelling [44, 45, 46]. Errors associated to the construction stage can be such as degradation of the insulation during transport, storage and implementation, variations between the project and its implementation (product performance and/or quantity) and poor workmanship [47, 48]. In the operational

stage, we could cite causes such as: malfunctioning equipment and non-optimal use of the building by the occupant [49]. Figure 2.2 shows an example of poor workmanship during insulation implementation that would lead to increase the energy performance gap.

Assuring the real performance of building present many advantages. At building reception, it could validate its performance after construction to ensure the results of the investment and to identify potential malfunctioning that could lead to over energy consumption during the building operation stage. It could also be useful in the context of energy performance guarantee contracts to: monitor operations, optimize performance and validate the good achievement performance of the building, avoiding the responsibility of a problem outside the operating perimeter. Ensuring the real performance could also potentially help to benefit from public policy management, subventions and quality labels. For constructors, it might be interesting in the framework of internal quality control and to have experience feedback to better design new buildings. It could also be used as a tool to communicate building insulation quality to its tenants, shareholders and public authorities [50].

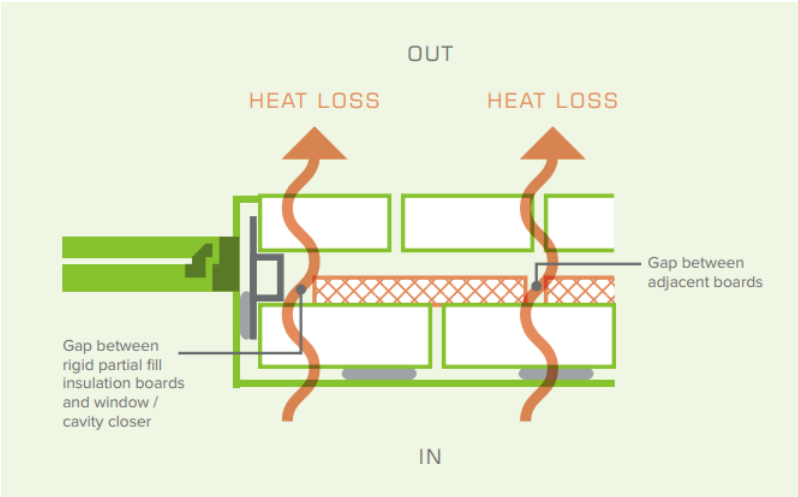


Figure 2.2 – Example of a potential source of energy performance gap due to defaults in the construction phase: space between insulation boards leading to increased heat loss [51]

Even though occupant behavior and preferences play a significant role in the energy consumption [52, 53, 54, 55] the contributions from building envelope and systems quality cannot be neglected. The use of tests and agreed protocols for in-situ measurements of the building envelope performance is one important measure for closing the gap.

2.2 Multi-family housing and tertiary sector buildings

Multi-family housings (MFH) and tertiary sector buildings (TSB) contrast with single-family housings (SFH) by their larger sizes. This aspect alone can already bring significant challenges for the application of in-situ energy performance protocols. In this subsection, we are going to describe some aspects of these two building typologies and their impacts on overall energy consumption in the French context.

2.2.1 Multi-family housings

Multi-family housings are buildings with more than one dwelling unit. It has a large spectrum regarding the size and number of units, going from large single-family houses, that have been subdivided into apartments, to high-rise MFH, which may contain hundreds of units. They are typically defined as low-rise, mid-rise, and high-rise MFH. Low-rise buildings have typically two to three stories, mid-rise have four to eight stories, while buildings taller than eight stories are considered high-rise, and can often have other uses such as offices and stores [56].

The typology composition of building stock varies among the EU member states (figure 2.4), but in average MFH accounts for 50% of residential building stock in Europe [57]. In France, 44 % of the residential building stock is represented by MFH [58]. In figure 2.3 the residential building stock is divided by date of construction and typology, with MFH in the left and SFH in the right of the red line. It shows that two thirds of MFH stock is constructed before the first thermal regulation in France (RT 1974), which presents thus a high potential for energy performance improvements.

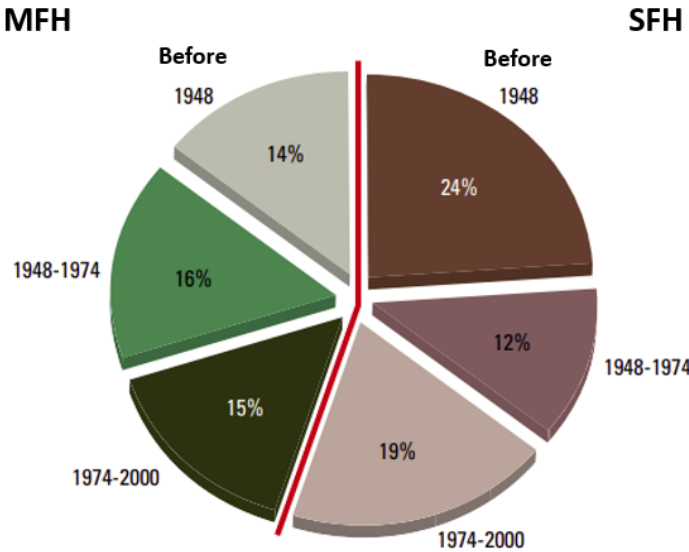


Figure 2.3 – Distribution of the residential stock by housing typologies and by construction time in France (number of units). Adapted from [59].

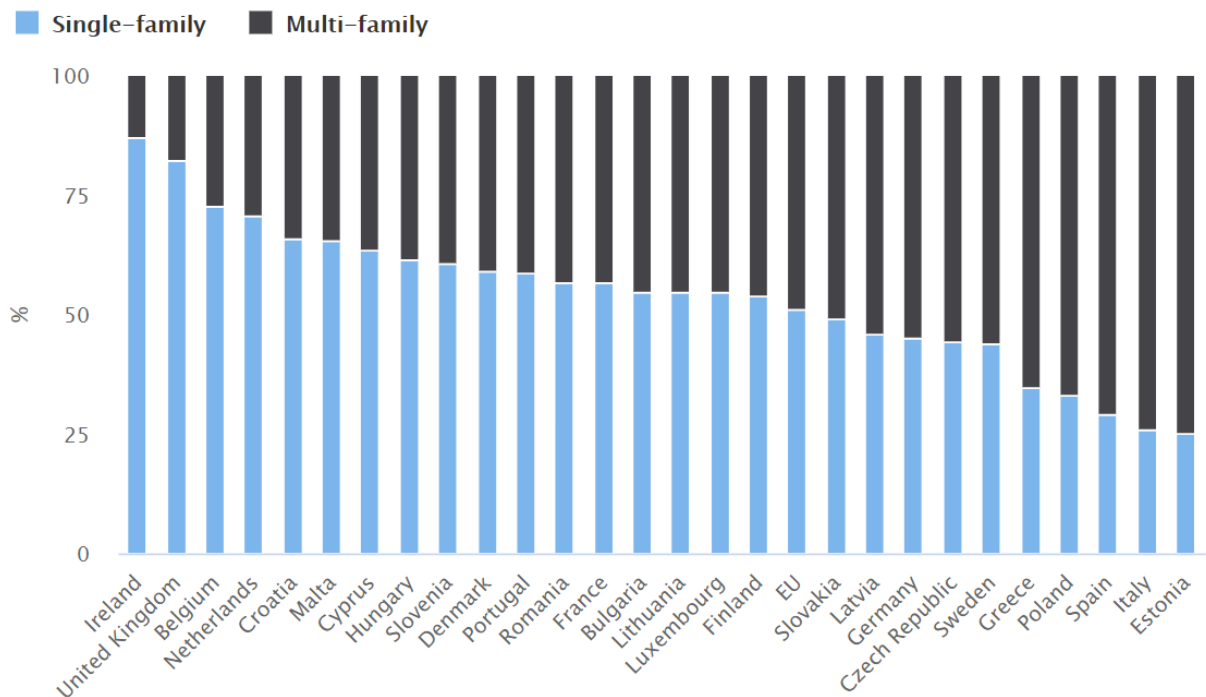


Figure 2.4 – Typology composition of residential building stock in different European countries: distribution of single and multi family housings [57]

2.2.2 Tertiary sector buildings

In the three sectors model, tertiary sector is responsible for providing services, while primary is associated to agriculture and secondary to industry. Tertiary sector buildings (TSB) include all of the infrastructure occupied by public authorities, associations and companies providing services. Different buildings are included in this TSB, such as offices, schools, healthcare centers, stores, warehouses, restaurants, hotels and buildings used for religious worship, culture and sports [60].

2.2.3 Energy consumption of MFH and TSB

In France in 2012, the residential-tertiary sector together was responsible for 18% of national GHG emissions. The average final energy consumption varies between the different buildings categories. The average consumption per square meter of SFH and MFH is similar, but in the tertiary sector, it strongly varies according to the developed activities [58].

In the MPEB project (in french *Mesure de la performance énergétique des bâtiments*), the energy consumption of the different building typologies was estimated, based on data from the French Ministry of the Ecological Transition from 2017 (table 2.1). In this estimation, TSB and MFH together represent more than half of the final energy consumed by the residential-tertiary sector.

Table 2.1 – Estimation of energy consumption per building typology in France. Adapted from [50].

Group	Typology	Number of units (M)	Total area (Mm ²)	Estimation of consumption (kWh/m ² /year)	Total final energy consumption (TWh)	Total
Residential buildings	SFH	16.2	1826	163	298	46%
	MFH (collective heating)	4.7	298		48	20%
	MFH (individual heating)	7.7	484	162.7	79	
Tertiary sector buildings	Offices		225	255	57	34%
	Hotel and restaurants		65	354	23	
	Commerce		212	236	50	
	Education		188	137	26	
	Community housing		70	190	13	
	Healthcare		115	236	27	
	Sport, leisure and culture		72	244	18	
	Transport		25	311	8	
Total			3580		647	

Even if the installation of efficient energy systems is necessary for reducing energy consumption in the residential and tertiary sectors, this measure alone is insufficient. Investing in thermally efficient building envelopes would decrease about 50% of energy consumption in these sectors [59]. In 2013 in France, 60% of the energy of residential buildings was used for space heating [61]. In figure 2.5, we can see that heating represent 43% of energy consumption in the French tertiary sector. Since heating accounts for an important part of final energy consumption in both groups, their building envelope thermal performance can have a significant impact on energy savings. Important policies on retrofitting existent buildings and reinforcing regulation for new constructions are necessary to reach the EU Commission objectives for 2030.

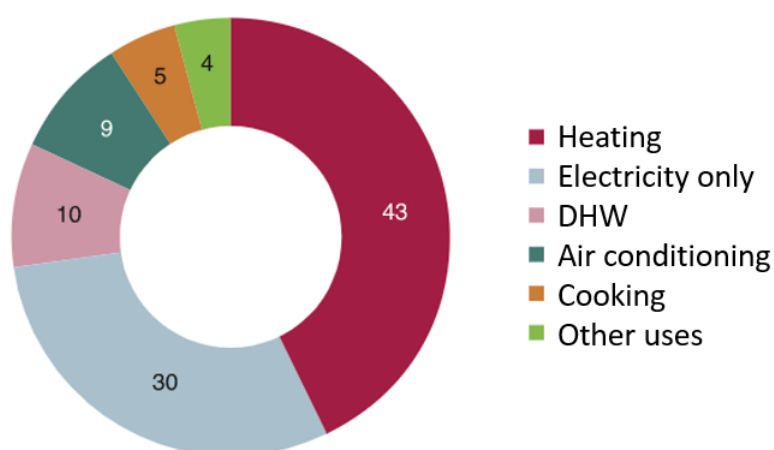


Figure 2.5 – Final energy consumption of the tertiary sector according to uses in France 2019 in % [62].

2.3 Chapter conclusion

MFH and TSB represent an expressive share of building stock and therefore of overall societal energy consumption. This reinforces the importance of assuring the intrinsic energy performance among those building typologies. The use of in-situ measurements to assess real BEP is a path for promoting and ensuring building quality. There are many available methods to verify BEP applied in different contexts, an overview of these methods are presented in the section 3.1 of the next chapter. As discussed before, occupants and systems play an important role on building total energy consumption. For avoiding these influences, some methods of BEP verification are concerned about the thermal performance of the building envelope that is only associated to the building intrinsic energy performance.

Among methods dealing with intrinsic energy performance, various protocols, mathematical principles and domains of applicability exist. Even though MFH and TSB present a relevant potential for energy savings, those methods relying on fast duration protocols have been mainly conceived for applying in single-family houses. One of the main challenges faced on large building typologies regards its dimensions and the consequent difficulties to apply a protocol in-situ. These difficulties can be partially overcome in methods relying on local equipment already installed in the building. However, most fast duration methods are conceived with an equipment kit, making difficult the task of instrumenting large buildings. In order to better understand the situation, the existent methods for assessing building envelope thermal performance with their applications and limitations in the context of MFH and TSB are presented in the next chapter.

Chapter 3

Building energy performance evaluation

Contents

3.1	A panorama on BEP evaluation	16
3.2	Basic concepts on BETPA	21
3.2.1	Analysis scale	21
3.2.2	Performance indicators	22
3.2.3	Heat balance in BETPA methods	24
3.2.4	Site conditions during protocol application	25
3.2.5	Inverse problems	28
3.3	Existent methods for BETPA	29
3.3.1	Averaging method	29
3.3.2	Linear regression	29
3.3.2.1	Co-heating	30
3.3.2.2	Energy Signature	31
3.3.3	Dynamic methods	33
3.3.3.1	ARX and ARMAX-modelling	33
3.3.3.2	State space model	33
3.4	Applications in the MFH and TSB context	42
3.4.1	Application of linear regression methods	42
3.4.2	Application of average method	44
3.4.3	Application of state space methods	45
3.4.4	Overview	45
3.5	Chapter conclusion	45

In this chapter we discuss about building energy performance characterization. Initially we show the big picture of approaches and contexts concerning real BEP. Then we delimit the meaning of envelope thermal performance, to get closer to the scope of this work, and the numerical indicators associated to it. After that, there is a literature review of existent in-situ methods, with more details on dynamic methods, since they were used as the basis for this work. Finally, we present some application in the context of multi-family housing and tertiary sector buildings to discuss their potentials and limits.

3.1 A panorama on BEP evaluation

Behind the concept of energy performance gap, there is the idea of assessing the real BEP. However, BEP is a broad subject that can be considered under different perspectives, as highlighted in section 2.1. Various objectives can be implicated in this domain, such as, inform, recommend, predict, measure and verify BEP. Also, different methods and mathematical models can be applied to comply with these multiple goals. In this section, we intend to present a panorama concerning contexts involving real BEP assessment and their methods.

As previously mentioned in section 2.1, EU Member States are encouraged to develop a national methodology to their Energy Performance Certificate. It is used to rate dwellings according to their energy consumption and greenhouse gas emissions, giving an understandable grade for energy efficiency from A to G [63]. The level A is associated to very energy efficient buildings, while G is associated to the worst level of efficiency. It is a very popular BEP communication, since EU Commission required them to be included in advertisements when announcing the sale or renovation of a building and it can have impacts on the property market value [64, 65]. The objective of Energy Performance Certificates is mainly informative, to help the stakeholders to make better decisions regarding building energy efficiency. Overall, simplified input parameters are combined in a mathematical model to give a BEP diagnostic. To do so, large amount of descriptive data are collected, such as building type, date of construction, presence of mechanical ventilation, type and year of heating system, U-value from walls and windows, construction type (heavy, medium, light) and others. With exception of energy bills, that can be used in some cases in the process, this methodology is not based on time-series analysis of measurement data describing building energy behavior.

It remains one of the largest database on BEP in Europe, supporting research and governmental policies in the domain [66]. However, it is debatable whether it has the capacity to accurately predict real BEP. A comprehensive study developed in Switzerland, over more more

than 1000 retrofitted buildings, found out that the input parameters of their national Energy Performance Certificates are poor predictors of building final energy consumption [67]. Another study in UK verified that simplifications in the method input data overestimates up to 70 % the buildings potential primary energy savings [68]. A study in France found that modelling simplifications regarding the heating data can overestimate energy savings up to 40 % [69]. This tool communicates in a simple way BEP for general population, that does not necessarily have technical knowledge of the domain. Even if it is an important measure to incentive BEP, complementary methods might be needed for more accurate information about BEP [70].

Going further than the informative goals of Energy Performance Certificates, there are the energy audits, that provide a complete assessment of building energy consumption characteristics. The objective is to detect the sources of energy waste, to evaluate the corrective measures to be adopted [71, 72]. It is thus suitable to be applied before retrofitting a building to establish a quantified and argued proposal of energy saving programs, and in some cases, it can facilitate access to governmental incentives. This analysis takes into account the five following building uses: heating, domestic hot water, cooling, lighting and ventilation. The HVAC systems are verified, as well as the building envelope thermal insulation quality. It establishes precise scenarios, considering the number of occupants and their behavior. However, a level of simplification is needed, since monitoring devices are expensive and can bring discomfort to occupants [73]. Part of power load is considered through estimations and some building characteristics are inferred [74], which can increase the results uncertainties.

Another common mechanism used to support BEP is the Energy Performance Contracts. They present common tools and methods with energy audits, such as baseline models, however they differ in their objectives. The first aims to propose solutions, whereas the second aims to ensure that the solutions implemented have the expected results [75]. A long term monitoring of building energy behavior during occupancy stage is done to verify if it is in line with the objectives fixed in the design phase [76, 77]. Energy Performance Contracts are contractual obligations between a beneficiary and an energy service provider, with established budgets regarding an agreed level of energy performance [78]. Measurement and Verification (M&V) protocols are often used in this context, that is the process of planning, measuring, collecting and analyzing data for the purpose of verifying and reporting savings following the implementation of an energy performance improvement action [79]. It allows to understand the building's overall energy use, track energy savings attributed to new projects, or detect equipment and/or system issues that can have an impact on energy consumption [80]. It has been noted in many cases that contract failure can happen before its ending, due to difficulties related to the team working in the analysis, the lack of investment and maintenance over time [81].

Those contexts take into account energy consumption due to the 4 main factors, previously mentioned in section 2.1: weather, occupants, systems and building envelope. Although, to facilitate taking appropriate measures to improve BEP, it might be interesting to verify those factors separately. On this basis, we can mention important fields regarding real BEP, such as: occupancy estimation and detection (OED), model predictive control (MPC), system fault detection and diagnosis (FDD) and building envelope thermal performance assessment (BETPA). The first mentioned fields are subjects of extensive research, that are not detailed here, as they are out of the scope of this work. The building envelope thermal performance, also considered as intrinsic BEP, depends only on building physical characteristics and has a strong influence on building final energy consumption. A multitude of methods are proposed for BETPA, varying on their level of maturity, mathematical model and protocols. This field of BEP is the main concern of this research, for this reason, an overview of existent methods for assessing thermal performance of building envelope is further detailed in section 3.3.

Those mentioned above are the primary contexts where real BEP is addressed, which does not exclude the importance of other applications and research work on the domain. Remaining on the large picture of the subject, we present the main families of methods and models used in this broad field of BEP to situate better our approach. Since there are intersections among them and multiple viewpoints, often different terminologies can be used to describe a similar style of methodology.

Inside BEP domain and beyond, methodologies can be classified by their modeling principles as black-box, white-box and grey-box [82]. In the black box modeling input and outputs are known, but the relations between them are unknown. They are purely statistical and require a low level of information on building [83]. For this reason, it can be hard to give them a physical meaning, which might be important in some applications. White-box models demand a high level of knowledge of building physics, with detailed and large amount of input data. The relations between inputs and outputs are described with a predictable internal functioning [84]. A grey-box model, is a mix of both mentioned above, where there is partial knowledge of the system. The model is composed by a controlled and analytical part and other parts that needs the use of numerical optimization algorithms and statistical methods. BEP incomplete and uncertain data can often be a challenge, grey-box models can be an useful tool for different applications, namely BETPA, MPC, building load estimation, and building-grid integration and district scale energy modeling [85, 86, 87]. Resistor-capacitors thermal networks are a common example of gray-box models, which is further described in subsection 3.3.3.2.

The classification above gives base to understand the different methodologies on assessing BEP. We could then mention in the next paragraphs, the four main categories of methods existent

to approach the problem (table 3.1), even though intersections among them can exist.

The engineering methods use data describing building components, systems interrelated by heat transfer and thermodynamic equations to evaluate building performance [88]. The calculations are generally simpler than in other method, some does not take into account the dynamic processes in the building, but they can be applied to have indicators of building stock quality in order to take global measures. Examples of evaluation of BEP through engineering calculations are the Energy Performance Certificates and energy audits methodologies.

Simulations methods use computer based models to simulates the BEP under determined circumstances. They are as well called white-box models, since detailed information level about building physics is used in their dynamic calculations. These techniques are useful for modelling individual buildings, whether existing or at design stage of new buildings, when detailed information of building composition is available. However, disparities between modeled and actual energy performance can be significant, as discussed before in the section 2.1.1. In order to have reliable outputs that better represent building behavior, the dynamic thermal models of existing buildings can be calibrated. Although, to have precision and quality over all models inputs is a difficult task, since building is a complex system with a sheer number of parameters and BEP involves multiple phenomena. There is also no consensus on calibration techniques, since many options are available and, in some cases, the details of calibrated models are unrevealed [89]. Different sources of uncertainties can also lead to biases in the model, associated with measurements and the imperfect or incomplete knowledge of the building physics and environment [90]. A sensitivity analysis can be useful to identify the more influential parameters on BEP, which might be more carefully calibrated [91]. It has been found that model parameters dependent on occupancy behaviors, such as ventilation and temperature set-point, have an important impact on building energy consumption and should receive a special attention during calibration process [92], since they are highly correlated to total building energy consumption [93]. Software for dynamic building simulation is an important tool for the design of new buildings and the analysis of the existing ones. However, representing the actual BEP requires substantial effort to accurately measure the inputs and take into account all the sources of uncertainties.

Statistical methods are broad and go from simple averages and linear regressions, to more complex methods such as likelihood estimation, which estimates parameters of a probability distribution, given some observed data. These methods are largely applied in BEP context to predict the energy usage and energy index or to estimate parameters that explain thermal behavior of building and its elements and systems [94]. Most of methods used for BETPA are under this category. Their principles and mathematical models are further discussed in the

section 3.3.

Machine learning techniques are applied at different building life cycle stages. It can be applied to the prediction of building heat and energy load of already occupied buildings [95, 96, 97], to FDD [98, 99, 100], OED [101, 102, 103], or MPC [104, 105]. There are fewer applications to forecast energy consumption on early stages of design [106] and for quantification of thermal performance [15]. Their main drawbacks are the need of big amounts of data and, being black box models, the difficulty to give physical meaning for their findings. The quality of their outputs is strongly based on statistical procedures, as hypothesis testing, cross validation, and others [107].

Statistical methods and machine learning techniques fit in a larger category of data-driven methods, that includes as well Bayesian methods [108]. The methods of this category use data describing past states, to define a model to achieve a desired output, which accuracy depends on quality and richness of input data and modelling choices. They can be considered as grey-box or black-box models according to the model parameters physical significance [108].

It should be noted that even if these classifications help to have an overview on BEP assessment, their limits are not rigid and many methods have overlap with the use of hybrid models. In the following section, we enter more specifically in applications concerning this work. Some basic concepts in BETPA and the existent methods applied to it are detailed.

Table 3.1 – Comparison of main building energy performance evaluation methodologies [109]

Method	Inputs needed	Applications	Restrictions
Engineering calculations	Simplified building information	Design. End-use evaluations. Highly flexible.	Limited accuracy.
Simulation	Detailed building information	Design. Compliance. Complex buildings. Cases where high accuracy is necessary.	Dependent on user skill and significant data collection.
Statistical	Dataset of existing buildings	Benchmarking systems. Simple evaluations.	Dependent on statistical data. Limited accuracy.
Machine Learning	Large dataset	Buildings with highly detailed data collection. Complex problems with many parameters.	Models construction is complicated. Do not consider direct physical characteristics.

3.2 Basic concepts on BETPA

Before describing the specific methods that are used to building envelope thermal performance assessment (BETPA), it is important to delimit the concept of BEP (such as which elements are included in the analysis and the building conditions) and to define an indicator to represent it. The following subsections bring elements to clarify those aspects and to specify how BEP is addressed in this work.

3.2.1 Analysis scale

In the evaluation of thermal performance of a building, it is important to define the scale of the analysis: the building components, the building envelope or the whole building energy characterization [110]. Figure 3.1 illustrates the scale of characterization. The more we upscale in the analysis the more the level of complexity increases, with more parameters and thermal phenomena to be taken into account. In the up-scaling process, parameter agglomeration and simplifications are often made to enable the analysis. For instance, if the analysis is in the scale of a building component, such as a wall, physical information about each one of its layers might be valuable. However, if the characterization concerns the whole building envelope, this level of information might be simplified and agglomerated in a parameter representing the thermal behavior of one of a group of walls.

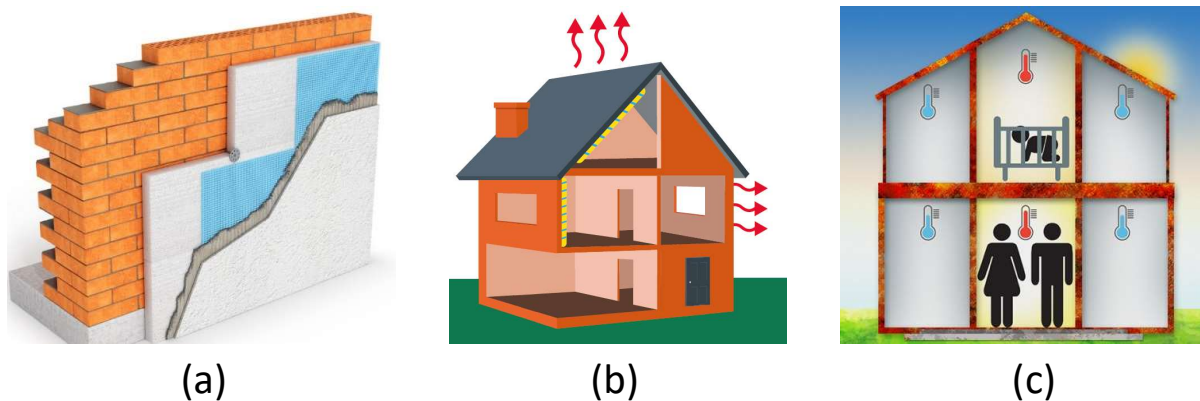


Figure 3.1 – Scale of BEP characterization: (a) building component, (b) building envelope, (c) whole building energy characterization

The characterization of building components is commonly done under laboratory conditions, with the test of samples, but in-situ techniques have started to gain attention in the past years [111]. Among them, we can mention the active methods [112] and the heat flux measurements [113, 114, 115].

With exception of extraordinary facilities, such as the Energy House from Salford University [116], the whole building envelope characterization can not be accomplished under laboratory

conditions. One difficulty of in-situ protocols resides in dealing with non steady state conditions. On the scale of this analysis, the performance of the building envelope alone is considered, however the test protocols can be realised with or without the presence of occupants and the utilisation of systems. In case those are included, modeling techniques might be used to separate (or neglect) the effects of each factor on the BETPA. Some protocols impose the application only on empty buildings, so then the test conditions can be better controlled. The advantage of this last option is the simplification of modelling, since the thermal phenomena related to other sources that exchanges through building envelope can be stopped or minimised. Nevertheless, a drawback of this option is the interference in the normal building use, turning them into invasive approaches. Invasive methods are often more suitable to be applied just after construction or important retrofit actions, while buildings are not yet occupied. However, this type of protocol should last as short as possible due to the vacancy cost [117]. These protocols are less convenient to be applied during the buildings' operation phase, because they disturb its occupancy.

When coming to the whole building energy characterization, occupancy and HVAC and local energy generation systems are also included in the analysis. However, as discussed in the former section, these estimations do not represent intrinsic thermal performance of the building, but strongly depend on the occupants behaviors and systems.

In this work, we focus on the factors related to building energy performance, concerning its physical characteristics, not its situation. We limit the analysis scale on the level of whole building envelope characterization. For this reason, most of methods presented in the section 3.3 are related to BETPA.

3.2.2 Performance indicators

It is important to have ways to assess and represent the energy performance numerically. The appropriate indicator to be used will depend on the scale of analysis. Building envelope is a combination of multiple building elements, and if we want to represent it as the set of those, we could represent their performance one by one. In this case, the U-value of the windows and walls could be characterized. It would also be possible to verify in a qualitative way the presence of thermal bridges and imperfections on the wall with the use of infrared thermography [118, 119]. Different numerical indicators are related to building envelope thermal performance. In this work we are mostly concerned about the stationary characteristics of building envelope. The main indicators related to this objective can be seen on table 3.2.

Air tightness is another important parameter of BETPA, since infiltration is a source of thermal losses through the building envelope. Infiltration is the unintentional air flow through the building envelope, which is different from ventilation that is a deliberate circulation of

air between indoor and outdoor environment. The blower door test is commonly used to characterize infiltration under various wind and leakage scenarios [120]. The main parameters related to these phenomena can be seen on table 3.2.

Table 3.2 – Different indicators concerning building envelope. Adapted from [121, 122].

Object	Indicator [unit]	Description
Windows	U_g [W/(m ² /K)]	Thermal transmittance of the glazing
Walls	R_c [m ² .K/W]	Thermal resistance of a homogeneous wall
	U_w [W/(m ² .K)]	Thermal transmittance of a homogeneous wall
Infiltration	Q_{4Pa} [m ³ /(h.m ²)]	Air permeability at 4 Pa
	q_4 [m ³ /h]	Air leakage rate at 4 Pa
	C [m ³ /(h.Pa)]	Air leakage coefficient
	n [-]	Air flow exponent
Building	HTC [W/K]	Heat transfer coefficient of building envelope (only transmission)
	U_b [W/(m ² .K)]	Surface heat transfer coefficient of building envelope (only transmission)
	HLC [W/K]	Heat loss coefficient of building envelope (transmission + air infiltration losses)
	BLC [W/K]	Heat loss coefficient of the whole building (transmission + infiltration + ventilation losses)

The performance indicators in building level are related to different extent of thermal phenomena. If only the thermal losses by transmission through building envelope are analysed, is the indicator to be used. It can be divided by the envelope surface in order to be more easily comparable among buildings of different sizes, what gives the U_b indicator. In case the infiltrations are also included in the analysis, HLC might be used. The HLC quantifies the amount of energy needed in steady state to maintain a temperature difference of one degree between the inside and the outside [123]. When the analysis scale is focused on building envelope, the main two indicators used to represent its energy performance are HLC and HTC, the second does not take into account the losses by air infiltration through the envelope (H_{inf}). Their mathematical formulas are represented from equation 3.1 to 3.3. Even though they can be mathematically calculated, it is hard to assure that the values of its parameters in a real building are conforming with the project, which was the object of the discussion in the section 2.1.1.

$$HLC = HTC + H_{inf} \quad (3.1)$$

$$HTC = \sum_{i=1}^p \psi_i \times L_i + \sum_{j=1}^q \chi_j + \sum_{k=1}^r U_{w_k} \times A_{w_k} \quad (3.2)$$

where:

- ψ_i is the heat flow of a linear thermal bridge i (W/m.K);
- L_i is length of a linear thermal bridge i (m);
- χ_j is the heat flow from a point thermal bridge j (W/K);
- U_{w_k} is the thermal transmittance of an exterior homogeneous wall k (W/(m².K));
- A_{w_k} is the area of an exterior homogeneous wall k (m²).

$$H_{inf} = \rho_{air} \times c_{air} \times Q_{inf} \quad (3.3)$$

where:

- ρ_{air} is the air density (kg/m³);
- c_{air} is the specific heat capacity (J/(kg.K));
- Q_{inf} is the infiltration rate (m³/s).

The HTC and H_{inf} , and logically HLC, are uncorrelated from effects deriving from HVAC system and occupants behavior, so then they characterize the building intrinsic energy performance. They are useful indicators in the building design and to rate its envelope quality, being largely used in the domain of BETPA [124, 125, 126, 127]. The minimum level of thermal phenomena taking place during an in-situ BETPA test is associated to the HLC indicator, since infiltration losses are related to the undeliberate air circulation; hence, they cannot be avoided. In case the losses by mechanical ventilation are included in the analysis, what goes beyond intrinsic BEP, the BLC indicator might be used. In this larger scale, of whole building characterisation, other indicators related to energy use over a time span can also be applied, but they are out of the scope of BETPA.

3.2.3 Heat balance in BETPA methods

Most of BETPA methods rely on the building single zone heat balance, that can be represented as in equation 3.4 [128]. Even though there is always a level of thermal dynamics happening to a building in real conditions, some hypotheses can be made to consider it as negligible, which are the so called quasi-steady state conditions. In this case ϕ_{inf} and ϕ_{tr} can be integrated in the losses through envelope characterized by the HLC and the interior and exterior temperature (T_e), as can be seen in equation 3.5.

$$C \times \frac{\partial T}{\partial t} = \phi_h + \phi_{int} + \phi_{sol} + \phi_v + \phi_{inf} + \phi_{tr} \quad (3.4)$$

where:

- T is the average indoor temperature of the zone (K);
- C is the effective heat capacity of the zone thermal mass (J/K);
- ϕ_h is the heat flow from heating systems (W);
- ϕ_{int} is the internal heat gains (W);
- ϕ_{sol} is the solar gains (W);
- ϕ_v is the heat exchange due to ventilation (W);
- ϕ_{inf} is the heat exchange due to infiltration through the building envelope (W);
- ϕ_{tr} is the heat flow due to transmission through the building envelope (W).

$$HLC \times (T_i - T_e) = \phi_h + \phi_{int} + \phi_{sol} + \phi_v \quad (3.5)$$

Equation 3.4 and 3.5 allow to separate two main families on BETPA methods, the first group considers the thermal dynamic behaviour of building thermal mass, while the second relies their method on a steady state hypothesis. For neglecting the dynamic term, one should say that during a specific time span the total heat absorbed and released by the building thermal mass are equal. This hypothesis can be defended by the use of enough long time steps associated to a cyclic period. This is typically longer than a day, so the effects of thermal dynamics on building envelope have a smaller importance regarding the other heat flows. On one hand, this hypothesis simplifies the techniques used for modelling resolution, with the heat balance represented by a linear equation. On the other hand, it implies in longer protocols for acquiring enough data points to characterize the envelope performance.

In opposition, dynamic methods take into consideration the variation of indoor temperature due to the energy stocked and released by the building thermal mass. This liberate the constraint of using long time steps for data measurements and aggregation, which is an advantage for having shorter test protocols. However, in this case, the heat balance equation is an ordinary differential equation, implying in more complex resolution algorithms for the HLC estimation.

3.2.4 Site conditions during protocol application

Another important aspect to be considered when applying a BETPA method is the presence of occupants during the test. Occupants behavior results in a series of thermal phenomena in the buildings. It is thus related to how each other term, non intrinsic to the building, in the heat

balance equation should be taken into account. This aspect splits again BETPA methods into two groups: those applicable to occupied buildings and those requiring a vacant building for its protocol application, also called invasive methods.

The first group allows more freedom in the protocol choices, since occupants thermal comfort and routine is not a matter of concern. Based on this, many thermal flow that are associated to a building in usage can be minimised or nullified. It allows then the use of simpler models comparing to tests done in occupied buildings. However, whilst the use of vacant buildings presents modelling advantages, it impacts the building normal usage and can restrain the protocol application in many situations. This subject was already investigated in the framework of the IEA Annex 58 [13], and is more mature compared to the application of BETPA methods in occupied buildings.

The second group brings the advantage of being a non invasive test, with little disturbance to building normal usage. Nevertheless, as mentioned before in chapter 2, occupant behavior is a major factor on building energy consumption. Estimating and predicting occupancy is not an easy task and is the subject of extent research in the building energy domain. The main challenge is that occupants can choose their behavior at each time, which is an extra difficult in the modelling process . Each one of their choices can impact building energy consumption and can lead to different local thermal phenomena. Predicting and modelling it, is thus associated to the need of voluminous data measurements.

Deepen the knowledge on the thermal phenomena happening in the building during a test protocol application helps to get the big picture of how occupancy relates to BETPA methods. Equation 3.6 to 3.9 presents the mathematical expressions of the parameters from equation 3.4, which are not related to intrinsic BEP [128]. Based on this, we can reflect about the extension of occupants influence a building thermal balance.

$$\phi_h = \phi_{h,sys} \times \eta_{h,sys} \quad (3.6)$$

$$\phi_{int} = \phi_{int,Occ} + \phi_{int,Ap\&Li} + \phi_{int,Wat} + \phi_{int,rec} \quad (3.7)$$

$$\phi_{sol} = \sum_{i=1}^n g_i \times A_i \times I_{sol,i} \quad (3.8)$$

$$\phi_{v,t} = \rho_{air} \times c_{air} \times \sum_{p=1}^r Q_{v,p} \times b_{v,p} \times (T_{ext} - T_i) \quad (3.9)$$

where:

- $\phi_{h,sys}$ is the power of the heating system (W);
- $\eta_{h,sys}$ is the overall system efficiency (–);
- $\phi_{int,Occ}$ is the heat flow from occupants (W);
- $\phi_{int,Ap\&Li}$ is the heat flow from appliances and lighting (W);
- $\phi_{int,Wat}$ is the heat flow related to hot water and sewage (W);
- $\phi_{int,rec}$ is the recoverable losses related to HVAC systems (W);
- g_i is the g-value of a transparent envelope element i (–);
- A_i is the effective area of a transparent envelope element i (m^2);
- $I_{sol,i}$ is the direct and diffuse solar irradiance (W/m^2);
- $Q_{v,p}$ is the ventilation flow rates (m^3/s);
- $b_{v,p}$ is a ratio to adjust external air temperature in case it is previously treated (–).

Occupants can choose to heat or not the building and regulate its temperatures, affecting then the heat flow due to the heating system (equation 3.6). The occupants interfere in all elements of equation 3.7, for instance, by the heat released directly from their bodies and by using appliances, lightning and DHW in the building. Occupants might choose on the state of the shutters and curtains, affecting the solar gains (equation 3.8). They can choose as well about the opening of windows and doors in the building and sometimes on the mechanical ventilation system, directly affecting air flow rate in equation 3.9. Therefore, performing BETPA methods in occupied buildings implies taking into account many thermal phenomena related to the situations mentioned above. For doing so, besides the need of more instrumentation for measuring the relevant parameters of these equations, it also requires accurate modelling for them. A study on how to take into account all these factors has been conducted in the framework of the recently concluded IEA Annex 71. Further information on the topic can be found in its respective reports [129].

Overall, a vacant building allows a larger choice on temperature scenarios and protocol conditions. This favor the control and annulment of thermal flows related to occupancy and HVAC systems and the minimisation of solar gains. Consequently, the experimental data expresses fewer thermal phenomena and simpler models can be hence applied to describe the building thermal behavior. Simpler models present advantages in comparison with more complex ones, such as the need of less input data, minimizing measurement errors and having fewer variables and casual relationships [130, 131]. In addition, in an occupied building, it is harder to defend the hypothesis of a homogeneous zone temperature [128], since the choices of occupant affects all thermal phenomena happening during the test. The invasive methods

had also been more broadly studied and are a step further in maturity concerning real cases application. For all these reasons, even though the use of invasive methods has consequences on buildings normal usage, they have often been the option of many BETPA methods.

3.2.5 Inverse problems

Most modelling applications are stated in two categories: the forward and the inverse problems. The first ones predict outputs based on model parameters and input data. In the second group, part of model parameters are unknown and might be determined from physical models, input and output data. The unknown parameters are estimated from comparison between model outputs with experimental data [132]. A representation on the these two categories of problems is shown on figure 3.2, where M represents a model and θ the vector of its parameters.

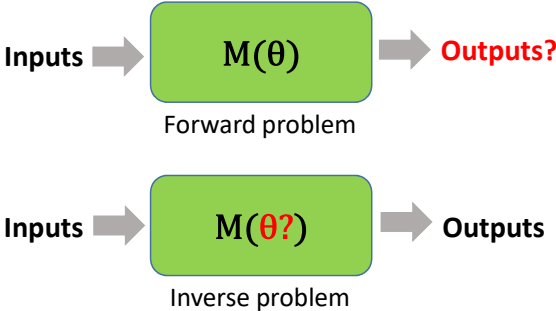


Figure 3.2 – What is investigated in forward and inverse problems

In the case of inverse problems, the physical phenomena should be initially modeled, describing how the parameters of the model translate into experimentally observable effects. Then the phenomena takes place in reality and the approach consists in tuning the parameters to approximate the model outputs to the experimental data [133]. Overall, it consists in training models through measurements. In BETPA, it can be applied to find representative parameters from building thermics through indirect measurements.

Even though inverse problems are widely used in the engineering domain, it can be challenging to assure that they are well posed. First of all, a well posed problem presents an existent solution. This solution should then be unique and its behaviour should change with the variation of the initial conditions. In case of ill-posed problems, the experimental observations are not sufficient to well estimate all model parameters, and the model can approach the observations while deviating from the real parameters. In some cases, multiple combinations of parameters can come to a similar solution. It is therefore necessary to add constraints or priors to reduce the space of possibilities in order to reach a unique solution [134]. The identifiability

of the model to a determined measurement data could be verified in order to assure that it is possible to estimate the parameters within a finite confidence interval [135]. Finally, models should be validated with techniques based on their parameters estimates, on their outputs and residuals and using different datasets than the one used for model training [135].

The methods presented in the following section are stated as inverse problems, aiming to learn physical properties of the building, such as heat loss coefficient and heat transfer coefficient, based on indirect measured data during the experiment.

3.3 Existent methods for BETPA

There are currently different methodologies, with capabilities and limitations, to address BETPA. We can divide those with physically representative parameters, in three main families: averaging method, linear regression and state space models [136]. The following subsections elucidate aspects on those methodologies families.

3.3.1 Averaging method

This method consists in averaging the heat flow and the difference between inner and outer temperature during a time span. It has been often applied for wall characterization, but it can be also applied to BETPA. Equation 3.10 is used for the HLC calculation in this method [137].

$$HLC = \frac{\sum Q}{\sum \Delta T} = \frac{\sum_{t_k=1}^n Q_{t_k}}{\sum_{t_k=1}^n (T_{i,t_k} - T_{e,t_k})} \quad (3.10)$$

Where Q is the power (W), T are temperatures (K) and n is the number of measured points. It is indicated for winter conditions and for situations without wide variation in external temperatures, since building dynamic thermal properties is not taken into account [137]. This method is then appropriated for quasi steady state conditions and when solar gains can be negligible [138]. Although, an improved average method has been proposed, where solar and internal gains can be estimated and included in the calculations [139, 140]. The integration period is an important criteria, for assuring the hypothesis of neglecting some of the building heat dynamics phenomena [141].

3.3.2 Linear regression

The approach using linear regression is also appropriated to determine stationary thermal properties. The period of testing is divided in shorter intervals in which the temperatures and

the heat flux are measured. Then, these values are plotted in a chart of temperature versus heat and a linear regression determined. The inclination of the line is representative of the heat loss coefficient. Equation 3.11 shows the mathematical representation of this approach.

$$Q_{t_k} = HLC \times (T_{i,t_k} - T_{e,t_k}) + \varepsilon_{t_k} \quad (3.11)$$

Where ε_{t_k} is the error between the measured and modeled heat input. The disadvantage of this approach is that it evaluates only stationary properties and does not bring more information about the dwelling dynamic behavior [137].

3.3.2.1 Co-heating

An example of method based on linear regression is the co-heating test. It consists in maintaining the internal temperature constant (typically 25 °C) in an unoccupied dwelling during a period of one to three weeks and measuring the amount of energy dispensed [142]. Different equipment are required to perform this test in a dwelling, including: temperature and relative humidity sensors, electrical fan heaters, air circulation, thermostatic controller, energy meters, and data-logger. Besides this, the installation of other items can be required to measure weather data such as a weather station, a pyranometer and a data-logger. This test is used to compare the as-built measured and the designed heat loss [143], being associated to the intrinsic BEP.

A linear regression of the daily heat input versus the difference between indoor and outdoor temperatures is applied [143]. For more precision, the daily averaged solar inputs can be added to the electrical heaters energy data to better represent the daily heat inputs [144]. The HLC is calculated by the inclination of the fitted line. Figure 3.3 shows the fitting of a co-heating test data, and the energy performance gap in the studied building.

This method is well stabilised in the domain of BETPA, been already widely applied in-situ. It is often used in research to give a HLC reference value, in order to promote comparison between other BETPA methods [125, 14]. However, the method is based on daily averaged data, what implies either in few measurement data points or long protocol duration [146]. It is recommended to have at least one week of measurements for assuring the test quality. As previously discussed in subsection 3.2.4, to limit vacancy costs, invasive methods should last the shortest the possible. For this reason, if time is a constraint on test application, other methods might be considered.

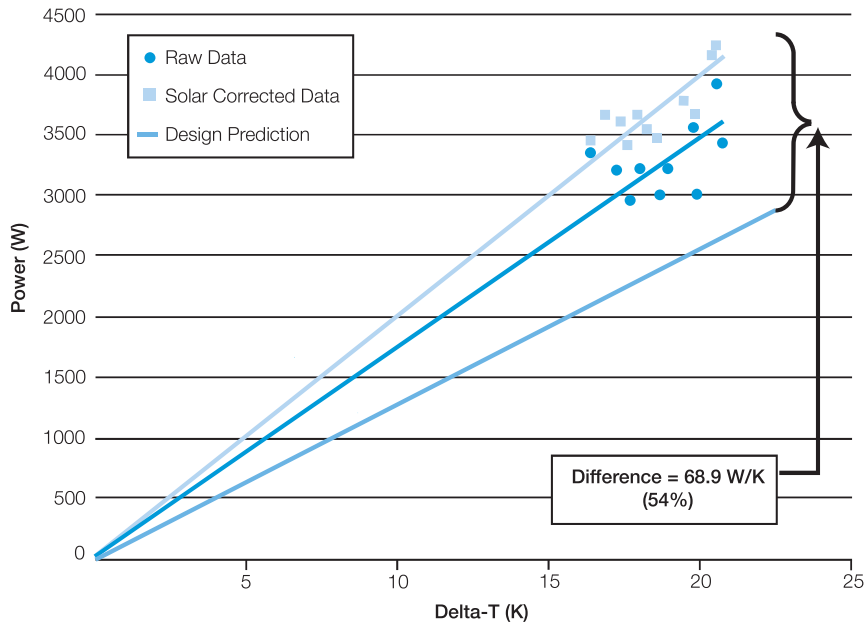


Figure 3.3 – Example of co-heating data – power versus internal and external temperature difference (Delta-T) [145]

3.3.2.2 Energy Signature

Another method broadly used is the Energy Signature. It can be used for buildings in occupation and it is typically a long-term method. There are variations of this method regarding the length of the period of averaging data, the amount and type of collected data.

A variation used to analyze heating consumption in the absence of detailed measurements of thermal magnitudes of the buildings was described by Zayane in 2011 [147]. In this variation, the data can be measured daily, weekly or monthly, and usually they include winter period. A simplification used is the substitution of the difference between indoor and outdoor temperature by just the external temperature, considering that the variations in internal temperatures can be negligible. The equation (3.12) shows the mathematical formula for describing this test.

$$Q = \alpha + \beta T_{ext} \quad (3.12)$$

The coefficients α and β are estimated by linear regression from a cloud of points corresponding to the data collected at the level of the building. Figure 3.4 illustrates an example of energy signature curve considering only the external temperature with a sub-period of one month. Another variation that intends to take into account the different climatic conditions replaces the measurement of external temperature by degree-days, allowing better comparison among buildings. This method, in all variations, has the advantage to demand relatively low detailed data and to be non-intrusive, however it takes a long time to be performed [147].

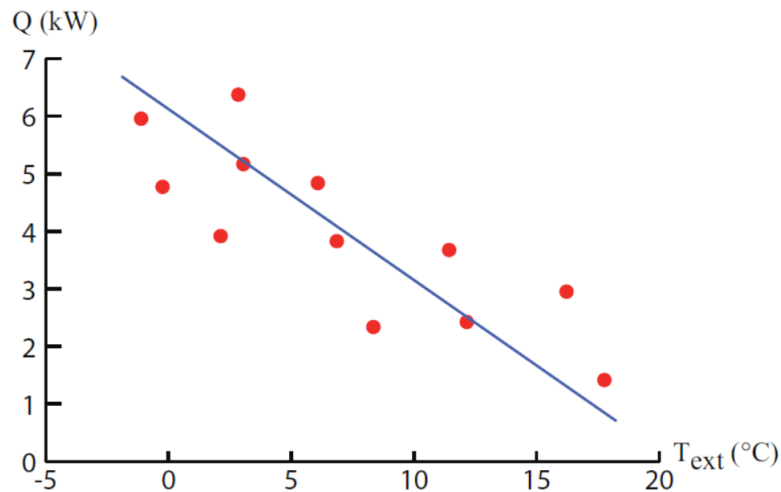


Figure 3.4 – Energy Signature curve according to the outside temperature [147]

A more detailed variant of Energy Signature considers the difference between internal and external temperatures in the temperature term using daily or weekly averages. The use of daily averages has shown realistic estimation of parameters. In addition, the heat term is decomposed in parts, as the power supplied for heating, the power gained with no cost and the power that is dynamically stored and released. If, for example, the heat is supplied by district heating, then the power supplied for heating would be the total amount of power input from the district heating system minus the one used for heating water and the one lost from the system. In the free power can be included the power gained from solar irradiance, from household electricity and the heat generated by occupants. The term relative to the dynamics of the building can be neglected for light construction materials, considering the time frame in daily or longer averages. The estimation of the HLC and U-value is more reliable for large differences between internal and external temperatures, and it is usually appropriated to estimate the parameters under cold conditions [148].

The main drawback from the Energy Signature method is the duration of analysis that goes from several months to years and it is usually done with low amount of measurements presenting then a high level of uncertainty [149]. The energy signature is commonly used in context of Measurement and Verification (M&V) and building management, but less to identify building envelope performance [121]. However, with the popularization of smart meters and thermostat loggers that record data regarding energy consumption and temperatures, this technique can become an interesting alternative for whole building characterization [150].

3.3.3 Dynamic methods

3.3.3.1 ARX and ARMAX-modelling

Differently from the methods above mentioned, these modelling techniques take into account the dynamics of the experimental data. ARX stands for Auto-Regression with eXtra inputs, meaning that the models present a correlation between the present output and its previous value, and the same for its inputs [14]. The ARMAX is a more complex case of ARX models, where a moving average (MA) model relates linearly the output dependant variable to the stochastic term in the model (noise) [151].

These are models of lagged dependent and independent variables and are suitable to be used in time series data. A variable having the possibility to explain the behavior of a dependant variable is also called covariate [152]. One disadvantage of this method is that the covariate coefficients can be hard to be interpreted [153]. It can be represented with the use of black-shift operators, that works as lag-operators in time series analysis [154].

These modelling techniques can be used to estimate building static properties from data of with in-situ methods [155]. In this case, the indoor temperature can be considered as a dependant variable and the heat flow in the building and the outdoor temperature as the covariates. Equation 3.13 shows an example of ARX model that could be applied to identify building thermal characteristics [14].

$$\varphi(B) \times T_{i;t} = \omega_h(B) \times (\phi_{h;t} + \phi_{int;t} + \phi_{sol;t} + \phi_{vent;t}) + \omega_e(B) \times T_{e;t} + \varepsilon_t \quad (3.13)$$

Where $\varphi(B)$, $\omega_h(B)$ and $\omega_e(B)$ are back shift operators and ε_t is the noise. It is possible to estimate the HLC by the stationary gain of the transfer function [14]. One advantage of this approach is the easiness to change the order of the polynomials describing the dynamics of the building [156]. The main drawback is related to the lack of physical interpretation of the covariates separately. In order to have a reliable model to represent the building thermal behavior, it should be carefully chosen inputs and outputs polynomials with appropriated order leading to irrelevant autocorrelation and cross correlation of residuals [14].

3.3.3.2 State space model

State-space models, can be used for a simplified representation of the heat dynamics in a building and building components. “The concept of the state of a dynamic system refers to a minimum set of variables, known as State variables that fully describe the system and its response to any given set of inputs.” [157]. It consists in a mathematical model with inputs, outputs and state variables that are related by differential equations. The values of state variables evolve through time depending on the values they have at previous time and on the input

variables values. The model can be represented by a matrix notation if the functions are linear combinations of states and inputs. In this case, the state variables are expressed as vectors to simplify the comprehension of the inputs, outputs and states. The following equations represent a matrix system, where the first is the state equation and the second is the output equation. The matrix A and E contain just parameters, without any input variable nor state variable.

$$C \times T' = A \times T + E \times U \quad (3.14)$$

$$Y = J \times T + G \times U \quad (3.15)$$

where:

- T is the state vector;
- T' is the derivative of the state vector;
- U is a vector made of the driving forces;
- Y is the vector of the outputs;
- C is the diagonal matrix of the node capacities;
- A contains all exchange terms between the nodes;
- E contains the exchange terms between the nodes and the driving forces;
- J relates the outputs to the nodes;
- G relates the outputs to the driving forces.

The solution of the state space matrix system is presented in equations (3.16) to (3.21). Initially, the vector T of temperatures is separated into a dynamical and a steady state part, as in equation (3.16) [158].

$$T = T_0 - A^{-1} \times E \times U \quad (3.16)$$

Then, the matrix $C^{-1} \times A$ that multiplies the vector of dynamical temperatures T_0 is diagonalized, and the states are represented by the vector X , as in the equation (3.17).

$$T_0 = P \times X \quad (3.17)$$

where P is a matrix where each column is composed by the eigenvector of $C^{-1} \times A$, whose eigenvalue $-1/\tau$ is the corresponding diagonal element of F . Then, the diagonalized system is described as in equations (3.18) and (3.19).

$$X' = F \times X + B \times U' \quad (3.18)$$

$$Y = H \times X + S \times U \quad (3.19)$$

where:

$$B = P^{-1} \times A^{-1} \times E$$

$$H = J \times P$$

$$S = G - J \times A^{-1} \times E$$

This system solution, for one time step Δt , is presented in equations (3.20) and (3.21) [158]. The identification of the mathematical model from the system can be done from measuring its inputs and outputs.

$$X^{n+1} = \exp(F \times \Delta t) \times X^n + \exp(-\Delta t/\tau_i) \times B \times (U^{n+1} - U^n) \quad (3.20)$$

$$Y^{n+1} = H \times X^{n+1} + S \times U^{n+1} \quad (3.21)$$

RC thermal networks are used in state-space modelling applied to the identification of building thermal properties. They are simplified models often used to represent building physical properties and can as well be applied for modeling building systems [159, 160]. The RC classical electrical network find analogies in building thermics, as presented in table 3.3 [161].

Table 3.3 – Parallel between parameters from electrical and thermal RC networks

Electrical parameter	Thermal parameter
Voltage	Temperature
Current density	Flux density
Current	Power
Electric charge	Heat quantity
Electrical conductivity	Thermal conductivity
Electrical resistance	Thermal resistance
Electrical capacity	Thermal capacity

The amount of differential equations is equal to the amount of thermal capacities in the RC thermal network and it defines the model order. Each node of the network is represented by a temperature (state) that is measured for a determined duration. These models are often used to solve inverse problems, where the inputs are known and optimisation algorithms can be used to estimate some of the parameters components of the model.

The physical meaning attributed to the model parameters brings one first advantage of this approach: the possibility to convert them into building envelope thermal performance indicators. Although, in some cases the physical meaning behind some parameters should be carefully interpreted, such as for the thermal capacitance. The lumped capacitance representing the thermal mass of the building is not exactly correspondent to the combined thermal capacitance of all building components. It depends as well on the experimental conditions and which parts

of the thermal mass had been thermally solicited during the test.

The combination of RC models and state space representation for solving an inverse problem is considered as a grey-box modelling. It presents much fewer parameters than when using RC thermal networks in white-box modelling, as in simulation softwares. This is another advantage of this approach, the use of relatively few parameters to describe a complex system as building thermal behavior.

In addition, differently from the methods in the first family, this approach takes into account the dynamic phenomena in the building. Since weather and indoor temperature conditions are constantly changing, we can not assume a building is in a steady state condition. However under low variation in those parameters, and with time steps long enough to neglect some dynamic behaviors, we could consider it under quasi-steady state conditions. Since RC thermal networks identify the dynamic behavior of the building, it is possible to apply shorter time steps in the data collection and agglomeration, what enables the use of a faster protocol for BETPA. This can be a special advantage when using invasive methods, in which the building might be unoccupied during test protocol. In contrast with the also dynamic ARX/ARMAX-models, it presents the interest of having parameters that are often physically interpretable [162]. However, if there are identifiability problems, the physical meaning behind the parameter estimate can be uncertain. In order to avoid structural and practical non-identifiability, the model should not have parameter redundancy and the data should be of quality [163]. In the same time oversimplified models might not explain well the building dynamic behavior. Model selection procedures can be used to find a suitable RC model structure [164, 165].

The use of RC thermal models is internationally well established, with applications in both punctual research cases and developed protocols and methods. On one hand, punctual researches on the domain allowed to give the theoretical basis on gray-box modelling application, such as the work from Madsen, Bacher and others[162, 164, 166, 167]. On the other hand, complete methods with a developed protocol allowed to apply this approach on different real and modeled buildings. The next paragraphs are dedicated to present the methods with a developed protocol for BETPA using RC thermal networks, with a significant recognition in France and even in international community.

3.3.3.2.1 QUB

QUB (Quick U-value of Buildings) is a method developed by Saint-Gobain to identify the global heat transfer coefficient in a short period. The method protocol consists of a temperature stabilization in the studied area followed by a heating phase at the beginning of the evening and finally a free evolution phase. The last two phases must be performed during the night

without occupancy to avoid any additional power sources [168]. The electrical model used for this method consists of a single resistance and a single thermal capacity (RC)[169], presented in figure 3.5.

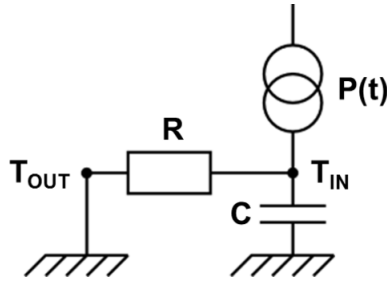


Figure 3.5 – RC thermal network model for QUB method [170]

Equation (3.22) presents the thermal balance of this model, where the solar radiation is not taken into account.

$$P = HLC(U^{n+1} - U^n) + C \frac{dT_{int}}{dt} \quad (3.22)$$

$$HLC = \frac{a_1 P_2 - a_2 P_1}{a_1 \times \Delta T_2 - a_2 \times \Delta T_1} \quad (3.23)$$

Although a RC model represents the thermal phenomena, the mathematical solution is based on linear regression. It is applicable under specific test conditions to guarantee its validity, such as the outside temperature should not present high variations during the experiment, specially in the cooling phase [171]. This method is not adapted for wide variations of external temperature, but it can be reproduced on a good part of the year [149]. An uncertainty up to 15% is attributed to HLC results, which is based on maximum deviation among repetitions of test application [170]. In spite of that, the uncertainty of input parameters is not propagated to the HLC estimate uncertainty.

3.3.3.2.2 EPILOG

EPILOG (Evaluation de la Performance Intrinsèque de LOGements) was developed by the research group ETB from ARMINES-Mines ParisTech in collaboration with INES (National Institute of Solar Energy) between 2016 and 2018. It was an initiative inside the project PACTE (Programme d'Action pour la qualité de la Construction et la Transition Énergétique) which aimed to develop tools to measure the intrinsic energy performance of buildings [172]. EPILOG method uses a state space representation of a RC thermal model to solve an inverse problem with an optimization algorithm. The purpose of the EPILOG method is to identify the global

heat loss coefficient (HLC) and the largest time constant using a short period measurement [48].

In this method, a constant heating power is applied in a building for two days followed by two days of free evolution. The indoor and outdoor temperatures are measured during these four days. In order to minimize the impact of solar gains and ventilation, the test is done with closed windows and shutters and with the ventilation system turned off.

EPILOG presents a flexibility regarding the dimension of the RC model, meaning that the amount of resistances and capacitances present in the model can change according to the boundary conditions, the geometry and composition of the building. In EPILOG work the following model dimensions were explored: 2R2C, 3R2C, 4R3C, 5R3C, 6R4C, 7R4C, 8R5C, 13R8C, 19R9C. The number of parameters to be searched depends on the dimension of the RC thermal model. There is one variable for each resistance and capacitance in the model. In addition, there are variables representing the initial temperature in the nodes of the model with exception of the initial internal temperature that is already known. The initial values attributed to the variables are random. Figure 3.6 shows one of the RC models from EPILOG method [173].

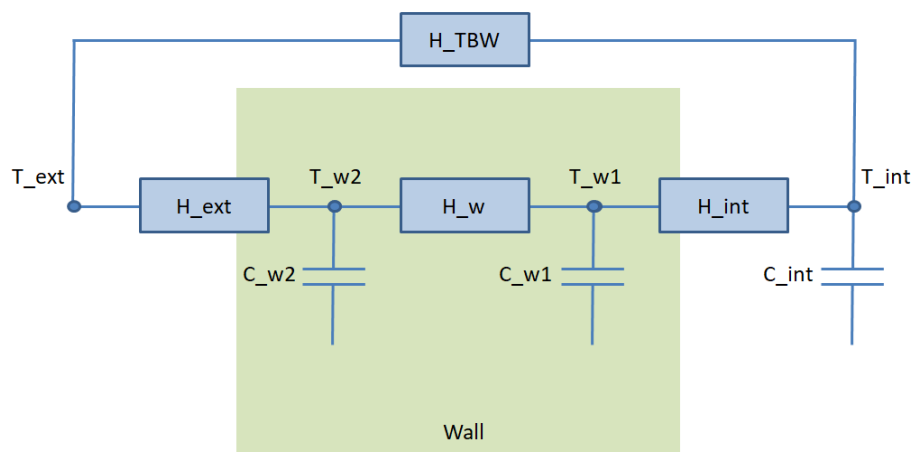


Figure 3.6 – Model 4R3C: one of EPILOG RC thermal network models

where:

- T_{int} is the temperature of the studied area (°C);
- T_{ext} is the outdoor temperature (°C);
- T_{w1} is the temperature of an internal node in the walls (°C);
- T_{w2} is the temperature of an external node in the walls (°C);
- C_{int} is the thermal capacity of the study area (Wh/K);
- C_{w1} is the thermal capacity of an internal node in the walls (Wh/K);
- C_{w2} is the thermal capacity of an external node in the walls (Wh/K);

- H_{int} is the heat transfer coefficient between the center of the walls and the studied area (W/K);
- H_w is the heat transfer coefficient between the wall nodes (W/K);
- H_{ext} is the heat transfer coefficient between the environment and the walls (W/K);
- H_{TBW} is the heat transfer coefficient related to thermal bridges and windows between the environment and the studied area (W/K).

The internal temperature is calculated based on the initial values of parameters according to the RC thermal model and the driving forces (heating power, external temperature and boundary temperature conditions). The Mean Quadratic Error between the vectors of the measured and calculated internal temperature is calculated. An optimization algorithm is used to minimize the Mean Quadratic Error varying the values of the parameters. The parameters corresponding to the optimal solution are used to calculate the global heating loss coefficient of the building and the principal time constant.

3.3.3.2.3 ISABELE

The development of the ISABELE (In Situ Assessment of Building Envelope performances) method by CSTB began during the first half of the 2010 decade. It was developed with the aim of characterizing the thermal performance of individual housing. The method, then known by the acronym EVAREPE (EVALuation à Receipt des Performances Energétiques), used an experimental protocol quite similar to that of today, heating the building and with a measurement of the injected powers as well as interior and exterior conditions. It allows the identification of the building envelope HTC with a test duration of 5 to 15 days [174].

Initially, the test protocol also presents a heating phase followed of a free evolution phase [175] but, differently from QUB, it presents a controlled temperature instead of constant power. Moreover, for buildings that require 2 or 3 days to achieve the steady state, a longer analysis period seems necessary to have an acceptable error.

For developing the test protocol a heating module must then be installed in each room, except in those which are not usually heated or small rooms. The modules are: a convector and a fan to heat, an air temperature sensor positioned at the most relevant location, an electricity meter to measure the consumption of all the elements of the module, a recording system that acquires the various module. These modules are illustrated in figure 3.7.

Initially the RC thermal model used in French Thermal Regulation (RT 2012) was used to represent building thermal behavior [175]. Figure 3.8 presents this model, with five thermal resistors and one capacitance. The resolution of the problem was done with the least squares minimization.



Figure 3.7 – a) ISABELE heating module, b) SENS sensors [176]

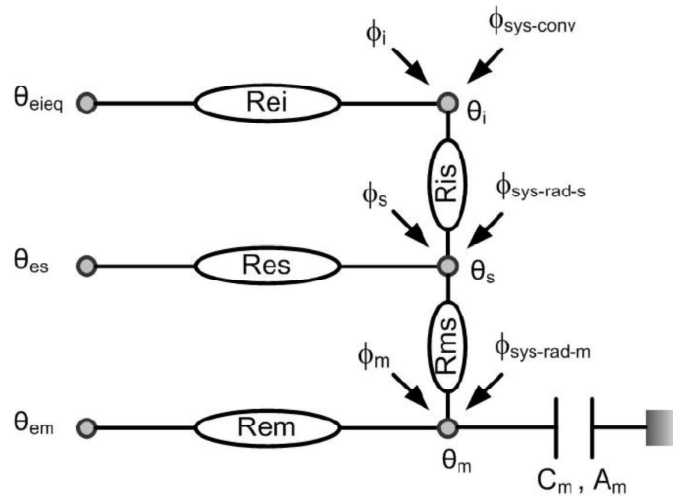


Figure 3.8 – RC thermal network model used initially in ISABELE method [175]

The initial method has significantly evolved and improved in performance. Some of these improvements are for such as: taking into account of the air infiltration rate [177], use of different thermal models and the automatic choice of one adapted to the building and a rigorous treatment of uncertainties, based on a Bayesian probabilistic approach [178, 122]. The resolution algorithm has been changed then to CTSM-R, used for fitting the RC model parameters. This framework provides the identification and estimation of gray-box models, based on maximum likelihood and Kalman filtering principles [179].

In total, a set of 20 RC network thermal models were available to represent different buildings. These models increases in complexity concerning the number of thermal capacities, from one to three. In all the models the output variable is the indoor air temperature (T_i). Some parameters commonly present in the models are: the outdoor temperature, the thermal resistance due to the air infiltration rate (R_{inf}), the interior convective and radiative thermal resistance (R_{is}) and the global equivalent outdoor temperatures for heavy and light walls (T_{em} and T_{es} , which are calculated from the data collected by the SENS sensors) [176].

ISABELE was first applied on test cells [122], and further it has been deployed on a large number of real cases during the PACTE program. Its reliability has thus been demonstrated in cases of new single-family homes for tests lasting around 4 days.

3.3.3.2.4 SEREINE

The SEREINE project (Solution d'Evaluation de la performance Energetique INtrinsèquE) aims to consolidate and develop knowledge about the methods of measuring the intrinsic energy performance of buildings. The project is a continuation of the PACTE program (Action Program for the Quality of Construction and Energy Transition) from which ISABELE and EPILOG were developed to new single-family houses. Since both methods are based on similar principles, SEREINE project aims to merge these two methods into one and adapt it to renovated buildings and also to collective housing.

In SEREINE, RC thermal models from ISABELE and EPILOG were added, opening the possibilities to new building configurations. One of RC thermal models is presented in figure 3.9, where the resistances R_{ms} and R_{em} associated with the inertia C_m represent the heavy walls. C_i is the inertia of the internal mass and R_{es} is the light walls thermal resistance.

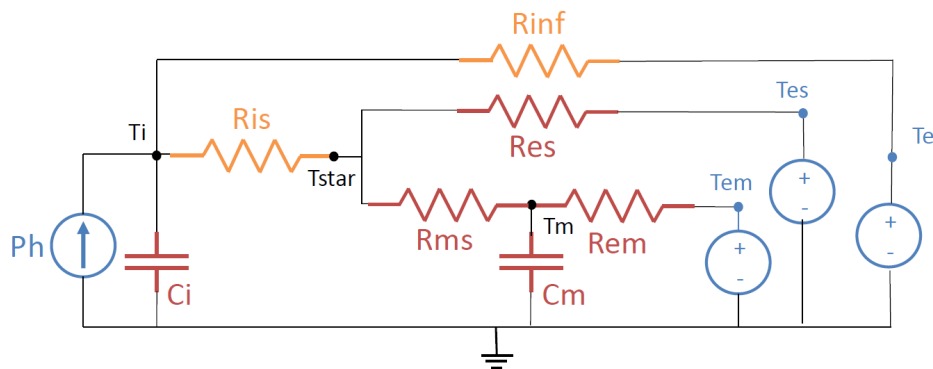


Figure 3.9 – Exemple of RC thermal network model from SEREINE method [176]

Later in the SEREINE method, the R_{is} was considered negligible. Then the node T_{star} , that represents the equivalent interior temperature (a combination of the air temperature and the average radiant temperature) was also neglected from the RC thermal network.

Another difference from ISABELE to SEREINE is the use of PySIP optimization algorithms, developed by the Savoie Mont Blanc University, instead of CTSM-R. SEREINE project is ongoing and the results of its development are being recently released.

3.4 Applications in the MFH and TSB context

Numerous methods based on state models are proposed for individual houses, but applications on larger buildings are rarer. Mainly steady state methods have been applied in MFH and TSB, such as the energy signature and EBBE methods. Some of BETPA applications for these buildings typologies found in the literature are presented in this section.

3.4.1 Application of linear regression methods

The Energy Signature method can be applied to MFH and TSB, however the estimation is dependent of occupants and systems in the building, so it is not just related to the intrinsic building thermal performance. The main drawback of the Energy Signature method is the duration of the analysis, which ranges from several months to several years.

In a study applying of energy signature method on TSB, it has been verified that the time step depends on the building usage pattern. Shorter time steps (daily) are allowed for buildings with continuous usage, as hospitals, but longer data collection might be used to TSB with discontinuity on occupation [180].

Another linear regression method is EBBE method (Energy Balance of the Building Envelope), that is applied for occupied buildings over a long period of time. It was developed in the late 2000s by the CETE, now CEREMA, as part of the PREBAT project, when it has been largely applied over France [181]. The protocol does not require to impose a heating power or a specific temperature set point. The test is preferably done during a heating season and the measurements last several weeks or months. During this time, measurements in hourly time steps should be made for: heat expended by the heating system, indoor and outdoor temperature, electrical consumption of the air extractors and global horizontal solar radiation [182]. The thermal model is based on the equation (3.24).

$$Q^{chauff} + Q^{app.int} + Q^{app.sol} + Q^{pert.ventil} + Q^{pert.perm} + HTC(T_{int} - T_{ext}) = 0 \quad (3.24)$$

where:

- Q^{chauff} is the heating output delivered in the heated zone to the building [W];
- $Q^{app.int}$ is the internal heat input of the building [W];
- $Q^{app.sol}$ is the solar input received in the building [W];
- $Q^{pert.ventil}$ is the losses related to the air renewal by ventilation [W];
- $Q^{pert.perm}$ is the losses related to the renewal of the air due to the airtightness defects of the building [W].

Another application in a large typology building was made with co-heating test, even though it is commonly applied to single-family homes. In a master thesis from 2015, adaptations were made to the co-heating protocol to apply it to a small tertiary sector building [183]. This was the case with a 200 m² community building located in Sweden. Due to its size, the amount of equipment required to perform a standard co-heating test would result in high costs. Therefore, the standard test was only carried out on part of the building. Unfortunately, in this case the measured power includes losses to the external environment, by infiltration and also to adjacent rooms. The average heat loss coefficient is calculated using the equation (3.25).

$$U_{m,meas,corr} = \frac{\dot{Q} - \dot{Q}_{inf} - \dot{Q}_{tr,is}}{A_{surf} \times \Delta T} \quad (3.25)$$

where:

- U_m is the average heat loss transfer ($W/(m^2 \cdot K)$);
- \dot{Q} is the measured power (W);
- \dot{Q}_{inf} are the losses by infiltration (W);
- $\dot{Q}_{tr,is}$ are the losses to the adjacent rooms (W);
- A_{surf} is the area connected to the heated interior (m^2);
- ΔT is the difference between the indoor and outdoor temperature.

The infiltration losses \dot{Q}_{inf} are calculated with the results of the blower door test, according to (3.26) and (3.27). $\dot{Q}_{tr,is}$ can be calculated with equation 3.28.

$$\dot{n} = \frac{\dot{n}_{50}}{20} \quad (3.26)$$

$$\dot{Q}_{inf} = \dot{n} \times \rho \times c_p \times \Delta T \quad (3.27)$$

where:

- \dot{n}_{50} is the air flow rate at 50 Pascal (m^3/s);
- \dot{n} is the air flow in (m^3/s);
- ρ is the air density in (kg/m^3);
- c_p is the specific heat capacity of the air in ($J/(kg \cdot K)$).

$$\dot{Q}_{tr,is} = \left(\sum K_{i,is} + \sum \Psi_{k,is} \times l_{k,is} + \sum \chi_{j,is} \right) \times \Delta T \quad (3.28)$$

where:

- $K_{i,is}$ is the conductance of each part of the building (W/K);
- Ψ_k is the conductance of a thermal bridge in the form of a line ($W/K/m$);

- l_k is the length of a linear thermal bridge (m);
- χ_j is the conductance of a point-shaped thermal bridge (W/K);
- ΔT is the difference between the indoor and outdoor temperature.

The entire building was also tested with the use of the local heating system, which was already equipped with a building level electricity and power meter. The building's radiators were mostly placed close to windows, which is not the configuration recommended by the standard test, which would be in the center of the rooms. Another variation from the standard test is the non-use of fans, for economic reasons.

The theoretical value of U_m , mean was calculated, according to ISO criteria. The values of thermal bridges are obtained from a simulation with the appropriate software. The results of the appropriate co-heating tests, applied to the entire building, give smaller deviations from the theoretical value than those applied only to a part of the building. Tests for the entire building gave results closer to the benchmark, so the study indicates that the protocol is more suitable for testing an entire building rather than part of a building.

3.4.2 Application of average method

An application of this method was made for a commercial building in Bilbao, Spain. The building had a complex geometry, with an irregular facade and had four floors. The building, built in 1970, has been renovated and tests have been carried out before and after the works. In this study, an *HLC* value is calculated for each floor of the building. These values are then added. It is considered that the heat exchange between interior walls is canceled in 3.29 [139].

$$HLC_{sum} = \sum_{i=1}^L \sum_{j=1}^M HLC_{F_{i,j}} \quad (3.29)$$

Internal inputs, such as appliances and occupants were not taken into account for this analysis. However, the test being carried out during the winter period, it is considered that these gains have relatively less weight with respect to the heating demand. The minimum measurement time used was 72h, as this period was shown to be sufficient during testing to have *HLC* stability of $\pm 10\%$ for the last 24h [141].

There is no benchmark for *HLC* values in this study. The co-heating method was not considered as a reference, due to the size of the building and also to the impossibility of leaving the building totally unoccupied during a winter month, since it is not a period vacation. However, several *HLC* measurements were performed on each stage and the results were consistent with each other. This method must be validated for buildings presenting an indicator reference.

3.4.3 Application of state space methods

Different from single-family homes, the question of the measurement perimeter arises for collective and tertiary buildings. The tests can be applied to the whole building or otherwise to a part of it, for example in an apartment. The QUB method was applied to a collective housing apartment from the 1960s located in the Stockholm region (Sweden). For the estimation of heat fluxes to the neighbors, the QUB / e method was used (explained in the next section). The HLC was estimated as for a QUB test and then corrected to take into account only heat losses to the external environment [184].

In the MERLiN project, the ISABELE method was applied for the entire collective building of 800 m² distributed over four floors on the ground floor [185]. The test lasted 13 days, during which each apartment was equipped with an ISABELE module. For heating, the existing system was used (collective gas heating). The heat input was measured by an ultrasonic calorimeter at the boiler. The test exhibited high uncertainties until the end of the measurement period, where the 95% confidence interval was 86% of the measured value (mainly due to a technical data reporting problem). Even with this extended range, the theoretical value calculated by the design office was found below the measured value.

3.4.4 Overview

A synthesis of the BETPA methods applied to MFH and TSB in the literature review are shown on the table 3.4. The short or very short-term measurement methods applied to MFH and TSB are proof of concept, while the long-term methods have a higher level of maturity regarding large buildings. Here, the methods are considered mature when they have been applied *in-situ* to more than five buildings. Notably, the energy signature have been applied to large typology buildings; however they are either very long-lasting or limited to winter period. Another concern is the treatment of results uncertainties, that are not considered in these methodologies. The state space approach has the advantage of presenting a short test duration and enabling the calculation of uncertainties on the estimated indicator. However, it has not yet been broadly tested in MFH and TSB and many adaptations need to be taken to be applicable to these typologies.

3.5 Chapter conclusion

It is important to measure the actual BEP to ensure quality and close the energy performance gap. A building is a complex system and the definition of its energy performance is a vast domain used for various applications. The strategy used to assess the real BEP depends on

Table 3.4 – Different methods for BETPA on the context of MFH and TSB

Method	Possibility of site occupation	Indicator [W/K]	Data time step	Total test duration	Usual building typology	Application on MFH and TSB	
						Literature review	Maturity level
ISABELE		HTC	1 h	2 to 4 days	SFH	Whole MFH	Proof of concept
QUB	Non	HLC	10 min	8h to 14h	SFH	Part of a MFH	Proof of concept
Co-Heating		HLC	1 day	One month	SFH	Whole and part of a TSB	Proof of concept
Energy signature		BLC	1 day to 1 month	One heating season	All	Whole TSB and MFH	Mature method
EBBE	Oui	HTC	1 week	One heating season	All	Whole TSB and MFH	Mature method
Average method		HLC	10 s to 5 min	About a week	All	Whole TSB	Proof of concept

the available information, the building conditions and which thermal phenomena might be described. Different methodologies are available to assess building energy performance, varying on their objectives and applicabilities.

In this work we are concerned about the building envelope thermal performance assessment (BETPA), for this reason the main existing methods to assess HLC and HTC indicators were presented. Inside the domain of BETPA there are methods with different mathematical approach, protocol and level of maturity. They can be adapted to the application in single-family housings (SFH) and/or multi-family housings (MFH) and tertiary sector buildings (TSB). Mainly steady state methods have been applied in large typology buildings, such as the energy signature and EBBE methods. As in in-situ conditions, building envelope is not under steady-state regime, these methods typically use long time steps to minimize the importance of the dynamic heat fluxes. Consequently, their total measurement duration are longer, ranging from several weeks to several years.

Some of the existent methods are categorized as invasive when they require vacant buildings for their application. The use of invasive methods can be considered when aiming BETPA, since a vacant building allows to get rid of extra complexities related to occupancy, HVAC systems and to minimise solar gains. Hence, with an experimental data expressing fewer thermal phenomena, simpler models can be applied to describe the building thermal performance. Simpler models present advantages in comparison with more complex ones, such as the need of less input data, having fewer variables and casual relationships and minimizing measurement errors [130] [131]. Another advantage of simpler models is related to inverse problem techniques. A more

complex model has more degrees of freedom and need to be more constrained to avoid ill-posed problems.

When the objective is to develop a protocol to be applied to different buildings, avoiding extra complexity can be an asset. A model that is more complex usually describes in details particularities of a specific building. However, these specificities are not always generalizable to other buildings. Modelling occupant behavior is already a challenge for a unique building and presently many efforts have been made in order to correctly predict it [186] [187] [188] [189]. Not surprisingly, it has been found that the occupancy patterns between seasons and weekdays varies significantly among different dwellings [190]. In addition, it has been found that the accuracy of the occupancy patterns based on onboard monitoring system in TSB can be accurate, but it is dependant on the level of occupancy [191]. Modelling building envelope performance considering occupants with distinct habits for different buildings and multiple contexts present an extra difficulty to BETPA in MFH and TSB. Many efforts have been made in the freshly finalised project Annex 71, "Building Energy Performance Assessment Based on In-situ Measurements", to clarify and unify the methods of BETPA on occupied buildings. However, it is necessary an extensive monitoring data in each building for achieving reliable results of HLC and the different hypothesis in the modelling process can increase the bias associated to this indicator. Although this initiative clarifies the perspectives of BETPA methods in occupied buildings, the studies have been conducted only in the SFH context.

Presently, there are no mature fast duration methods adapted to large building typologies, which presents a potential for developing new methods to answer this demand. Considering the extra complexities related to the size of MFH and TSB compared to SFH, it seems logical in a first step to avoid secondary thermal phenomena during test protocol. For this reason, in this work we choose to develop a protocol applicable to vacant buildings. However, invasive methods might be as fast as possible to limit vacancy costs. RC thermal network thermal models are strong candidates to develop a short measurement time method, since they take into account the thermal dynamic phenomena related to building thermal mass. They have the advantage of presenting physically interpretable parameters, in comparison with the also dynamic ARX/ARMAX models. Among the proposed methods using RC models, EPILOG and ISABELE methods present a flexibility regarding the model order and season of protocol application. SEREINE method is an evolution of both methods together presenting advantages of both of them. In addition, ISABELE and SEREINE methods present a methodology to estimate the uncertainties in the final BETPA indicator, increasing its reliability when correctly applied. Another important aspect was the facility to access the measurement equipment due to the CSTB collaboration in this work. This was also a valuable asset to choose studying further ISABELE

and SEREINE methods in the context of large typology buildings.

Nevertheless, ISABELE was conceived to SFH application and SEREINE method is still under development. In order to make them applicable to TSB and MFH, it is thus necessary to make adaptations in the method protocol and estimation process. The following chapter presents these methods in a higher level of details. In sequence, the main challenges for applying them to MFH and TSB and the strategies used to face it are discussed.

Adapting ISABELE and SEREINE methods to MFH and TSB

Contents

4.1 A general BETPA method	51
4.1.1 Protocol of a BETPA method	52
4.1.2 Estimation process in a BETPA method	55
4.1.3 Limits of a BETPA method	58
4.2 ISABELE and SEREINE methods	60
4.2.1 Protocol	60
4.2.1.1 Equipment	60
4.2.1.2 Heating scenarios	62
4.2.1.3 Duration of protocol	63
4.2.1.4 Requirements	64
4.2.2 Estimation process	64
4.2.2.1 An overview of the data processing	64
4.2.2.2 RC network thermal Models	65
4.2.2.3 Measured and estimated parameters	68
4.2.2.4 Identified parameters	70
4.2.2.5 Model selection	71
4.2.2.6 Uncertainty propagation	71
4.2.2.7 Reporting	74
4.3 Challenges of testing MFH and TSB	74
4.3.1 The main challenges of the global approach	75
4.3.1.1 Proposed solutions	77

4.3.2	The main challenges of the sampling approach	83
4.3.2.1	Proposed solutions	85
4.4	Strategy for testing the approaches	93
4.4.1	Virtual experiments	94
4.4.1.1	Model	94
4.4.1.2	Energy dynamic simulations	96
4.4.2	In-situ experiments	98
4.5	Strategy for analysing the results	98
4.5.1	Result quality indicators	99
4.5.2	Method improvement process	102
4.6	Chapter conclusion	103

As presented in section 3.3, ISABELE method has been developed to SFH. The SEREINE method is under development and it aims to answer the needs of BETPA in retrofitted SFH and also MFH, the latter receiving contributions of the present work. The objective of this chapter is to propose solutions for the following question:

How to **adapt ISABELE/SEREINE BETPA methods** to *large typology buildings*?

In order to answer this question, a deeper comprehension on the emphasized concepts and their correlations is desirable. Firstly, it is pertinent to understand the principles of general BETPA methods, so then modifications can be proposed in a coherent manner. For this reason, in section 4.1 we discuss about the main components of a general in-situ method (the protocol and the estimation process) and its limits. Based on the knowledge acquired in the previous chapter, we glimpse the shapes these elements take in the BETPA context. This discussion supports a better understanding on how each of these components are affected while adapting an existing BETPA method.

Considering that the defined goal is to adapt an existing BETPA method, it is thus important to understand its principles and functioning in a higher profundity. A more detailed description of ISABELE/SEREINE methods is presented in section 4.2. This exercise allows the comprehension of its limits regarding the application in large typologies.

Based on this information, two main adaptation approaches were proposed. The first consists in the global approach, where the protocol is applied to a whole MFH or TSB. However, it can present inconveniences concerning the instrumentation of large buildings. Therefore, a sampling approach was also proposed, where only a part of the building is tested. In this case, other challenges are faced, specially in the estimation process. In section 4.3 we analyse how the

protocol and the estimation process can be impacted by changing the original building typology of these methods through the lens of each approach. The encountered challenges are then roughly analysed. According to their importance and study possibilities, we propose to further investigate some of them.

In section 4.3 we analyse how changing the building typology, from SFH to MFH and TSB, impacts the method. The challenges and possibilities related to both approaches are then raised, to propose a protocol and estimation process for each. They need therefore to be tested and the application of tests under different conditions is useful to define the method limits. It is thus necessary to find tools to apply these methods, that is the point of discussion in section 4.4, where two main strategies are used: virtual and real test applications. After that, the results from these tests should be verified. In section 4.6 we present the metrics of verification and the process used to improve the method.

4.1 A general BETPA method

An in-situ method consists in applying locally a protocol to acquire data that is further modelled for a specific objective. The method can be divided then into two main parts: the protocol and the estimation process. The protocol is a procedure with a set of rules and techniques applied together for the method data acquisition. One could do an analogy of a protocol with a culinary recipe [192], but instead of getting a tasty cake in the end, one would aim to achieve quality data. In both cases, before starting to follow the recipe, one should already know what is aimed to be achieved in the end. However, the right materials should be used and all the steps should be carefully followed to successfully accomplish the task [193].

Going further in this analogy, the estimation process would start when we eat the cake to give the body energy. To achieve this goal the food has to pass through a digestion process, that can be divided in many smaller physiological processes: ingestion, the mechanical and chemical breakdown of food, nutrient absorption, and elimination of indigestible food [194]. An intermediate step before one start eating the cake is to take it out of the oven, cut off a piece of it and place it on a plate. In the same way, the output data from the protocol needs to pass through a preprocessing to match with the input from the estimation process. The latter consists in a set of techniques used to connect the data (model input) to achieve a desired output. As in the digestion process, estimation can be a complex operation, composed by a combination of various models, with different inputs, principles and objectives. Its principles are based on scientific fields as physics, statistics, computational science and others. It is a domain as vast as the limits of the sciences behind it. It already exists multiple modelling techniques and the

possibilities are still growing with all the horizons computational science opens. Inside all these possibilities is important to assure that the chosen technique is appropriated to the data and to achieve the determined goal. There are many procedures for model validation and criteria used to verify its quality, as cross-validation, assuring its identifiability, dynamic stability and small white-noise residuals [156]. On the whole, estimation process is not always a piece of cake!

In the attempt to develop a method, some guidelines should be followed. Initially, it should be clear what is intended to be characterized. Based on this information, it can be decided which physical quantities should be measured and how (protocol). After that, it should be defined how to go from the collected data to the desired output (estimation process). Once these two parts are defined, the capability of the method to achieve the desired output should be verified. It is then important to know the limits of the method regarding its applicability and its validity. Once the protocol, the estimation process and the method limits are defined, the method development is concluded. It can be then applied inside its pertinency domain. A method application is called here a *test*. Based on the state of the art in the previous chapter and for a better comprehension of BETPA methods structure, in next subsections we extend on its principle components and interactions. This discussion aims to provide bases to the augmentation on the impacts of adapting a method for another building typology.

4.1.1 Protocol of a BETPA method

As mentioned before in chapter 3, many methods are available for BETPA, combining different protocols and modelling techniques. In BETPA in-situ methods, we are interested in physical parameters related to the building envelope thermal behavior. This phenomenon should therefore be emphasized during test protocol, so then it can be well distinguished from measurement noises and undesirable physical perturbations. Most of the equipment and procedures in a BETPA protocol are applied to assure that enough heat flow passes through building envelope and that the hypothesis assumed during the test are respected. We could point the following aspects to be considered in the perspective of a BETPA protocol definition:

- The equipment used for test
 - To induce thermal phenomena
 - * Heating equipment
 - * Fans
 - To measure thermal phenomena
 - * Temperature sensor
 - * Weather related sensors

- * Ventilation related sensors
- * Thermal flow sensors
- * Energy meters, and others
- Heating scenarios
 - Control
 - * Temperature
 - * Power
 - With a variation profile
 - * Fixed to a value during the test
 - * Varying along the test
 - At a certain time
 - * Before the beginning of the test (preheating)
 - * During the test application
 - At a certain location
 - * Inside the test perimeter
 - * In the boundaries of the test perimeter
- A set of requirements
 - Regarding site occupancy
 - * Building can be freely occupied
 - * Building can be occupied if inhabitants respect protocol conditions
 - * Building must be vacant
 - Regarding the use of local building systems
 - * Space heating system
 - * Space cooling system
 - * Ventilation system
 - Regarding building envelope conditions
 - * State of windows, shutters and doors
 - * State of infiltration pathways
- Duration of protocol
 - Minimum test duration for an acceptable output
 - Optimum duration for output quality

The equipment used for test can be from a dedicated kit or from the building systems. In both cases, this is directly associated with data quality. Even though the best data quality is

desired, this can reach economical boundaries. In the framework of Annex 71, the idea of using a decision matrix to rate different methods according to their accuracy and the quality and cost of the data was proposed [195]. It can be seen in figure 4.1 that different methods require different level of data and of outcome accuracy. More costly data is usually associated to more accurate estimation outputs. A compromise in the data quality can be chosen in cases where the level of accuracy is not an important matter of concern.

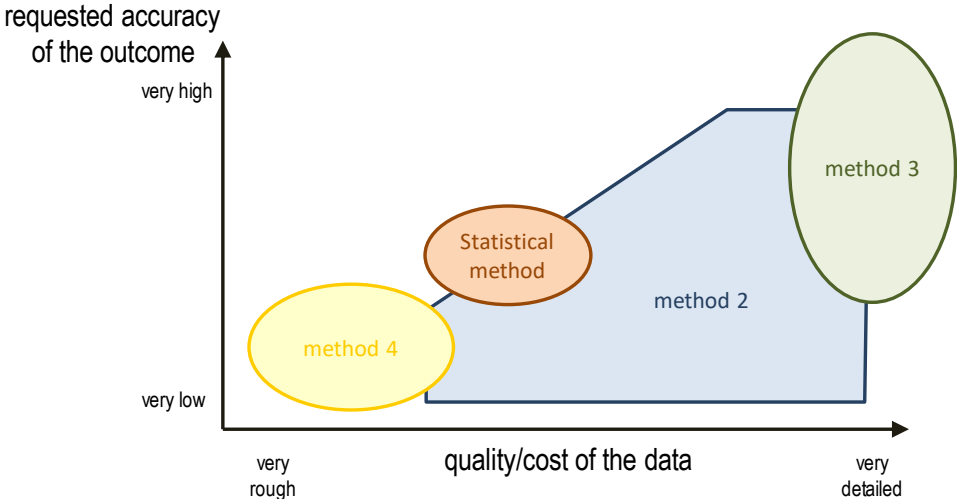


Figure 4.1 – Decision matrix linking the methods to the quality of the input data and achievable accuracy of the outcome[195]

The heating scenario is an important component of a BETPA method, since it provides the signal for testing the envelope thermal performance. In the case of methods applied to occupied sites, it is usually not possible to determine the heating scenario, since the test is constraint to the building normal usage. When dedicated invasive methods are applied, more possibilities are open to the protocol and choices can be made for optimal test conditions. We could define four moments/spaces potentially concerned by BETPA method: a, b, c and d shown in figure 4.2.

<i>Measured perimeter</i>	Boundaries	(a)	(b)	
	Indoor areas	(c)	(d)	
		Before the test	to	During the test

Figure 4.2 – Relevant questions to define a protocol heating scenario in a BETPA method.

If it is relevant and possible to control the temperature in parts (a), (b) and (c), a heating scenario can be defined. Part (d) concerns the tested area during the protocol application. In this case a heating scenario is always relevant, but not always possible to be applied. In invasive methods, there is the possibility to apply a heating scenario, and the following questions can be useful to define it:

- The heating scenario is controlled by power or temperature?
- How is the evolution of this control in time, fixed or varied?
- Which levels of temperature differences it has with with (b) and (c) ?

The requirements are important to be respected to assure the protocol is tuned with the estimation process. They are usually more restrictive in the invasive methods, since more freedom is given for the protocol application. The duration of a protocol concerns the quality of the method results. There is a minimum amount of data for which the modelling part starts to give reliable results. In some cases, the results can have higher accuracy with additional data, so then there is a time length for which the method performs better.

4.1.2 Estimation process in a BETPA method

In a solid method the protocol and the estimation process should be tightly aligned. The method protocol should provide quality data for the modelling regarding its quantity, accuracy and relevancy. The latter meaning that the data must contain enough information on the aspects targeted by the estimation process. If the input data of a model is poor, it is mostly probable that the output will follow the same tendency: garbage-in, garbage-out. As mentioned in the introduction of this section, the estimation process can be complex and compounded of many sub parts. Figure 4.3 represents the correlations of the protocol with the estimation process and the main components of the latter.

The output data of the protocol can pass through a preprocessing step where, first, corrupted or inaccurate data are corrected or removed (cleansing), then part of the data is selected (reduction) and it is finally changed to the appropriated formats (wrangling) to the downstream purposes [196] (estimation process).

The modelling part can be composed of one or many complementary models. A model in physics can be defined as "a representation of structure in a physical system and/or its properties" [197]. It can be useful to describe, to explain, predict, design and control physical phenomena [198]. Once a model is defined, its structure and implications can be analyzed to extract valuable information. This process is known as model-based inference [198].

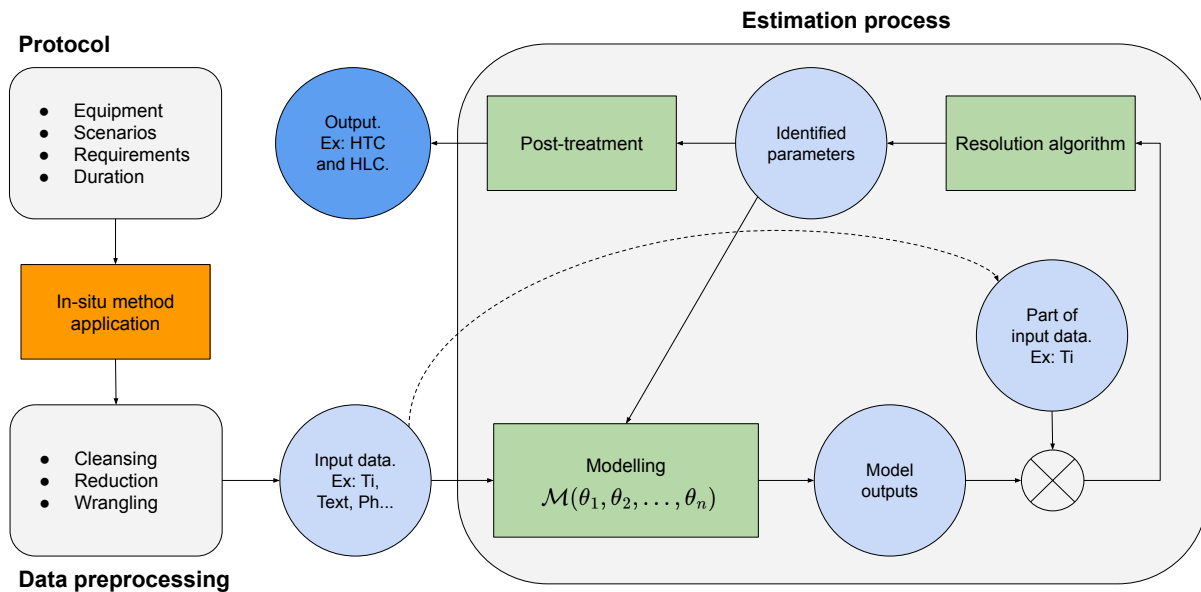


Figure 4.3 – Schema of a BETPA method with the main components of the estimation process.

In BETPA methods models are used to describe the thermal phenomena happening during a protocol application, as previously presented in section 3.3. The models imply hypothesis on how these thermal phenomena should be taken into account. The combination of the model hypothesis with a mathematical framework gives the model structure. In summary, there are four main mathematical frameworks that could be distinguished among the principle existing BETPA methods, as presented in figure 4.4

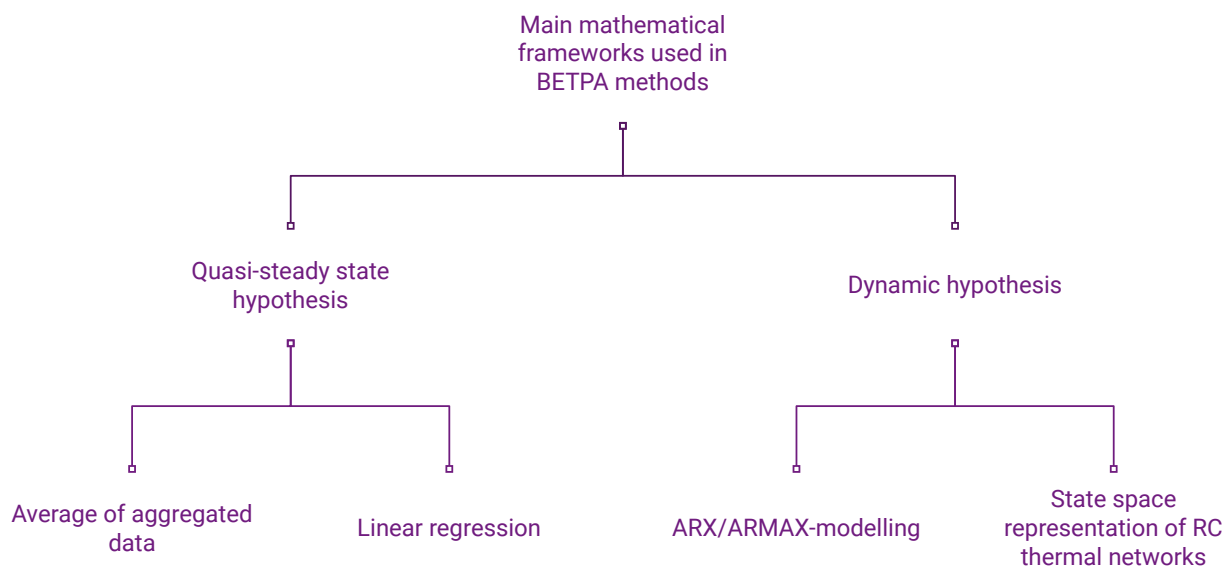


Figure 4.4 – Main mathematical frameworks used for BETPA methods

Different models are used among the existing BETPA methods, depending on the mathematical framework and on the hypothesis made on the thermal phenomena occurring during the in-situ test. Also the resolution algorithms can vary among the modelling techniques,

as for the static methods they are the inclination of a line defined by aggregated data or by a linear regression. The optimization algorithms are a special type of resolution algorithms, where the parameters are optimized based on a determined criteria. Some criteria that are commonly used in this field are the ordinary least-squares and the maximum likelihood. The optimization relies on the idea that the model outputs should be the closest to a comparable part of the experimental data. Once all the sub models (if any) are solved and the parameters are estimated, the model itself is defined. In some BETPA models a post-treatment is applied to part of the acquired information to calculate the final indicator, such as the HTC or the HLC.

To assure a final indicator accuracy, the estimation process should be able to take into account all the relevant phenomena happening during the protocol application. Different strategies can be used to deal with the heat flows unrelated to building intrinsic energy performance. The thermal phenomena that are not associated to the thermal exchange through the building envelope could be treated with one or more of the solutions below:

- Minimised by protocol conditions
- Neglected by modelling hypotheses
- Modeled with additional data collection and/or mathematical descriptions

As discussed in section 3.2.4, the protocol of a method should match the following estimation process, otherwise parasite thermal phenomena can be embedded in the indicator estimation. For understanding this phenomena we could divide the heating flow in the following categories:

- Flow of interest: a heat flow that is directly associated with the method output
- Secondary flow: a heat flow that can occur during a BETPA protocol, but it is indirectly associated with the method output

A parasite flow is a secondary flow that is not properly treated in the method. It could happen in the following conditions:

1. A secondary flow is naively ignored in the conception of the model structure
2. The measures taken to minimise a flow are not effective enough
3. The hypothesis used to disconsider the secondary flow are not valid

In the second item the words "minimize" and "effective enough" carry the idea that it could have an acceptable degree of parasitism. It happens when we consider the dimension of a parasite flow negligible regarding the dimension of the flow of interest. We could define a level

of parasitism as in equation 4.1. The idea is that this ratio remains the smallest possible to do not influence the method final output accuracy.

$$LP = \frac{\phi_{parasite}}{\phi_{interest}} \quad (4.1)$$

For this reason in BETPA protocols it is important to enhance the flow of interest by applying a *enough* temperature gradient with the outdoor environment. This reasoning resonates with the idea behind the relation between signal and noise. We could consider in this case the flow of interest and the parasite flow respectively as our signal and the noise. If a BETPA method targets to characterise the building HLC, the flows of interest are the ϕ_{tr} and ϕ_{inf} . However, if the HTC is visioned, then ϕ_{inf} becomes a secondary flow. In any case, a secondary flow that is not negligible should be modeled to be taken in account by the method. Again, if the quality of these secondary models are not good enough, a level of parasitism can be present. So the quality of the overall estimation process depends on the quality of each model used in the process and its hypothesis.

4.1.3 Limits of a BETPA method

Every method has a limit, meaning that it should be applied inside a certain domain. We could define the method limits as the perimeter of the intersection of two domains:

- Applicability domain: where it is feasible to apply the protocol.
- Validity domain : where test results of the estimation process remain reliable.

The combination of these two defines the method limits or its pertinency domain. Figure 4.5 represents graphically the pertinency domain of a method.

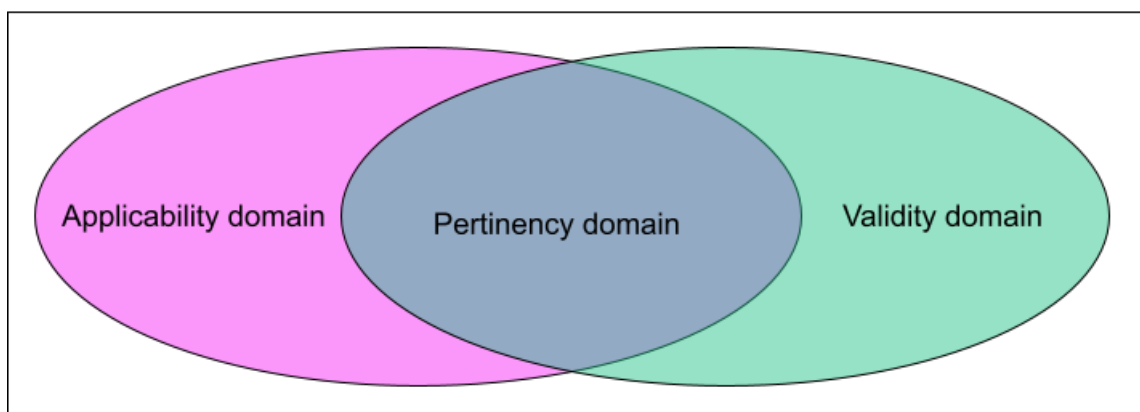


Figure 4.5 – Representation of the pertinency domain of a BETPA method.

This space dimension depends on which parameters are important to a determined method. In BETPA method the building characteristics and weather conditions are important parameters,

since they are directly related to the dimension of the flow of interest. For a BETPA method applied to occupied buildings, aspects such as HVAC systems and occupant behavior should be considered, while for an invasive BETPA method, where most of secondary flows are minimised, the envelope characteristics would be the main matter of interest. This would include the building size, shape, materials, insulation level and location.

We could for instance divide the building stock and the weather conditions into different subgroups. Figure 4.6 represents an intuition on the limits of a BETPA method developed to SFH, that could be occasionally applied to small TSB and MFH. Typically, the validity domain is reduced in summer comparing to the other seasons, due to the difficulty to apply a big enough temperature gradient with the outdoor environment.

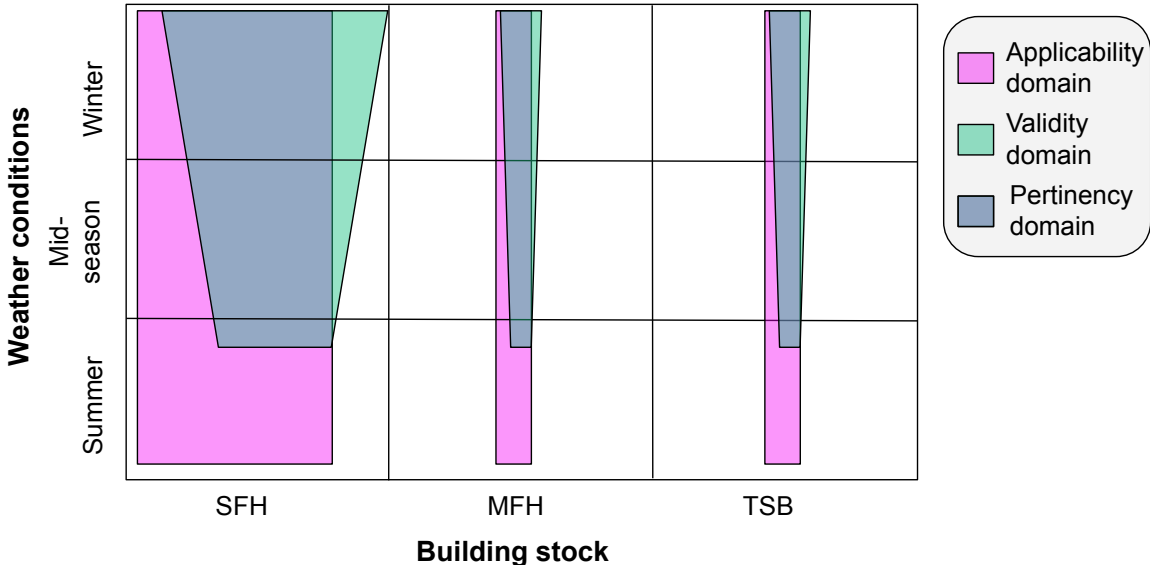


Figure 4.6 – Intuition about the pertinency domain of a BETPA method developed for SFH, when applied to MFH and TSB and for three different weather conditions.

This representation reflects the challenges of extending a method to a part of the building stock it was not initially designed to, as from SFH to MFH and TSB. The method might be initially applicable to an important part of the SFH building stock. It also might perform better during colder months, having more valid results during winter than summer. However, if no modifications are done to the method it would be applicable to a restrict part of MFH and TSB, mainly to those with smaller size, comparable to SFH. The combination of the applicability and validity domain would not cover then an important part of building stock.

In order to cover a larger area in the MFH and TSB building stock, adaptations should be developed into the method. In this case, as in the goal of this thesis, one should carefully understand the applicability and validity domain of the method after adaptations. Although, it could be hard to precisely define its limits, since it depends on applying the method in buildings

with varied characteristics that could be present in the building stock. This analysis should be combined with the behavior of the method under different weather conditions. Taking into account all the possibilities inside this space of parameters would be a laborious work, but main tendencies can be analysed by the study of some specific cases.

4.2 ISABELE and SEREINE methods

ISABELE and SEREINE are complex methods, with specificities regarding equipment and requirements in the protocol part and based on various modelling techniques. The complexity of those methods bring a challenge regarding their adaptation out of their pertinency domain. Disturbing the protocol and the estimation can impact the whole process to achieve a reliable estimation of the final indicator. In the section 3.3 an overview on ISABELE and SEREINE method was presented. In this section this former general description is complemented with information in a deeper level. This allows further to highlight which parts of the protocol and estimation are more likely to be affected when adapting them to MFH and TSB.

SEREINE is a method that is still under development and is based on ISABELE method. Since both of them share most of its principles, a unique description is presented for both methods. In the case of particularities and evolution on SEREINE method, it is specifically mentioned. The idea in this section is to give more details, especially on the estimation process, so then the path to come to a final indicator (HLC or HTC) and its meaning is clarified to support the comprehension of chapters 5 and 6. Although, the modelling part is strongly related to the protocol: the type of data available and its quality. For this reason, additional information is given on the in-situ equipment and procedures. Also highlighting the role of the protocol equipment supports the reasoning of the section 4.3 on the main challenges of applying those methods on MFH and TSB.

4.2.1 Protocol

4.2.1.1 Equipment

As already described in the previous chapter, by and large, the protocol consists of heating a building in a controlled way and measuring different quantities associated to its thermal behavior, such as temperatures and heating power. The ensemble of equipment used in a ISABELE/SEREINE test application is called protocol equipment kit, or just kit. It has been developed targeting the application in SFH. This kit allows to heat the building and measure quantities related to thermal phenomena during the test, typically including:

- 1 data-logger
- 7 Controllers
- 7 Electric heaters
- 7 Fans
- 2 Outdoor temperature sensors
- 8 Equivalent outdoor temperature sensors (SENS)
- 1 irradiance sensor

The equipment of the ISABELE and SEREINE methods are illustrated in figure 4.7.

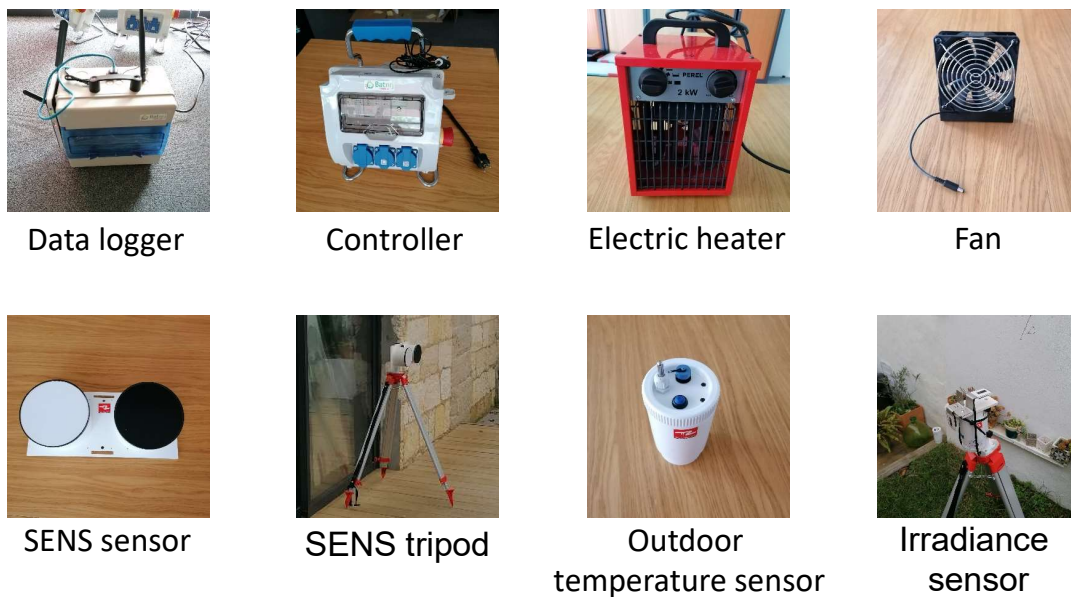


Figure 4.7 – Modules in ISABELE/SEREINE kit. Adapted from [199].

Three of these modules are always implemented together: the controller, the electric heater and the fan. The controller has four roles in the experimental setup:

- Measure the local temperature
- Pilot the operation of the fans and heater according to a scenario previously settled
- Measure the energy dispensed by these other two modules.
- Communicate with the data logger: to receive the piloting commands and to send the acquired data.

Simplified RC thermal network models are used in the modelling: the building is considered as one unique heating zone and a single temperature represents the state of the indoor temperature. Even though there will always exist heat flows inside a certain volume that is not under steady-state conditions (as any real building), efforts should be made to approach the hypothesis of temperature homogeneity. For this reason, the ideal recommendation for the protocol is to implement at least one set of controller, electric heater and fan per room, to assure

more homogeneity in the indoor temperature during the test. The fan is also implemented with this goal, by improving the convection heat transfers; it increases the temperature homogeneity inside a room. In SEREINE there are initiatives taken to increase the temperature homogeneity among the different room in a SFH, with the use of a central controller to modulate the heat power of different heaters, which is still under development.

The electric heater is an interesting system for the protocol equipment, since it is portable, and presents close to 100% efficiency [200], meaning that all electricity consumed is converted in thermal energy. Since the heating delivered during the test is one of most influential inputs of the following modelling part, it is important to assure the quality of this data. Other heating systems could also be used, but then the efficiency would have to be periodically verified in order to assure the right heating input.

In addition, there are also temperature sensors that are decoupled from the triple module for heating. Those are the external temperature sensors, that are mainly used in boundary non heated areas, and the SENS sensor. The latter is used to measure an equivalent outdoor temperature, where the effects of radiation and precipitation are added to the external temperature. More details can be found on a paper describing its principles [201]. Besides the equipment used for measuring and applying a heating scenario, there is also the data logger. It is connected by radio waves with the controllers and temperature sensors, so then all data are centralised by this device. It is also connected to an online interface, where all data can be accessed during and after a protocol application.

4.2.1.2 Heating scenarios

In ISABELE, the temperature scenario is based on a fixed value varying from 25 °C to 35 °C depending on the outdoor temperature. No preheating is applied to the building or conditions imposed on the boundary areas of the test. In SEREINE, the signal is preheating plus pseudo random power (PSA) that allowed to get reliable results with shorter test protocols. An example of a temperature scenario from ISABELE method is presented in figure 4.8 and one PSA signal from SEREINE method is shown on figure 4.9

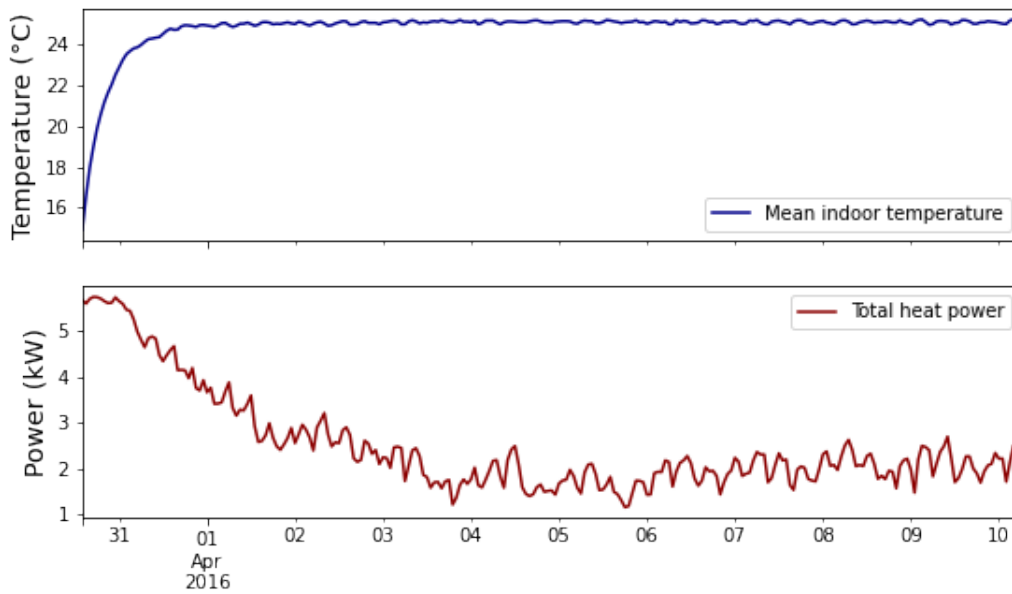


Figure 4.8 – Example of a heating scenario with stable temperature from ISABELE.

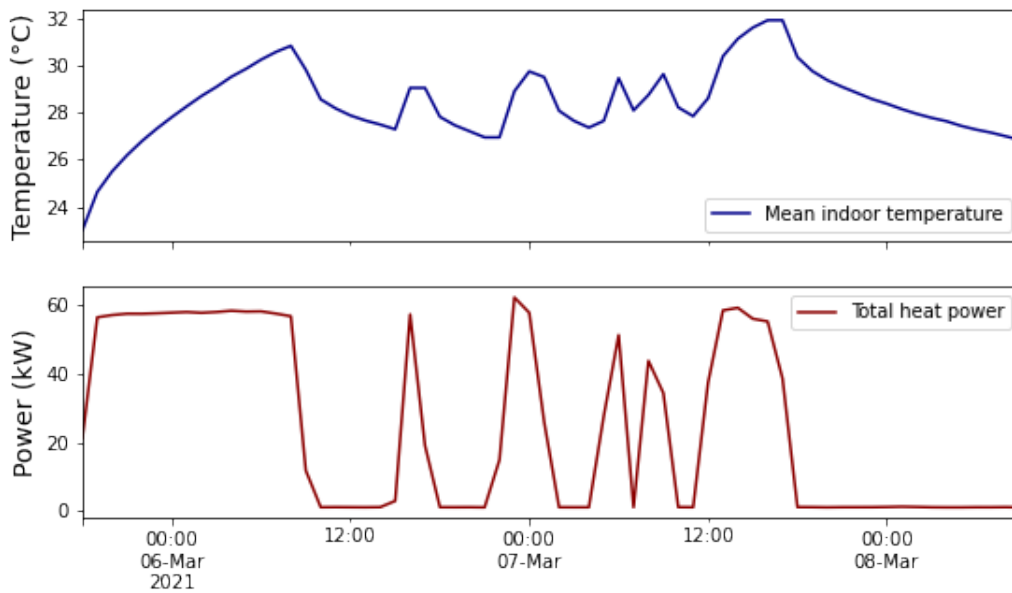


Figure 4.9 – Example of a heating scenario with PSA power signal from SEREINE.

4.2.1.3 Duration of protocol

The duration of ISABELE protocol was about 4 days, but results could still improve with a week or two. One of the main goals in SEREINE is to shorten this duration to reduce the constraints of building inoccupation. The use of power variation and consequently of the indoor temperature variation during the test allows to have more informative data regarding the dynamic thermal behavior of the building. Using these techniques nowadays allows to reduce the building immobilisation time to one to two days for SFH typologies insulated from the inside

and with cold enough outside temperatures.

4.2.1.4 Requirements

An unoccupied building not only has the advantage of negligible internal heat gains, but also the control of other heat flows unrelated to building intrinsic energy performance. Both methods are based on vacant buildings where the protocol tries to minimise the secondary flows happening during the test. For this reason, the building must have closed windows and doors to limit natural ventilation. The shutters are closed for minimising solar gains. The ventilation pathways must be taped in order to also minimise infiltration. In addition, all HVAC systems should be off, so then thermal phenomena is produced in a controlled way by the equipment kit.

4.2.2 Estimation process

ISABELE and SEREINE methods apply different modelling techniques and mathematical methods together to come to a desired output. It is essentially treated as an inverse problem, even though some sub parts are treated as forward problems. In this subsection we bring elements to the comprehension of the estimation process in a whole. A level of knowledge on these methods is necessary for understanding the implications of further modifications on them. Although, they have been and are still being developed from a large group of researchers. If one needs a deeper level of details, references can be further consulted.

4.2.2.1 An overview of the data processing

As mentioned before, all the data from the protocol are stored in an online platform from where it can be remotely accessed. There are different outputs from the protocol part, such as:

- a csv file : with the sensors measurement data
- a json file: with the experimental setup, with information regarding the sensors and the test location, duration, etc.
- a excel or xml file : with description of the building composition and properties.
- data on the weather conditions during test, either measured locally (csv file) either acquired remotely by online weather services.

In addition to those above mentioned, an yml file independent from protocol is defined. This file defines aspects regarding the modelling and numerical settings, for instance the RC thermal network models to be tested and some parameters of uncertainty propagation. All those inputs are given to the runner to achieve the outputs, the main being the HLC and HTC estimations and

their probability distributions. The data from all the process are stored in a json file and finally a report with graphical representation of the results is generated. In SEREINE there is a work in progress on reducing the number of input files. A schema of the whole process is represented in figure 4.10. An example of these files formats is presented in Annex A..

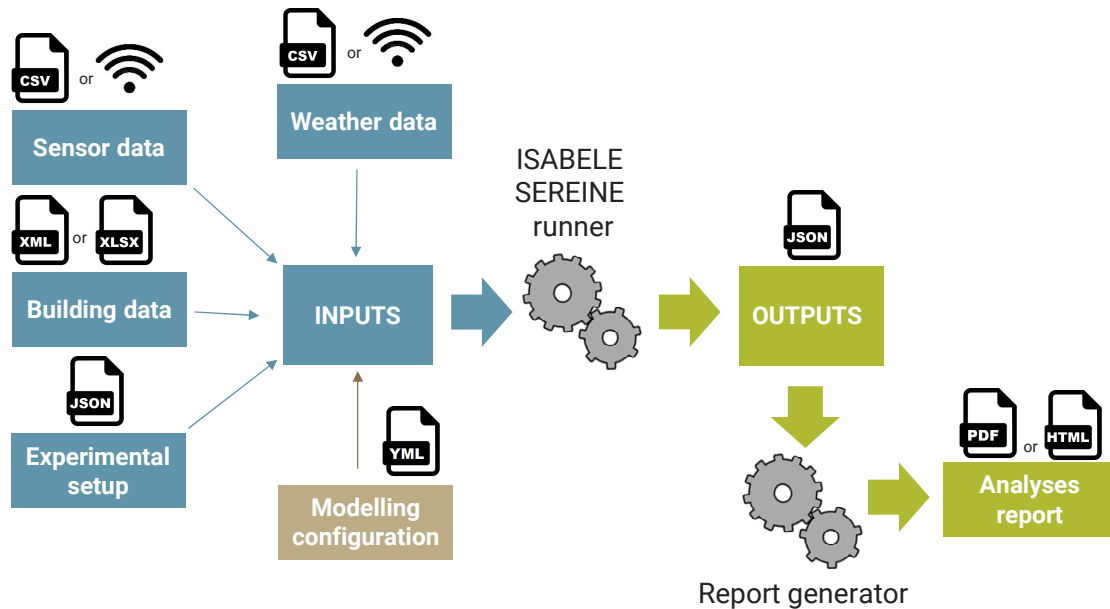


Figure 4.10 – Overall schema on the data process of ISABELE and SEREINE methods. Adapted from [202]

The following parts (from 4.2.2.2 to 4.2.2.6) aim to clarify the ISABELE/SEREINE runner that is the estimation process of these methods.

4.2.2.2 RC network thermal Models

In ISABELE, a total of 20 different RC network thermal models were available to represent buildings with different configurations. These models increase in complexity concerning the number of thermal capacities, from one to three. Other variations regard the position amount and connections among the thermal nodes and resistances. In all the models, the output variable is the indoor air temperature (T_i). The boundary conditions are: the outdoor temperature, the thermal resistance due to the air infiltration rate (R_{inf}), interior convective and radiative thermal resistance (R_{is}) and the global equivalent outdoor temperatures for heavy and light walls (T_{em} and T_{es}) which are calculated from the data collected by the SENS sensors. Details on all the models can be found in the PhD thesis from Simon Thébault [122].

In SEREINE, RC network thermal models from ISABELE and EPILOG were added, opening the possibilities to new building configurations. The (R_{is}) parameter has been removed to simplify the model structure, since it seemed to have minor relevance in the models. There are in

total 24 models, varying from order one to six. They also had added more external conditions, such as the temperature in the adjacent spaces as ground, garage, basement ceiling and attic floor, that can be now directly represented in the RC model. However, the use of models with elevated order and number of boundary conditions is still under evaluation because it might induce identifiability problems in some cases.

An example of one model present in both methods is showed in figure 4.11, followed by its state space representation and final indicators calculation. Some of the RC thermal network parameters are measured during the experiment (blue), others are estimated with forward modelling approaches (yellow). The main parameters regarding building envelope are treated in an inverse problem perspective, they are estimated using an optimization algorithm (red).

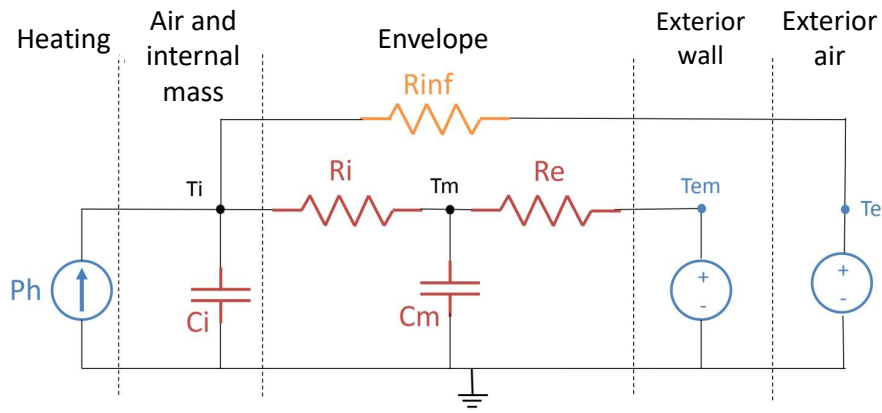


Figure 4.11 – Model M2_TmTi: a second order SEREINE RC thermal network model. Adapted from [122].

The equations describing this model are presented below. Equations 4.2 and 4.3 show a state space representation similar to that presented in subsection 3.3.3.2. Equations 4.4 to 4.7 show the components of each matrix from equation 4.2. Equation 4.9 is the vector of parameters to be identified by the optimization algorithm. Equations 4.10 and 4.11 show the relations between some of the identified and estimated parameters with the performance indicators.

$$dX_t = (AX_t + BU_t)dt + Qdw_t \quad (4.2)$$

$$y_t = CX_t + v_t \quad (4.3)$$

$$A = \begin{pmatrix} \frac{-(R_e + R_i)}{C_m R_e R_i} & \frac{1}{C_m R_i} \\ \frac{1}{C_i R_i} & \frac{-(R_i + R_{inf})}{C_i R_i R_{inf}} \end{pmatrix} \quad (4.4)$$

$$B = \begin{pmatrix} \frac{1}{C_m R_e} & 0 & 0 \\ 0 & \frac{1}{C_i R_{inf}} & \frac{1}{C_i} \end{pmatrix} \quad (4.5)$$

$$X = \begin{pmatrix} T_m \\ T_i \end{pmatrix} \quad (4.6)$$

$$Q = \begin{pmatrix} \sigma_m & 0 \\ 0 & \sigma_i \end{pmatrix} \quad (4.7)$$

$$U = \begin{pmatrix} T_{em} \\ T_e \\ P_h \end{pmatrix} \quad (4.8)$$

$$\theta = \begin{pmatrix} R_e \\ T_i \\ C_m \\ C_i \end{pmatrix} \quad (4.9)$$

$$H\hat{T}C = \frac{1}{\hat{R}_e + \hat{R}_i} \quad (4.10)$$

$$H\hat{L}C = H\hat{T}C + \frac{1}{\hat{R}_{inf}} \quad (4.11)$$

Different from the deterministic state space models presented in the previous chapter, these are stochastic state-space models. The latter can increase the parameters estimate uncertainty, but gives more consistent and reliable results compared to the deterministic approach [127]. For this reason, in these equations, there are additional terms to represent the system errors with independent Gaussian noise. The terms Qdw_t and v_t represent respectively the process noise (Wiener process) and the observation noise.

It is noticeable in figure 4.11 that many thermal phenomena that could happen in a building are not represented in the model. Since these methods require a vacant building, the occupant heat gains, lightning and appliance heat flow, heat due to DHW, local HVAC system and natural ventilation are not taken into account in the RC thermal model. The requirements imposed during protocol application allow the simplification of the modelling part.

Solar gains are not directly considered as previously in equation 3.8. Given that all shutters are closed during protocol application, solar gains through transparent surfaces are highly reduced, but it is impossible to impeach the solar gains through opaque surfaces. This effect is taken into account by an equivalent outdoor temperature T_{em} measured by SENS sensors. In case SENS sensors data is not available, the equivalent outdoor temperature can be estimated by equation 4.12 [201]. The absorptivity coefficient is estimated according to the external surface color.

$$T_{em} = T_{out} + \frac{\alpha_s \times I_s - F_r \times h_r \times (T_{out} - T_{sky})}{h_c + h_r} \quad (4.12)$$

where:

- T_{em} is the equivalent outdoor temperature (K);
- T_{sky} is the sky temperature (K);
- α_s is the absorptivity coefficient of the exterior wall (-);
- I_s is the solar irradiance on the exterior wall (W/m²);
- F_r is the form factor between the exterior wall and the surface seen by the wall (-);
- h_r is the radiant heat transfer coefficient (W/m².K);
- h_c is the convective heat transfer coefficient (W/m².K).

The following paragraphs explain how all RC thermal network parameters are taken into account in ISABELE and SEREINE.

4.2.2.3 Measured and estimated parameters

These parameters are components of the RC thermal network model, even though they are not directly implicated in the final HTC calculation. They are represented in the figure 4.11 in blue and yellow colors.

Heating power

It is the total amount of energy dispensed during the test at each time step. Energy consumption data from all the different modules are added together.

Temperatures

The temperature data is estimated as in the description below:

- Indoor temperature: the arithmetic average of the temperature sensors data associated with each controller placed inside the house.
- Outdoor temperature: Values coming either from on site measurements with an outdoor sensor or from online data of the closest weather station.
- Equivalent outdoor temperature: first the equivalent outdoor temperature of each SENS sensor (T_e) is calculated, as in equation 4.13. It is done an interpolation of the temperatures measured by its white and black plates (T_{white} and T_{black}), using the value of the envelope element absorptivity (α_{elem}) and the absorptivity from each plate (α_{white} and α_{black}). Then, the building envelope is divided in representative parts, such as parts of the wall, roof and windows. A SENS sensor is associated with each of these parts according

to their orientation and inclination. Finally, the overall equivalent outdoor temperature is calculated by a weighted average of the SENS sensors temperatures, based on the surface (S_k) and U-value (U_k) of each envelope part (k) (equation 4.14). The theoretical U-value can be found in the building project files for new buildings.

$$T_e = \frac{T_{black} \times (\alpha_{elem} - \alpha_{white}) + T_{white} \times (\alpha_{black} - \alpha_{elem})}{(\alpha_{black} - \alpha_{white})} \quad (4.13)$$

$$T_{em} = \frac{\sum_{k=1}^n (T_{e_k} \times S_k \times U_k)}{\sum_{k=1}^n S_k \times U_k} \quad (4.14)$$

Infiltration estimation

The final indicator in ISABELE is the HTC and in SEREINE it can be either the HTC or the HLC. When the HTC is aimed, it is necessary to separate the infiltration heat losses during the test from the results. In ISABELE the infiltration losses are represented in the form of a thermal resistance connecting the outdoor and the indoor temperature states, as in the figure 4.11. In SEREINE it is represented directly by an equivalent heating source into the node T_i . The Equations 4.15 and 4.16 show the respective formula of each one of these parameters.

$$R_{inf} = \frac{1}{\rho_{air} \times c_{air} \times Q_{inf}} \quad (4.15)$$

$$P_{inf} = \frac{T_e - T_i}{R_{inf}} \quad (4.16)$$

where:

- R_{inf} is the thermal resistance related to air infiltration ($K \times W^{-1}$);
- ρ_{air} is the air density ($kg \times m^{-3}$);
- c_{air} is the specific heat capacity of the air ($J \times kg^{-1} \times K^{-1}$);
- Q_{inf} is the airflow infiltration rate ($m^3 \times s^{-1}$);
- P_{inf} is heat flow due to infiltration (W).

In order to estimate Q_{inf} it is necessary to apply a blower door test before the estimation process. Indicators from this test, as the air leakage coefficient and exponent, C_L and n , with their respective uncertainties are used to characterize the building air tightness. Other experimental data, such as wind speed, indoor and outdoor temperatures are used in the ISABELE and SEREINE infiltration model [122]. Additionally, building data on the height of the zones, facade areas, roof and slope and terrain class (urban, country, open) are used in the aerologic

model. Equation 4.17 presents the relation between the blower door coefficients, the pressure difference (ΔP) and the envelope areas (A_{facade} and A_{roof}) to calculate the air infiltration rate.

$$Q_{\Delta P, surf} = \frac{C_L}{A_{facade} + A_{roof}} \times \Delta P^n \quad (4.17)$$

In order to estimate the ΔP , the values of outside and internal pressure are necessary. The first are calculated using standardized pressure coefficients (from standard NFE51-766, previous EN 15242), wind and temperature measurements. Five components are taken into account, one in each, in the down and top part of the facades, in the leeward side and the windward side and also in the roof [177]. Figure 4.12 present the five components considered in this simplified model. The internal pressure is calculated with an optimization algorithms to maintain the mass flow balance in the zone [177]. The airflow $Q_{\Delta P, surf}$ (in m^3/h) is finally calculated in each of the five branches and added in a total airflow estimation.

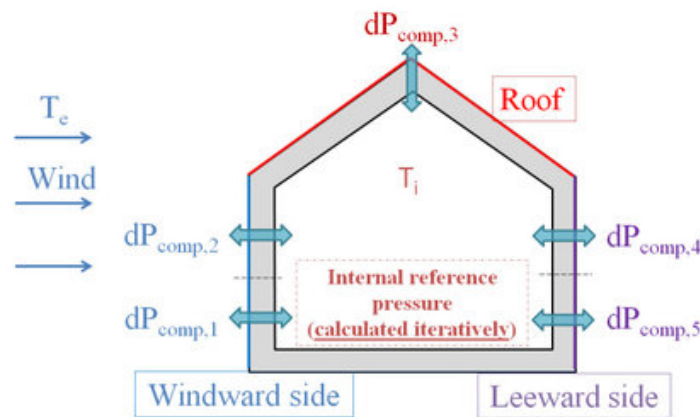


Figure 4.12 – Simplified representation of the airflow network used in the EN 15242 without ventilation [177]

4.2.2.4 Identified parameters

We consider here as *identified parameters* those estimated by the optimization algorithms. They are typically the capacities and some of the resistances of the RC thermal network model. For example, in the figure 4.11 the identified parameters are those coloured in red. This is the concern of an inverse problem, since some model parameters are initially unknown and estimated based on measured data. As already mentioned, the mathematical structures of the models are based on stochastic state space representation of ordinary differential equations.

Different frameworks can be used to optimize the parameters of such models in this type of inverse problem. In ISABELE method, the optimization algorithm used for fitting the RC model parameters is CTSM-R, developed by the Danish university DTU. This framework, provides the

estimation of gray-box models, based on maximum likelihood and Kalman filtering principles. In SEREINE, it is used pySIP, an optimization algorithm developed by the University of Savoie Mont Blanc. This framework’s frequentist approach shares the same principles of CTSM-R on the parameter identification. An asset of pySIP is that it is fully developed in python as the main code of ISABELE and SEREINE. More resources on the principles of these frameworks can be found in the literature [122, 203, 204, 205].

4.2.2.5 Model selection

The idea in this part is to select a model among the available models that better fits measured data. For this purpose, each available RC thermal network model is fitted with the help of the optimization algorithm. As output of each fit, among other information, there is a value for the likelihood function and also a value of HTC or HLC estimated from the model parameters. The model selection process starts using the simpler models and increases in complexity (number of model parameters) at each step. The likelihood of a fitted model is then compared with the previous one. The tests allows to verify if the increase in the likelihood value is worth of the increase of the model complexity [122]. In addition, the uncertainty of HTC in the selected model might be lower than the HTC mean value to take into account the significance of the result. A synthesis on this process is presented in figure 4.13.

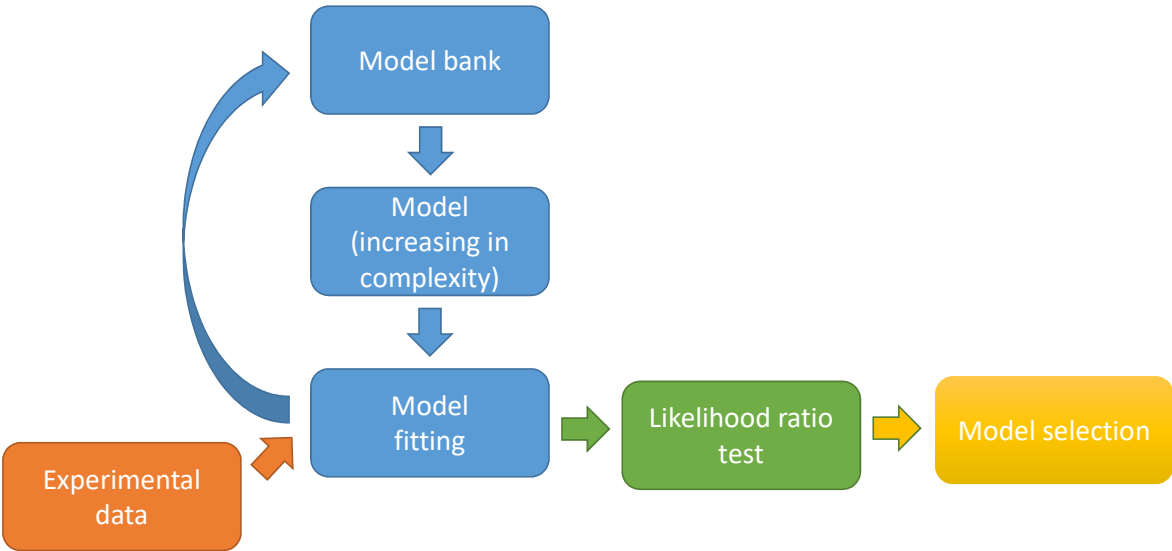


Figure 4.13 – Schema of model selection in ISABELE method

4.2.2.6 Uncertainty propagation

Two main categories of uncertainties are considered in these methods: stochastic and systematic. Figure 4.14 illustrates the bias related to those different categories and the combination of them.

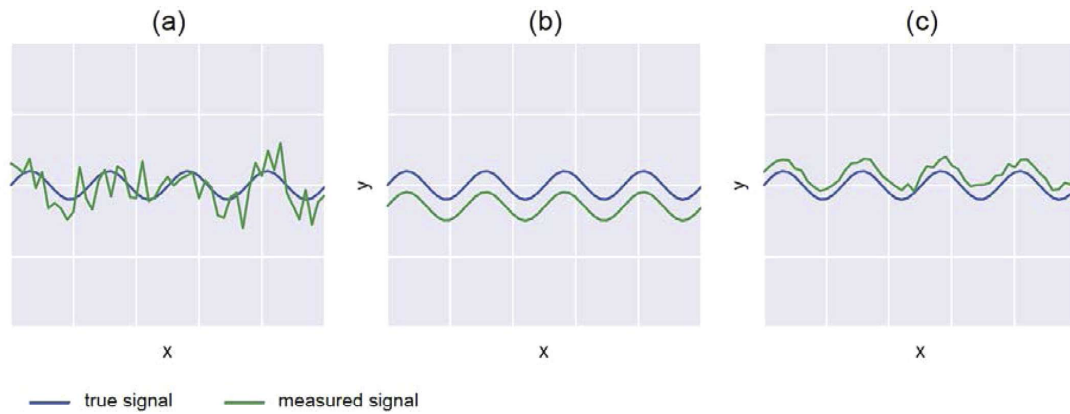


Figure 4.14 – Examples of measured signals with (a) purely stochastic error, (b) purely systematic error, and (c) a combination of stochastic and systematic errors [178].

Stochastic uncertainties

The stochastic uncertainties are associated to the optimization of the RC thermal network model parameters. These uncertainties are related to the profile of the likelihood function in the zone nearby the optimum value. In this way, each output parameter and each model state equation error is represented by a Gaussian, with an associated standard deviation. As presented before in 4.2.2.2, the final indicator (HLC/HTC) is a mathematical function of some RC thermal network parameters (resistances related to the envelope). For this reason, those parameters uncertainties can be propagated to the final indicator through an analytical formula, following the JCGM recommendations for the evaluation of uncertainty of type B [206].

Systematic uncertainties

Although the stochastic uncertainties are already taken into account, it has been verified that an additional uncertainty source could be quite influential on the final indicator quality [178]. This is related to an offset on the measurements, such as a sensor that presents a persistent deviation from the real value. This is related to the capability of equipment to measure the real physical quantity. For instance, it has been observed that small deviations in the indoor temperature value would have significant impacts on the final indicator results. For this reason, this source of uncertainties are also taken into account for some of the input data given to the resolution algorithm. The parameters and how they are considered in this analysis are presented below:

- Heating power [%]
- Indoor temperature [°C]
- Outdoor temperature [°C]
- Black SENS plate temperature [°C]
- White SENS plate temperature [°C]

- Black SENS plate absorptivity [-]
- White SENS plate absorptivity [-]
- Exterior wall absorptivity [-]
- Wind speed [%]
- Indoor convective heat transfer coefficient [$\text{W}/\text{m}^2/\text{K}$]
- Indoor radiative heat transfer coefficient [$\text{W}/\text{m}^2/\text{K}$]
- Pressure coefficients from the EN 15242 [-]
- Air leakage coefficient (CL) from blower door test [%]
- Air leakage exponent (n) from blower door test [%]
- Temperature of a non heated boundary area with measurement [$^{\circ}\text{C}$]
- Temperature of a non heated boundary area without measurement [$^{\circ}\text{C}$]
- Temperature of the soil for houses with a direct contact to it [$^{\circ}\text{C}$]

Instead of considering an absolute value for these inputs, a probability function is associated to them. A range corresponding to the I95 limits of a Gaussian distribution is set to each one of these inputs.

In ISABELE, since the uncertainty propagation method is highly computationally intensive, a sensibility analysis is first used to choose the most influential parameters. For doing so, the Morris method of sensibility analysis is applied to determine the five most influential parameters. These parameters are then sampled with Saltelli sampling and then propagated by a quasi-Monte Carlo method. Their probability functions define the space of parameters to be researched. For each set of values, a fit is done with the optimization algorithms, which gives as outcome a Gaussian distribution. This process is repeated about 300 times with a different set of input values. The ensemble of indicator Gaussian results are added and combined in a new probability distribution function.

In SEREINE, the sensitivity analysis and the uncertainty propagation are done together in the whole space of uncertain parameters. The quasi-Monte Carlo method is used with the sobol sequence generator by Frances Y. Kuo and Stephen Joe [207] with at most 300 samples.

Final indicator estimation and uncertainty

Once these two steps of uncertainty propagation are concluded, the indicator (HTC or HLC) is represented by a probability distribution. The estimated value of the indicator is the average value between the 95% confidence interval (I95) borders. The uncertainty of the indicator is represented as the percentage difference between the indicator value and the 95% confidence interval (I95) borders. A schema of the uncertainty propagation and the indicator estimation is presented in figure 4.15.

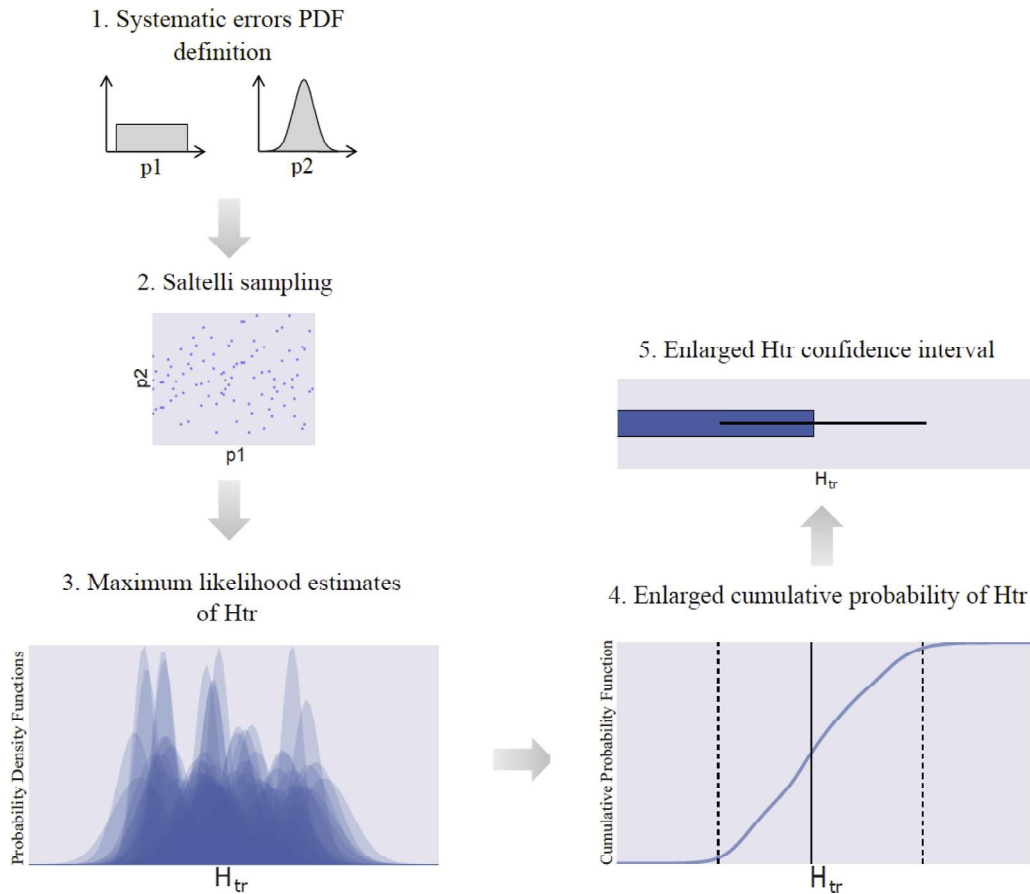


Figure 4.15 – Illustration of the uncertainty propagation procedure [178].

4.2.2.7 Reporting

Once all the estimation process is finalized an automated report with the main outputs is generated. This includes the location and duration of the test, the measured boundary conditions, the final indicator estimation and probability function and the evolution of the results over time, among other information.

4.3 Challenges of testing MFH and TSB

When aiming to adapt ISABELE and SEREINE methods to MFH and TSB, the first difference that becomes apparent with the SFH tests is related to their dimensions. This aspect alone can bring many challenges regarding the protocol application. As explained in the previous section, the protocol of these methods includes instrumenting each room in a building with equipment for heating, air circulating and temperature measuring. Performing this operation in large building typologies can be challenging and even lead to an impediment for protocol application. Furthermore, in some cases it would not be possible to vacate the whole building to apply a BETPA invasive test. For this reason, two main approaches were considered to adapt

the method into large building typologies:

- Global approach : the BETPA protocol is applied to the entire building.
- Sampling approach : the BETPA protocol is applied to parts of the building.

The first would be considered when it is possible to have the whole building available during the protocol application. It would typically happen in the context of new buildings before occupancy or heavy refurbishment, where the duration of the test is not a strong constraint as for most retrofitted buildings. In this case, the measured perimeter would normally coincide with the building envelope. This presents challenges facing the implementation of a protocol in a large building; for instance, how to apply a controlled temperature and how to measure the energy dispensed during the test. These approaches and their related issues are further discussed in the subsection 4.3.1.

The second envisioned strategy could be considered when the protocol application in the whole building is an obstacle for performing the test. It would suit the context of retrofitted buildings, where it is necessary to limit the constraints on the occupants. In this case, the measured perimeter includes parts of the building envelope, but also of the shared walls with the adjoining spaces, such as intermediate floors, party and partition walls. The indicator of such test would not represent the whole building, but samples of its envelope. In this approach, the main challenge is related to the heat flow passing through the shared walls, typically not insulated, and how to assure that they do not influence the accuracy of the envelope indicator. The difficulties related to this approach are presented in the subsection 4.3.2

4.3.1 The main challenges of the global approach

One important challenge of the global approach is the fact that the protocol application requires a vacant building. In the context of one household it could already be disturbing to free a site for four days, when it involves a larger number of people, the situation is even more critical. Evidently, this is in case of occupied buildings, such as in BETPA application after retrofitting works. In the context of new buildings, in-between construction and occupancy phases, if enough time is allocated to a test application, this would not be a matter of concern. However, if the test time is not integrated into the delivery process, the builder might have no interest in leaving the building vacant for several days, since often there are contractual penalties for delay in the delivery date of the constructions. This aspect, more than a challenge, can be considered one limitation of the global approach: the difficulty to have an entire building available enough time to perform the test.

Besides this first aspect, the size of the building can bring technical difficulties for the protocol application. Most of BETPA invasive protocols consist in implementing an *in-situ* heating kit equipment in the tested SFH to achieve a desired temperature gradient with exterior environment and hence induce the heat transmittance flow. The possible larger size of MFH and TSB make this approach technically difficult and even impossible in some cases. In ISABELE, as mentioned in subsection 4.2.1.1, each room of a house should be equipped with a set of three modules: an electrical heater, a fan and a controller. There are 7 of this module set per protocol equipment kit, which represents roughly two thirds of its total volume. One kit can be transported by a large car or a small commercial vehicle (figure 4.16). Currently, the size of the kit is about to be miniaturised in the SEREINE project. The equipment kit was conceived for the application into SFH up to 120 m².

When testing a low-rise MFH, it could be considered to bring multiple kits, depending on the equipment availability and the transportation possibilities. It could be considered to distribute the heating modules more sparsely to be fairly divided along the total area. However, this should not be done to the extent such that the building presents high indoor temperature inhomogeneity.



Figure 4.16 – Vehicles with the whole equipment of ISABELE/SEREINE methods version 2020.

If we consider a mid-rise MFH apartment, for example, with 5 floors and 4 apartments per floor, using the same strategy would imply in a logistical problem for material transportation. Also, the amount of equipment available by a testing center might not be enough to cover the whole site needs. In the case of high-rise MFH, this question should not even be raised. As for MFH, the same reasoning applies to TSB buildings of equivalent size.

If HTC indicator is searched, another modelling problem befalls the adaptation to larger typology buildings. After all, an *in-situ* method cannot be conducted without infiltration losses

through the building envelope. For this reason, if it is aimed to assess the losses by transmission alone, an additional modelling technique should be applied to estimate H_{inf} . ISABELE/SEREINE presents an infiltration model based on equation 3.3 where Q_{inf} is a function of the wind speed and the blower door test results, which might be applied to the SFH before the analysis takes place. Seeing that the official protocol for blower door test in MFH and TSB is done through a sampling approach, it is hard to base ISABELE/SEREINE aerolic model for the whole building on these values. In addition, the air infiltration between the apartments or offices is not taken into account in the current model, which will tend to overestimate the infiltration rate of the whole building when using local measures.

4.3.1.1 Proposed solutions

Four main issues were raised above in order to adapt ISABELE/SEREINE methods to large buildings, namely:

1. Whole building vacancy during protocol application;
2. Equipment volume and protocol logistics;
3. Indoor temperature homogeneity;
4. Air infiltration losses modelling.

The first one is situational, and a proposed adaptation regards the use of the other approach, testing partially the building. The second only questions the test protocol, coming from the modification in the method application domain. The third problem interrogates both: the protocol and the modelling. The protocol in its capability of assuring quality data and the model in its base physical hypothesis. As mentioned before, most BETPA methods are based on the single zone thermal balance. If there are large temperature spatial variations in the tested volume, the single zone model would rather be unconsidered. The last challenge is mainly related to the estimation process, but it could be avoided if the indicator to be used is the HLC.

In order to enable the method application, those aspects should be considered for each case or group of cases. As mentioned in section 2.2, MFH and TSB present wider possibilities of typologies than SFH, regarding their size, shape and uses. A unique solution is then not practicable to be applied on the whole MFH and TSB building stock. For this reason, each of these points are analysed individually in the next paragraphs. It discusses how these challenges are taken into account and, when it is possible, also solutions are proposed to be further investigated on their limits and potentials.

4.3.1.1.1 Site vacancy

Allowing occupancy in the building during the test would imply reformulating the whole modelling process of ISABELE/SEREINE methods. Since this condition is a requirement for the application of these methods, this parameter will not be further studied. It will be integrated in the limitation of method - that is, when it is not possible to have vacancy in a building during the protocol prescribed duration, the case will be deemed out of the method applicability domain.

4.3.1.1.2 Equipment volume and logistics

Coming to the first item list, applying these methods could be without considerable effort for a small TSB and low-rise MHF. However, as discussed above, when building size starts to increase, using a heating kit equipment can be non-viable. The preparation of the whole building would already be time consuming, including actions such as: masking all the windows, blocking all air intakes and installing the kit modules. For a SFH test, if the windows do not have shutters, they are then masked with cardboard. In case of large buildings, this solution would be impracticable and it should be given a preference for testing buildings with manual or electrical shutters. Even if it is the case, more man-hour should be allocated to perform all these actions.

When it comes to the kit modules, the volume of the equipment can be an issue for the protocol application. It might bring logistic problems related to the the availability of enough modules to instrument the whole building and their transportation into the tested site. The modules implemented in each room of a SFH (the controller, the electrical heater and the fan), represent more than half of the equipment volume and this would exponentially increase for large buildings. Unless the interior modules are significantly miniaturised, it is unrealistic to use these modules to apply the protocol heating scenario in large buildings. A logical solution would thus be to use the building local heating system to perform the test.

When applying this solution, the heating system should be accessible and possible to be piloted during the test. The control and regulation of it will depend on the heating system type. MFH and TSB can present multiple technologies for system heating. Under winter conditions, the local heating system is expected to have enough power to achieve a considerable temperature difference with the outdoor environment, which is necessary for enhancing the heat flow of interest. During mid season, the capability of the heating system should be verified, according to the weather in the test location. In summer, it is mostly likely that the local heating system would not be adapted to give an important temperature gradient with exterior. This brings a first level of constraint: the power and control of the heating system are not dimensioned for a BETPA test, but for normal building usage. The limitation of the system would be usually a compromise between thermal comfort and energy savings in an occupied building.

It is true that the method quality strongly depends on the level of indoor and outdoor temperature gradient produced by the used heating system. However, the quality of the data from this system is also crucial for accurate estimations. It has recently been concluded in the framework of Annex 71, that the quality of the heating power data was the most influential parameter to the indicator quality, among many other studied parameters, such as solar gains, infiltration and ventilation, occupancy and indoor temperature [14]. For this reason, supposing that the local heating system is used during a protocol application, the energy delivered by it should be accurately measured.

Therefore the following practical aspects should be considered, to enable the use of the local heating system:

- Capacity of the system for heating the building under the protocol required conditions
- Possibility of accessing and piloting the local system
- Possibility of measuring the delivered heat power during the test

It is important to assure that the envisioned heating scenario is applicable with the local heating system. It is then necessary to have ways to acquire the data of the power delivered during the protocol application and to assure its quality. Different heating systems would provide distinct possibilities regarding these aspects. For investigating the limits of a protocol based on the use of the local heating system to perform the heating scenario, a discussion on the types of systems and their possibilities is included in chapter 5.

4.3.1.1.3 Homogeneity of indoor temperature

This aspect is dependent on the resolution used to the issue above. The temperature homogeneity inside the building will be influenced by the capacity of the heating system to heat the building evenly. If the equipment kit is used to perform the test, it should be assured sufficient quantity of modules per area to provide a well distributed heating source. If the local system is used, then this is conditioned by the original distribution system in the building. The non heated areas of a building should also be considered, as this could be the case for the common areas. Areas that do not dispose heating distribution can induce to more temperature dispersion in the building. In some cases, this could be handled by equipping these areas with the kit controller and electrical heaters to assure a set temperature, in addition to the local system.

In order to have a more descriptive data of the global temperature evolution during the test, an average of the data from the scattered sensors in the building can be used. This is already the case of ISABELE/SEREINE methods in the SFH context, where a simple average of

the indoor temperature data takes place. A possibility to improve this estimation is to use a weighted average of the indoor temperature data. It can be weighted either by the floor area covered by each sensor or by the volume of air associated with each sensor.

These averages require the collection of additional information about the floor area and the ceiling heights associated with the different sensors, which could be taken from the plans and measurements. It also requires an extra action in the data preprocessing of associating each sensor to its representative volume or area. This volume average solution was used in the estimation process of the virtual tests for the global approach in chapter 5. Nonetheless, this solution is limited, as a significantly dispersed indoor temperature could still affect the quality of the estimation process output.

The common areas can be an ambiguous boundary between the heated spaces and the exterior. They should be carefully analysed to define the test measured perimeter and how to deal with their temperature data. The presence of insulation between the dwellings and these areas should be noticed, since it is not usually present as for the exterior walls. If there is insulation, these areas can be considered as buffer spaces and their temperature data would be included in the equivalent outdoor temperature. It is therefore necessary to close the doors of the dwellings giving to these spaces and to implement temperature sensors (SENS or exterior sensor) in these spaces.

Sometimes there is no insulation between the common areas and the dwellings, so they might be included in the measured perimeter. In such circumstances, it is important to assure these areas temperature in respect to the protocol heating scenario. If common areas are heated by the heating system distribution, it is not necessary to go further in the solution. If it is not the case, they are not necessarily considered as unheated areas. In case its volume is enclosed enough in another heated area presenting insulation to the external environment, this space can be considered as a heated area.

In some MFH and TSB several of these situations could occur simultaneously, with a part of the common area being considered as a buffer space and other part being considered inside the measured perimeter. We could think for instance of a mixed function building, with the ground floor serving commercial purposes and the rest intended for residential uses. In such situation, when performing a test it could be decided to let the ground floor be unheated, as a boundary area, and the common areas in each floor be part of the measured perimeter. This choices are logically associated with the presence of insulation among the spaces, since the idea is to test the thermal performance of the building. Although, the measured perimeter can be differently defined in some cases, but then the protocol should be performed in accordance with the estimation process and it should be clear what is being measured. What counts is that the

areas included in the measured perimeter present similar values of temperature and that the spaces considered in the boundaries of the system have their temperatures associated to the equivalent outdoor temperature.

Another possibility for dealing with the non homogeneities in a large building would be to consider the use of a multi-zone RC thermal network model. For example, based on the reasoning above could be the use of a two-zones model, one zone for the areas with heat distribution system and another for those without. An example of a possible multi-zone RC thermal network model is presented in figure 4.17.

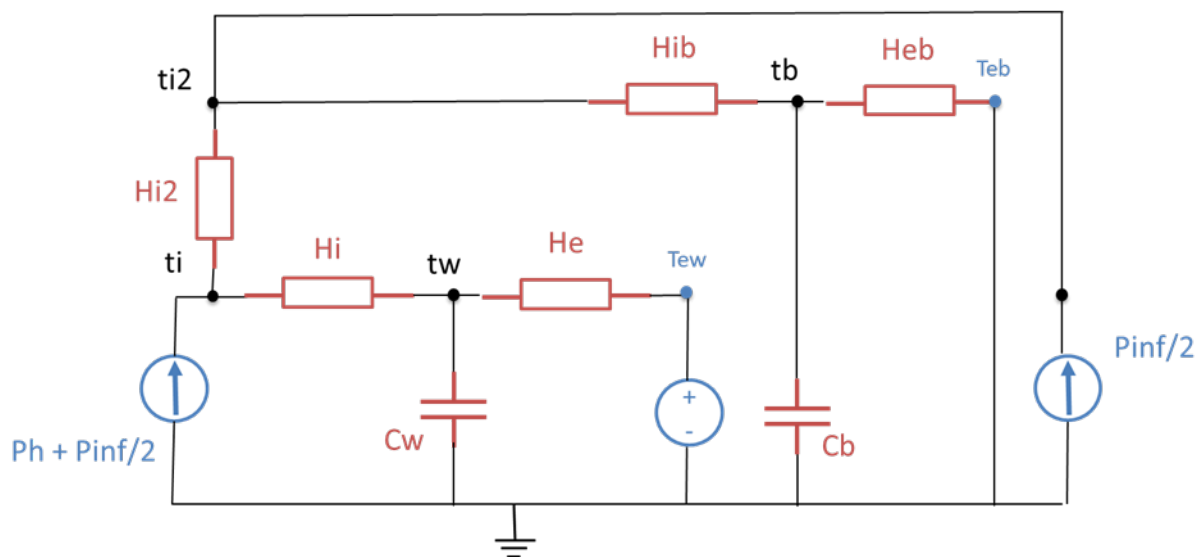


Figure 4.17 – Examples of a potential multi-zone RC thermal network model for the global approach. Adapted from [208].

This strategy was not further tested in this work. The definition of the zones related to the measured data could be challenging in some cases, as when there is no clear insulation among parts of the building. The temperature might be not homogeneous in the totality of the building, but also do not present enough dispersion to define two different states. This should be analysed case by case, according to the configuration of the tested building. It would be more difficult to generalize a multi-zone model among different buildings configurations. In addition, the use of multi-zone models would imply more complex systems, with an increased number of variables. The number of variables, in special having parallel thermal resistances, could bring identifiability problems, with many combinations of possible estimation to some of the parameters. For this reason it was chosen to develop the work with single zone RC thermal network models. In this case, it is chosen either to include the common areas in the measured perimeter (with or without extra actions to assure the temperature of those areas) or to make them as boundary of the system (buffer zones).

In order to assure a better temperature homogeneity inside the measured perimeter it is

preferable to apply a stable heating scenario as in ISABELE protocol with a fixed setpoint temperature during the test. Due to the difficulties to assure the single zone balance in a large building, the pseudo-random power heating scenario used in SEREINE method is not considered as a viable option.

Another question when changing the test scale is related to the thermal capacity of the whole building. A more important inertial behavior is expected when comparing to a test applied to SFH. This would be likely due to the internal mass, with greater presence of intermediate floors, party walls and partitions; but also, possibly due to the heating system, in case of water distribution system and underfloor heating [208]. This could imply longer test protocols to achieve an homogeneous temperature. Strategies, such as preheating the building before protocol application could be useful for limiting the building vacancy time. This strategy and the expected ranges of protocol duration for assuring method quality are investigated in chapter 5.

4.3.1.1.4 Modelling infiltration losses

The choice to estimate the infiltration or not comes with the question regarding which indicator is expected in the end of the method application. If the HLC is aimed to be estimated, there is no need for modelling infiltration losses. However, if one is interested only in the building envelope transmission losses, there is the need to decouple the infiltration losses from the final indicator.

As mentioned in part 4.2.2.3, the infiltration is normally estimated with a simplified model. This model requires data from a blower door test applied to the building. In the SFH context it is not a matter of concern, since both tests are applied to the entire building. Meanwhile, in large size buildings, the blower door test is applied through sampling methods [209]. The test coefficients are then related to the tested areas, the sampled apartments or offices. This hampers the use of the air infiltration model in ISABELE/SEREINE runner, since the blower door test coefficients do not match with the whole building infiltration behavior. Research has been developed in order to apply the blower door test in a whole TSB with innovative technologies, as coupling an auxiliary pressure generator during the test [210]. This solution would allow to have the blower door test coefficients for the entire building and ease the infiltration losses estimation. The use of other technologies has been also proposed, such as the CO₂ decay method in a TSB to decouple the H_{inf} from HLC [211].

Another possibility, in case the openings connecting the multiple floors could be closed, would be to test the air leakage of each building floor, depending on the building size. In this case, the infiltration rate would be the combination from each floor, if we consider that the air rate between floors is negligible.

Besides the difficulties related to achieve an infiltration coefficient for the whole building or an important part of it, the infiltration model used for SFH might not be suitable to be applied into large buildings. The separation of the air volume among the flats or offices prevents the air from circulating freely in the building, as it is assumed in the current model [208]. In this way, the real infiltration rate is expected to be lower than the one estimated by the model. To deal with this question, the doors of the different areas should be kept open to enhance the inner air circulation. However, the possibility of performing this operation depends on the measured perimeter that was defined. In addition, when a global coefficient is available, the results from the present aerologic model could be submitted for a post-processing. Considering the assumption that the infiltration rate would be lower in the presence of air barriers, the infiltration rate could be considered as a percentage of the one estimated by the current model. In alliance with this measure, an increased value of uncertainty should be associated to this estimation.

4.3.2 The main challenges of the sampling approach

In view of the constraints discussed above on the application of ISABELE/SEREINE methods to an entire MFH or TSB, a sampling approach could be considered. This approach consists in applying the method to sampled dwellings, in which a part of the building envelope is tested. It has the advantage to skip the issues related to the equipment volume. Since the tested area is equivalent to those of SFH, the ISABELE/SEREINE kits can be easily applied. Also the current aerologic model could be easily applied, since the blower door test could be performed in the tested apartment. In addition, the hypothesis on indoor temperature homogeneity would be applied as for SFH.

Nonetheless, new challenges come with this approach. Figure 4.18 illustrates the floor of a MFH, in which the protocol could be applied to the apartment in blue. The measured perimeter, inside the borders of the blue area, is composed of a part of the building envelope (in red) shared walls with other apartments (in green) and with the common area (in yellow). Depending on which floor the tested apartment is situated in the building, it can have either the envelope or shared walls above and underneath it. This highlights the two principal challenges of this approach. The first is related to the interpretation of the method indicator, since it would represent just part of the building envelope. In addition, this indicator might contain contributions of the thermal bridges that are shared between the tested and adjacent areas. The second regards the protocol and the estimation process, in how to assure that the flows passing through the shared walls do not affect the quality of the HTC estimation.

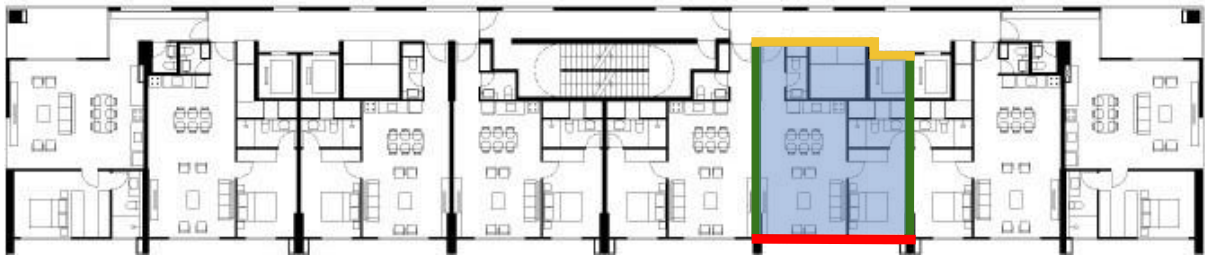


Figure 4.18 – Example of the measured perimeter and the boundaries in a sampling approach method application. Adapted from [212].

The walls between apartments and those leading to common areas can be isolated or not according to the building design. Although, when facing another heated area, they usually do not have insulation or they might have a thin layer for acoustic purposes. In any of those cases, the U-value of these walls would be comparatively higher to the exterior walls in high-performance buildings. For this reason, the heat flow passing through these walls can be considerable during a protocol application, depending on the temperatures applied on both sides of the wall. Since the objective of the method is to characterize the envelope, this flow, if not properly treated by the method, would be a parasite flow that could potentially influence the indicator estimation.

A study developed in the framework of IEA - Annex 58 applied a dynamic gray box methodology to identify the HLC from a part of a twin house [213]. In this study, the measured perimeter was also different from the building envelope. Even though it was conducted in the context of SFH, this shares the idea of sampling an area inside a wider building. It was verified that the envelope was responsible for just 30 % of the total HLC, which means that, if an important temperature gradient is applied between the two houses, considerable heat losses to the boundary zone inside the building would happen. A study addressing the thematic of energy performance gap in MFH, defended that the internal heat transfers, due to temperature differences between apartments, are an important explanatory factor of the household energy consumption. It was found that an apartment on the top floor would present the double of energy consumption than one in an intermediate floor, due to the larger surface-to-volume ratio with external walls [214]. Both of these researches highlight the importance of the flow passing through the shared walls in a building.

In addition of calling the attention to the internal heat flows in a building, the latter research raises another question concerning the sampling approach: in which parts of the building the test should be performed? A simulation study, in a master thesis about energy performance of MFH, concluded that the apartments situated in the angles of a building present a higher energy consumption than those located in the middle of it [215].

A simulation study from a master thesis concluded that one apartment situated in the corner

of the last floor of a MFH could consume 60 % more energy than one apartment situated in the middle of the building, considering both follow the same heating scenario [215]. The apartments and offices in a building can present different surface-to-volume ratio with external walls. In addition to this, the composition of the envelope may vary according to the chosen area to be tested. All these questions are further investigated in the following paragraphs.

4.3.2.1 Proposed solutions

Three main challenges were identified above in order to adapt ISABELE/SEREINE methods to a sampled apartment in a MFH or office in a TSB, namely:

1. Indicator interpretation
2. Sampling choices
3. Heat flow through the shared walls

4.3.2.1.1 Indicator interpretation

This issue is related to the difference between the tested and estimated perimeters during a protocol application. The first concerns the perimeter of the area in which the test was applied. The second concerns the parts of this perimeter that were aimed to have their thermal behavior estimated. To illustrate this problem, the total HLC coefficient of a sampled area is presented in equation 4.18.

$$HLC_{tot} = H_{inf_{tot}} + HTC_{ext} + HTC_{shar} \times \left(\frac{T_m - T_i}{T_e - T_i} \right) \quad (4.18)$$

where:

- HLC_{tot} is the heat loss coefficient of the total perimeter in a sampled are, including exterior and shared walls (W/K);
- H_{inf} is the coefficient of losses by air infiltration (W/K);
- HTC_{ext} is the heat transfer coefficient to the outside environment (W/K);
- HTC_{shar} is the heat transfer coefficient to neighbouring spaces (W/K);
- T_m is the temperature on the other side of the shared wall (°C);
- T_i is the indoor temperature (°C);
- T_e is the outdoor temperature (°C).

Usually, the HLC_{tot} of a tested area can be used to estimated the heat power needed to maintain a level of temperature differences between the indoor and the outdoor environments. For this reason, the temperature difference ratio (inside the parenthesis) is applied, accounting for the difference between the adjacent space and the exterior temperatures [216]. However, this

definition shows that the HLC of the whole tested area depends on T_m , which is not desirable for an indicator of building intrinsic thermal performance.

In cases where the walls separating apartments are insulated, one could aim to assess the performance of the whole measure perimeter. The HLC_{tot} and HTC_{tot} would have a similar meaning as the one for SFH. Although, an important insulation between heated areas is not the rule, since it does not result in significant energy savings. In these cases, it is harder to consider the HLC_{tot} or HTC_{tot} of the whole measured perimeter, in view of its dichotomous thermal behaviour. Although the measurement of such indicator would not bring major challenges for being estimated, it would not be representative of the intrinsic thermal performance of the building. In addition, the low insulation of the shared walls would induce to high HLC_{tot} and HTC_{tot} walls, that are not representative of the envelope thermal performance.

If the test is applied to estimate the building intrinsic thermal performance, that only depends on the building characteristics, an indicator related to the envelope of the tested area should be used, such as the HTC_{ext} or HLC_{ext} . In the end, this is the part of the building usually targeted by BETPA methods. Estimating the envelope thermal performance is also coherent with the original goals from ISABELE/SEREINE methods. However, this approach does not provide directly an indicator relative to the whole building envelope, but only to a portion of it. This problem is more of a theoretical concern about how and for what the indicator is going to be further used. An indicator is relevant if it gives a reference to understand the object in its context. Different possibilities can be envisioned for the interpretation of this value, as presented below:

- The direct use of the indicator with comparison among similar cases.
- The use of a threshold value for determining the thermal performance of a sampled area.
- The representation of the indicator per a area.

The first would make sense if many similar apartments are tested, so then the indicator itself would have a meaning regarding the quality of the envelope performance. The second would be inspired by tests like the blower door test, where a determined criteria is used to define the sampled areas and a threshold indicator value is associated to the tested area quality. Results with a performance below this reference would be considered out of the standards. This could be defined, for example, for a specific sampled space location in a large building.

Another possibility is to use different levels of envelope thermal performance to rate the its quality, using a surface indicator. The units of the HTC and the HLC are in Watts per Kelvin, and they normally represent the behavior of the whole building envelope. Instead, we could consider to divide the the HTC_{ext} by, for instance, the tested envelope area, so then it would represent a

equivalent U-value of the apartment's envelope. In this way, it could be compared to a reference scale, such as that from the new French Energy Performance Certificate from July 2021 [217], presented in table 4.1.

Table 4.1 – The insulation performance level as a function of the envelope's average thermal transmission coefficient (U_{bat}). Adapted from [217].

Insulation performance	U_{bat} ($W.m^{-2}.K^{-1}$)
Very good	< 0.45
Good	$0.45 < \leq 0.65$
Medium	$0.65 < \leq 0.85$
Poor	> 85

This approach is interesting when analysing the tested area envelope, but if the goal is to generalize the indicator to the whole building, it should be carefully interpreted. This surface indicator would not describe a unique building component, as usually for U-values, but it includes the thermal characteristics of multiple walls - potentially with different compositions - also of the thermal bridges and windows. For instance, if one aims to multiply such value by the total envelope area, this could mislead to an erroneous global indicator.

The pertinence of this idea depends on how the sampled area represents the whole building. If the aim is to use the surface indicator to represent the whole building, the percentage of the different components in the sampled area should be representative of the whole envelope. In buildings where the insulation of the walls and roof are in the same order this could be more consistently applied. Sampling different areas of a same building to achieve such representativeness of the whole envelope can also be considered. In case the goal is just to evaluate the overall insulation level of the tested area, this question would not be a problem.

Another option would be to divide this indicator by floor or living area. Although it would not give a reference for the whole building thermal behavior, it could be useful for the tenants and potential buyers of a space. This would emphasize the advantages of intermediate floors in the losses to the exterior. In these indicators per area, the use of HTC would be more pertinent, since it would be more contestable to divide the $H_{in,f}$ by a certain area. Going beyond this theoretical discussion, it is important to first assure that such approach is feasible and can provide reliable results to be further interpreted. This is the matter of the discussion in the points below.

4.3.2.1.2 Sampling choices

As mentioned before, the position of a tested area is an important criteria regarding the envelope sampling and it can potentially influence the heat flow taking place during an in-situ

test. This could also be thought as a matter of a proportion between the exterior and shared walls in the measured perimeter, depending on the test location. To address this problem we could define a surface ratio, as shown in equation 4.19.

$$\Gamma_{S_{ext-shar}} = \frac{S_{ext}}{S_{shar}} \tag{4.19}$$

Figure 4.19 presents some choices of sampling areas in a MFH. One idea would be, such as in case 1 of the picture, to aggregate different apartments until a level that is feasible and convenient to apply the test with the equipment kit. This would be an intermediate option between the global approach and the sampling approach applied to a single apartment. It would be less restrictive than the global approach, since the building do not need to be entirely vacant, the available apartments could be tested. This would allow more flexibility in the choices of the building envelope parts to be tested, with a representation potentially closer of its whole behavior. Multiple combinations of apartments and offices would be possible to compose the test measured perimeter. Although, the problematic would be similar to those of the global approach, concerning the size of the tested area and its availability for being tested.

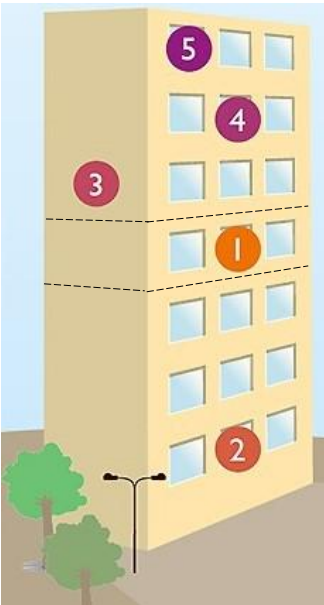


Figure 4.19 – Different possibilities for the tested areas in the sampling approach. Adapted from [218].

Another option, that would be more similar to a SFH protocol application is to test a single apartment or office in a large building per time. The location of the chosen area would then affect the parts of the envelope that are being tested and the surface ratio. The areas in the corner of a building, horizontally and vertically or both have a higher surface ratio than those

in the middle of the building. Continuing to analyse the mid-rise building from figure 4.19, it could be chosen a area in the ground floor (case 2), so then the low part of the envelope is tested and also sections of the exterior wall. An intermediate apartment in the horizontal corner could be chosen to just test the walls and in the same time have (case 3) two tested façades. A horizontal and vertical intermediate area (case 4) presents the lower surface ratio among the possible tested locations. Contrary to this an area located in a horizontal and vertical corner would present the higher surface of exterior walls in the tested perimeter. For instance, case 5 would have a high surface ratio, but also test the roof and the walls of the building.

The choice of the tested area would be then subjected to three main factors:

1. Their availability for testing (vacancy);
2. The parts of the envelope aimed to tested (roof, walls, ground floors, openings);
3. The surface ratio of these areas.

The first and the second items are dependent on the available conditions for test and its goals. They are more related to a practical character of the method application than to its scientific background. The last item could be though influential in the method quality, what need to be further investigated. This part would be better set with simulations, to define the potentials and limits of applying the test in different parts of a building. Section 6.2 presents a study developed to investigate this question. Coming to this topic, next section addresses exactly the use of simulations to develop the method for its application to large buildings.

4.3.2.1.3 Heat flow through the shared walls

As shared walls have typically high U-values, they can be crossed by a large heat flow during the protocol application. We could represent the term relative to the transmittance through the shared walls (HTC_{shar}) from equation 4.18, so then each HTC element is detailed in the form from equation 3.2. This can be seen in equation 4.20.

$$HTC_{shar} = \sum_{m=1}^s \left(\sum_{j=1}^p \psi_j L_j + \sum_{k=1}^q \chi_k + \sum_{l=1}^r U_{sharl} A_l \right) \quad (4.20)$$

where:

- ψ_j is the heat flow of a linear thermal bridge (j) [W/(m.K)];
- L_j is length of a linear thermal bridge (j) [m];
- χ_k is the heat flow from a point thermal bridge (k) [W/K];

- U_{shar_l} is the thermal transmittance of an homogeneous part of a shared wall (l) [W/(K.m²)];
- A_l is the area of an homogeneous part of a shared wall (l) [m²].

The HTC_{shar} is the sum of the HTC from the different shared walls (m) in the tested area. In the hypothesis the shared walls are poorly insulated, the effect of thermal bridges could be negligible and equation 4.20 could be simplified. In this case, in steady state condition, the heat flow going to adjacent spaces would be described by equation 4.21.

$$\phi_{shar} = \sum_{m=1}^s \left(\sum_{l=1}^r U_{m_l} A_{m_l} \times (T_m - T_i) \right) \quad (4.21)$$

If the terms of the equation 4.21 are measured or estimated, the steady state flow among neighbours could be estimated. If the temperature in both sides of the wall are stable, this hypothesis could be considered. This heat flux could be therefore represented in the RC thermal models by adding a power source ϕ_{shar} connected to the indoor temperature node, such as in the figure 4.20.

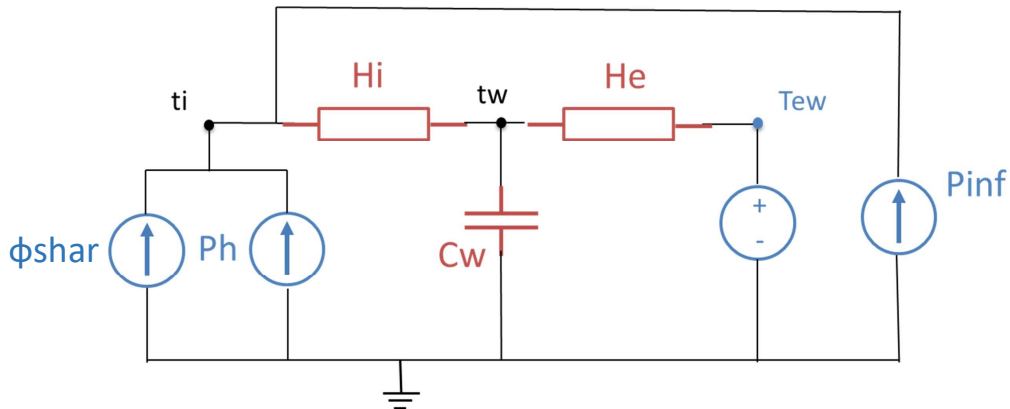


Figure 4.20 – Example of a RC thermal network model with the addition of a power source ϕ_{shar} to represent the neighbour heat flow. Adapted from [219].

However, the estimation of ϕ_{shar} can be hampered by the lack of information on the shared walls. In many field cases, there is not an extensive description on the shared wall thermal characteristics, assuming then an U-value for them could be then a challenge. The less information is available about this variable, the more uncertainty should be associated to it. The bias associated with the U_{m_l} value could be associated with the level of knowledge available on the thermal characteristics of the walls. In general, one could assume five levels of prior knowledge associated with this value [219]:

1. Any previous knowledge on the shared wall

2. Presence or absence of insulation by site inspection.
3. Type of shared wall by site inspection and date of construction of building (typical materials).
4. Detailed description of the shared wall materials : thickness (e_{mat}) and thermal conductivity (λ_{mat}).
5. Identification test carried out beforehand on the walls.

In the French Standardised Summary of the Thermal Study (RSET), which is mandatory for new buildings, the information on the shared walls is not available. If no further documents are available about these walls, it could be aimed to get more information by inspection during the in-situ test. A U-value based on a professional knowledge of the types of walls, the ranges of thicknesses used and the conductivity of the materials could be used. Depending on the site possibilities, it would be either the first, second or third case. Anyhow, a wide bias should be thus associated with the U_{m_i} value, which would be potentially degrade the HTC_{ext} result.

A more optimistic situation would be when the thermal characteristics of shared walls could be detailed in the new or retrofitted buildings' project documents. In this case, a theoretical U-value could be calculated to these walls according to equation 4.22.

$$U_{shar} = \left(\frac{1}{h_1} + \frac{1}{h_2} + \sum_{mat=1}^n \frac{e_{mat}}{\lambda_{mat}} \right)^{-1} \quad (4.22)$$

The following usual surface exchange coefficients h_1 and h_2 could be considered according to the wall position:

- $h_1 = 5.9 \text{ W/m}^2/\text{K}$ and $h_2 = 10 \text{ W/m}^2/\text{K}$ for intermediate floors
- $h_1 = h_2 = 7.7 \text{ W/m}^2/\text{K}$ for vertical shared walls

In this case, differences between actual and design performance must still be taken into account. As a security option, an uncertainty of the order of 20 % in U_{shar} could be considered. Going beyond this, the thermal transmittance of the shared wall could be tested separately, using a dedicated method to wall characterization. This would give a more accurate U-value for these walls, although this implies extra steps and complexity to the protocol. Moreover, even for the best level of information, there is still an uncertainty associated with this value. The effects of measurement sampling on the wall and non-uniformity have to be considered.

Considering the other terms of equation 4.21, the surfaces of the shared walls must be collected manually in-situ or calculated from the area blueprints. In addition, the temperatures

need to be measured in each side of the wall. This would be subject to the availability and authorisation of the neighbour for implementing a temperature sensor. Depending on the intervention possibilities in the adjacent areas, it could be adopted a temperature level similar to that of the tested area, so then the flows passing through the shared walls would be minimized. But even in this case an uncertainty should be associated to this flow, which could bring high uncertainties in the final result. In the contrary, if the neighbouring areas are not heated, the flow passing through these walls would be significant relative to the power required to carry out the test. This will thus have a bigger impact and if not well taken into account by the model, would affect the exterior HTC estimation. It should be considered that there is an uncertainty associated with the temperature measurement of the neighbouring dwellings and the U-values of its walls.

Another possible solution would be to directly measure the heat flow passing through the shared walls during the in-situ test. This could be done with the use of heat flow meters in each of the shared walls. The advantage of this option would be taking into account the dynamic phenomena in these walls. Also, this estimation method would release the constraint on the instrumentation and/or immobilisation of the neighbouring dwelling. However, it would imply more equipment and complexity of the protocol application. The number of heat flow meters to be installed can be difficult and time consuming during protocol installation. More man-hour should be available for this operation, in comparison to a test using just the standard equipment kit. The number of sensors would increase with the shared walls areas, which could be troublesome in spaces with a small ratio $\Gamma_{S_{ext-shar}}$. In addition, the fixation of the sensors could leave marks on the walls, which can be not well accepted by the dwelling tenants.

A question that is also raised is the capability to estimate the heat flow passing through a wall by the measurement at specific points. In walls presenting important heterogeneity along the area, or with defects in specific points, this could be problematic. An infra-red camera could be used before the test to make a diagnosis of the different areas of each wall. The uncertainty associated to these measurements will be addressed with experimental work in section 6.4.

In this work, the steady state hypothesis for neighbours flow estimation will be called *indirect method*. The second option, with the measurements through heat flow meters, will be called *direct method*. Table 4.2 shows a comparison on the benefits and drawbacks of each of these methods. Both of these methods for estimating the neighbours heat flow are further investigated in chapter 6.

Table 4.2 – Benefits and drawbacks of the methods for taking into account the neighbours heat flows. Adapted from [219].

	Indirect method	Direct method
Measured quantity	Temperature	Heat flow
Benefits	<p style="text-align: center;">Technical simplicity:</p> <ul style="list-style-type: none"> - No new types of sensors added to the kit. - Additional temperature sensors to neighbours with wireless communication. - Protocol implementation time comparable to that of a SFH. 	<p style="text-align: center;">Precision (to be confirmed):</p> <ul style="list-style-type: none"> - Neighbour heat flow directly measured, avoiding estimation errors. - Measurement uncertainty of the flow associated with the quality of the measurements: possibility of reducing the uncertainties of the indicator. - Consideration of the shared walls inertial behavior: suitable for heavy walls (e.g. concrete partitions). - Measurements a priori independent of neighbours availability or agreement. - Temperature measurement in neighbouring dwellings not required.
	Drawbacks	<p style="text-align: center;">Uncertainty:</p> <ul style="list-style-type: none"> - Neighbour flow calculated from an estimated data. - Accuracy of the U-value estimate depends on the information available on the shared walls and its quality. <p style="text-align: center;">Access to neighbouring areas:</p> <ul style="list-style-type: none"> - Need to measure temperatures in neighbouring areas. - Dependent on their agreement and availability.

4.4 Strategy for testing the approaches

In order to study the strategies proposed in the section above, they must be tested under different conditions to verify their pertinency domain. Real test applications are costly and time demanding. They imply at least an available vacant building where the protocol can be applied. In addition, it might be a new or retrofitted building, for which the envelope quality is aimed to be verified. Usually more efforts are made to know in detail the quality of a good solution, since by simple inspections a bad solution can be identified, with no need of further investigation. Furthermore, in-situ measurements imply transport and installation of equipment, bringing a logistic dimension to the tests. For reasons of availability, costs and all the difficulties associated

to real tests, they are going to be applied in a more advanced step of the protocol investigation.

Initially for testing the different approaches, energy dynamic simulations seem to be the most adapted solution. Software for dynamic building simulation are a white-box modelling tool, where very detailed information on building physical properties are combined with descriptive equations to simulate the building's thermal behavior. Different software are available for these goals and there are recognized methodologies, such as Bestest - that is based on ASHRAE standards [220, 221, 222] - and others [223], to validate their capacity to accurately simulate reality.

In the subsection 4.4.1 we describe how the virtual experiments were conducted: the chosen software for dynamic building simulation and the reference model used for the study. Later, in subsection 4.4.2, we present the assets of in-situ method applications.

4.4.1 Virtual experiments

The virtual experiments were simulated with the software PLEIADES and COMFIE. They were created in the beginning of the 90s' [224] in a reference French research center: the present ETB group ("Eco-conception et thermique des bâtiments") of the CES ("Centre d'Efficacité énergétique des Systèmes") part of the ARMINES grouping [225]. PLEIADES is the software used for the realization of digital models and COMFIE is used for the dynamic thermal simulations. In this work we call the ensemble of both as P+C.

These software have been maintained by the editor IZUBA Energies [226] and refined through different initiatives [227] over the years. They are broadly used in French BEP context and have been already verified and validated [228, 229, 90]. It is considered a reliable tool for simulating a BETPA method application. A license on this software was provided by ARMINES and IZUBA for the development of the present work. The simulation with features going beyond the possibilities of the commercial version of the software were performed by ARMINES.

4.4.1.1 Model

MFH and TSB can widely vary in size, shape and construction technique. A detailed analysis of the French residential building stock was done in 2017 [230]. Table 4.3 shows some information present in this report regarding the building type and representation in the MFH building stock. A column regarding their size category was added concerning the typical number of floors in each one of the different MFH building types. Mid-rise MFH are those presenting from 4 to 8 floors, low-rise refer to those inferior to this and high rise to those superior

Table 4.3 – Analysis of French MFH building stock in 2017 by building type and size category

Construction period	Building type	Quantity	Size category
Before 1948	Building "de bourg"	11%	low-rise and mid-rise
	Hausmannian building	10%	mid-rise
	Eclectic building	4%	mid-rise
	Building HBM	1%	mid-rise and high-rise
1948 – 1974	"Pastiche" building	3%	low-rise
	"Bourgeois" building	2%	mid-rise
	Intermediate MFH	3%	low-rise and mid-rise
	Various small collective	20%	mid-rise
	"Bars"	12%	high-rise
	Towers	< 1 %	high-rise
1975 – 2000	Intermediate MFH	1%	low-rise and mid-rise
	Various small collective	5%	mid-rise
	"Bars"	6%	high-rise
	Towers	< 1 %	high-rise
	MFH from 1982 to 1989	8%	mid-rise and high-rise
	MFH from 1990 to 2000	11%	mid-rise and high-rise

According to this data, the French building stock of MFH is strongly represented by mid-rise buildings. Although many other building sizes should be considered, this choice seems then to be a coherent attempt to study BETPA applied into MFH. A PLEIADES model of a mid-rise MFH with 16 apartments was provided by ARMINES. This model was based on a real 4 story building from a French city close to Lyon. The original building was built in 1978, and has undergone a massive retrofitting in 2012. The energy consumption before work was classified from French DPE as class E (231 to 330 kWh/m²/year) and after retrofitting it became class B (51 to 90 kWh/m²/year) [231].

Regarding the PLEIADES model, its structure and type of materials were kept the same as the original one. However, the level and position of the insulation and the thermal bridges values were modified to correspond to a high-performance building envelope in the present standards for renovation. Table 4.4 shows the global characteristics of the building model with the main areas of interest. Figure 6.11 shows the 3D vision of the PLEIADES model.

Table 4.4 – Global characteristics of building model in Pleiades Modeller

Whole building	
Number of apartments	16
Total living area (m ²)	1048
Ground floor area (m ²)	354
Exterior wall area (m ²)	799
Total envelope area (m ²)	1508



Figure 4.21 – Axonometric view of the building model in Pleiades Modeller

4.4.1.1.1 Characteristics of building components

For the components of the building, the material properties (such as λ , C and ρ) proposed by the standard library of P+C were used. The walls compositions are based on references for high-performance retrofitted buildings [232]. In the beginning, the values of the thermal bridges were kept from the original model, with more optimistic values that could be thought for a new building. Later, the prescriptions from the French thermal regulation for existing buildings [233] were used to define these values, according to each type of insulation, thickness and thermal resistance of components. The details on the building components thermal properties are presented in Annex B.

4.4.1.1.2 Reference indicators

A very important asset of virtual method applications is the possibility to have a known value for the final indicator. In a virtual test, the environment can simulate both real and controlled conditions. The combination of a totally controlled heating scenario with a stable outdoor condition allows to put the building in a steady state. This way, indicators representing building envelope static thermal properties, such as HLC and HTC, can be precisely calculated. This enables to verify the outcomes from the different tested strategies and gives a powerful tool for quality criteria. The reference value for each tested case is shown in the dedicated chapters.

4.4.1.2 Energy dynamic simulations

As previously mentioned, one of the advantages of using a virtual environment is the possibility of trying a method under different configurations. When adapting a method to a new domain, we should resist to draw conclusions from one single simulation. Although a single

simulation can provide a starting point for comparison, it seldom allows a full comprehension of a system's natural tendencies. Model experimentation is preferably done in an exploratory way by trying different simulations to help to understand the trends of a system [198].

By comparing multiple simulations, we can study the method limits and have insights on its behavior in a specific model. For this reason, multiple experimental plans were performed for global and sampling approaches. Each experimental plan tries, in an exploratory manner, to see the behavior of the method when the protocol or the estimation process are modified. The experimental plans present variations of many simulation parameters. The main studied parameters regards the protocol temperatures and the weather conditions. The idea is both to develop the method and to study its pertinency domain. The simulations done to address these problems are presented in details inside the chapters dedicated to each one of the approaches (Chapters 5 and 6). In this part we focused on the common assumptions done for these simulations.

All the simulations were performed using weather files from the Thermal Regulation 2012 (RT2012), from French cities such as Trappes, Nancy, La Rochelle and Nice. In the simulations with solar gains, it was considered an equivalent outdoor temperature, as in a real protocol application it would be measured by SENS sensors. For the calculation of T_{em} , the equation 4.12 was simplified, reducing the term related to the form factor, as in equation 4.23.

$$T_{em} = T_{out} + \frac{\alpha_s \times I_s}{h_c + h_r} \quad (4.23)$$

The absorptivity coefficient of the exterior wall α_s is set to 0.6, since it is the value related to the exterior walls in this PLEIADES model. The solar irradiance (I_s) was calculated for each direction and inclination of exterior walls and roof. In COMFIE algorithms manual, radiant and convective heat transfer coefficients are combined into a global coefficient that depends on the surface position and its emissivities. The values present in the manual are listed in table 4.5. The emissivity of all exterior surfaces of the model is 0.9 and it was considered normal wind conditions for the h_{ext} .

The T_{em} calculations were developed in order to assure that the hypotheses of the method are respected in the virtual test application. It is important in virtual tests to have consistent assumptions and data transformations providing sufficient amount of data. The ISABELE/SEREINE runners provide two possibilities for the data time step: five minutes and one hour. The first simulations done in this work were based on a time step of one hour, since the idea was to have a global vision on the system behavior. In the commercial version of P+C, this is the minimum time step for the simulations outputs. Once the dynamic behavior of the

building was aimed to be further investigated, the simulation time step was changed to one minute and this data was later averaged to five minutes. In these cases, the simulations were performed directly by ARMINES, that had the possibility to change the output time steps.

Table 4.5 – Combined radiant and convective heat transfer coefficients for surfaces in COMFIE software [234]

Position of the wall	Emissivity	h_{int} [W/(m ² .K)]	h_{ext} for the wind exposure [W/(m ² .K)]		
			normal	sheltered	severe
Vertical	0.9	8.13	18.2	12.5	33.3
	0	3.29	14.9	9.1	33.3
External ceiling	0.9	9.43	22.2	14.3	50
	0	4.59	18.9	11.1	50
External floor	0.9	6.67	20	20	20
	0	1.78	20	20	20
Horizontal internal	0.9	8	-	-	-
	0	3	-	-	-

4.4.2 In-situ experiments

Once the methods were tested in a virtual environment, the limits of these methods were studied and then protocols were applied in real buildings could be developed. Since the aim is to develop an applicable method for MFH and TSB, the in-situ tests are important to verify their feasibility in real life. Differently from virtual experiments, difficulties regarding equipment and measurements can appear on site. It is relevant to have the real dimension of these difficulties and to acquire experience to face them. Both global and sampling approaches, were applied in real buildings at least one time. The results of these in-situ tests can be seen in the following chapters regarding each approach.

4.5 Strategy for analysing the results

In order to improve the method in the context of large buildings, multiple energy dynamic simulations were performed. The experimental plans enable to qualify the method results according to the protocol and the estimation process used. In the interest of this analysis, it was necessary to first define result quality indicators to be used to understand the method behavior with the different input data. The used quality indicators are presented in subsection 4.5.1. With these tools, it was possible to perform a process to study and improve the method, which is discussed in subsection 4.5.2

4.5.1 Result quality indicators

Since the virtual model provides a reference value for HTC, it is possible to apply criteria to analyse the quality of the method. In this work a comparative testing of the estimation process output with the reference value is used as a relative test. To analyse the relative difference of the estimated HTC to the reference, the bias, defined in equation 4.24, was used. The closer this value is to zero, the more accurate is the test result.

$$bias = \frac{HTC_{ref} - \widehat{HTC}}{HTC_{ref}} \quad (4.24)$$

Besides a low bias value, it is desirable that the estimation output present a limited level of uncertainty to have more precise results. As explained in part 4.2.2.6, the uncertainty of the indicator is represented as the percentage difference between the center and the borders of the 95% confidence interval (I95) of the result. Different from the bias, the uncertainty does not take into account the reference value, it is only relative to the estimated indicator and the dispersion of its probability density. Initially in this work, a threshold of 15 % in the bias and 35 % in the uncertainty were considered to defined a result as acceptable. Therefore, a result that respects both conditions would have an acceptability of 1, as shown in equation 4.25.

$$acceptability(bias, unc) = \begin{cases} 1, & \text{if } bias \leq 15 \% \wedge unc \leq 35 \% \\ 0, & \text{otherwise} \end{cases} \quad (4.25)$$

Since the acceptability is a dummy variable, it has the advantage to separate the results into two groups and allows an easy understanding of the method behavior under different conditions. However, this analysis criteria lacks sensibility on the level of the results quality. In figure 4.22, the results of four different (a,b,c,d) tests applied in a same dwelling are presented. The reference HTC value is the same for all of them (in red), the bias percentage is presented besides the estimated HTC (vertical blue continuous line). According to equation 4.25, the test (a) would not be acceptable, since its bias is superior to the 15 % threshold. Tests (b), (c) and (d) respect both criteria of this equation and would be therefore considered as acceptable. However, by visual inspection, it is evident that the distribution (b) shows more similarities with the test that was rejected (a) than with the test (d) that was also accepted. The latter presents a notable lower bias and also a reduced uncertainty, being a high quality result. Therefore the lack of information on the level of quality of the results is a drawback of using this variable in this analysis that is essentially multi criteria.

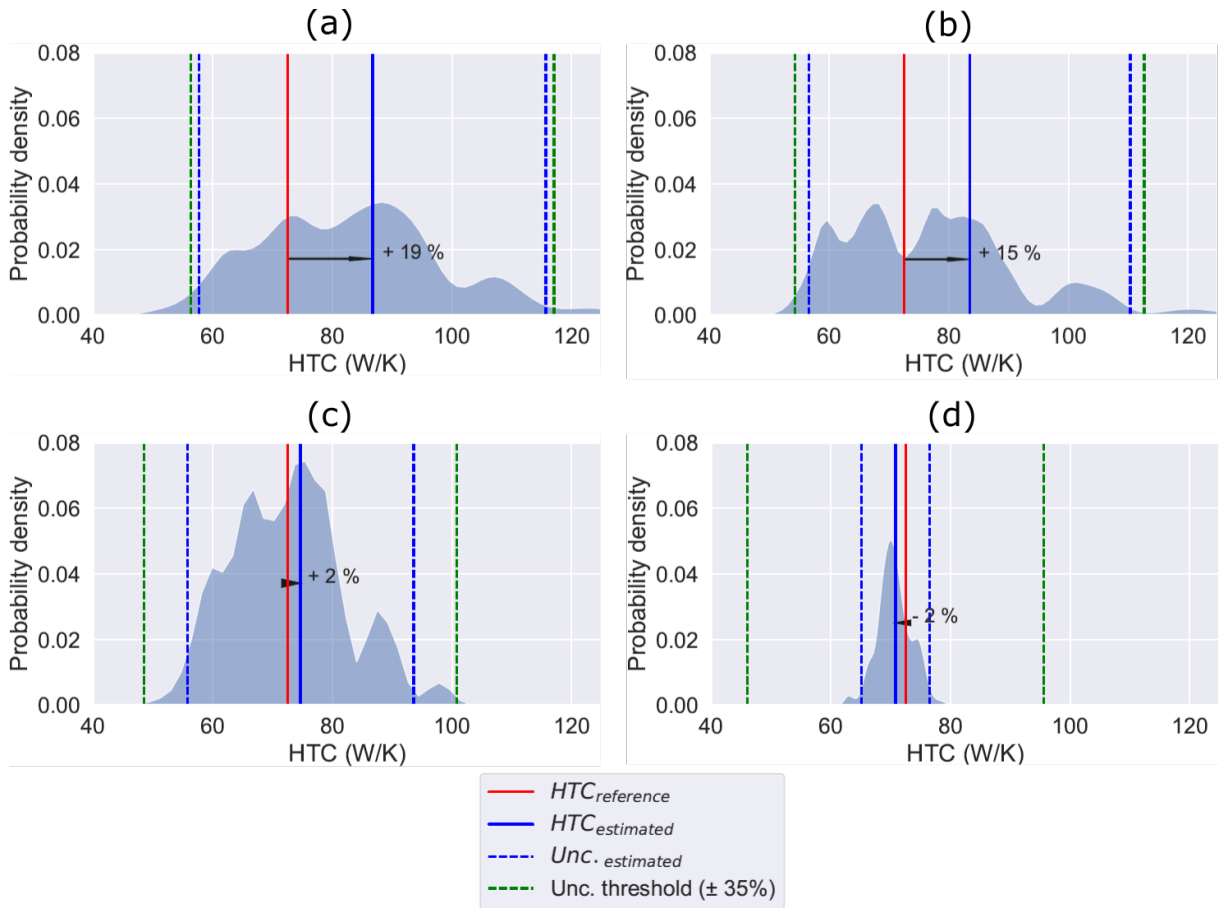


Figure 4.22 – The probability density of four different tests with the results bias and uncertainty

In order to access the information from the result probability function, another variable inspired in a recent work from Sarah Juricic [235] was considered further in this work as a quality criterion. This is the interpretability indicator that represents the intersection of an interval centered in the reference indicator value and the probability distribution of the estimated result. This variable can assume continuous values between 0 and 1, since the maximum area under the probability density function is equal to 1.

Figure 4.23 shows a graphic representation of the interpretability indicator for an interval of $\pm 15\%$. The value of this indicator is equal to the value of "b" minus "a" in the cumulative distribution function of the result. The interpretability is mathematically expressed in equation 4.26, where $f(x)$ is the result probability density function and i is interval range that is been analysed (in the example above it is 15%).

$$interpretability = \int_{HTC_{ref}(1-i)}^{HTC_{ref}(1+i)} f(x) dx \quad (4.26)$$

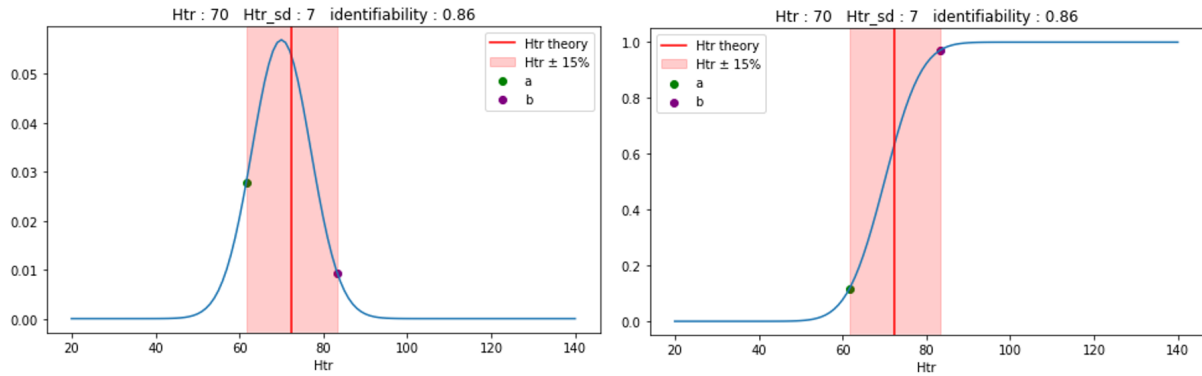


Figure 4.23 – Representation of the interpretability indicator with cumulative distribution function and probability density function of the result [236]

In figures 4.24 and 4.25 the same cases from figure 4.22 are again graphically presented. Here, the HTC estimation, uncertainty and the interpretability are presented in the top of each case. The intersection of the cumulative distribution function with the $\pm 15\%$ interval are shown. The results quality from cases (a) and (b) are closer and much inferior than those from cases (b) and (d). This highlights how the use of the interpretability, when compared to the acceptability, gives a clearer vision on the results quality. Another advantage of this quality indicator is to resume the effects of the bias and the uncertainty into one unique value.

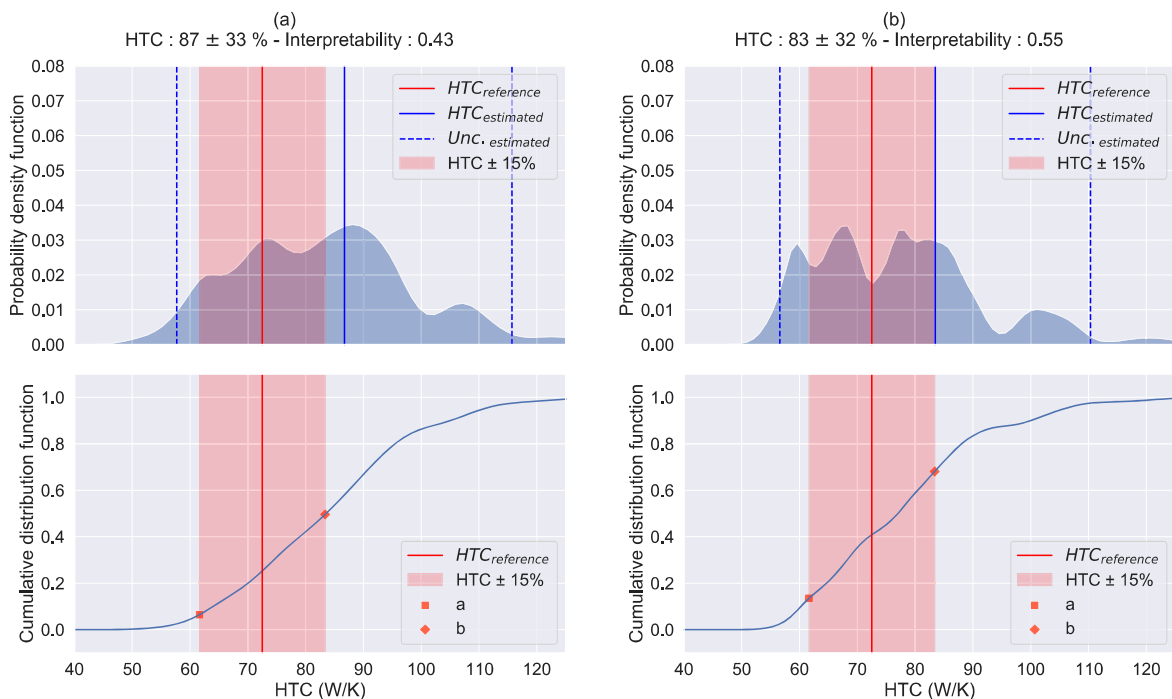


Figure 4.24 – Representation of the interpretability indicator with the cumulative distribution function and the probability density function of the result for the cases a and b.

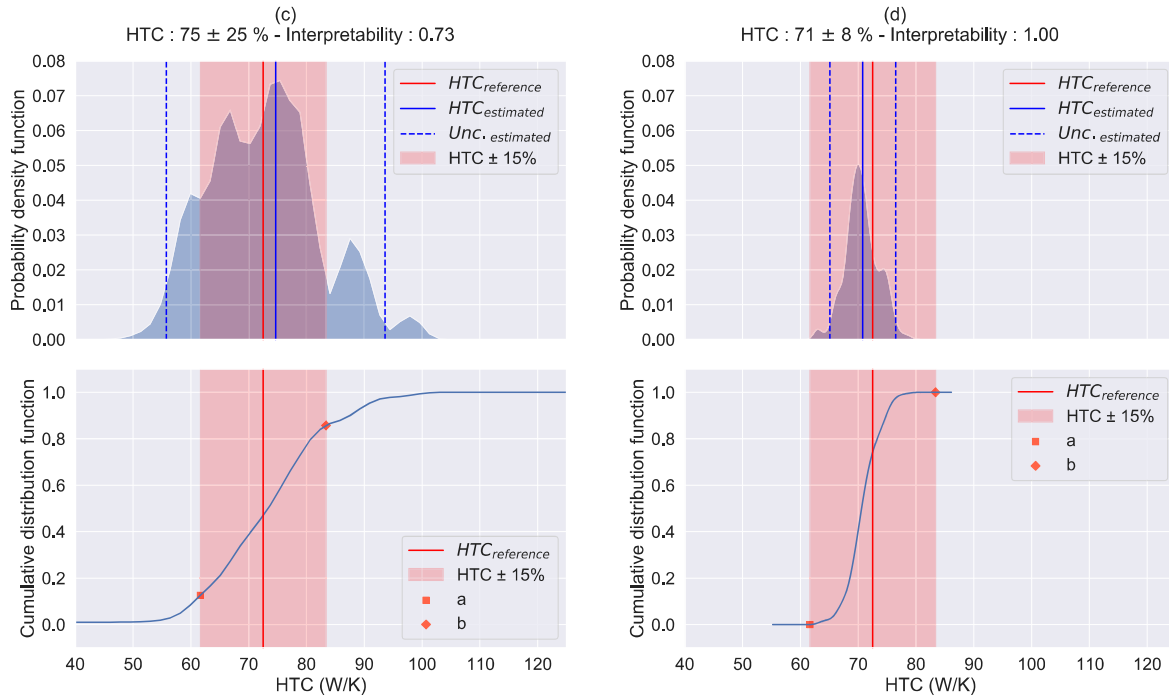


Figure 4.25 – Representation of the interpretability indicator with the cumulative distribution function and the probability density function of the result for the cases *c* and *d*

The interpretability indicator shows the nuances of results quality through a continuous variable. However, when studying the method through multiple tests, a continuous variable might not be the easiest way to estimate if the method performed well enough. In this case, a threshold value for the interpretability could be defined to facilitate the analysis of the results quality. The combination of both criteria can be applied, using first the results from the acceptability to define the group of acceptable results. The minimum interpretability value in the acceptable results group, can be used as a threshold for this continuous variable.

4.5.2 Method improvement process

In the virtual tests, where a reference for the estimation results is available, this value can be compared to verify the capability of the whole method to achieve a reliable result. Once the result of one test is analysed, an iterative process can be applied to improve the method and to study its limits. This opens doors to a cycle of method improvements, where the quality of the outputs is a way to access the whole process quality, as presented in figure 4.26.

The analysis of each test from an experimental plan can be seen as an iteration of this cycle. This process could be repeated multiple times, so then a better understanding of the influential parameters on test quality can allow to adapt either the protocol or the estimation process. Aspects in the protocol, such as its duration and the heating scenarios were vastly studied in the experimental plans. Concerning the estimation process, mainly in the sampling

approach two different alternatives were tested, that are presented in the dedicated chapter of this approach. The method limits regarding the weather conditions were also studied in the case of this approach.

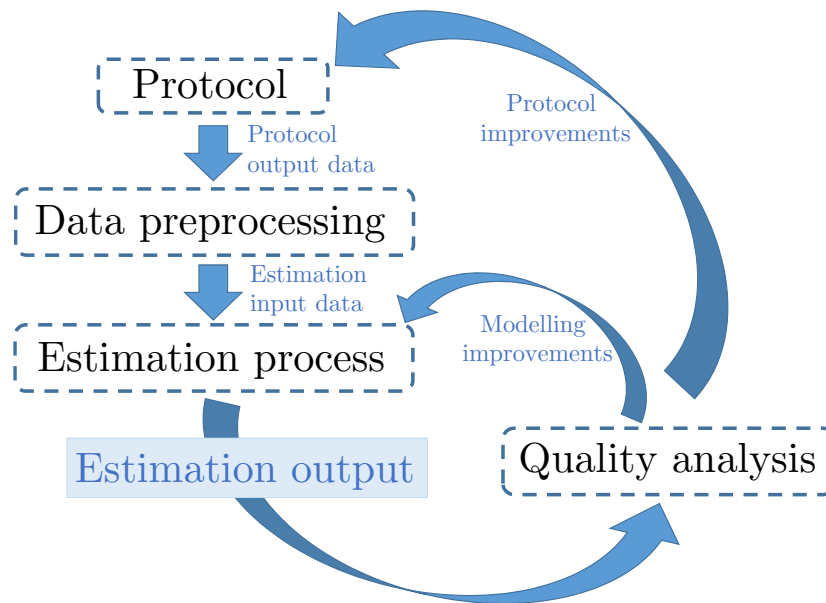


Figure 4.26 – General representation of a method improvement process based on model result quality

The following chapters are showing the results of the exploratory attempts used to understand the method limits and potentials, to finally propose possible solutions to various conditions. Since the different alternatives present advantages and drawbacks, multiple methods are studied and proposed, being suitable to different situations. All this investigation process is the subject of discussion in the following chapters.

4.6 Chapter conclusion

BETPA methods are composed by a protocol and an estimation process that should be aligned to identify the thermal behavior of the building envelope. They are conceived to certain building types and test conditions in which their results are valid. Their pertinency should be investigated if applied to other building types and conditions.

ISABELE/SEREINE are complex methods composed of an extent estimation process to model the thermal phenomena taking place during a test. ISABELE was initially conceived to be applied to SFH and the adaptation for building of larger bring new subjects to be treated, of a technical, scientific and operational nature. To allow a measurement on a majority of operations, two measurement approaches are proposed: a measurement on the scale of the whole building (global approach) or on parts of it (sampling approach). Each approach has different advantages

and disadvantages and both are investigated in this work.

The global approach has the advantage to analyze the envelope of a building in its entirety, but at the cost of many conditions, such as the entire building must be released for several days. This would limit the applicability of this approach on the field in some cases. The large size of the measurement area also implies changes in terms of the equipment used in the test. A possibility is the use of the existing heating system to reduce the volume of material to be transported to the site. This solution depends though on the condition of local heating system and on the possibility to measure the power delivered during the test.

In contrast, in the sampling approach, the tested area has similar dimensions to SFH, which facilitates the protocol application. However, the presence of thermal flows towards the adjacent spaces can hamper the HTC and HLC estimation. This heat flow can have a significant impact on the measured indicator and for this reason it need to be well estimated. Two approaches are proposed to estimate this heat flow: the indirect and direct methods. In the first the temperature of the adjacent spaces are measured, in the second the flow is directly measured by the use of heat flow meters.

In order to study the proposed solutions, numerical simulations are used with the advantage of having a known indicator reference. This allows the use of result quality indicators, which are applied to verify how well the whole method performed in a certain scenario. In chapter 5 and 6 these approaches are further investigated.

Chapter 5

Global approach

Contents

5.1	Characteristics of local heating system	106
5.2	Dynamic thermal simulations	111
5.2.1	Reference indicator	112
5.2.2	Experimental plan	112
5.2.3	Results analysis	114
5.2.3.1	Dispersion of results	114
5.2.3.2	Acceptable results	117
5.2.4	Discussion	122
5.3	In-situ test	122
5.3.1	Site description	122
5.3.2	Implementation of equipment in-situ	123
5.3.3	Estimation algorithm results	126
5.3.3.1	HLC indicator	126
5.3.3.2	Air infiltration estimation	128
5.3.3.3	HTC indicator	130
5.3.4	Discussion	131
5.4	Chapter conclusion	132

In this chapter the global approach is further discussed. In section 5.1, a discussion on the local heating systems and the possibilities they could offer during ISABELE/SEREINE method application are presented. Later, in section 5.2, virtual applications of the method with variations

in some of the protocol parameters are presented. The idea in this section is to study the method behavior in a large building and the optimal protocol configuration for it. Subsequently, in section 5.3 the results of an in-situ test applied to a low-rise MFH are shown. Finally, in section 5.4, the main conclusions on the global approach are exposed.

5.1 Characteristics of local heating system

As presented in the former chapter, the use of the local heating system can be a strategy to reduce the equipment used for protocol application. Multiple heating system technologies can be present in MFH and TSB, offering different possibilities concerning the system control and heat measurements.

A heating system consists of three main parts: heat generator, distribution system and heat exchangers [237]. In order to better understand the possibilities it can provide for an in-situ test, it is necessary to know the technologies that are used locally. Table 5.1 presents some common types of solutions for heating system components.

Table 5.1 – Some of the possible technologies for the local heating system components

Generators					
<i>Boiler</i>	<i>Heat pump</i>	<i>Joule effect</i>	<i>Stove</i>	<i>Hot air generator</i>	<i>District heat</i>
Gas	Air/water	Electric	Biomass	Combustion	-
Oil	Water/water		Coal	Electric	
Biomass	Air/air		Oil or LPG		
Electric	Geothermal				
Distribution systems					
<i>Hot water network</i>		<i>Refrigerant distribution</i>	<i>Air network</i>	<i>Natural air circulation</i>	
Medium or low temperature (<65°C)		-	-	-	
High temperature (65°C)					
Heat exchangers					
<i>Joule effect</i>	<i>Hot water radiator</i>	<i>Hot air blower</i>	<i>Radiant ceiling</i>	<i>Heated floor</i>	<i>Other</i>
Convector	Medium or low temperature	-	-	-	-
Radiant panel	High temperature				
Other					

Two main types of installations can be adopted in large buildings: centralized or decentralized. In the first case the heating system is conceived for the whole building, typically with one or more generators placed in a common area. The distribution system crosses the building to deliver heat from the generator to the heat exchangers located in each heated area. In the decentralized installation, the heating system is conceived for each apartment or office.

The ENL survey (in French "*Enquête Nationale Logement*", in english national housing survey) has been conducted since 1955 and the in 2013 it accounted 27,000 interviews. It is the major statistical source for describing the French residential building stock and the conditions in which households occupy their main residence [238]. In the ENL survey from 2013, the share of centralized heating systems in MFH is 42 % [239], the absolute values are presented in table 5.2.

Table 5.2 – Distribution of heating system installation type in SFH and MFH (%) according to ENL database.

<i>Heat installation</i> <i>Typologie</i>	SFH	MFH	Total
Decentralized system	14 139 751	6 720 264	20 860 015
Centralized system	49 796	5 060 919	5 110 716
Independent devices	1 432 532	329 357	1 761 889
Others or no heating	259 525	67 650	327 176
Total	15 881 604	12 178 191	28 059 795

Another data source is the PHEBUS survey developed by the French ministry of ecological transition, provides statistics on fuel poverty and vulnerable populations are over-represented in it. The building heating system, among other topics are described in this survey [240]. The survey took place in 2012 on 2,300 housing units, from which 690 were located in MFH. The centralized systems represent 30 % of cases for MFH in this survey. Since the size of the PHEBUS MFH sample is not as vast as for SFH, and the total sample is smaller than that from ENL survey, the statistics in this part are based on the latter. No survey data was found on TSB heating systems types, although it can be expected an expressive share of centralized systems in this building typology.

The centralized installations are more adapted to be integrated in the test protocol, since the control and the measurement can be done in one single place. In case of decentralized systems, it need to be done on the multiple systems present in the building. This operation can be complicated, depending on the number of dwellings and the required equipment.

The type of installation and components in a heating system should be verified previously to a protocol application in a large building, defining the way to control and measure the heat delivered during the test. Figures 5.1 and 5.2 present the main technologies used in the generator in MFH, according to ENL survey.

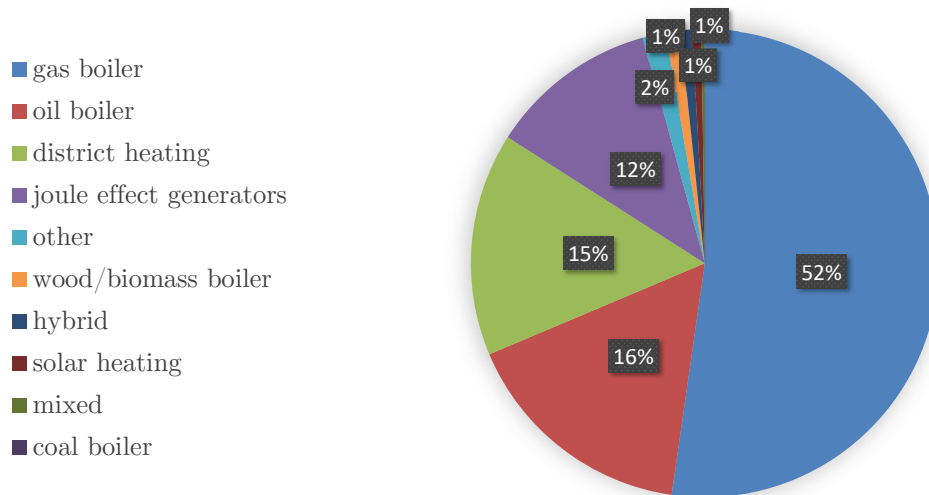


Figure 5.1 – Distribution of generator types for centralized heating systems according to ENL database.

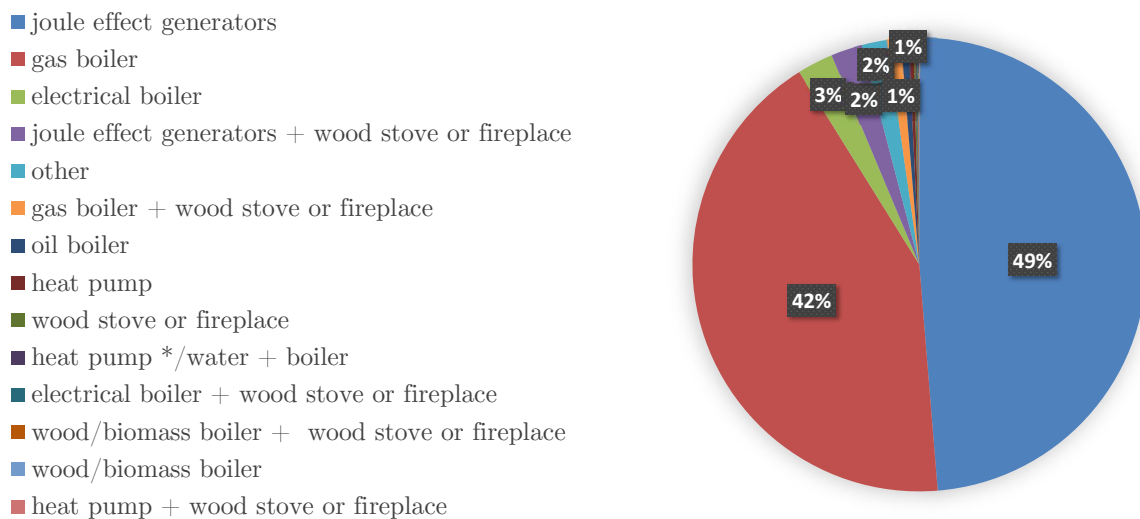


Figure 5.2 – Distribution of generator types for decentralized heating systems according to ENL database.

Boilers and district heating represent the majority among centralized systems. While for decentralized systems, the electrical heaters account for half of the studied sample, followed by boilers with various fuels.

When preparing a protocol application using the global approach, the possibility of operating the heating system should be guaranteed during the test. The generator of a central heating system may be located in a locked area for security reasons, and its operation might need the intervention of an external professional. In case of district heating, the substation connecting the main network to the building's own heating system should be accessible. Setting the temperature for a test include actions in the generator, but can also include the regulation of the heat

exchangers in the whole tested area. If the heat exchangers present thermostatic valves or electric controller, they need to be set in a way to assure similar temperatures among the different building areas.

In case of decentralized systems, the access and regulation of the generator is normally feasible. However, the multiple systems should be set to achieve an homogeneous temperature. Specially if the systems are not controlled by a set point temperature, assuring a similar behavior among the areas can be a challenge.

The measurement of the heat delivered during the test strongly depends on the technologies that are adopted in the building and local system components, such as those mentioned in table 5.1. When a Building Automation System (BAS) is available locally, it could be used to access data relative to the building space heating. In this case, the heating system heat input and electrical consumption within the building should be available with a frequency of at least 1 hour. However, if it is not the case, additional equipment need to be added to the measurement kit in order to access this data.

For system with hot water distribution systems, the heat could be measured directly in the main pipe going towards the building. A non-intrusive calorimeter allows to measure the heat passing inside a pipe that has a liquid flow. It uses ultrasonic and temperature sensors to estimate the heat flow passing through a pipe. The pipe material, thickness and diameter need to be set previously to the experiment, as well as the characteristics of the liquid (commonly water). Figure 5.3 shows the installations of the calorimeter and its sensors close to the building main heating pipes.

This equipment could be thus added to the experimental kit when applying the global approach. It is a costly equipment and, for this reason, it would be used only in buildings with a centralized system. The distribution system should also consist of hot water networks, such as for systems with boilers, some heat pumps and district heat generators. An additional condition is that the main pipes serving the building should be accessible to install the calorimeter.

Another possible distribution system in centralized installations, besides liquid based networks, are the air networks. Such cases are often integrated to ventilation systems, that, besides supplying air, allow space heating with heat exchangers. Stoves also directly generate hot air; however, they are usually used locally in decentralized systems and are not designed to heat the whole building [241]. In case of air network distribution systems, if the air flow rate and air temperatures are measured, the delivered heat can be estimated. This have not been further investigated in this work, since it does not seem to be significantly used in the MFH context, though it can be more present in TSB.

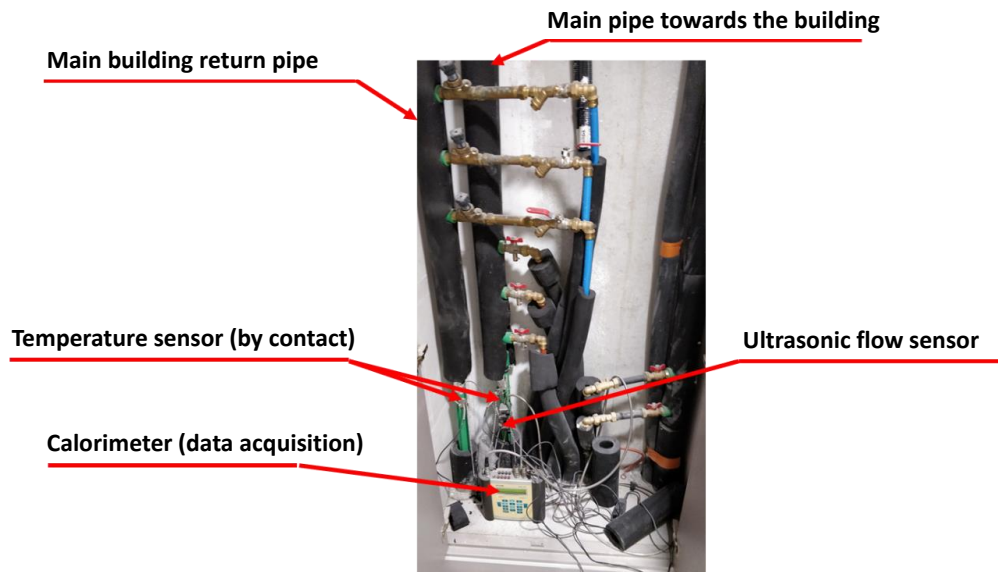


Figure 5.3 – Example of installation of the calorimeter sensors at the main building heating pipes [185].

As already mentioned, the use of local decentralized systems can be more challenging in large buildings. The reasoning for decentralized systems possibilities is more based on the type of generator than of distribution systems. The households with combustion systems would not be considered as feasible. It would be possible to measure the fuel consumption in some cases, but then the boiler or stove efficiency would need to be known. Since this value could vary with the equipment usage and age, and sometimes even being unknown, this option is not considered in this work. As previously stated, the use of a calorimeter in the heating pipes of multiple dwellings would be too expensive.

Even though it is more difficult when comparing to centralized systems, the use of electrical heat generators could be considered. In France, the communicating electricity meter, Linky, can be used to provide information on the energy used in a household. The data is provided by the main operator of the electricity distribution network in France (Enedis) in an hourly basis with the request of the household occupants. Another possibility would be to use a pulse counter in the Linky. Considering to install equipment for measuring the electricity would include the use of ammeters or optical counter on the electric board/meter. Even if they have a more affordable price than a calorimeter, it can be complicated for a large amount of dwellings. In case of joule effect generators, the system efficiency is close to 1 so the measured values could be directly applied. For heat pumps, the coefficient of performance (COP) value should be known to determine the heating delivered during the test, it would bring a level of uncertainty to these measurements.

Based on the considerations above and the data from ENL survey, figure 5.4 brings up in which cases the local approach using the local heating system would be possible, difficult

and very difficult for MFH in France. In overall it was considered possible to apply the global approach in the decentralized systems with hot water distribution network. The cases of decentralized systems with electrical energy source generators were considered as difficult to apply the method. The decentralized system with combustion generators were considered as very difficult to be treated by this approach. The unknown category includes the systems without a precise description inside the category others of the ENL database. These data give a magnitude for the applicability of the global approach. This graphic disregards the buildings with a BAS, which would increase the method’s applicability domain.

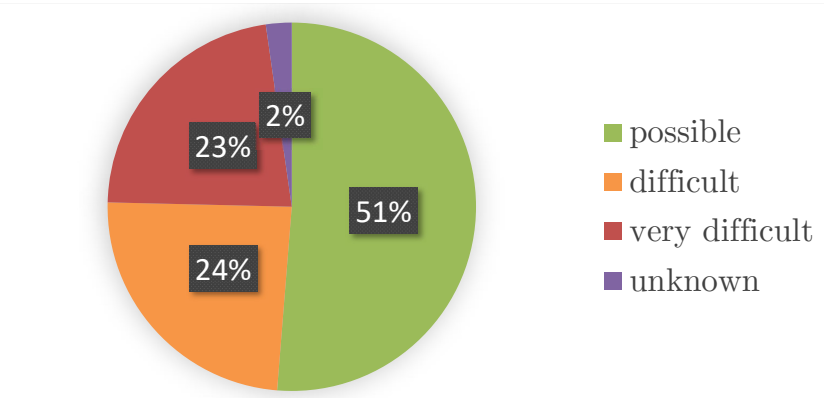


Figure 5.4 – Protocol feasibility of global approach using local system in French MFH building stock, according to ENL database.

Even inside the group considered as possible, other criteria should be met to the realisation of the test: the generator should be drivable and the main pipes accessible. Another important aspect can be the power delivered by the heating system, which should meet the test setpoint temperature. In the majority of cases, the setpoint temperature applied as for the SFH, with a constant heating power to maintain 35 °C, would be hardly achieved in most cases [208]. The feasibility of the protocol should be considered case by case. The question of the setpoint temperature and the power of the local heating system are addressed in the experimental plan developed in the next section.

5.2 Dynamic thermal simulations

To be able to test different protocol conditions and have a reliable reference value for HTC indicator, the methodology in this section is based on a numerical study. An experimental plan was developed to verify the impact of the indoor temperature before and during protocol application, as well as the power of the heating system. This aspects can be an important constraint in the global approach, since the heating would be limited to the local system capacity. Another objective is to verify the possibility of application of ISABELE method in this

building typology with acceptable HTC results, regarding its bias and uncertainty. The fact that the thermal mass of the building is much higher than that of SFH could also be a challenge concerning the demanded time to stabilize the method results.

The immobilisation time during test is an important factor, since the protocol application disturbs the building normal usage. However, an unduly short test duration can lead to poor results of indicator. Another goal in this analysis is therefore to minimize building immobilization time through an optimized protocol.

5.2.1 Reference indicator

The model was tested with 3 different thermal zones distributions. Initially, the whole retrofitted building was considered as a unique thermal zone. Then, the heated areas (apartments) and the unheated areas (common areas) were considered as two distinct thermal zones. Finally, one thermal zone was attributed to each of the 16 apartments and to each of the 5 common areas, with a total of 21 different thermal zones. In each of these three distinct configurations, a fictitious weather condition was applied, with a fixed outdoor temperature and without solar irradiation. The indoor heating scenario was also set to a fixed value, so then the building could achieve steady state conditions. Under this condition, it was possible to calculate the HTC as the proportion between the power delivered to heat the building and the temperature differences between indoor and outdoor environments. The infiltration rate is set equal to zero, for this reason the values of HLC and HTC are the same for this model. The HTC value of 889 W/K was calculated, independent of the number of zones in the model. All the simulations done later in this work were based on 21 thermal zones for the building.

5.2.2 Experimental plan

Several virtual experiments of the ISABELE method were applied to the case study's thermal model. The test beginning date was January 1st and the weather file used is for the city of Trappes, France, located close to Paris (issued from the French Thermal Regulation 2012). The scenarios used in the simulations are described below.

1. General scenarios

- 100 % of window occultation;
- No infiltration rate;
- No ventilation, occupation and electrical gains during the test.

2. Indoor temperature scenarios

- 16 heated thermal zones (HZ), one per apartment;
- 5 unheated thermal zones (UHZ), one per circulation area;
- The representative temperature of the building is a volume average of all thermal zones.

3. Heating scenarios

- Only applied to heated zones;
- The maximum power of each heated zone was defined as a proportion of the total maximum power respecting the volume ratio of zones.

The building model has a concrete structure (the detailed description is in Annex B.) and the capacity of the method to deal with its inertia level is a matter of concern. The influence of rising indoor temperature time on the quality of HTC results was studied during this work. For this goal, variations of the test protocol were tested, such as: the maximum heating power, the set temperature during the test and the preheating temperature before the test started. In addition, different test durations were analysed. The values considered on this parametric study are shown below.

- Maximum power:
50 kW, 65 kW, 80 kW;
- Pre heating temperature:
Absent, 16 °C, 18 °C, 20 °C;
- Setpoint temperature:
20 °C, 25 °C, 30 °C, 35 °C;
- Test duration:
12 hours, 1 day, 2 days, 4 days, 6 days, 8 days, 14 days.

The preheating of the building could be beneficial in the context of in-situ tests applied to collective housings [242]. It was then considered as a potentially influential parameter on test quality. For the cases without preheating, since the building is considered as unoccupied before the test, the initial indoor temperature is a consequence of thermal exchanges with the environment during 15 days before the test start.

The experimental plan consists of all the combinations of the parametric variations presented. In total, 48 different simulations were made with P+C. Each simulation returns the indoor temperature and energy consumption profile. The output data from the virtual

simulations are used as an input of ISABELE algorithm and a HTC value with an associated uncertainty is estimated for each variant .

5.2.3 Results analysis

Considering the 48 different test configurations and the 7 test durations, a total of 336 different experiments were performed. 95 % of these experiments converged to a result of HTC with the use of the optimization algorithm. All tests that diverged (the algorithm was not able to deliver a HTC) had at most 1 day of measurement duration, for longer test duration all results converged. The main parameter used to analyse the results quality was the bias between the measured and theoretical HTC.

5.2.3.1 Dispersion of results

The results dispersion according to the various parameters (duration, power, setpoint and preheating) can be seen between figures 5.5 and 5.8. The vertical red lines are equivalent to $\pm 15\%$ of bias. The test duration is, as expected, very influential on the dispersion and also on the quality of the results. The red vertical lines are a reference of the $\pm 15\%$ bias range. The longer the test, the lower the dispersion and the observed bias in the results (Figure 5.5).

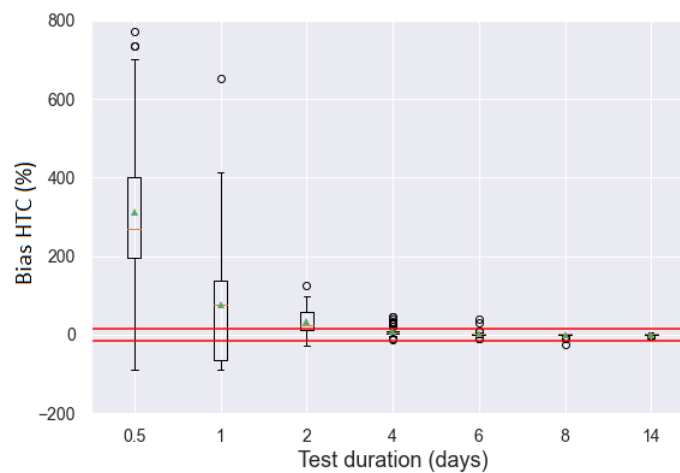


Figure 5.5 – Dispersion of HTC bias according to test duration

Since the test duration is very influential in the results quality, the results here are shown for two different groups: the first days of test and those with duration longer than two days. Figure 5.6 shows the dispersion of the results according to the maximum heating power. For the first test durations the smaller power gives results more centered, although they still very dispersed. Possibly the fact that these variants are heated slower, they have less dispersion of temperature among the different thermal zones, which means the average temperature is closer to that of

the experiment. The maximum heating power seems to have less impact on the dispersion of the results for longer test duration, but the highest power present just one result out of the $\pm 15\%$ of bias boundary.

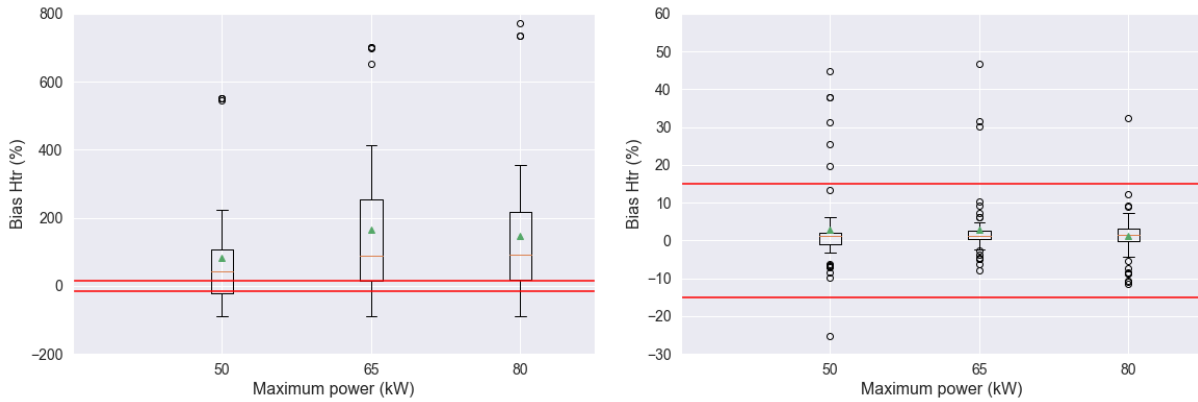


Figure 5.6 – Dispersion of HTC bias according to maximum power for tests until 2 days (left) and tests longer than 2 days of duration (right).

Figure 5.7 present a non linear y-axes, due to the variants without preheating ($0\text{ }^{\circ}\text{C}$). The results have lower dispersion and bias for the variants with $20\text{ }^{\circ}\text{C}$ of preheating temperature. The variants without preheating show higher dispersion than the others for both groups. In Figure 5.8, the variants with the lowest setpoint temperature ($20\text{ }^{\circ}\text{C}$) present lower bias for shorter test duration and the highest setpoint temperature present more points out of the bias limits for longer test duration.

In this test case, it is relevant to have preheating and lower test temperatures. To better understand the influence of indoor temperature dynamics, these two parameters were combined into a temperature delta, which is directly related to the time of temperature rise during the test. The temperature delta ($\Delta T_{beg-end}$) is calculated as in the equation 5.1.

$$\Delta T_{beg-end} = T_{indoor_{setpoint}} - T_{indoor_{beginning}} \quad (5.1)$$

The dispersion of this parameter can be seen in the figure 5.9, where we observe a tendency of less dispersion and better precision of the results for a moderate $\Delta T_{beg-end}$, between 10 K and 15 K. Figure 5.10) shows this parameter bias dispersion for the shorter and longer test durations. For the first days of test the higher $\Delta T_{beg-end}$ are associated with the bias dispersion. For duration longer than 2 days, tests with very low $\Delta T_{beg-end}$ have bias close to zero and the highest temperature difference still show a very large dispersion. This could be explained by the fact that with higher $\Delta T_{beg-end}$ the dynamical phenomena are more relevant during the first days of test and HTC is a steady state indicator. Also, higher $\Delta T_{beg-end}$ could be associated with

more thermal heterogeneity among the thermal zones, which is not taken into account in the mono zone RC thermal models.

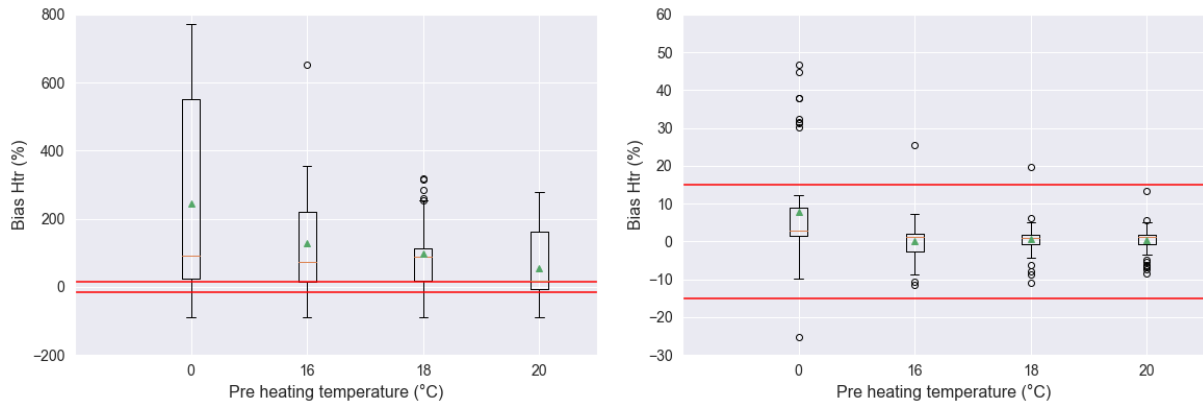


Figure 5.7 – Dispersion of HTC bias according to preheating for tests until 2 days (left) and tests longer than 2 days of duration (right).

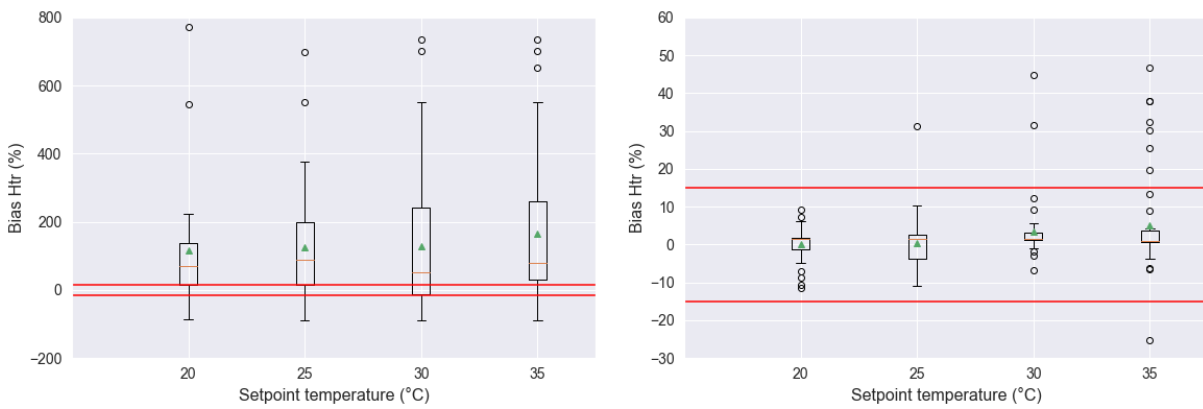


Figure 5.8 – Dispersion of HTC bias according to setpoint temperature for tests until 2 days (left) and tests longer than 2 days of duration (right).

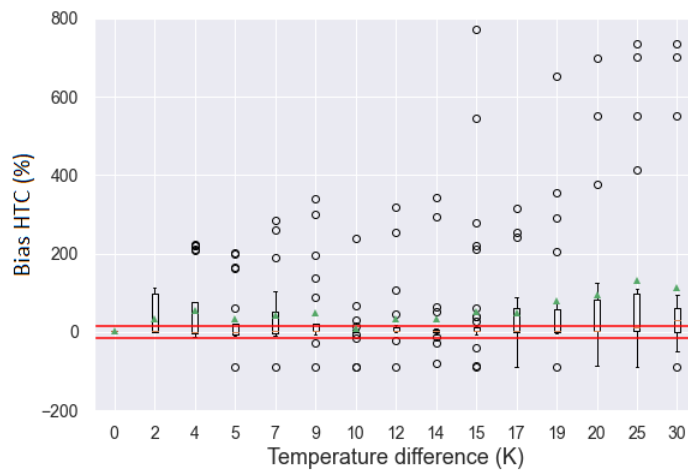


Figure 5.9 – Dispersion of HTC bias according to the $\Delta T_{beg-end}$ (K) of temperature for all duration

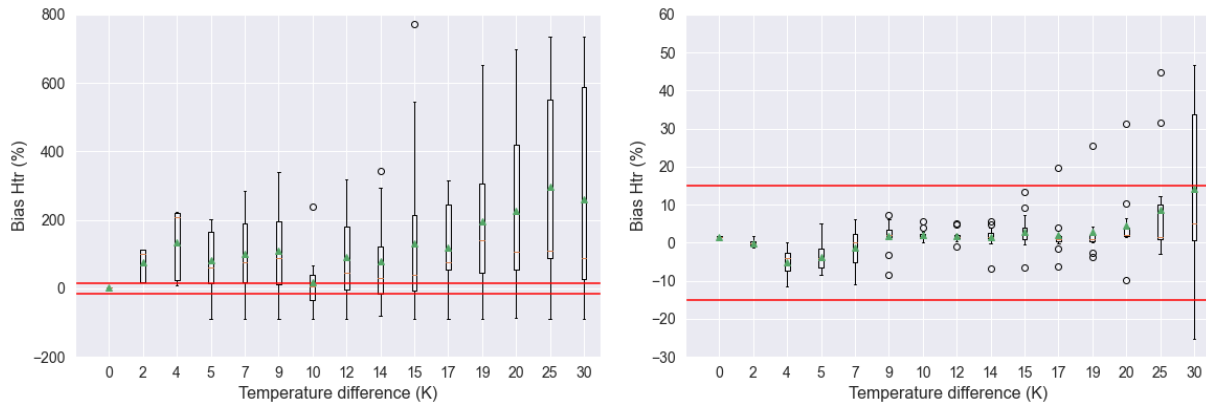


Figure 5.10 – Dispersion of HTC bias according to the $\Delta T_{beg-end}$ (K) of temperature for tests until 2 days (left) and tests longer than 2 days of duration (right).

5.2.3.2 Acceptable results

The HTC results should have a value close to the reference, with an uncertainty high enough to comprise the reference value and low enough to keep its significance. To classify a result as acceptable a limit of 15 % was considered for the HTC bias and 35 % for the uncertainty of the result.

Among the convergent results, 61 % of the results meet the bias criterion and 81 % of the values meet the uncertainty criterion. A total of 185 results, or 58 % of convergent experiments, meet these two criteria at the same time. The following figures show the characteristics of the experiments which presented results were considered acceptable.

Figure 5.11 shows the histogram of the HTC bias for tests more than two days of test duration. There is a concentration of results within ± 10 % HTC bias. Among these results 94 % of the results meet the bias criterion and 98 % of the values meet the uncertainty criterion, with 93 % of them respecting both criteria. The results that did not meet these criteria are mainly those without preheating.

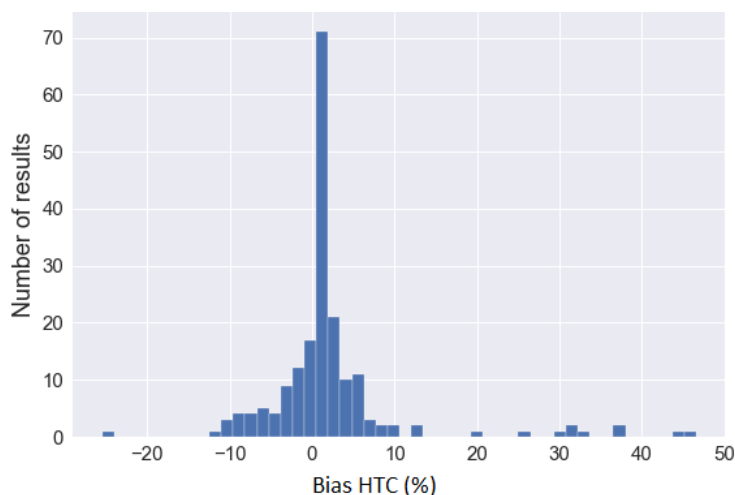


Figure 5.11 – Histogram of HTC bias for tests longer than two days

Figure 5.12 shows the percentage of acceptable results for each tested $\Delta T_{beg-end}$, with a distinction between tests with and without preheating. Among the virtual experiments, the following $\Delta T_{beg-end}$ were studied: 0, 2, 4, 5, 7, 9, 10, 12, 14, 15, 17, 19, 20, 25 and 30 K. Experiments without preheating have an initial indoor temperature of 5 °C. Thus, we obtain four configurations without preheating with the four setpoint temperatures used, which give the following four $\Delta T_{beg-end}$ values: 15 K, 20 K, 25 K and 30 K. The combination of the three preheating temperatures with the four setpoint temperatures gave twelve different $\Delta T_{beg-end}$ values. For this reason, some bars contain a result with preheating or without preheating or a combination of these two.

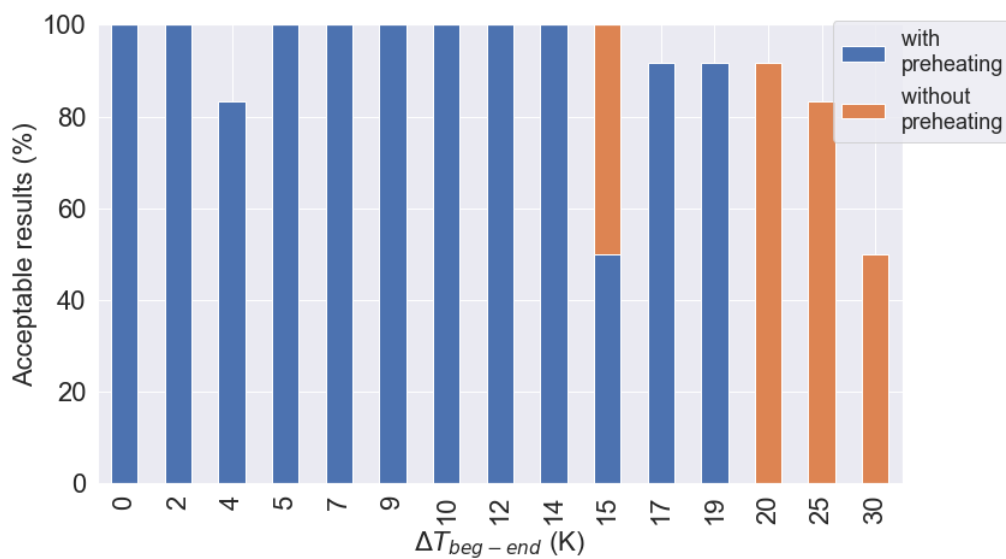


Figure 5.12 – Percentage of acceptable results per $\Delta T_{beg-end}$ for tests longer than two days

A lower percentage of acceptable results is observed for the higher $\Delta T_{beg-end}$ (30K). When analysing the results with and without preheating, for tests that show a similar $\Delta T_{beg-end}$, the temperature difference appears to be more influential than the preheating. The $\Delta T_{beg-end}$ of 15 K is the only case in which the two tests were carried out: with a configuration without preheating and set temperature at 20 °C and the other configuration with preheating at 20 °C and set temperature at 35 °C. The percentage of acceptable results between these two configurations is the same. The percentage is also equal for two tests with a similar $\Delta T_{beg-end}$ (with preheating 19 K and without preheating 20 K delta).

Since a large number of variants was tested, not all the temperature and results evolution are illustrated here. But two extreme cases, regarding the $\Delta T_{beg-end}$, are detailed to illustrate the difference in temperature dispersion between zones for each case. The temperature evolution, boundary conditions and model selection for these two experiments can be seen between figures 5.13 and 5.16.

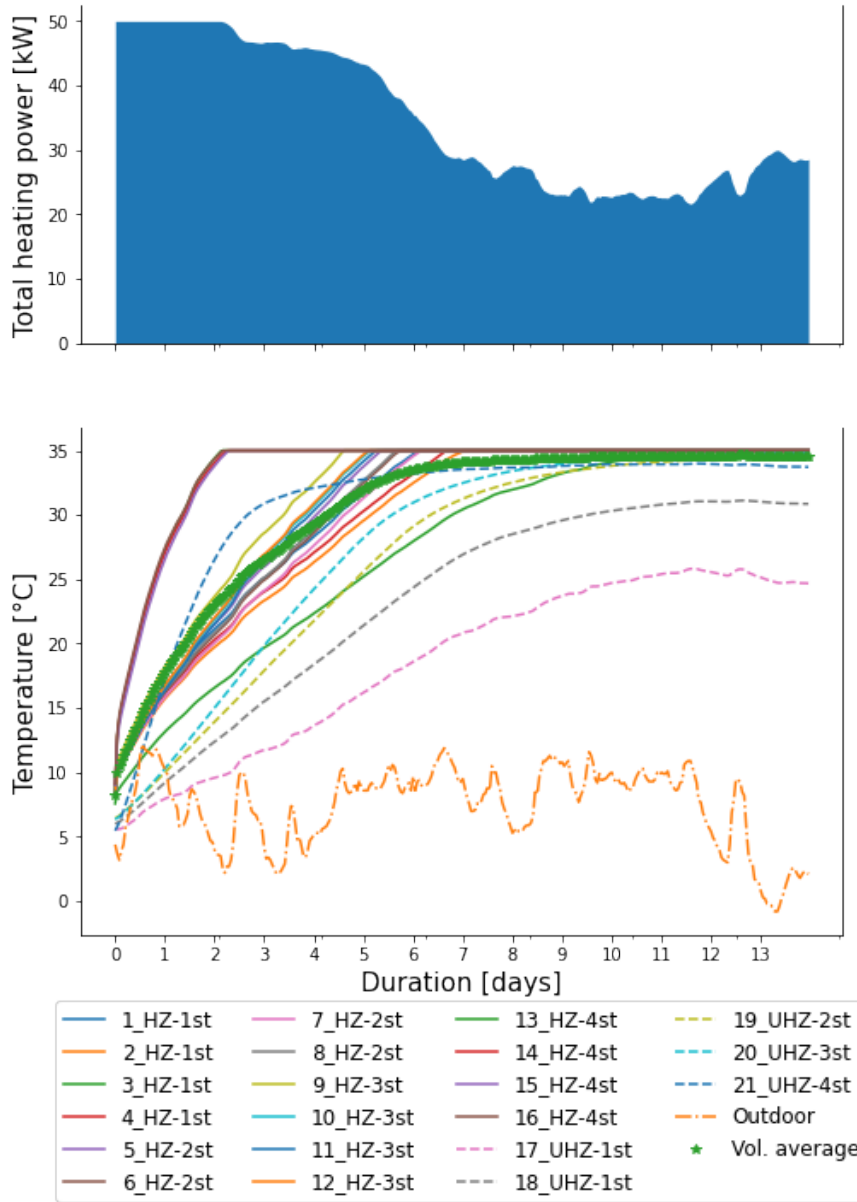


Figure 5.13 – Heating power and temperature (variant: 50 kW and 30 K of $\Delta T_{beg-end}$)

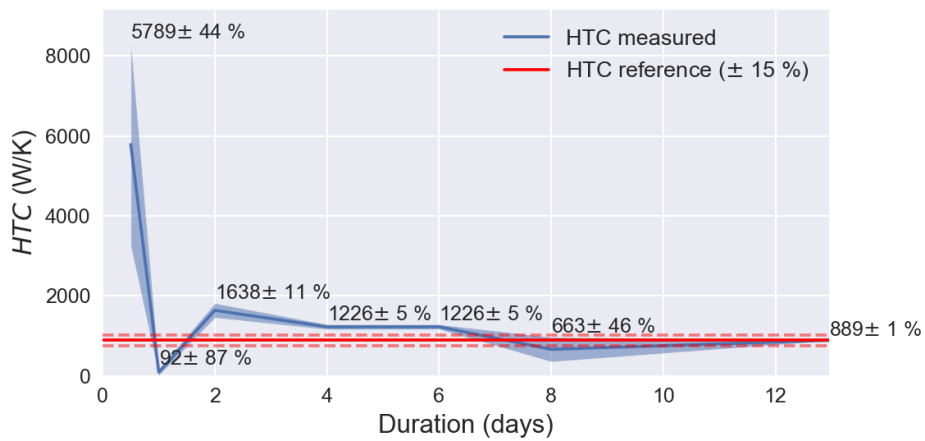


Figure 5.14 – HTC progression with test duration (test: 50 kW and 30 K of $\Delta T_{beg-end}$)

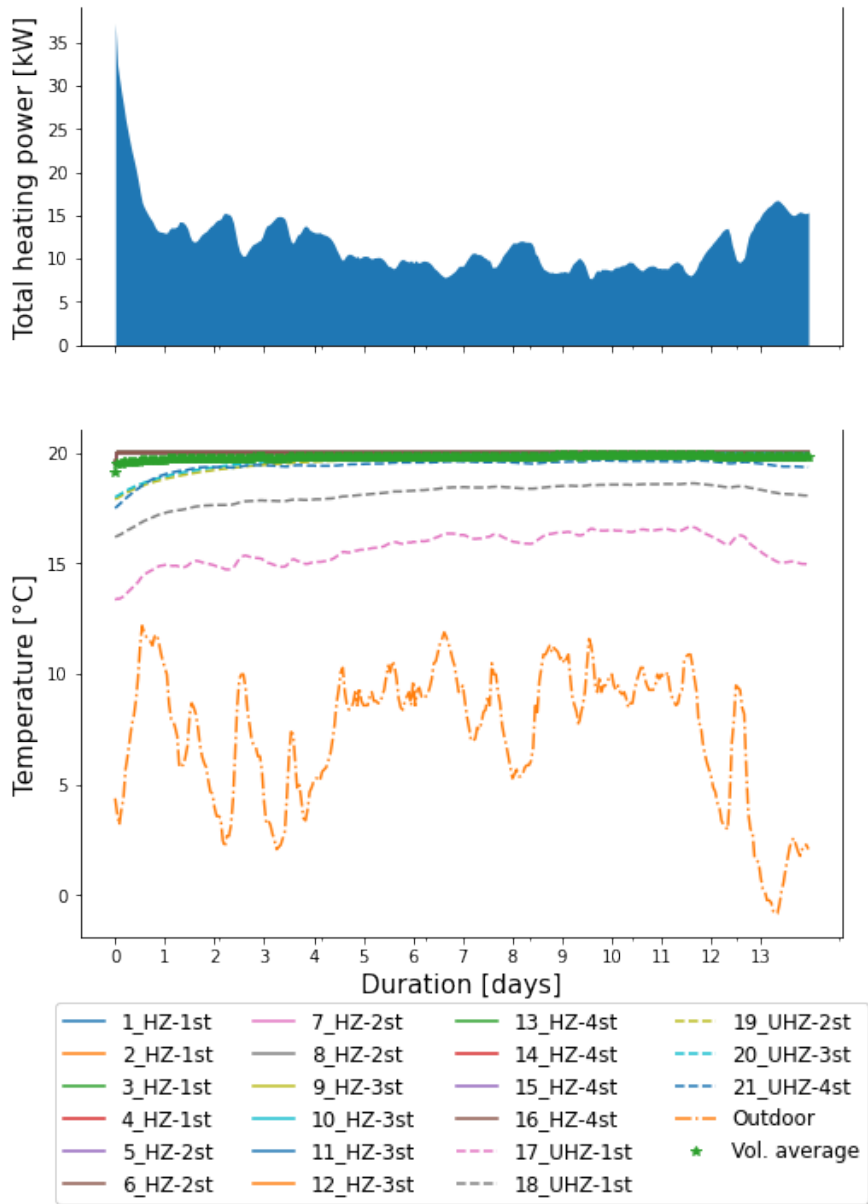


Figure 5.15 – Heating power and temperature (test: 80 kW and 2 K of $\Delta T_{beg-end}$)

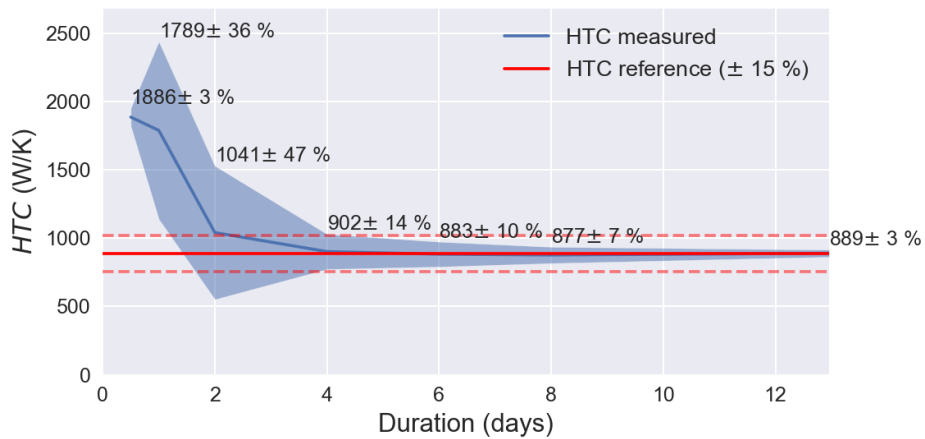


Figure 5.16 – HTC progression with test duration (variant: 80 kW and 2 K of $\Delta T_{beg-end}$)

The first case presents a $\Delta T_{beg-end}$ of 30 K considering that the outside temperature at the start of the experiment is 5 °C. This experiment has also the lowest maximum heating power tested, which further increases the time for reaching the setpoint temperature. The second case has a $\Delta T_{beg-end}$ of 2 K, presenting less dispersion among the zones temperature than the first case. In addition, the optimization algorithm converges faster to acceptable HTC results in the experiment with less dispersion of temperatures between zones.

Figure 5.17 supplement the information in figure 5.12, with an additional axis for test time. Each position in the Z axis represents the percentage of acceptable results between the three powers tested. Thus 4 values are possible on the Z axis: 0 %, 33 %, 67 % and 100 %. This shows that for high $\Delta T_{beg-end}$ it is necessary to have a longer test time to have a higher percentage of acceptable results. Note that after 6 days (except for the test with the highest delta) the tests have 100 % acceptable results.

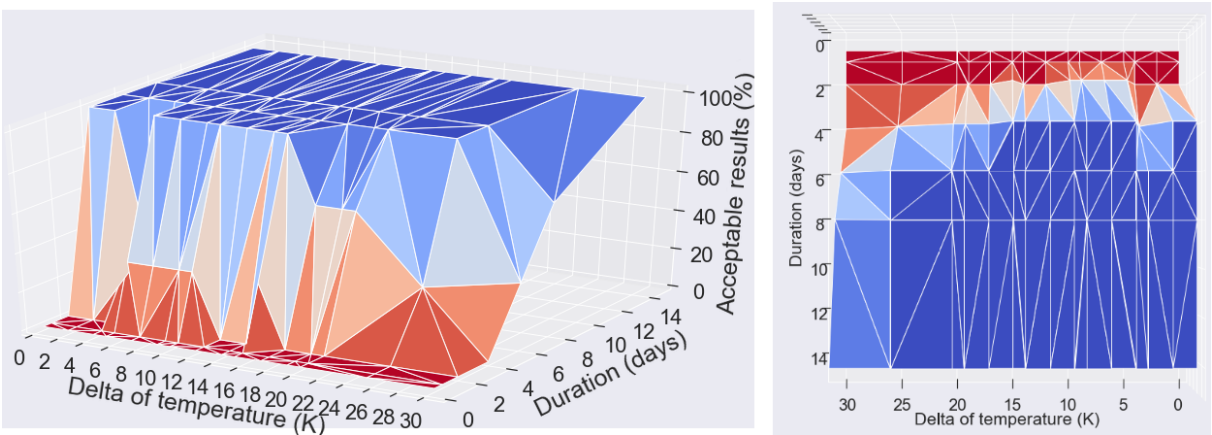


Figure 5.17 – Percentage of acceptable results per delta of temperature and duration - lateral vision in the left and superior vision in the right

This phenomenon is perhaps explained by the dispersion of temperatures between the zones. A trend is perceived when comparing the evolution of the zones temperatures: the greater the temperature difference between the setpoint and the initial temperature, the more time is needed to have uniformity between the zone temperatures. This temperature dispersion phenomenon is important for this building, which has five non heated zones considered inside the test perimeter. Temperature dispersion can prevent the algorithm from working properly, once the thermal models used have a single node for the indoor temperature. The interior temperature considered by the optimization algorithm is the volume average of the temperatures of each zone, which remains only a representation of the multiple temperatures measured.

When the test measurement time is limited, moderate $\Delta T_{beg-end}$ should be preferred. For this building, tested in winter weather conditions, four days of testing time would be sufficient to have 100 % acceptable results using a $\Delta T_{beg-end}$ between 5 K and 15 K.

5.2.4 Discussion

The test duration and the temperature difference from the beginning and the end of the test were the most influential parameters in the quality of the HTC indicator. The longer the test duration the lower the influence of the protocol in the HTC quality. However, one of the objectives is to reduce the building immobilization time. It was observed that in four days of measurement, the variants with a moderate $\Delta T_{beg-end}$ presented acceptable results, with an HTC bias inferior to 15 %.

As a conclusion of this work, the usage of preheating in the building and the use of a $\Delta T_{beg-end}$ of at most 15 K are recommended for winter conditions. Four days of test measurement time is enough for reliable results when there is preheating, in this collective housing. All the tests were performed during winter, for a unique weather conditions, the test duration for other seasons has to be further studied.

In this work high $\Delta T_{beg-end}$ is associated to non acceptable results, however most of these variants were not preheated. Future works could separate the effects of pre heating and $\Delta T_{beg-end}$ in the quality of HTC results.

In the course of SEREINE project, the algorithm has evolved, but the analysis here presented were developed before these modifications. In this way the presented results are all based on ISABELE method. A similar analysis could be further done using SEREINE estimation algorithms.

5.3 In-situ test

The global approach was applied in-situ to a small MFH located in Sallanches, a French city close to Grenoble. The building size allowed the application of two complete ISABELE/SEREINE measurement kit.

5.3.1 Site description

The instrumented building is a set of three renovated apartments from 1840. The apartments are located on the ground floor (63m²), the first floor (63m²) and the second floor (88m²). Figure 5.18 presents one of the building facades.

The apartment on the ground floor has boundaries with:

- the outside
- a cellar on approximately half of the low floor (the remainder being on ground level)
- the unheated common areas
- the upper apartment at the R+1 (shared wall)



West facade

South facade

East facade

Figure 5.18 – Pictures of the MFH building facades in Sallanches site

The apartment at the R+1 has boundaries with:

- On the outside
- the unheated common areas
- an unheated neighboring apartment (shared wall)
- the lower apartment on the ground floor (shared wall)
- the upper apartment at R+2 (shared wall)

The apartment at the R+2 has boundaries with:

- the outside
- the attic floor
- the unheated common areas
- a heated apartment (shared wall)
- the apartment below the R+1 (shared wall)

The insulation was carried out from the inside (20 cm on average on the exterior walls and low floors, 12 cm on the unheated common areas, 40 cm on the lost attic, 8 cm towards the adjoining dwellings). The intermediate floors (adjoining) were heavily insulated (30 cm of insulation).

5.3.2 Implementation of equipment in-situ

A test using the global approach was conducted from February 6 to 12, 2020 (on the three apartments). The sufficiently small size of the building allowed the use of two SEREINE kits. Indeed, the use of the existing heating system could not be realized due to lack of preparation

(it would have been theoretically possible by the use of the Joule effect boilers and the recording of the electrical consumption). The location of the modules is shown in figure 5.19. Figure 5.20 shows some pictures taken during the equipment installations. The irradiance sensor was placed outside the lost attic (on the south facade). The SENS sensors were placed:

- 1 on the South facade (on the R+1)
- 2 on the East facade (at R+1 and R+2)
- 2 on the West facade (at R+1 and R+2)
- 1 in the unheated common areas (at R+2)
- 1 in the lost attic (horizontal)

The outdoor temperature modules were placed:

- 1 in the cellar in the basement
- 1 in the unheated common area (ground floor)
- 1 in the neighbouring unheated dwelling (at R+1)
- 1 in the heated neighbouring dwelling (at R+2)

The LEMMI modules were distributed as follows in the building: Ground floor:

- 2 in the living room
- 1 in the bathroom
- 2 in the bedrooms (1 per room)

On the R+1:

- 1 in the living room
- 1 in the corridor
- 2 in the bedrooms (1 per room)

At the R+2:

- 1 in the living room
- 2 in the big room
- 1 in the bathroom
- 1 in the bedroom

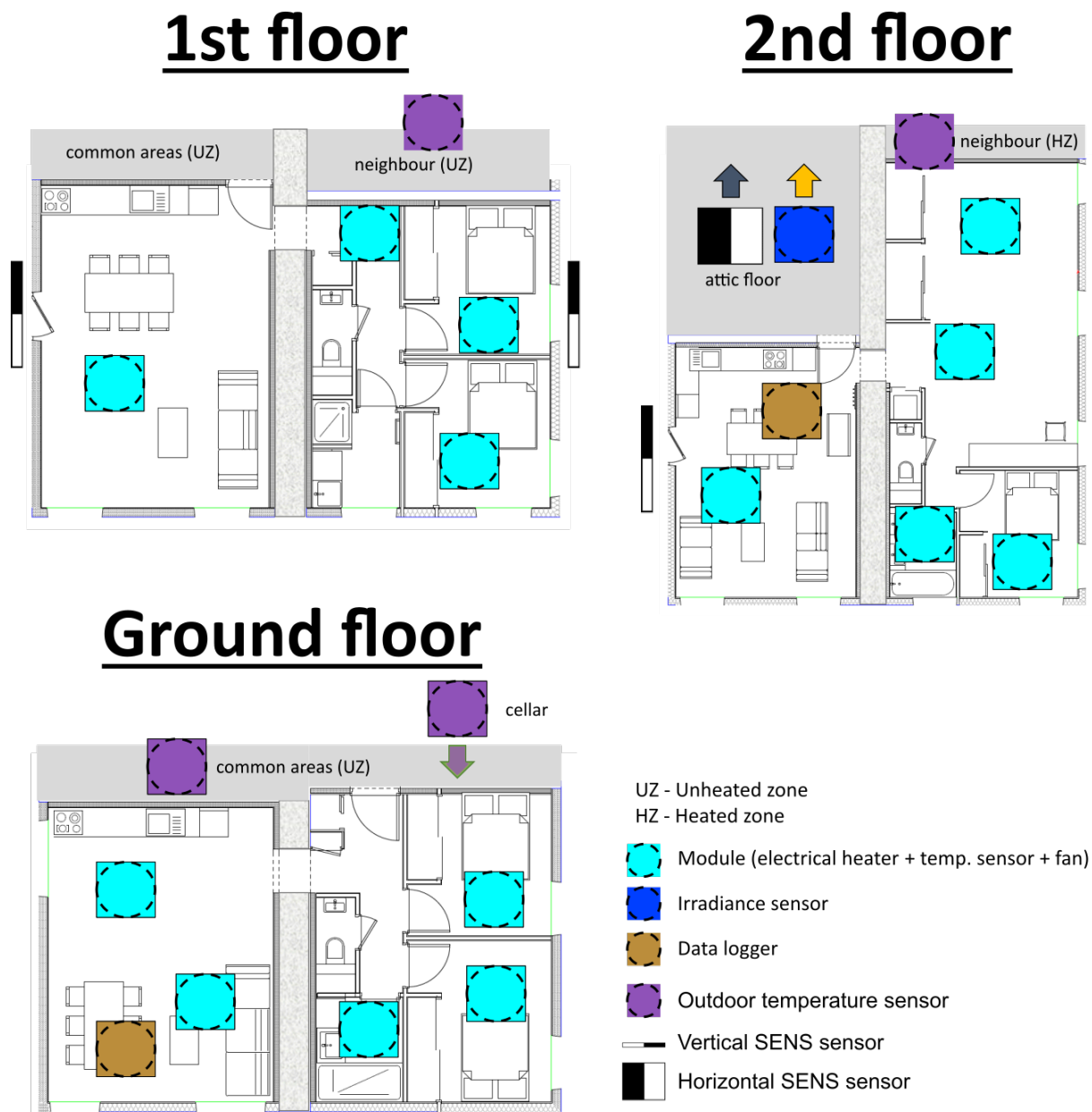


Figure 5.19 – Location of the sensors during the measurement by global approach of the Sallanches site [208]

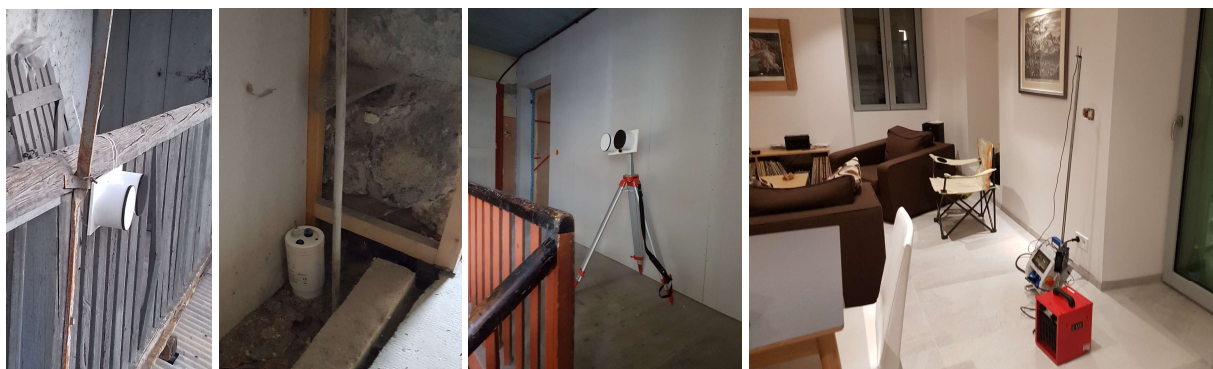


Figure 5.20 – Pictures of some of the equipment installed outdoor and indoor at the Sallanches site [208]

5.3.3 Estimation algorithm results

5.3.3.1 HLC indicator

The studied building presents shared walls with a neighbour building. For this reason, when applying the global thermal losses, the HLC indicator includes:

- Losses by transmission to the outside and to the ground
- Losses by infiltration
- Losses to neighbouring building

The data issued from the protocol was analysed with ISABELE and SEREINE codes with a time step of 5 min and 1 hour. The results are presented in the figures 5.21 to 5.24. In each of these figures the dark blue line connects the estimated HLC value for each test duration. The light blue band gives the uncertainty associated to this value. For durations under one and a half days the algorithm estimation is not yet reliable, which is understandable considering the comparable lack of data and the nature of inverse problems. These durations can present really elevated uncertainties and/or estimations out of the final indicator range.

The reduction of the analysis time step seem to have beneficial consequences on the uncertainty level for both algorithms, but in particular for ISABELE. This effect is coherent with the expectations, since with a five minutes time step there is twelve time more data than for one hour, considering the same test duration. In general the uncertainty has the tendency to diminish with the increasing of data, until stabilized to a value. Although, high variations between two consecutive durations might be the result of changing the selected RC thermal model. First order models were in some cases selected in the beginning when less data is available: for half day duration using SEREINE with five minutes and one hour time steps and until one and a half days for ISABELE using a one hour time step. After that, even though different model structures were selected, all of them were second order models. Once a single model is chosen in consecutive durations, the behavior tends to stabilize, or to present a gradual reduction of uncertainty.

From two and a half days of measurements, the results converge to similar HTC values, even if the uncertainty varies among them. The analysis using five minutes time step starts to present a stable result, with acceptable uncertainties from one and a half days (around 15 %). In general, SEREINE algorithm seems to present more stable results over time for this in-situ test. However, this indicator does not express the level of external thermal insulation, with combined effects of infiltration and the partition walls. For this, it is necessary to evaluate the losses by infiltration and the losses between buildings. The latter should bring additional uncertainty, that will have to be evaluated.

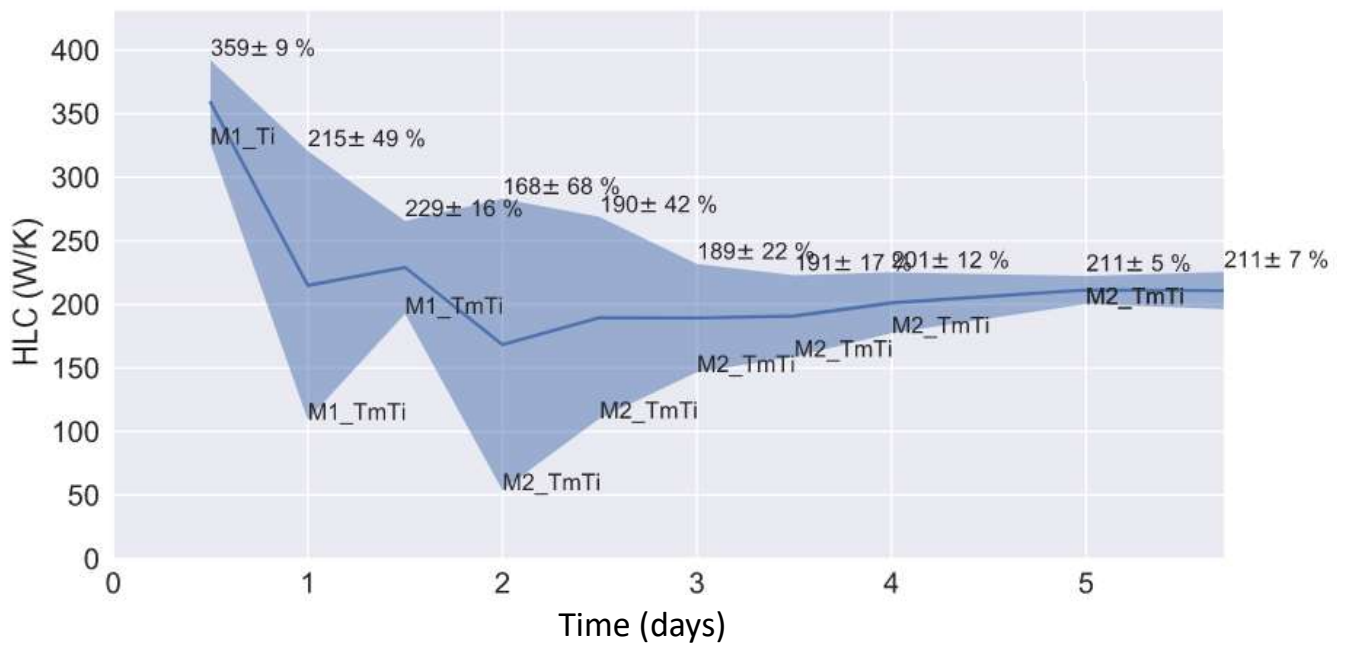


Figure 5.21 – Sallanches site progression of HLC results using ISABELE estimation algorithms and a time step of 1 hour

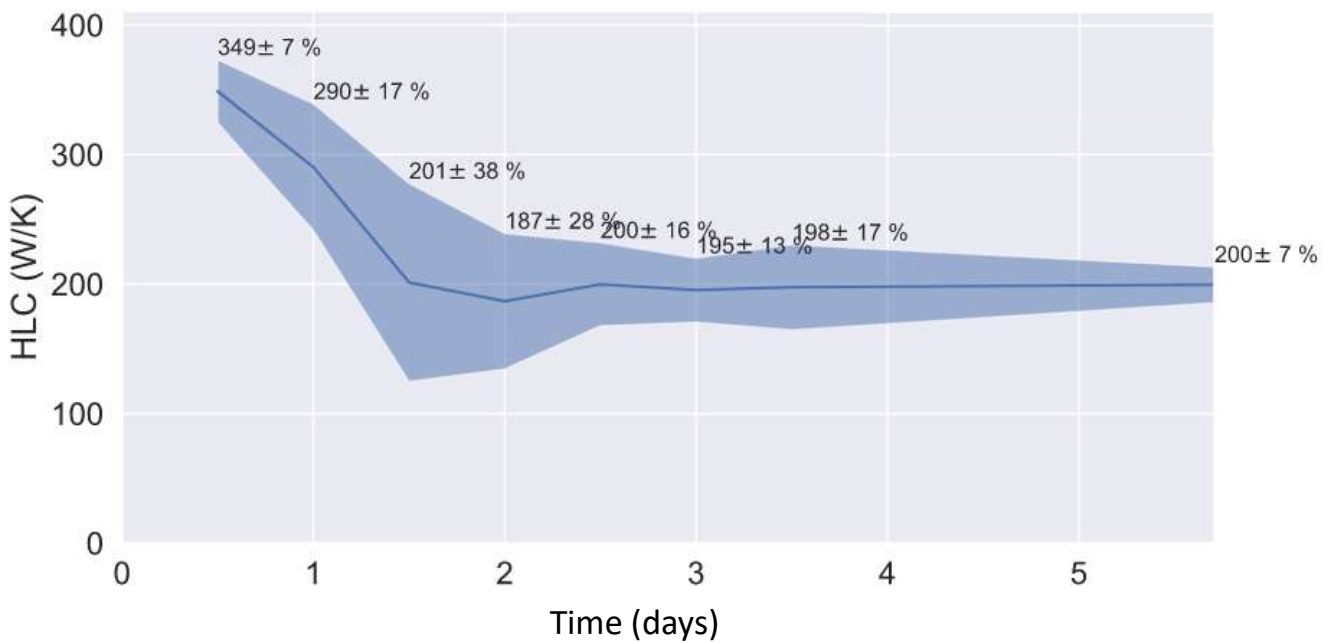


Figure 5.22 – Sallanches site progression of HLC results using SEREINE estimation algorithms and a time step of 1 hour

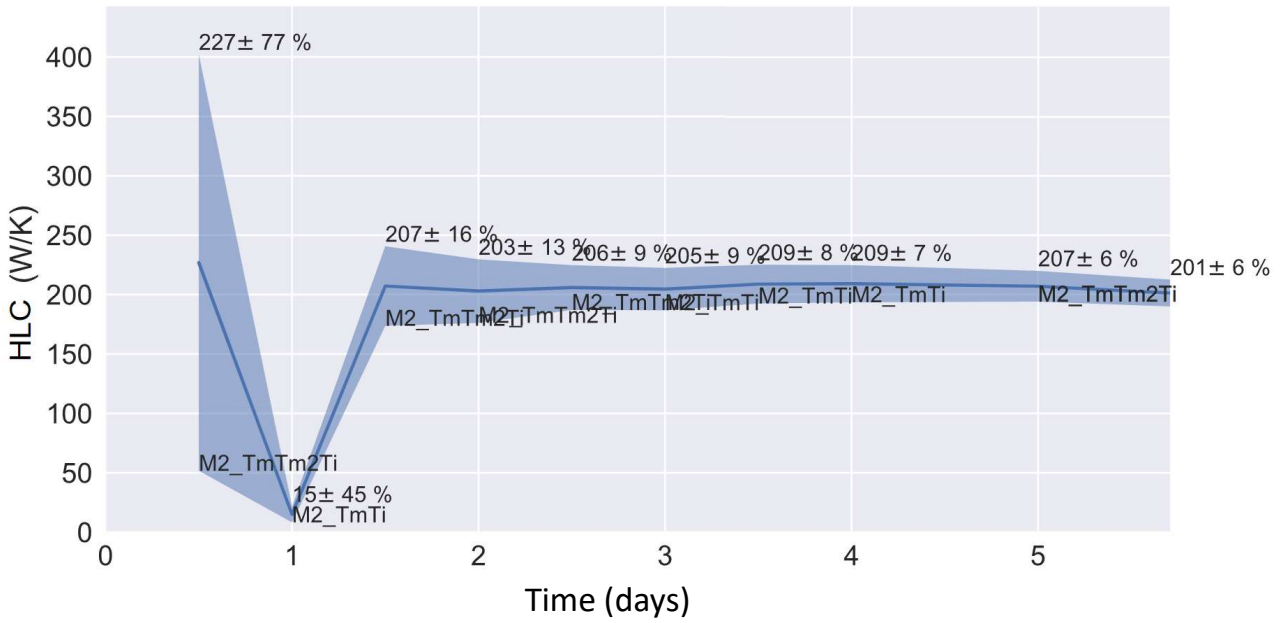


Figure 5.23 – Sallanches site progression of HLC results using ISABELE estimation algorithms and a time step of 5 min

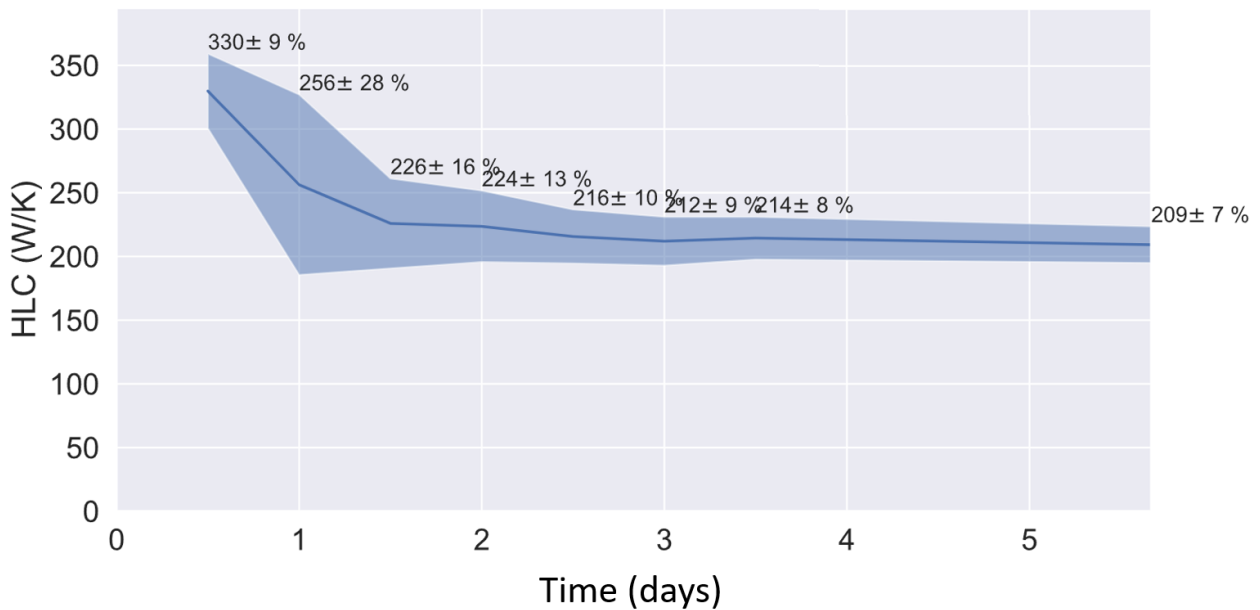


Figure 5.24 – Sallanches site progression of HLC results using SEREINE estimation algorithms and a time step of 5 min

5.3.3.2 Air infiltration estimation

Blower door tests were applied to each apartment of the building, on February 19. Its indicators are presented in table 5.25. Excellent results were obtained for the three apartments, with $Q_{A_{pasurf}}$ levels lower than $0.6 \text{ m}^3\text{h}^{-1}\text{m}^{-2}$ (level required for new SFH, knowing that for new MFH, the requirement is $1 \text{ m}^3\text{h}^{-1}\text{m}^{-2}$). As an indication, the average level of $Q_{A_{pasurf}}$ overall building (average weighted by A_{tbat} heat loss surfaces) is $0.22 \text{ m}^3\text{h}^{-1}\text{m}^{-2}$.

Apartment	Atbat (m ²)	Q _{4pa,surf} (m ³ /h/m ²)	n50 (vol/h)	Leakage coefficient CL (m ³ /h/Pa ⁿ)	Leakage exponent n	Correlation coefficient
2nd floor	173	0,09 ± 8%	0,73 ± 6%	4.47 ± 11%	0.881 ± 4%	0.999
1st floor	68,7	0,57 ± 12%	1,09 ± 6%	18.1 ± 18%	0.575 ± 9%	0.997
Ground floor	69,0	0,23 ± 81%	1,01 ± 31%	8.63 ± 85%	0.906 ± 41%	0.942

Figure 5.25 – Permeability indicators main measures for MFH in Sallanches [208]

The ground floor test has very high uncertainties on the measured indicators. This is due to a very poor correlation of the measurement points (0.942) probably due to a gust of wind or a parasitic leak during the measurement. Despite these uncertainties, the $Q_{4pasurf}$ confidence interval remains in the "excellent" category below $0.45 \text{ m}^3\text{h}^{-1}\text{m}^{-2}$.

In order to estimate the air infiltration losses, two hypothesis were considered for this test:

1. Evaluating a "maximum" infiltration rate from the most unfavorable measurement and neglecting the internal air barriers. The maximal $Q_{4pasurf}$ measured among the apartments is used as an upper limit for the whole building. The infiltration rate is then evaluated at half of this maximum value, with an uncertainty of $\pm 100 \%$. The middle value is used in the air infiltration estimation, as for a SFH case. This is a security option to represent the envelope permeability, but have a high level of uncertainty in the estimations.
2. Measuring the leakage coefficients and index of all apartments and using them to calculate the infiltration rate in each apartment. Since this building is a low-rise, this hypothesis is applied. Even though this is more accurate than the first approach, this would be hard to apply to larger buildings, since all apartments and offices would need to be measured. The applied infiltration rate uncertainty are similar to that for SFH (around $\pm 50 \%$).

Figure 5.26 illustrate these two hypothesis. Based on these two hypothesis, the H_{inf} was estimated for the tests. The evolution of this parameter results for both of them over the time is shown in figure 5.27. Figure 5.28 details the air losses for each apartment for hypothesis 2.

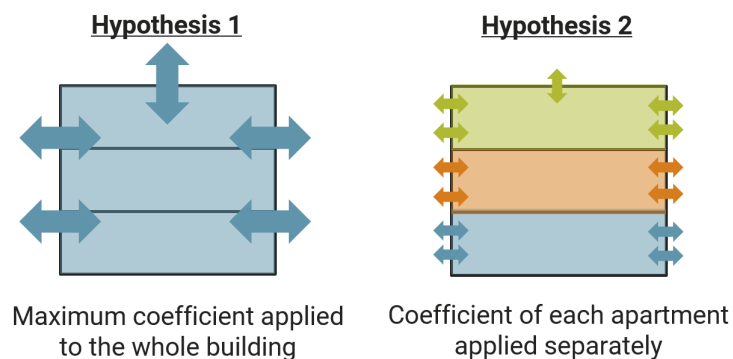


Figure 5.26 – Hypothesis on the blower door indicators to estimate the air infiltration losses during the test in Sallanches site with the global approach [219]

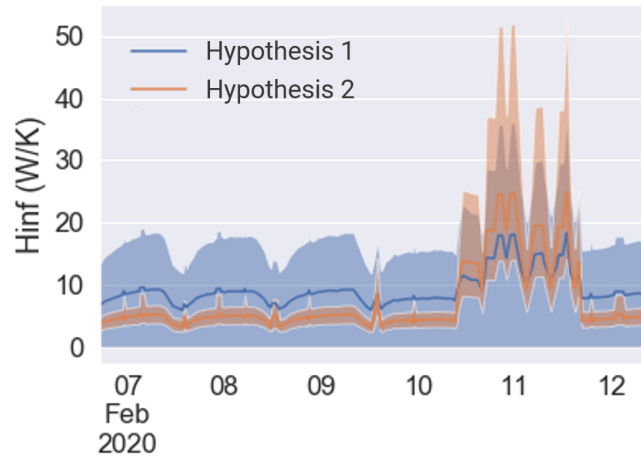


Figure 5.27 – H_{inf} estimation based on hypothesis 1 and 2 during the test in Sallanches site with the global approach [219]

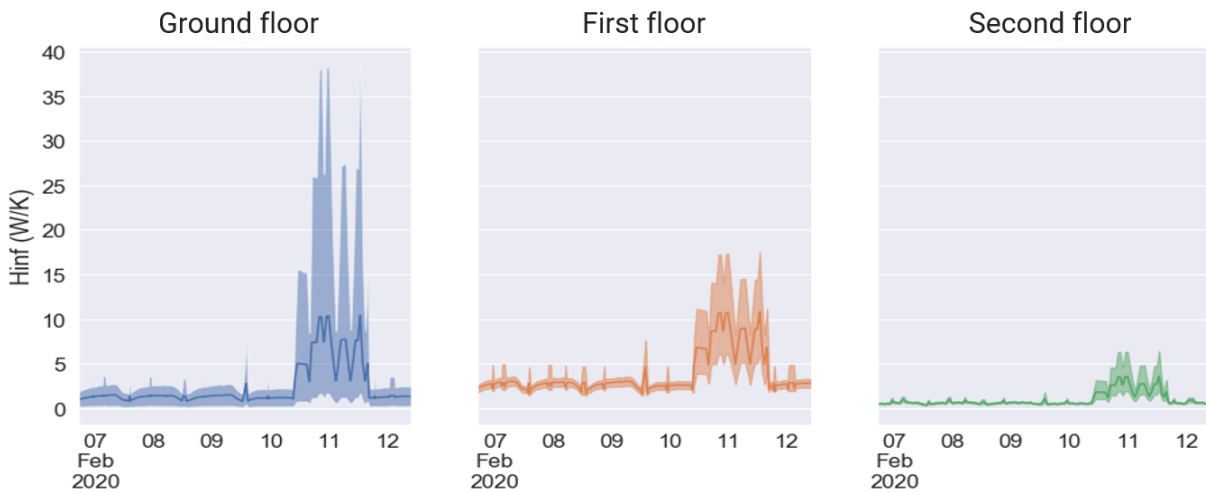


Figure 5.28 – H_{inf} estimation of each apartment for hypothesis 2 during the test in Sallanches site with the global approach [219]

5.3.3.3 HTC indicator

Once the H_{inf} was estimated the HTC of the building could be calculated. The analysis of HTC for both hypothesis were based on SEREINE algorithms, with a time step of one hour. The result of the analysis using hypothesis 1 for the estimation of H_{inf} is presented in figure 5.29 and that using hypothesis 2 in figure 5.30. The level of the infiltration losses compared to the heat loss coefficient is small, for this reason the difference between HLC and HTC is not significant. Comparing these figures with the progression shown before in figure 5.22, it can be perceived a decrease on the estimation and a slightly increase of the uncertainties. It is expected that the uncertainties would increase, once the parameters related to the air infiltration and their uncertainties are taken into consideration for HTC estimation. Finally, in this case, where the H_{inf} is relatively low, the difference of the results among the hypothesis 1 and 2 is not

significant. Even though both hypothesis have wide differences in the values and uncertainties, they remain small when compared to the HTC value.

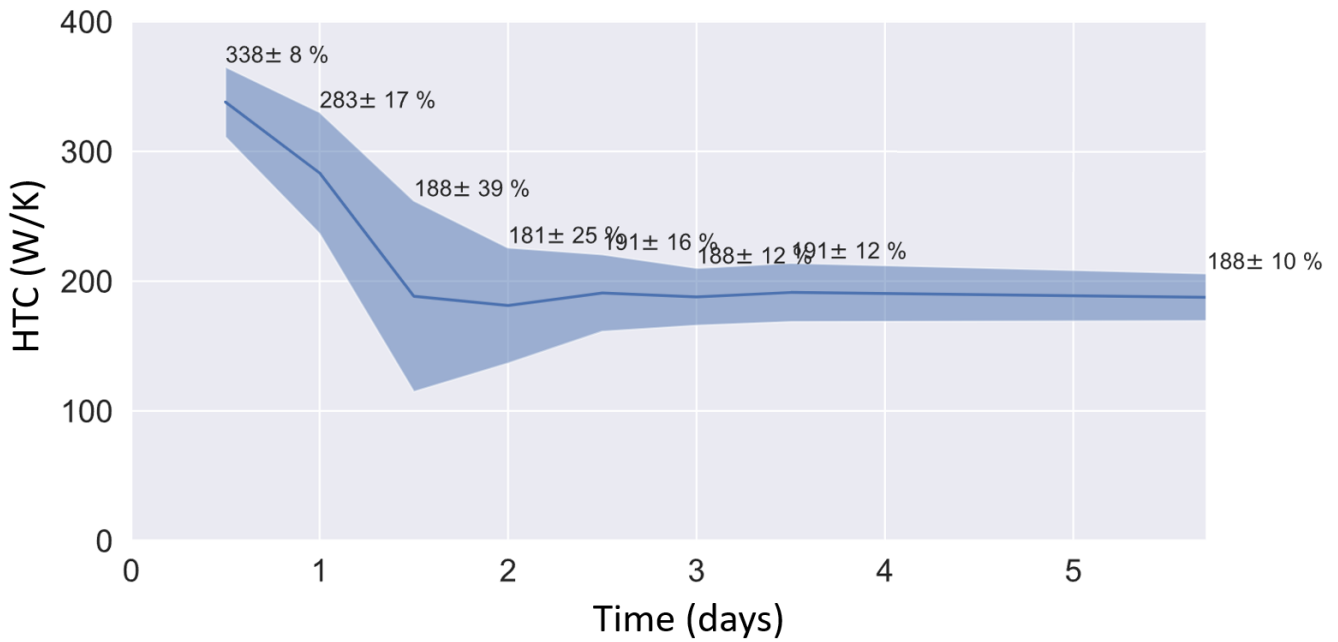


Figure 5.29 – Sallanches site progression of HTC results using SEREINE estimation algorithms with a time step of 1 hour and the hypothesis 1 for the estimation of H_{inf} .

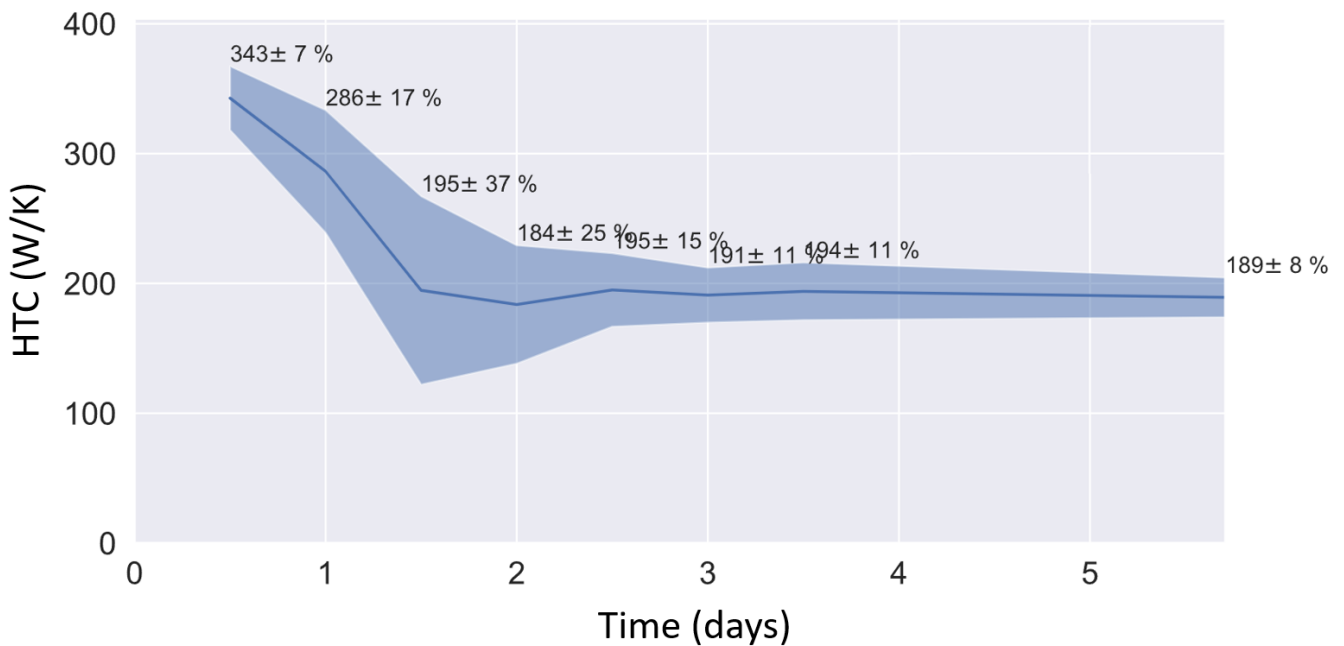


Figure 5.30 – Sallanches site progression of HTC results using SEREINE estimation algorithms with a time step of 1 hour and the hypothesis 2 for the estimation of H_{inf} .

5.3.4 Discussion

The measurements could be carried out on a real case of a low-rise MFH with the current equipment. The preliminary results obtained are encouraging, in the way that the global loss

coefficients (HLC indicator) measured seem to converge after 2 days of testing with a relatively low uncertainty.

In this case the building air tightness was high, therefore the estimation of H_{inf} had low influence in the HTC results. However the estimation of air infiltration in large buildings can present a difficulty for the global approach, especially for larger buildings with more significant air infiltration losses. Further researches are to be carried out in order to obtain an accurate estimation of H_{inf} for those cases.

5.4 Chapter conclusion

This chapter is dedicated to the development of the global approach for estimating the thermal losses of large buildings envelope. The size difference of these buildings with SFH implies a certain number of new subjects to be treated, of a technical, scientific and operational nature. The global approach has the advantage to analyze the envelope of a building in its entirety, but at the cost of many conditions (for example, the entire building must be released for several days). For low-rise MFH and small TSB, multiple equipment kits could possibly be used. If a larger size building is to be measured, an option would be changing the heating device (e.g. using the existing system) in order to make the volume of material to be transported to the site reasonable.

Using the local heating system could be an alternative for large building, however this approach will therefore only be possible for a limited number of cases. The system should be accessible, operational, controllable and measurable. These conditions would vary according to the system and also from site to site. In general, the use of the local devices was considered possible when the technology used is that of hot water network in centralized systems. Electrical generators in decentralized systems are considered to be a more difficult option, since the operation and measurements should be done in multiple points. This method would therefore present a strong constraint regarding the site characteristics and have a limited applicability domain. Based on the ENL survey, which brings data on residential buildings heating systems, the global approach would be possible in half of the French MFH stock and be difficult in one quarter of it. This analysis did not take into account the buildings with more technological systems, such as BAS, that could provide the heating input data. When more buildings have this technology, the global approach would increase its applicability domain.

Virtual protocol applications were designed to show the most influential parameters on the HTC estimation quality. The P+C model presented in Chapter 4 was tested under different conditions. 336 variations from a protocol inspired by ISABELE method were tested with

this model with variations in parameters of the protocol, such as duration, heating power, setpoint and preheating temperature. The test duration and the temperature difference from the beginning and the end of the test were the most influential parameters of the protocol. As expected, longer test durations are associated to higher quality estimations. Low temperature difference had also a positive impact on the measurement accuracy. With four days of data, and no elevated temperature difference, most results were acceptable regarding bias and uncertainty. This conclusion apply for winter and need to be confirmed with other weather conditions.

A proof of concept of the global approach was taken in a low-rise MFH, in which it was possible to use the measurement kits. In this occasion ISABELE and SEREINE estimation algorithms were applied with time steps of five minutes and one hour. All analysis came to similar results after two and a half days of measurements. The air infiltration losses were addressed using two different hypothesis, one that majors the infiltration and another more accurate that requires a blower door test in each apartment. Even when different levels of air leakage estimation were presented, HTC results were not significantly affected, since the building has a good air tightness level. Despite the difficulties during the protocol application, enough data was collected and stable results were achieved. Further development should be considered to estimate the air infiltration losses for larger buildings.

Chapter 6

Sampling approach

Contents

6.1 Impact of neighbour heat flows	137
6.1.1 U_{eq} ratio	138
6.1.2 Surface ratio	138
6.1.3 Temperature difference ratio	140
6.2 Static method for exploring the sampling approach	142
6.2.1 Result uncertainty with the indirect method	144
6.2.2 Result uncertainty with the direct method	146
6.2.2.1 General discussion	148
6.3 Indirect method for neighbours flow estimation	149
6.3.1 Ranges of U_{shar} uncertainty	149
6.3.2 Virtual experimental plan	150
6.3.2.1 Variation on the exterior walls insulation location and shared walls inertia	152
6.3.2.2 Variation on the setpoint and preheating temperature	156
6.3.2.3 Variation on the test and weather conditions	160
6.4 Direct method for neighbours flow estimation	167
6.4.1 Ranges of φ_{shar} uncertainty	168
6.4.1.1 IUT experiment	168
6.4.1.2 CEA experiment	170
6.4.1.3 Discussion	179
6.4.2 Virtual experimental plan	180
6.5 In-situ test application	184
6.5.1 Building description	184

6.5.2	Experimental description test	187
6.5.3	Results and discussion	190
6.6	Chapter conclusion	192

Given the difficulties of applying the global approach in some MFH and TSB, regarding the site vacancy and local heating system, the sampling approach is further developed in this chapter. For SFH or the global approach in large buildings, the limits of the tested area are commonly equivalent to the limits of the insulated envelope. However, it is not the case for the sampling approach, in which parts of the tested area are facing neighbour dwellings, offices or common spaces.

The heat flow passing through the shared walls can have a significant impact on the heat input data and therefore on the estimation process. The protocol of the sampling approach should be developed to master these heat flows to assure quality results of HTC_{ext} . In section 6.1, the importance of properly taking into account this flow is highlighted.

In section 6.2, a static model was used to explore different possibilities of the sampling approach and to have the big picture of its validity domain. The location of the tested area inside the building was studied, since it affects the surface ratio of exterior and shared walls and consequently the level of heat flow going towards neighbouring areas. Based on the outcome from this section, an apartment in the Pléiades model previously presented, is used to virtually apply the sampling approach in dynamic conditions in the following sections.

As mentioned before in chapter 4, two main methods for estimating the heat flow going towards the neighbours were considered. The first is the indirect method, where the temperatures are measured in each side of the shared walls and, together with their area and U-value, a heat flow is estimated. The second is the direct method which consists of measuring the flow with the use of heat flow sensor during the protocol application. Each method presents advantages and drawbacks and might be useful under different test conditions. For this reason, both of them were investigated in parallel.

In order to investigate these possibilities, many virtual experimental plans were conceived in Pléiades Comfie for the indirect method. In section 6.3, variations in the protocol and weather conditions are tested to study the limits of this method. The idea in this section is to study the method behavior in a sampled area and to test it under different experimental tests using heat flow meters to give a base of the uncertainties in this input data. In the same section a virtual experimental plan is presented using the direct method to estimate the neighbours heat flow. In section 6.5 both indirect and direct methods are applied in-situ. Finally, in section 6.6 the general conclusions on the sampling approach are drawn.

6.1 Impact of neighbour heat flows

In the sampling approach, shared walls are part of the tested perimeter and the heat flow passing through them can be significant during an in-situ test, depending on protocol conditions and wall thermal properties. Figure 6.1 represents an example of a sampled area to be tested, in which only part of the tested perimeter is facing the exterior environment, but the majority of it is facing the adjoining spaces.

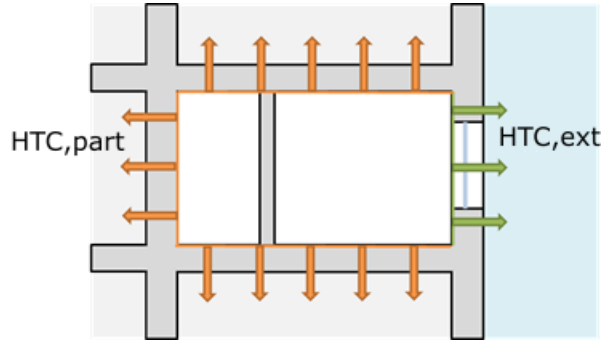


Figure 6.1 – Separation of thermal transmission coefficients to the outside and to adjoining spaces [219]

If the heat flow passing through the shared walls (ϕ_{shar}) is significant and not well estimated it would behave as a parasite flow in the estimation process and hinder the accuracy of the final indicator HTC_{ext} . The impact of the ϕ_{shar} in the estimation process depends on the magnitude of the heat flow going towards the exterior environment (ϕ_{ext}). It is therefore interesting to think in terms of relative heat flow between the tested area and both the exterior and adjoining spaces, as expressed in equation 6.1.

$$\Gamma_{\phi_{ext-shar}} = \frac{\phi_{ext}}{\phi_{shar}} \quad (6.1)$$

In order to simplify the analysis of this ratio, we could consider a surface equivalent heat loss coefficient U_{eq} , which represents the sum of all the losses by transmission (through certain walls, roof, floor, doors, windows and thermal bridges) divided by the surface areas. If we consider one homogeneous temperature in the adjoining areas, $\Gamma_{\phi_{ext-shar}}$ can be represented as in the equation 6.2. This can be alternatively represented by the product of three ratios, $\Gamma_{U_{eq_{ext-shar}}}$, $\Gamma_{S_{ext-shar}}$ and $\Gamma_{\Delta T_{ext-adj}}$, which are respectively related to U_{eq} , surface and temperature difference (equation 6.3).

$$\Gamma_{\phi_{ext-shar}} = \frac{U_{eq_{ext}} \times S_{ext} \times (T_{int} - T_{ext})}{U_{eq_{shar}} \times S_{shar} \times (T_{int} - T_{adj})} \quad (6.2)$$

$$\Gamma_{\phi_{ext-shar}} = \Gamma_{U_{eq_{ext-shar}}} \times \Gamma_{S_{ext-shar}} \times \Gamma_{\Delta T_{ext-adj}} \quad (6.3)$$

Two main strategies are considered to deal with the ϕ_{shar} : minimizing them and/or improving their estimation. This last representation of $\Gamma_{\phi_{ext-shar}}$ helps to give the intuition on how to minimize the impact of the ϕ_{shar} during a test. In case their estimation is not accurate or possible, increasing the $\Gamma_{\phi_{ext-shar}}$ could be used as a strategy to avoid the effects of parasite heat flows.

Actions in the protocol requirements and conditions could be taken to maximize each one of the following ratios: the U-value, the surface and the temperature difference. In some cases although it could lead to the method applicability domain restriction. Next subsections discuss some possibilities to maximize each term of the equation 6.3

6.1.1 U_{eq} ratio

The $\Gamma_{U_{eq_{ext-shar}}}$ is intrinsic to the building thermal characteristics and is hard to modify with protocol conditions, but could be included as a limit for the method applicability domain. If we consider that the U_{eq} ratio should be elevated for protocol application, the test would be limited to buildings with insulation on the shared walls or with poor envelope thermal performance. However, since it depends on building characteristics and would represent a strong limitation to the method applicability domain, this strategy is not desirable on a first attempt.

Another possibility would be to add insulation panels on the surface of the shared walls during the test. This strategy, even though it could seem theoretically interesting, would be unpractical to be applied in an in-situ test. It would imply a great amount of insulation panels and their installation on ceiling and vertical walls could also be problematic. In case of a furnished apartment, the furniture could impeach the installation of the insulation panels. In order to minimize the impact of the ϕ_{shar} during a test, all strategies related to U_{eq} ratio could be considered.

6.1.2 Surface ratio

The surface ratio depends on the building geometry and on the location of the sampled area. For instance, an apartment located in the middle of a building would present lower $\Gamma_{S_{ext-shar}}$ than one located in the corner of a building. As an indication, table 6.1 gives the $\Gamma_{S_{ext-shar}}$ according to the position of two apartment types in a building. A simple geometry shape was considered for them, the first is a square apartment with seven meters of width and length and the second is a rectangular apartment which is ten meters long and five meters wide. In both

cases, an apartment situated at the corner of a top or ground floor presents the higher $\Gamma_{S_{ext-shar}}$ equal to 100 %.

Table 6.1 – Ratio of exterior and shared walls for apartments located at different locations of the building

Apartment position	Wall surface (m ²)		Surface ratio
	Exterior	Shared	
Square apartments (7 m x 7 m x 2.5 m)			
Intermediate floor middle apartment	17.5	150.5	12%
Intermediate floor corner apartment	35.0	133.0	26%
Top or ground floor middle apartment	66.5	101.5	66%
Top or ground floor corner apartment	84.0	84.0	100%
Rectangular apartments (5 m x 10 m x 2.5 m)			
Intermediate floor middle apartment in the short side	12.5	162.5	8%
Intermediate floor middle apartment in the long side	25.0	150.0	17%
Intermediate floor corner apartment	37.5	137.5	27%
Top or ground floor middle apartment in the short side	62.5	112.5	56%
Top or ground floor middle apartment in the long side	75.0	100.0	75%
Top or ground floor corner apartment	87.5	87.5	100%

Another option for the sampling could be to aggregate different apartments to test a whole floor or two floors at once. This strategy could increase the $\Gamma_{S_{ext-shar}}$, but could bring similar issues as for the global approach, concerning site vacancy of all apartments and the volume of equipment required for testing them. Table 6.2 shows two hypothesis done with a building with four apartments per floor or six apartments per floor, without any common area. The dimensions of each apartment are equal to those of the square apartment presented above and the building geometry is simplified, without any common areas, with the apartments placed side by side.

Table 6.2 – Ratio of exterior and shared walls for aggregated tested areas located at different parts of the building

Tested area	Wall surface (m ²)		Surface ratio
	Exterior	Shared	
4 apartments per floor (2 x 2)			
One intermediate floor	140	392	36%
Two intermediate floors	280	392	71%
One top/ground floor	336	196	171%
Top/ground floor + intermediate floor	476	196	243%
6 apartments per floor (2 x 3)			
One intermediate floor	175	588	30%
Two intermediate floors	350	588	60%
One top/ground floor	469	294	160%
Top/ground floor + intermediate floor	644	294	219%

Figure 6.2 shows some of the different locations mentioned in tables 6.1 and 6.2. In the left part, the top floor corner (in red) and middle apartment (in pink) are represented, as well as the intermediate floor corner (in yellow) and middle apartment (in blue). In the right part of the figure, there are some possibilities of gathering different apartments to increase the $\Gamma_{S_{ext-shar}}$, such as testing the following areas: the top floor (in red), one intermediate floor (in blue) and the ground floor plus one intermediate floor (in green).

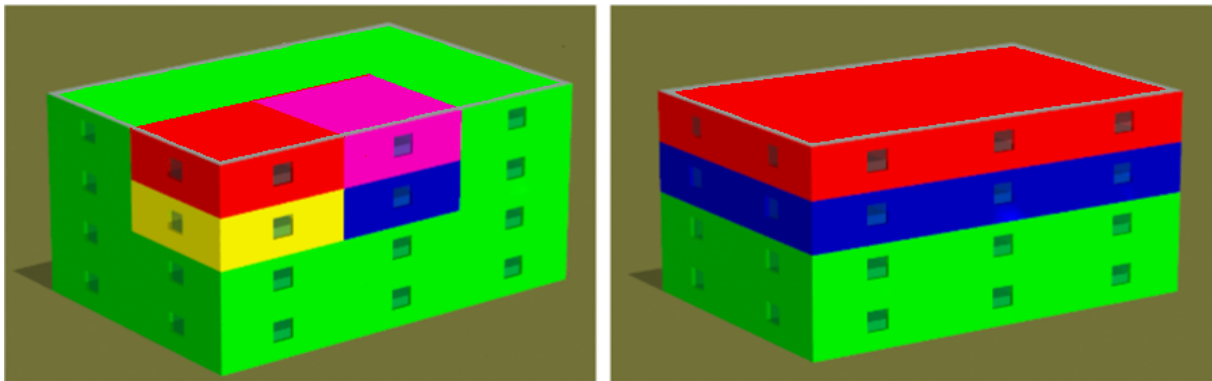


Figure 6.2 – Example of tested area location in a four-storey building with twenty-four apartments of 7 m x 7 m.

The surface ratio depends on the geometry of the building and of the tested area. Different areas could be chosen to be tested and to represent a sample of the building envelope. The higher the surface ratio, the better the conditions for the test. However, imposing a determined test location also means a limitation to the protocol applicability domain, reducing the possibilities of application on the field. For single apartments, those located on the corner of top or ground floor have the maximum $\Gamma_{S_{ext-shar}}$. Aggregating apartments increases the $\Gamma_{S_{ext-shar}}$ when compared to single apartments in the same floor. The possibility to apply the aggregation strategy should be verified case by case, according to the availability of the apartments and the equipment necessary for protocol application.

6.1.3 Temperature difference ratio

The $\Gamma_{\Delta T_{ext-adj}}$ is the ratio between the difference of temperature between the indoor and the outdoor environment ($\Delta T_{int-ext}$) and the difference of temperature between the indoor environment and the adjacent space ($\Delta T_{int-adj}$). It is the most flexible among the ratios, since it depends on the protocol conditions and is not related to the intrinsic characteristics of the building. However, it remains dependent on the exterior and adjacent temperatures.

The closer the temperature of the tested and the adjoining areas, the lower the heat flow among them. The strategy used to maximize $\Gamma_{\Delta T_{ext-adj}}$ is conditioned by the level of access and control in the adjoining spaces. Different scenarios could be considered for the constraints

regarding these areas [219]:

1. It is possible to access the adjoining spaces and to instrument and control their setpoint temperature.
2. It is possible to access the adjoining spaces and to instrument them, but not to control their setpoint temperature.
3. The adjoining spaces are not accessible during the protocol application.

The level of constraint would not only define the temperature control in the adjoining spaces, but also the method used to estimate ϕ_{shar} . In the first case, more freedom is given to the protocol application and ϕ_{shar} could be minimized by the use of a similar heating scenario in the tested area and in the adjacent dwellings. Both direct or indirect methods could be applied to estimate the heat flow that could still occur during the test due to imperfect temperature control and before temperature stabilisation.

In the second scenario, more restriction is given to the protocol application, but both methods could still be applied. However, in this case, it is expected to have higher levels of ϕ_{shar} , and the quality of these methods would have more impact on the final indicator. In the third scenario, since no sensor can be placed in the adjoining spaces, only the direct method could be considered. In the case of occupied retrofitted buildings, the access to adjoining dwellings can be a real constraint to the protocol application, since it depends on occupants agreement and on their availability during the beginning and the end of the test. For this reason, in some cases, only the direct method would be considered possible to be applied.

In the second and third scenarios the adjacent temperature can not be controlled, but still the temperature difference ratio could be maximized if the average temperature chosen by the neighbour is close to a suitable temperature for testing, with a enough high temperature difference between the indoor and outdoor environment. This condition would be typically achieved during winter time, when the neighbours also present an important temperature gradient with the outdoor environment. On one hand, this strategy seems to open some possibilities for the second and third scenario, on the other hand it may limit the period of the year during which the method can be applied.

Different strategies can be applied to maximize the $\Gamma_{\phi_{ext-shar}}$ and to minimize the impact of the ϕ_{shar} during a test. However this is still an intuition on how to improve the method accuracy. In the next section, a static model is used to explore different protocols, weather and building conditions, to give a numerical vision on the importance of ϕ_{shar} and the method limits.

6.2 Static method for exploring the sampling approach

In order to better understand the general behavior of the sampling approach a simplified model of the building thermal behavior was developed. In this model the thermal bridges, air infiltration and solar gains are not considered. Also the temperature and power are considered constant over time, to neglect the thermal dynamics happening during the test. The convenience of this hypothetical situation is that the HTC and its uncertainty can be calculated directly by a simple formula, which allows less computer intensive exploration of the sampling approach.

Under these particular conditions one model was developed to represent the indirect method and another to represent the direct method. Considering the simplifications of the model the HTC_{ext} can be calculated with equation 6.4 in the indirect method. The uncertainty of HTC_{ext} can be analytically calculated by direct formula with partial derivatives (equation 6.5) [219].

$$H\hat{T}C_{ext} = \frac{P_{heat} - \sum HTC_{shar}(T_{int} - T_{adj})}{T_{int} - T_{ext}} \quad (6.4)$$

$$u_{HTC_{ext}} = \sqrt{\left(\frac{\partial HTC_{ext}}{\partial P_{heat}}\right)^2 u_{P_{heat}}^2 + \sum \left(\left(\frac{\partial HTC_{ext}}{\partial HTC_{shar}}\right)^2 u_{HTC_{shar}}^2\right) + \left(\frac{\partial HTC_{ext}}{\partial T_{int}}\right)^2 u_{T_{int}}^2 + \left(\frac{\partial HTC_{ext}}{\partial T_{ext}}\right)^2 u_{T_{ext}}^2 + \left(\frac{\partial HTC_{ext}}{\partial T_{adj}}\right)^2 u_{T_{adj}}^2} \quad (6.5)$$

where:

$$\begin{aligned} - \frac{\partial HTC_{ext}}{\partial P_{heat}} &= \frac{1}{T_{int} - T_{ext}}; \\ - \frac{\partial HTC_{ext}}{\partial HTC_{shar}} &= \frac{T_{int} - T_{adj}}{T_{int} - T_{ext}}; \\ - \frac{\partial HTC_{ext}}{\partial T_{int}} &= \frac{-P_{heat} + \sum HTC_{shar}(T_{ext} - T_{adj})}{(T_{int} - T_{ext})^2}; \\ - \frac{\partial HTC_{ext}}{\partial T_{ext}} &= \frac{P_{heat} - \sum HTC_{shar}(T_{int} - T_{adj})}{(T_{int} - T_{ext})^2}; \\ - \frac{\partial HTC_{ext}}{\partial T_{adj}} &= \frac{\sum HTC_{shar}}{T_{int} - T_{ext}}. \end{aligned}$$

Equation 6.6 describes the HTC_{ext} calculation with the direct method, using heat flow meters. The uncertainty of HTC_{ext} is presented in equation 6.7 [219].

$$H\hat{T}C_{ext} = \frac{P_{heat} - \varphi_{shar} S_{shar}}{T_{int} - T_{ext}} \quad (6.6)$$

$$u_{HTC_{ext}} = \sqrt{\left(\frac{\partial HTC_{ext}}{\partial P_{heat}}\right)^2 u_{P_{heat}}^2 + \sum \left(\left(\frac{\partial HTC_{ext}}{\partial \varphi_{shar}}\right)^2 u_{\varphi_{shar}}^2\right) + \left(\frac{\partial HTC_{ext}}{\partial T_{int}}\right)^2 u_{T_{int}}^2 + \left(\frac{\partial HTC_{ext}}{\partial T_{ext}}\right)^2 u_{T_{ext}}^2} \quad (6.7)$$

where:

$$\begin{aligned}
 - \frac{\partial HTC_{ext}}{\partial P_{heat}} &= \frac{1}{T_{int}-T_{ext}}; \\
 - \frac{\partial HTC_{ext}}{\partial \varphi_{shar}} &= \frac{-S_{shar}}{T_{int}-T_{ext}}; \\
 - \frac{\partial HTC_{ext}}{\partial T_{int}} &= \frac{-P_{heat}+\varphi_{shar}S_{shar}}{(T_{int}-T_{ext})^2}; \\
 - \frac{\partial HTC_{ext}}{\partial T_{ext}} &= \frac{P_{heat}-\varphi_{shar}S_{shar}}{(T_{int}-T_{ext})^2};
 \end{aligned}$$

These models demand the following entry variables:

- Temperatures (all constants)
 - Interior temperature (T_{int}) [°C]
 - Exterior temperature (T_{ext}) [°C]
 - Adjacent temperature (T_{adj}) [°C]
- Geometry
 - Exterior to shared walls surface ratio ($\Gamma_{S_{ext-shar}}$) [%]
 - Intermediate floor to shared wall surface ratio [%]
- U-values
 - U-value of exterior walls [W/m²/K]
 - U-value of party walls [W/m²/K]
 - U-value of intermediate floors [W/m²/K]
- Input uncertainties
 - Uncertainty on the power measurement ($u_{P_{heat}}$) (default of ISABELE and SEREINE methods: $\pm 2\%$)
 - Uncertainty on the temperature measurements ($u_{T_{int}}, u_{T_{ext}}, u_{T_{adj}}$) (default of ISABELE and SEREINE methods: $\pm 0.5K$)
 - Uncertainty on the U-value of shared walls ($u_{HTC_{shar}/S_{shar}}$) [%] for the indirect method (varied)
 - Uncertainty on the measurement of heat flow meters ($u_{\varphi_{shar}}$) [W/m²] for the direct method (varied)

The values of input uncertainties represent a possible deviation the measurements of some input parameters might have with the real values. In this static study the input uncertainties are considered to respect a continuous uniform distribution between the values associated to them. An exception is the U-value of shared walls that is given directly in the standard deviation form.

The models were used to study the uncertainty level of the results according to different test conditions. For simplicity, the same U-value and input uncertainty level of the U-value of all shared walls were assumed. Once the intermediate floor and party walls have the same characteristics, the intermediate floor to shared wall surface ratio becomes irrelevant. The indoor and outdoor temperatures were chosen to represent a test under winter conditions, the respective temperatures used were 20°C and 5°C. The parameters were varied in this study according to the following ranges:

- U-value of the exterior walls: between 0.1 and 2 W/(K.m²)
- U-value of the shared walls: between 0.4 and 2.8 W/(K.m²)
- Surface ratio between exterior and shared walls: between 0 and 2.4
- Adjacent temperature (T_{adj}): 10, 15 and 20 °C
- Uncertainty on the U-value of shared walls for the indirect method: between 5 and 40 %
- Uncertainty on the measurement of φ_{shar} for the direct method: between 0.01 and 4 W/m²

The U-value ranges were based on common values presented on non insulated to well insulated walls. The surface ratio was defined from zero (most pessimist condition) to the maximum achieved by group of apartments, previously presented on table 6.2. The adjacent temperatures were chosen to give a $\Delta T_{int-adj}$ up to 10 K. The ranges of uncertainty levels used here were done by testing different values, starting from low values (most optimistic) until values where the uncertainty in the final results were mostly out of the acceptable range. Based on these assumptions, the level of HTC_{ext} uncertainty was graphically represented with the variation of the most influential parameters for each method. The results of the indirect method are shown in part 6.2.1 and those of the direct method are shown part 6.2.2.

6.2.1 Result uncertainty with the indirect method

The results of the static indirect method application are presented in figures 6.3 to 6.5. Color bars represent the uncertainty in the HTC_{ext} value, which corresponds to 1.96 times $u_{HTC_{ext}}$. Red areas represent the cases where the uncertainty is above 35 %, for which the results are considered to be less meaningful. The dashed vertical white lines are limiting the maximum $\Gamma_{S_{ext-shar}}$ usually achieved when testing a single apartment or office.

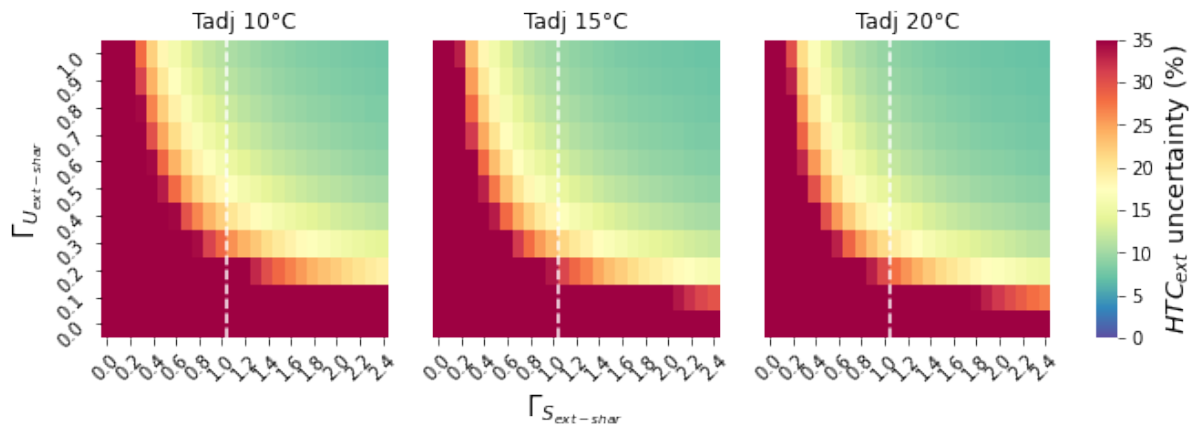


Figure 6.3 – HTC uncertainty according to U-value and surface ratio using the indirect method considering 5 % of uncertainty in U_{shar} .

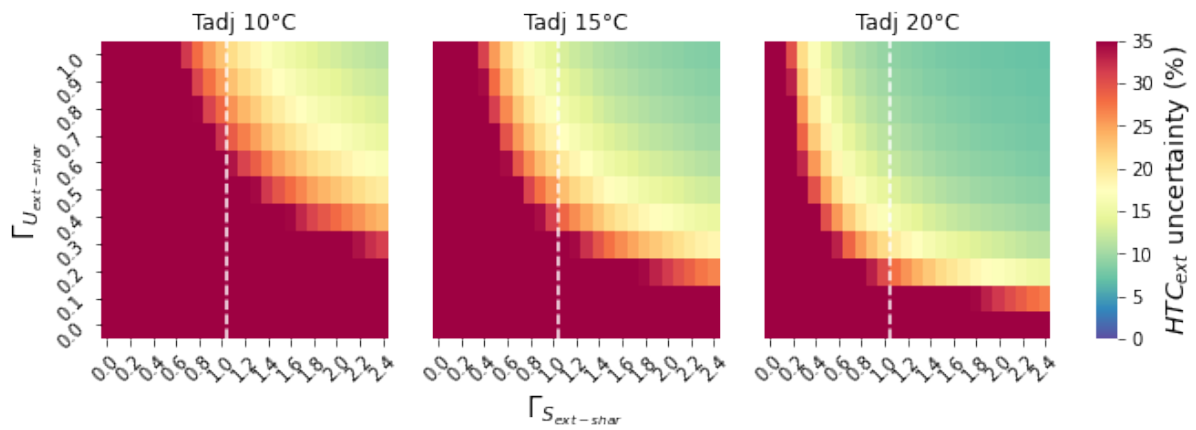


Figure 6.4 – HTC uncertainty according to U-value and surface ratio using the indirect method considering 20 % of uncertainty in U_{shar} .

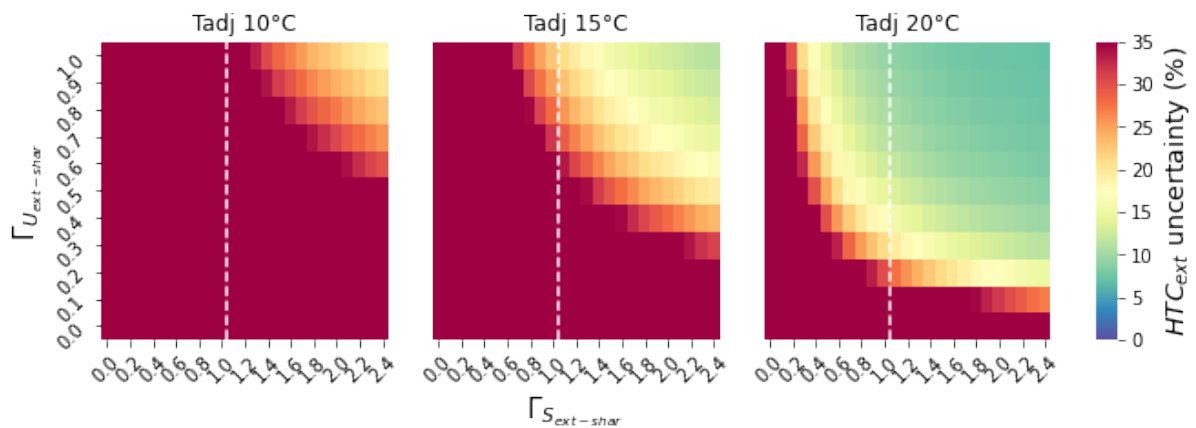


Figure 6.5 – HTC uncertainty according to U-value and surface ratio using the indirect method considering 40 % of uncertainty in U_{shar} .

The area above 100 % of surface ratio represents a test in aggregated areas, such as one or two entire floors in a building. In these graphics we present this ratio going up to 240 %, that

is about the maximum level achieved when aggregating two consecutive floors in a building, presented previously in table 6.2.

It can be seen among the three figures that the $\Gamma_{S_{ext-shar}}$ plays an important role on the final result uncertainty. The more this ratio increases, the less uncertainty there is in the results. If a single apartment or office is tested, it would be better to choose those located at the corner of the top or ground floor. Otherwise, aggregation of apartments or offices can be considered to perform the test and assure lower levels of uncertainty in the final indicator.

Once $\Gamma_{U_{ext-shar}}$ increases the uncertainty in the HTC also increases. This means that buildings with well insulated exterior walls and non insulated shared walls are more difficult cases to be treated, as expected. Considering that the input uncertainty of the U-values was a percentage of this value, less insulated walls present a higher ϕ_{shar} , but also an absolute higher uncertainties of U_{shar} than the insulated walls, both having an impact on the result uncertainties.

In addition, when the uncertainty associated to U_{shar} increases, the level of uncertainty in the final indicator raises, for cases with $\Delta T_{int-adj}$ different from zero. When T_{adj} is at the same temperature that the tested area, the uncertainty in U_{shar} does not have influence on the results, which is expected, since there is no heat flow passing through the shared walls. Decreasing the temperature difference between the interior and the adjoining spaces becomes therefore important for buildings with poor insulation on the shared walls, for which the losses to the neighbors are more important.

6.2.2 Result uncertainty with the direct method

According to equation 6.7, the input uncertainty of U_{ext} is not taken into account in the direct method, but the input uncertainty associated with the heat flow measurements impacts the final result uncertainty. The latter input uncertainty was then added to the analysis of the direct method. Figures 6.7 to 6.8 present the results of this analysis for the following values of input uncertainties: 0.01, 1, 2 and 4 W/m².

The trends related to $\Gamma_{S_{ext-shar}}$ and the $\Gamma_{U_{ext-shar}}$ are similar to that presented in the previous figures. When the input uncertainties of the ϕ_{shar} measurements are small, the validity domain of the method increases significantly when compared with the indirect method. If, in addition, the adjoining spaces have the same temperature as the tested area, the test could be applied to all apartments locations and buildings typologies. However, achieving 0.01 W/m² of input uncertainties of the heat flow meter measurements is unrealistic. In any case, the HTC_{ext} uncertainty strongly depends on the input uncertainties of the heat flow meters measurements. The temperature difference between the interior and the adjoining spaces has relatively less importance on the results of the direct method when comparing to those of the indirect method.

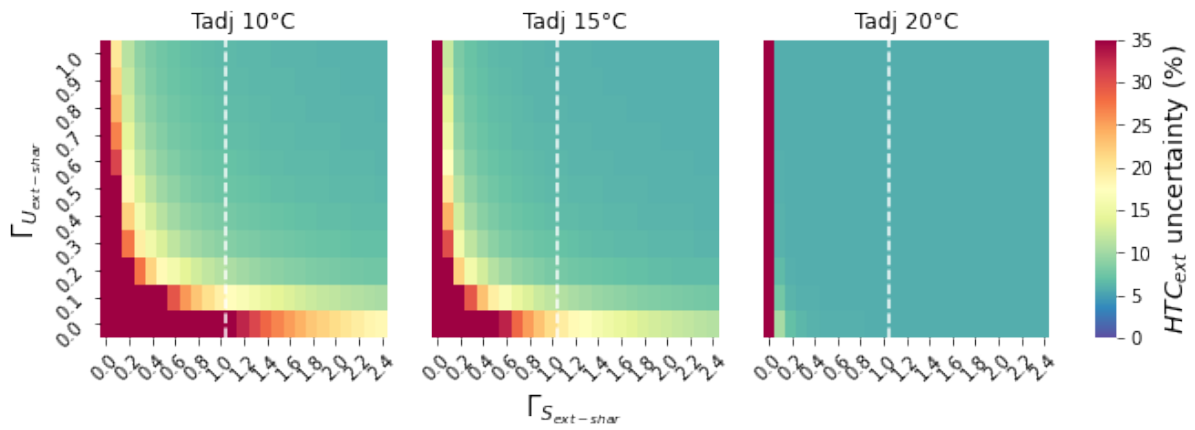


Figure 6.6 – HTC uncertainty according to the U-value and surface ratio using the direct method considering 0.01 W/m^2 of uncertainty in the heat flow meter measurements.

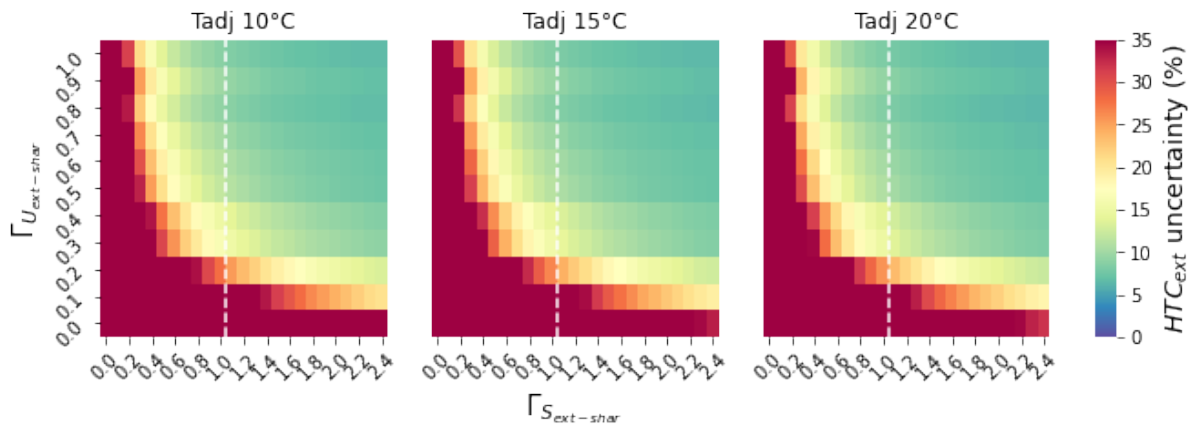


Figure 6.7 – HTC uncertainty according to the U-value and surface ratio using the direct method considering 1 W/m^2 of uncertainty in the heat flow meter measurements.

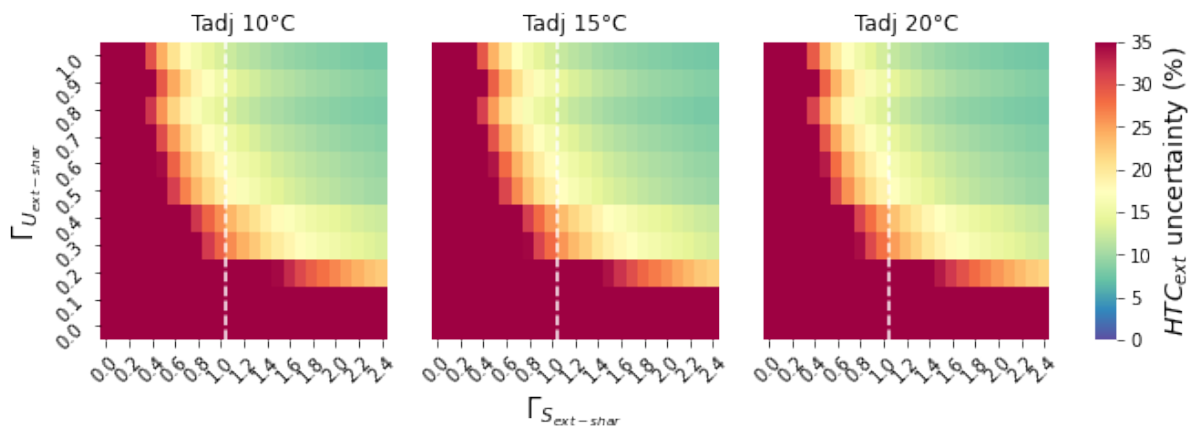


Figure 6.8 – HTC uncertainty according to the U-value and surface ratio using the direct method considering 2 W/m^2 of uncertainty in the heat flow meter measurements.

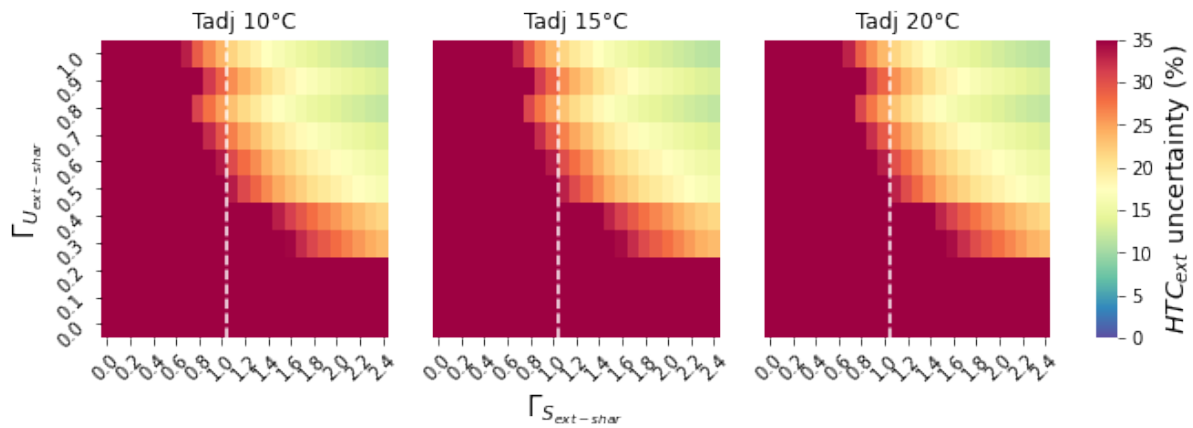


Figure 6.9 – HTC uncertainty according to the U-value and surface ratio using the direct method considering 4 W/m^2 of uncertainty in the heat flow meter measurements.

6.2.2.1 General discussion

This preliminary study guides on the choice of the area to be tested in a building. Testing an apartment or office located at the corner of the top floor would improve the method accuracy when we keep all other parameters unchanged. The presence of insulation on the adjoining walls, that is a rare condition, makes it possible to further improve the measurement accuracy when applying the indirect method. With this method, the level of thermal losses through the shared walls had a significant influence on the results. It should also be considered that in both methods the input uncertainties were directly or indirectly related to the shared walls U-value, so the level of input uncertainties increased with the increment of ϕ_{shar} .

Heating the adjoining spaces can also be a relevant strategy when applying the indirect method. The results uncertainty in the direct method are strongly dependant on the uncertainties of the heat flow meters measurements. The ranges of uncertainties expected from these measurements in real life should be further studied.

In general, the conditions that enhance the external heat flows (which are to be characterized) in comparison to the ϕ_{shar} , presented lower result uncertainties. This highlights the importance of increasing the $\Gamma_{\phi_{ext-shar}}$ during the protocol application. Although first conclusions can be taken from this study, it should be precised that this is based on a simplified steady state model, and in reality the dynamics may play an important role. When ISABELE/SEREINE algorithms are used, the uncertainty calculations are different, including other sources and might be higher than in this study. In order to understand the applicability domain of the indirect and direct methods, they should be simulated in conditions closer to the real application and these observations have to be confirmed with dynamic models. In the next sections, both methods are applied with dynamic simulations and *in-situ*.

6.3 Indirect method for neighbours flow estimation

The indirect method consists of the estimation of the ϕ_{shar} through a simplified calculation, based on the temperature in both sides of the walls and its surfaces and U-values. In part 6.3.1, hypothesis are made to define the level of uncertainty associated to the shared walls U-value. In part 6.3.2.3, different numerical simulations are presented to investigate the method behavior.

6.3.1 Ranges of U_{shar} uncertainty

The uncertainty associated with the shared walls U-values depends on the level of knowledge about these walls. This uncertainty has a significant influence on the HTC_{ext} final uncertainty and is therefore studied in this subsection.

We consider that the materials and layers of the shared walls would be detailed in the building description documents. In this case, an uncertainty characterized by a normal distribution with a standard deviation of 10% could be considered for the material conductivity [243]. An uncertainty of 10 to 15 % related to the wall layer thickness was used in the literature due to to workmanship [244, 245], but lower levels could be associated for factory made materials and those with certifications. In this study, a standard deviation of 10 % was associated to the wall layers thickness. The model walls composition is described in Annex B.

Concerning the superficial heat transfer coefficients, they represent the combined phenomena of convection and radiation. A uniform distribution between 5.5 and 11 W/m²/K was used, which represents the ranges for natural ventilation conditions, including values for vertical surface and ascending and descending heat flow in horizontal surfaces. The center of this distribution is 8.25 W/m²/K, while in Pléiades Comfie the superficial heat transfer coefficients used for internal vertical walls is of 8.13 W/m²/K and for internal vertical walls is of 8 W/m²/K, both for surfaces with an emissivity of 0.9.

Based on these ranges of variations for the parameters and on equation 6.8 a Monte Carlo uncertainty propagation with 10000 samples was conducted.

$$U_{shar} = \left(\frac{2}{h_{int}} + \sum_{m=1}^n \frac{e_m}{\lambda_m} \right)^{-1} \quad (6.8)$$

where:

- U_{shar} is the U-value of a shared wall (W/m².K);
- h_{int} is the indoor superficial heat transfer coefficient (W/m².K);
- e_m is the thickness of a material layer (m);
- λ_m is the conductivity of a material layer (W/m/K).

The distributions of the U-value for the shared walls of the P+C model are presented in figure 6.10.

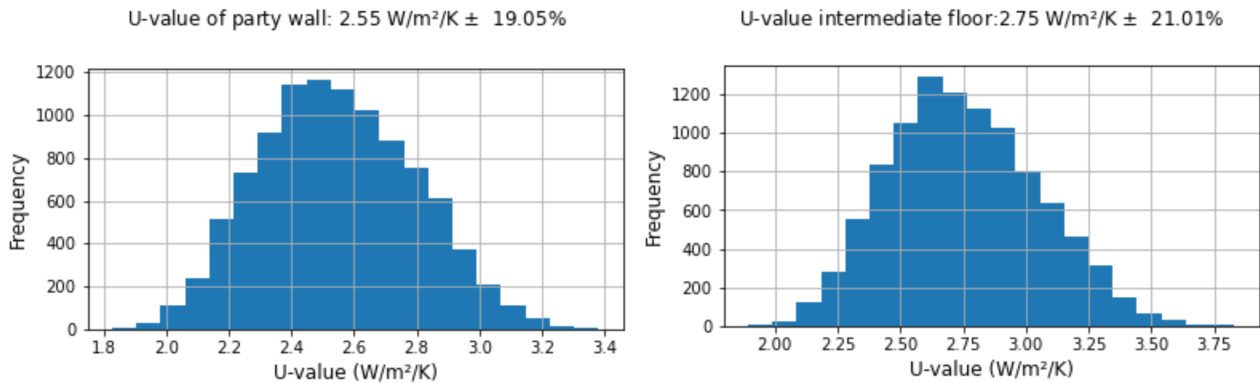


Figure 6.10 – Histogram of partition walls (left) and intermediate floor (right) U-value, obtained from the Monte-Carlo uncertainty propagation sample size of 10000

The estimates of U-value are 2.55 W/m²/K for the partition wall and 2.75 W/m²/K for the intermediate floor. Values calculated with equation 6.8, without considering uncertainties in the thickness and conductivity, are respectively 2.53 and 2.78 W/m²/K. The estimated value for both methods are coherent. The percentage uncertainties presented in this figure corresponds to the semi interval of 95 % confidence or 1.96 times the distribution standard deviation. Both uncertainties are around 20 % of the absolute U-value. This value will therefore be considered for the uncertainty of the shared walls U-values in the virtual experimental plan presented in this section. If the knowledge about the shared walls composition are lower, higher uncertainties should be considered for U_{shar} .

6.3.2 Virtual experimental plan

In this part different simulations were performed in Pléiades Comfie to study the behavior and limits of the sampling approach. The building model used for the global approach is the same one used in these simulations, with only one difference for the thermal bridges that were adjusted to correspond to a renovation level. The protocol and the site of the building vary among the different methods application to test different temperatures and solar radiation conditions. In Pléiades Comfie it is possible to analyze the solar radiation incident on each building facade, at any time of the year, which enables the use of the equivalent outdoor temperature in the tests for simulating the SENS sensors measurements.

The virtual tests are carried out on a corner apartment of the top floor, with two exposures (east and south) and modeled in a single thermal zone. The objective of this choice is to obtain the highest possible $\Gamma_{S_{ext-shar}}$, while testing a single apartment in the building. It has a 63m²

floor area, 107 m² of exterior walls and an equivalent area of shared walls.

In terms of the thermal characteristics of the building, the HTC_{ext} of the part of the envelope associated with this apartment is of 72.5 W / K. In order to calculate this value, the outdoor environment and the adjacent spaces were set with the same constant temperature and solar radiation was set equal to zero. The ratio between the power delivered and the temperature differences gives the HTC value (table 6.3).

Table 6.3 – HTC_{ext} reference value for the tested apartment in the building model in Pleiades Modeller

Indoor temperature (°C)	Outdoor temperature (°C)	Temperature difference (K)	Delivered power (W)	HTC (W/K)
5	0	5	363	72.6
10	0	10	725	72.5
20	0	20	1450	72.5

The HTC_{shar} was calculated with the respective surfaces and U-values of each shared wall and it is 287.0 W/K, which gives a $\Gamma_{U_{ext-shar}}$ of 25 %. This condition makes the test of this apartment difficult and the results are likely to have an elevated level of uncertainty. Although buildings with more elevated $\Gamma_{U_{ext-shar}}$ would provide better results, the choice of a building with a good envelope thermal performance is more representative of a situation where the method would be applied, such as after a massive retrofit action.

Figure 6.11 shows the location of the tested apartment, number 15, on the top floor. It shares walls with four different areas in the building: one unheated zone (UZ), two apartments in the same floor (14 and 16) and one apartment beneath it on the second floor (11).

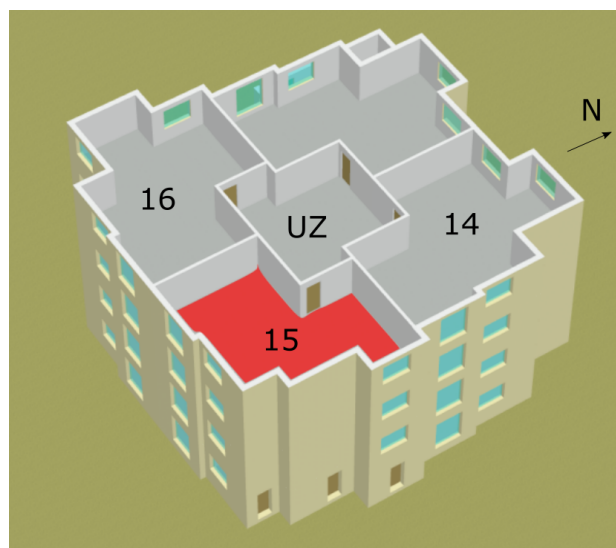


Figure 6.11 – Internal view of the building model top floor in Pleiades Modeller with floor of apartment n° 15 in red.

Equation 6.9 describes the heat flow passing through shared walls in an instant t , when applying the indirect method. It should be noticed that the ϕ_{shar} is considered as a steady state heat flow.

$$\phi_{shar;t} = U_{shar,hor} S_{11}(T_{15;t} - T_{11;t}) + U_{shar,vert} (S_{14}(T_{15;t} - T_{14;t}) + S_{16}(T_{15;t} - T_{16;t}) + S_{UZ}(T_{15;t} - T_{UZ;t})) \quad (6.9)$$

Different numerical experiments were performed with dynamic simulations to explore various test conditions. In all experimental plans, air infiltration was set to zero, so HTC and HLC are identical. Models of order higher than 1 were not stable in the results and with a low tax of convergence. This might be due to the simplicity of the model in the apartment level, with a single thermal zone. For this reason only first order models were used in this work. The two RC models used in the estimation process are presented in figure 6.12. The parameters in red are estimated by the optimization algorithm, the parameters in blue are measured and the parameters in yellow are estimated through other models.

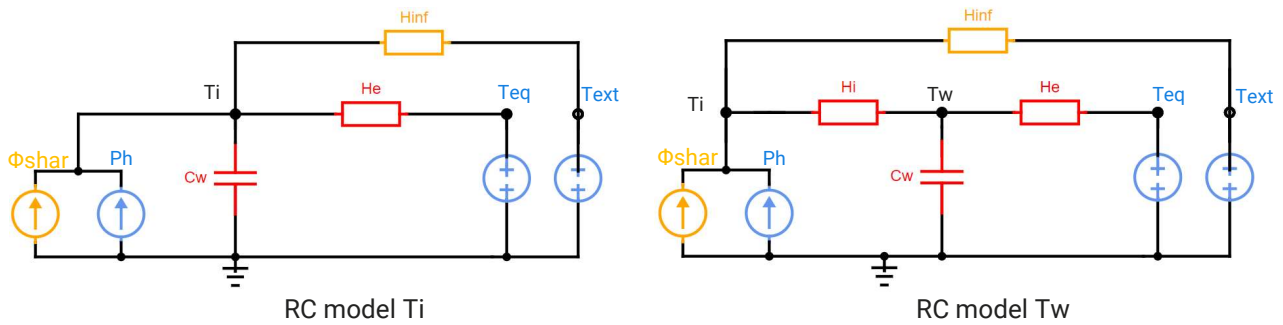


Figure 6.12 – RC thermal models of first order used in the estimation process of the numerical experiments.

In part 6.3.2.1 the shared walls composition and the insulation position in the envelope were varied to investigate the method behaviour for different building fabric. In part 6.3.2.2 the preheating of the building before test application and the setpoint temperature were investigated. Part 6.3.2.3 presents variations in the test setpoint temperature and test application all over the year through different weather stations.

6.3.2.1 Variation on the exterior walls insulation location and shared walls inertia

This experimental plan was performed using the weather data from the French city Trappes, close to Paris. All the tests were applied the same weather condition of winter and had a setpoint temperature of 22 °C. It was considered a preheating of the building before protocol application of 18 °C. It was considered that the adjacent apartments were occupied during the test and that

their temperatures could not be controlled. In order to perform the simulations, a scenario was chosen to represent the temperature in the adjacent apartments, as can be seen in table 6.4. In this scenario, one of the neighbours kept a constant temperature over time and two of them varied the setpoint temperature between night and day. The unheated zone in the middle did not have any temperature set, however, it is indirectly heated by the surrounding apartments.

Table 6.4 – Setpoint temperatures for the scenario with variation in the neighbours temperature in P+C

Apartment	Temperature (°C) for each hour of the day																							
	1	2	3	4	5	6	7	8	9	10	11	12	13	14	15	16	17	18	19	20	21	22	23	24
11	20	20	20	20	20	20	20	20	20	20	20	20	20	20	20	20	20	20	20	20	20	20	20	20
14	17	17	17	17	17	21	21	21	21	21	21	21	21	21	21	21	21	21	21	17	17	17	17	17
16	15	15	15	15	15	15	19	19	19	19	19	19	19	19	19	19	19	19	19	19	15	15	15	15
Others	16	16	16	16	16	16	20	20	20	20	20	20	20	20	20	20	20	20	16	16	16	16	16	16

The parameters that varied in the experience were the composition of the shared walls and the position of the insulation. A light and heavy wall variant was tested as shown in table 6.5. Concerning the exterior wall, the same materials and thickness were used from the model presented before in chapter 4, but the insulation was placed either on the inside or on the outside of the wall.

Table 6.5 – Shared wall characteristics for the heavy and light variants

<i>Variant</i>	<i>Shared wall</i>	<i>Material</i>	<i>Thickness</i> [cm]	<i>Surface mass</i> [kg/m ²]	<i>Thermal resistance</i> [K.m ² /W]
Heavy	Partition wall	Plaster	1	10	0.03
		Concrete	15	345	0.09
		Plaster	1	10	0.03
	Intermediate Floor	Concrete	20	460	0,11
Light	Partition wall	Plaster	2	20	0.06
		Hollow brick	5	36	0.10
		Plaster	2	20	0.06
	Intermediate Floor	Wood fiber	1.6	13	0.11

Finally, four compositions were considered: heavy walls and light walls with insulation by the inside and outside. Figure 6.13 presents the temperature profiles and the heating power for these four tests. The results progression for these variants is presented in figures 6.14 to 6.17. Only first order models were used, since they presented more stability over time and lower levels of uncertainty for this study case.

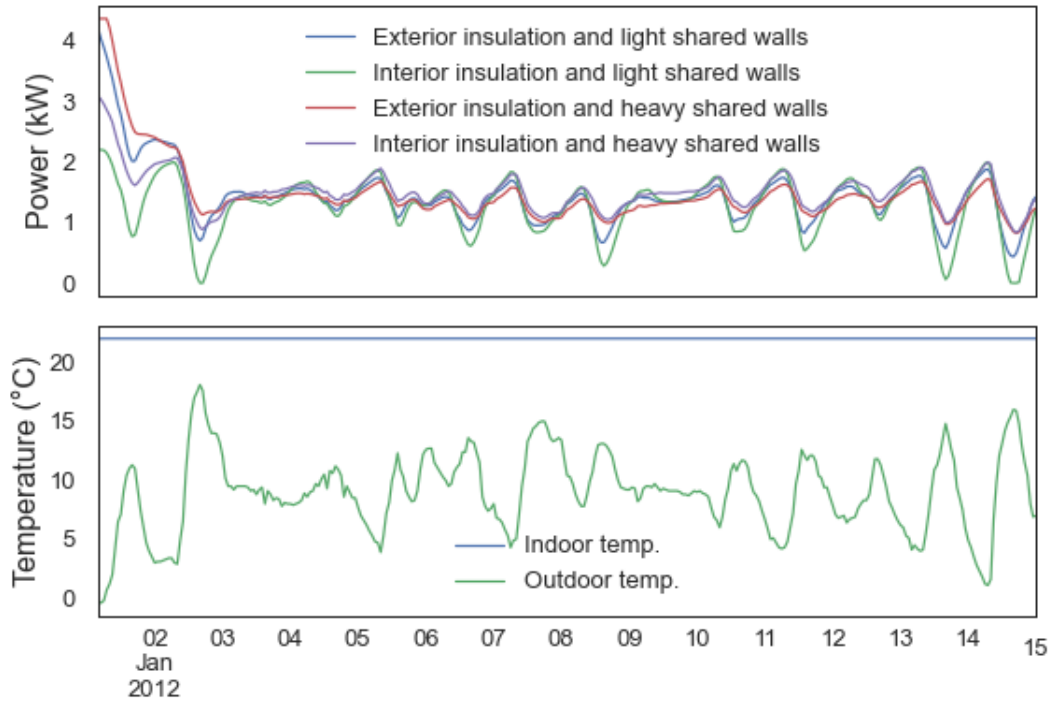


Figure 6.13 – Indoor and outdoor temperatures during the test

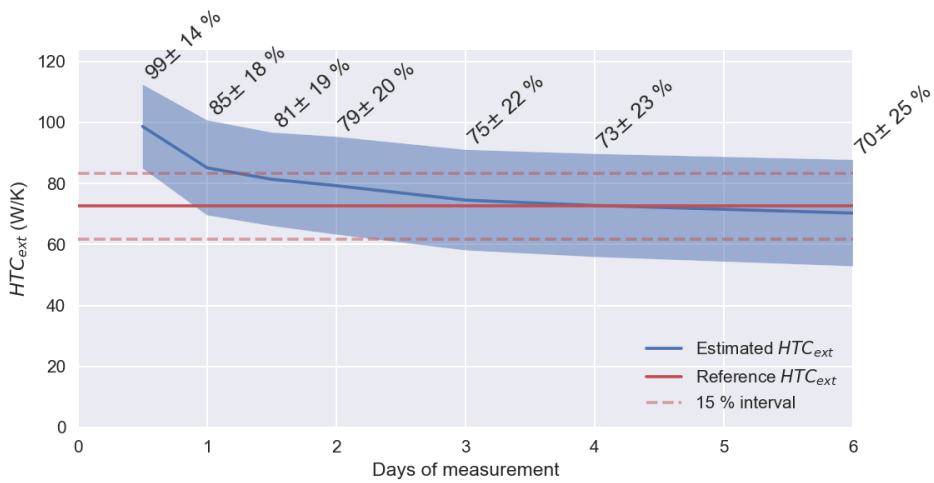


Figure 6.14 – Results progression for the variant with heavy shared walls and internal wall insulation

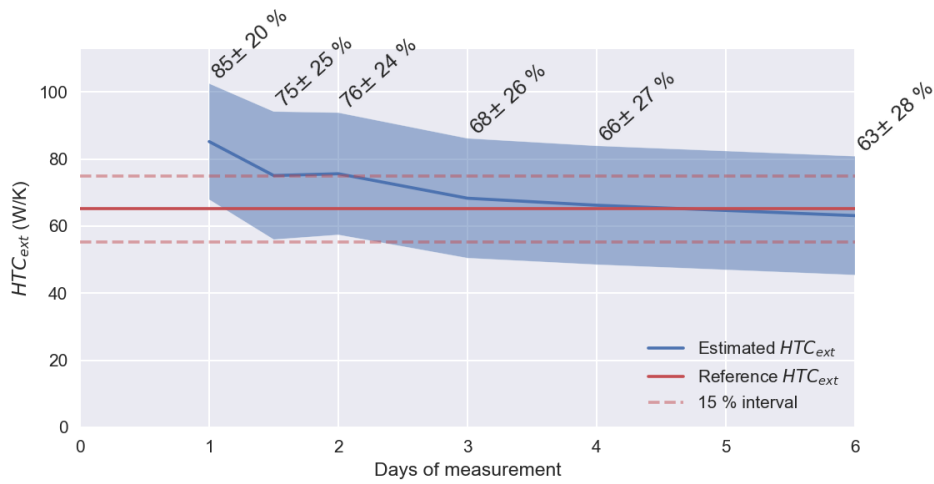


Figure 6.15 – Results progression for the variant with heavy shared walls and external wall insulation

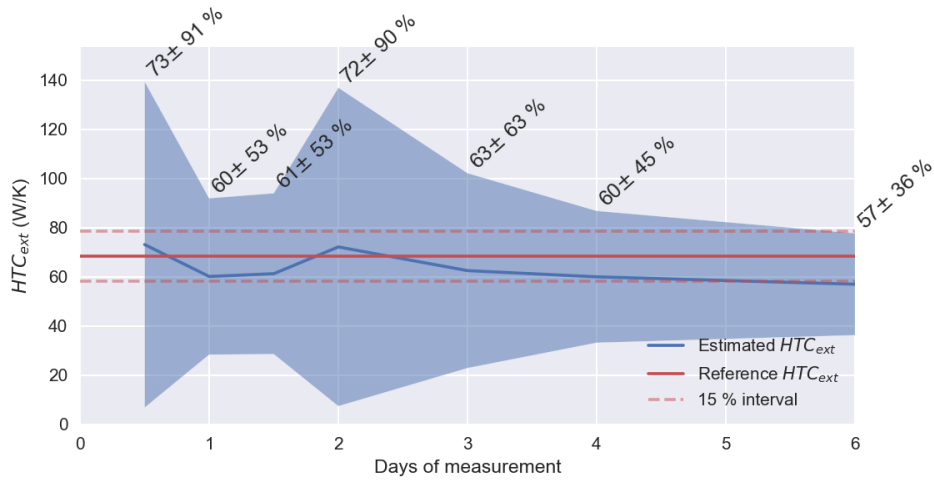


Figure 6.16 – Results progression for the variant with light shared walls and internal wall insulation

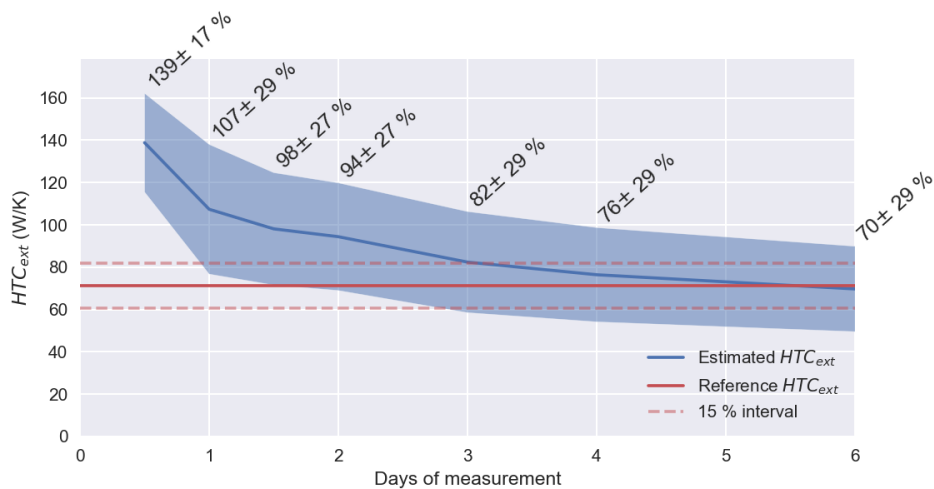


Figure 6.17 – Results progression for the variant with light shared walls and external wall insulation

It can be noticed that the variants with an external wall insulation needed more time to converge to the reference HTC_{ext} , which is expected since more time is required to heat the thermal mass of the exterior walls. These four results were for tests with preheating and 4 K of $\Delta T_{beg-end}$. In tests without preheating, the time required to converge in variants with an insulation on the outside might be even higher. In the next part the effect of the preheating is going to be presented to one of these building variants.

The variant of the shared walls does not play a clear role on the test results. For the variants with insulation on the outside, the results are similar, but with slightly higher uncertainties in the case of light shared walls. However, the variant with the lowest thermal mass among the four (insulation on the inside and light shared walls) presented unstable uncertainty levels, although the bias was low from the shortest test duration. This results are not intuitive, once the indirect method does not take into account the dynamics in the shared walls. It was expected that variants with lower thermal mass would perform better, since the calculated and real φ_{shar} are not shifted in the power time series. Other conditions and building compositions might be investigated to verify this effect, although it will not be the focus of this work.

6.3.2.2 Variation on the setpoint and preheating temperature

Another experimental plan was developed to investigate the advantages of preheating the apartment before the test. A two-week-fixed temperature period was used prior test for the variants with preheating. Even for the tests without preheating, the initial test temperature was about 16 °C, since the neighbours were heated all year round. According to the outcomes of global approach experimental plan, the temperature difference between the beginning and the end of the test ($\Delta T_{beg-end}$) was an influential parameter that allowed to make the results converge faster. For this reason different setpoint temperatures were used applying the same $\Delta T_{beg-end}$ of zero and four Kelvins. Its values, as well as those to which the tested housing is heated during the protocol, are given in the table 6.6.

This experimental plan and the following ones were simulated by Michaël Cohen, from Mines ParisTech. The building variant with heavy shared walls and insulation on the inside was used in this and all the following experimental plans. All these tests were performed under winter conditions, with the weather station of Nancy starting on 15th of January. The temperature of the adjacent spaces was considered variable over the day according to the scenario presented before in table 6.4. From these simulations, the equivalent outdoor temperature takes into account the solar gains per each building facade. Figure 6.18 presents the solar radiation for each direction (G_S, G_E, G_W, G_N), the outdoor temperature (T_{ext}) and its equivalent temperatures per facade ($T_{eq_S}, T_{eq_E}, T_{eq_W}, T_{eq_N}$) over the test duration.

Table 6.6 – Preheating and setpoint temperatures of the experimental plan.

Variant number	Preheating temperature [C°]	Setpoint temperature [C°]	$\Delta T_{\text{beg-end}}$ [K]
1	no preheating		2.2
2	14	18	4
3	18		0
4	no preheating		6.2
5	18	22	4
6	22		0
7	no preheating		10.2
8	22	26	4
9	26		0
10	no preheating		14.2
11	26	30	4
12	30		0

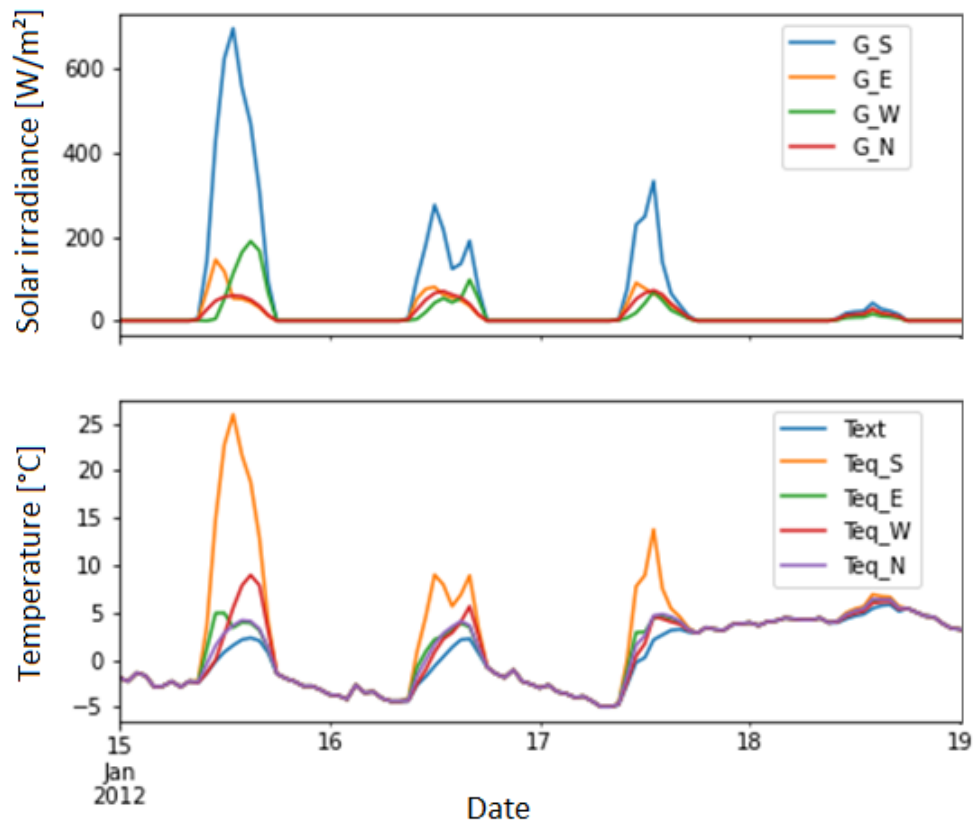


Figure 6.18 – Solar radiation per facade (top) and outdoor and equivalent outdoor temperatures (down) during virtual protocol application of second experimental plan.

The twelve variants were analysed with SEREINE algorithms using a test duration from half a day to four days. The results were considered as acceptable if they presented a bias inferior to 15 % and an uncertainty inferior to 35 %. Table 6.7 shows the statistics on the interpretability indicator, inner 15 % interval, for the results considered acceptable and unacceptable. It can be

seen that just one third of variants were acceptable with a very short duration of half day. For this short duration also the variants diverged, while for longer durations all tests converged. With the increment of test duration, more results became acceptable and from three days all twelve variants were acceptable. Regarding the interpretability of the results, 0.5 is the maximum interpretability value presented among the unacceptable results. Even though interpretability of 0.4 can be found among the acceptable results, the value of 0.5 is going to be used as a threshold of result quality in this study.

Table 6.7 – Statistical description of results interpretability according to acceptability and test duration.

Interpretability \ statistical description	Acceptability \ Duration (days)	Acceptable results						Unacceptable results			
		0.5	1	1.5	2	3	4	0.5	1	1.5	2
Amount		4	9	10	10	12	12	5	3	2	2
Mean		0.8	0.7	0.7	0.8	0.8	0.8	0.1	0.2	0.4	0.5
Standard deviation		0.0	0.1	0.1	0.1	0.1	0.1	0.1	0.1	0.1	0.1
Minimum value		0.8	0.5	0.4	0.5	0.6	0.7	0.0	0.1	0.3	0.4
25th percentile		0.8	0.5	0.7	0.7	0.7	0.7	0.2	0.1	0.3	0.4
50th percentile		0.8	0.6	0.8	0.8	0.8	0.8	0.2	0.2	0.4	0.5
75th percentile		0.8	0.7	0.8	0.8	0.9	0.9	0.2	0.2	0.4	0.5
Maximum value		0.8	0.9	0.9	0.9	0.9	0.9	0.2	0.2	0.5	0.5

Figures 6.19 to 6.22 present the interpretability of the 12 variants according to their setpoint temperature and $\Delta T_{beg-end}$. Only the diagonal of the area without preheating was tested. The areas in green are those not tested or that did not converge. The blue areas correspond to the tests with acceptable results and the red areas to those with unacceptable results. The areas with light color are correspondent to 0.5 of interpretability. The higher the interpretability of a test, the better its result.

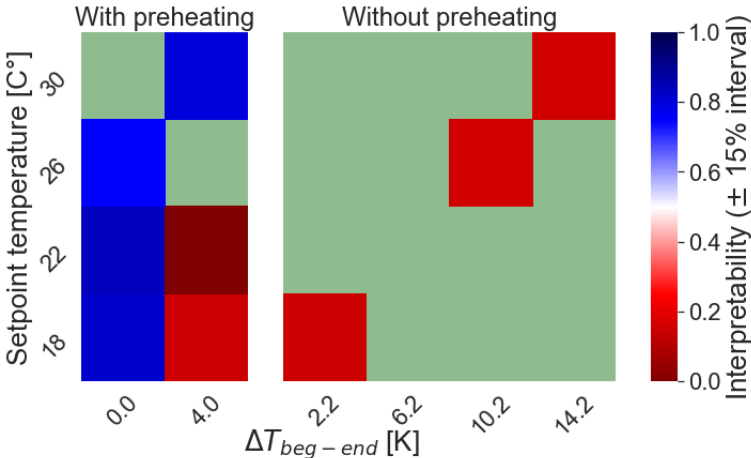


Figure 6.19 – Results interpretability for different protocol setpoint temperature and preheating conditions for half day of test duration.

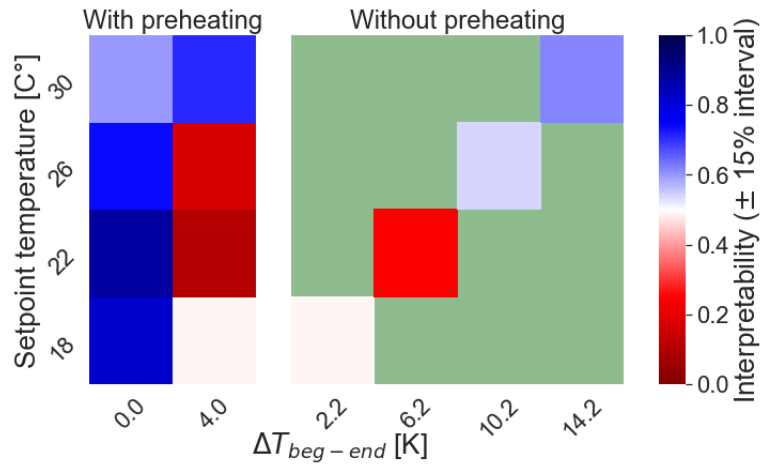


Figure 6.20 – Results interpretability for different protocol setpoint temperature and preheating conditions for 1 day of test duration.

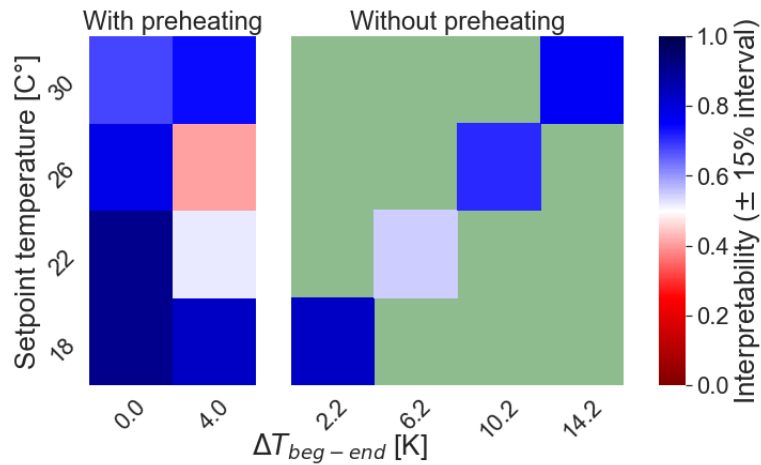


Figure 6.21 – Results interpretability for different protocol setpoint temperature and preheating conditions for 2 days of test duration.

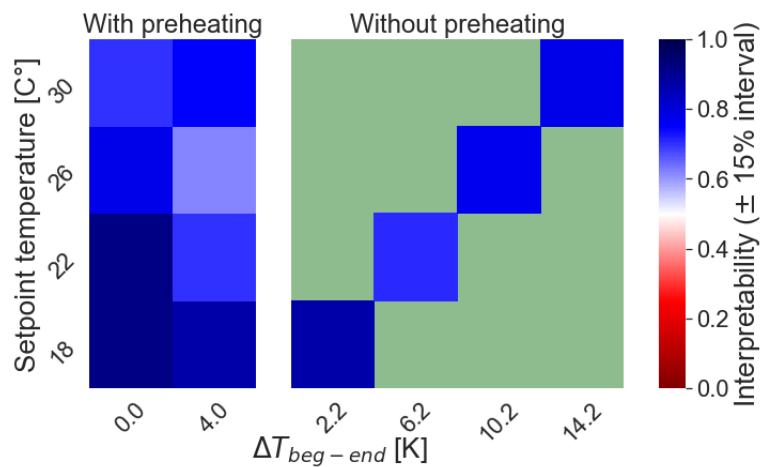


Figure 6.22 – Results interpretability for different protocol setpoint temperature and preheating conditions for 3 days of test duration.

In figures 6.19 and 6.20 it can be seen that, even for very short durations, most results were already acceptable if no $\Delta T_{beg-end}$ was applied. It reinforces the results from global approach, and indicates that preheating the building to the same temperature of the test can be a good strategy. This is mainly coherent during winter conditions, since the test setpoint temperature can be close to that considered comfortable for occupants.

However, for 0.5 days, even without $\Delta T_{beg-end}$, the variant with 30 °C test temperature diverged. This test temperature is also the one furthest from the adjacent spaces temperatures (T_{adj}). Considering the heated zones, T_{adj} is in average 17 °C during the night and 20 °C during the day, with a global mean of 18.8 °C. Although the variants with the highest setpoint temperature present an important signal towards outside, they are also those with higher φ_{shar} and the test conditions are therefore less optimal.

In figure 6.21 an unexpected result is presented: the extremes of setpoint temperature had better results. Maybe the contribution of the increased heat flow towards the exterior compensated the effect of the φ_{shar} estimation errors. From 3 days all results were acceptable and those with zero $\Delta T_{beg-end}$ and low $\Delta T_{int-adj}$ presented really high interpretability values (figure 6.22). The results for 4 days are not presented, since it has a similar behavior than that of 3 days test duration.

In general, preheating the building to the same temperature used during the test seems to be a good strategy to decrease the test duration, considering the place can be heated during one week before the test beginning with the local heating system. Under this condition and with test temperatures close to the T_{adj} , the indirect method performed well even for very short durations, such as half a day. These conclusions are taken for winter conditions, and it might be different when the outdoor temperature is higher.

6.3.2.3 Variation on the test and weather conditions

The goal of these numerical experiments is to multiply the number of tests to study the behavior of the method over the year and at different locations in France. They were performed using the weather stations of four French cities: La Rochelle, Nancy, Nice and Trappes. All tests begin on the 15th of each the month at 8 p.m., and follow a 2-week preheating period. The preheating temperature is the same as the setpoint temperature, thus a zero $\Delta T_{beg-end}$ is used in all these tests, since it was the best condition presented in the previous part.

In these experimental plans, the incident solar radiation on each of the building facades is extracted from the software and used in the SEREINE estimation algorithm. The time step of the data goes from one hour to one minute and the estimation process uses a time step of five min.

The experimental plan A was performed initially, to represent a protocol were the neighbours

do not have their temperature controlled, bringing less constraints in the method application. The study presented good results for winter period, however, tests applied during mid-season and summer presented low quality results. As an attempt to improve the estimation for other periods than winter time, a more invasive protocol was tried in experimental plan B. In this case the adjacent spaces are heated at the same temperature as the tested area, except for the unheated zone. This condition is expected to improve the results, since it decreases the φ_{shar} level, however a level of heat flow towards the unheated zone still exists.

A second attempt to improve the method behavior during warmer seasons was to allow higher values of indoor temperature. The experimental plan C was thus performed using the neighbours with variable temperatures, but with indoor temperatures limited to a higher temperature of 35 °C. Also, a higher $\Delta T_{int-ext}$ was used to determine the test temperature: instead of adding 10 K to the monthly mean outdoor temperature, a $\Delta T_{int-ext}$ of 15 K was used, based on the mean outdoor temperature of the four days following the beginning of the test.

The exact criteria used for defining the indoor temperature (T_{int}) and the adjacent spaces temperature (T_{adj}) in each of the three experimental plans are presented below. Table 6.8 shows the precise temperatures used for each test virtually applied in all the three experimental plans.

- Experimental plan A

- $T_{int} = T_{ext_{mean_{month}}} + 10 \text{ K}$, within the interval of 20 °C and 25 °C
- T_{adj} follows a variation pattern, different among neighbours and between day and night (table 6.4)

- Experimental plan B

- T_{int} is the same as experimental plan A
- $T_{adj} = T_{int}$

- Experimental plan C

- $T_{int} = T_{ext_{mean_{4days}}} + 15 \text{ K}$, within the interval of 20 °C and 35 °C
- T_{adj} is variable, same as experimental plan A (table 6.4)

Table 6.8 – Indoor temperatures (°C) for the experimental plans A, B, C.

City Month\Experimental plan	La Rochelle		Nancy		Nice		Trappes	
	A and B	C	A and B	C	A and B	C	A and B	C
January	20.0	26.1	20.0	20.0	20.0	22.0	20.0	20.0
February	20.0	20.1	20.0	20.0	20.0	25.5	20.0	20.0
March	20.0	24.4	20.0	27.8	21.7	27.9	20.0	20.0
April	20.9	25.8	21.3	26.4	23.5	27.2	20.0	24.3
May	25.0	32.9	25.0	26.6	25.0	33.5	22.9	29.3
June	25.0	35.0	25.0	31.5	25.0	34.4	25.0	34.7
July	25.0	35.0	25.0	35.0	25.0	35.0	25.0	30.2
August	25.0	33.7	25.0	32.5	25.0	35.0	25.0	35.0
September	25.0	34.2	25.0	29.8	25.0	35.0	25.0	31.2
October	24.5	29.3	23.0	24.4	25.0	31.9	20.0	23.6
November	20.0	23.3	20.0	23.2	22.1	28.1	20.0	20.2
December	20.0	21.5	20.0	20.7	20.0	23.0	20.0	20.0

The model selection process from SEREINE algorithm was initially used, in which model *ti* was more commonly chosen. However, the model selection process was still in development in the SEREINE project, while these analysis were conducted. So finally, both models, *ti* and *tw* (figure 6.12), were applied to each case, disregarding the model selection process. The model *tw* presented more convergent results and among them there is a higher percentage of results that finished the uncertainty propagation process. The results for a same test also presented a higher interpretability value compared to results using *ti* model, with an average of 11 % higher values. In addition, it has a larger number of acceptable results for 2 and 3 days duration, with 66 acceptable results against 26 of model *ti*. For this reason the following results presented here are solely for the estimation process with the model *tw*.

In experimental plan A, 10 % of the tests diverged while in experimental plan B this level decreased to 4 %. For experimental plans C all the tests converged. Although a test might converge, it does not imply that the uncertainty propagation process has been correctly performed. Whenever a test does not complete this process, the result is not going to be further analysed. This choice was taken to avoid misinterpretation by comparing results with different levels of information. The first have higher level of uncertainty, since they have passed through the uncertainty propagation process. The results that did not finish this process have an uncertainty close to a single fit in the optimization process, which is much smaller.

Once a result converged and passed the uncertainty propagation step, it was studied regarding the acceptability and interpretability criteria. Most of the results presented a stabilization of values from 2 days of test, some of them presented stable behavior earlier with 1 day of test duration. To verify this, almost half of the tests in the experimental plans were

conducted up to one week of duration.

Table 6.9 shows the mean interpretability value for these 7 days tests. It can be seen that from half of a day to one day there is an important improvement on the interpretability values, among all groups. From one to two days the interpretability still shows a significant increase. After that, although some improvements can be reached, they are probably not enough to justify an extra day of protocol application in-situ.

Table 6.9 – Mean interpretability for tests with maximum duration of 7 days by results acceptability.

Group\Test duration (days)	0.5	1	2	3	4	5	6	7
All results	27%	40%	45%	48%	48%	48%	49%	49%
Acceptable results	45%	60%	66%	68%	69%	67%	67%	68%
Unacceptable results	22%	38%	39%	41%	40%	41%	43%	42%

It should be considered that this duration depends on the context. In this study the building has internal wall insulation and the protocol requires preheating the tested area. The duration could be longer for cases with external wall insulation and without preheating the building. An example of a test with acceptable results is shown in figure 6.23.

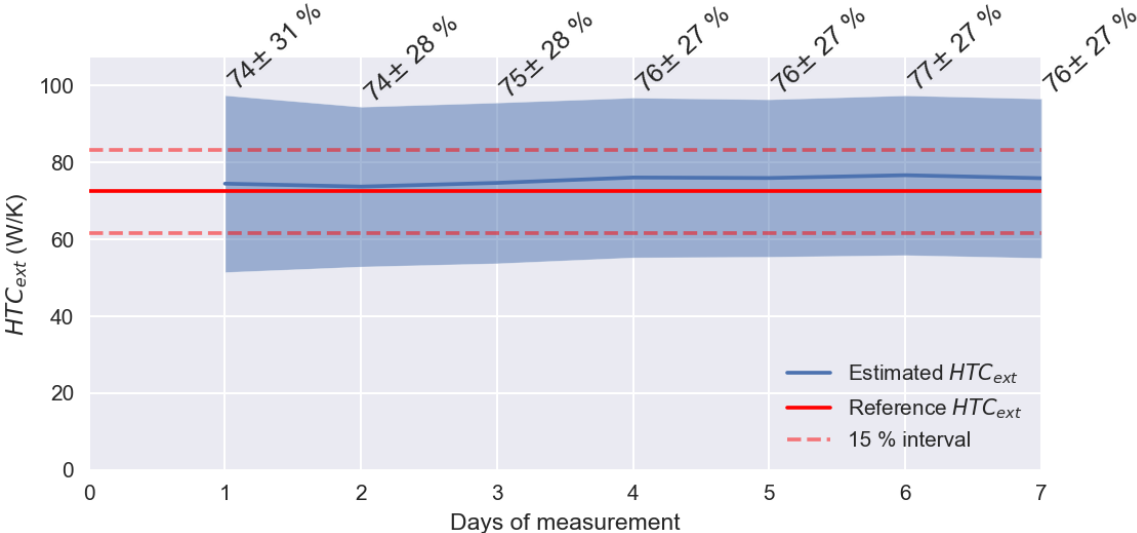


Figure 6.23 – Results progression for the numerical test performed in February in La Rochelle with experimental plan B.

The whole experimental plan was conducted with at least three days of duration, since it seems to be enough to stabilize the test results. A total of 144 results is expected per test duration in the ensemble of the three experimental plans. From these, only 25 % of the tests

converged and had the uncertainty propagation process completed within half a day of test duration. This value increases to 70 % for one day of test, and for 85 % for two and three days of test. Considering this, a really short duration of half a day should be avoided for a test application when similar experimental conditions are encountered in-situ. One day of test duration can be considered, but the ideal would be to test a building for at least two days.

Table 6.10 presents the results of interpretability for the tests that converged in the Experimental plans A, B and C for a two days duration. The empty values correspond to tests that did not converge or complete the uncertainty propagation process, for reasons which would require further investigation. The values without highlight failed to reach the criteria of bias inferior to 15 % and uncertainty inferior to 35 % and those in purple met both criteria. The values in blue met only the bias criterion, while those in red met only the uncertainty criterion.

Table 6.10 – Interpretability and acceptability for 2 days of duration

City Month\Experimental plan	La Rochelle			Nancy			Nice			Trappes		
	A	B	C	A	B	C	A	B	C	A	B	C
January	52%		50%	85%		85%	60%	63%	60%	69%	76%	69%
February	68%	65%	68%	66%	61%	66%	37%	42%	46%		68%	67%
March	46%	48%	50%	45%	44%	45%	33%	43%	44%	56%	53%	56%
April	47%	51%	43%	41%	37%	42%	42%	50%	44%	38%	38%	42%
May	18%	25%	36%	43%	68%	41%	23%	28%	37%	27%	27%	
June	12%	9%	27%	34%	51%		19%				33%	
July			34%	9%	19%	24%		17%		20%	23%	
August	24%	30%	36%	30%	41%	39%			29%	31%	39%	43%
September	31%	41%	40%	40%	49%	43%	14%	8%	40%	31%	36%	
October	37%	54%	41%	54%		58%	38%	44%	42%	42%	44%	50%
November	33%	30%	39%	43%	44%	51%	29%	33%	44%		52%	53%
December	76%		77%	73%	68%	73%		62%	61%	75%	74%	74%

Reached criteria:	 Bias	 Uncertainty	 Bias and uncertainty
--------------------------	--	---	--

The maximum interpretability was of 85 % with Nancy weather in January, that is also the month with the lower external temperatures during the test. Nice city presented the lower amount of acceptable tests, and it is the city with the highest average outdoor temperatures. The external temperatures seems to be a determinant factor in the results quality, which is an expected behavior, since it affects ϕ_{ext} levels. It can be seen that applying the test during winter improves the probability of achieving higher interpretability values and to have acceptable results. Although the attempts of heating the adjacent spaces and to increase the indoor temperature in overall increased the results interpretability, these strategies were not enough significant to reach acceptable results out of the winter months, with few exceptions.

Another tendency observed is that it was more challenging to reach the uncertainty criterion

than the bias. The bias criterion was commonly met in tests performed during mid-season and even during some summer months. However, the uncertainty criterion was mainly met during the colder months. The increased level of uncertainty is probably due to the increased level of input uncertainty in the U-value of the shared walls. In addition this building presents a $\Gamma_{U_{eq_{ext-shar}}}$ of 25 %, with a fairly good insulation on the exterior walls and no insulation on the shared walls. This condition makes the levels of uncertainty using the indirect method likely to be close to the determined limit, as presented before in section 6.2.

In table 6.10, the results are ordered by date of application, although a trend of convergence and interpretability level can be seen according to the seasons, this table does not show the exact exterior temperatures. The precise days tested in each month might also have an outdoor temperature, that is hotter or colder than the month average. In order to better understand the method behavior, this data was analysed according to the temperature differences with the outdoor environment and adjacent spaces (figure 6.24 and 6.25).

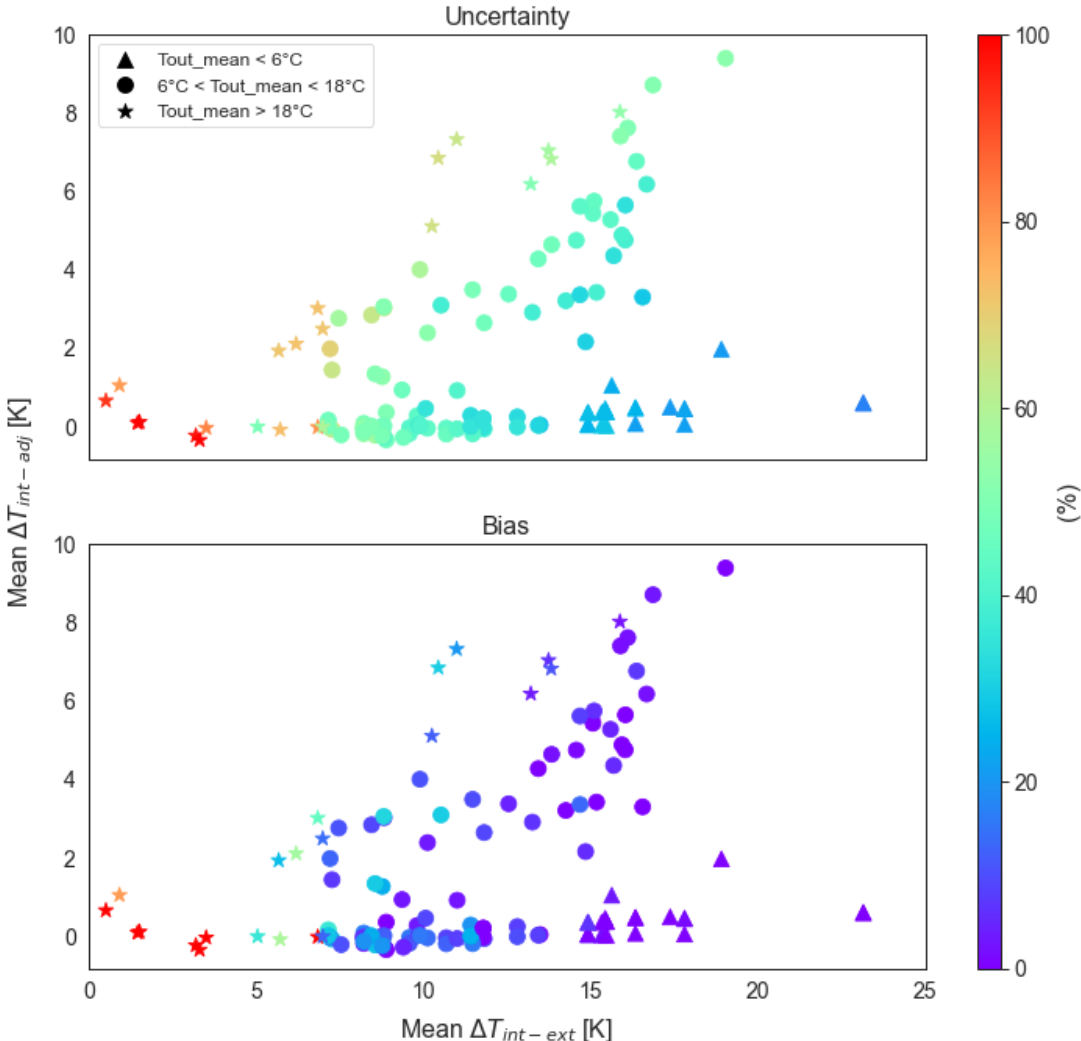


Figure 6.24 – Bias and uncertainty of results according to the mean $\Delta T_{int-ext}$ and $\Delta T_{int-adj}$ for 2 days of test in experimental plans A, B and C.

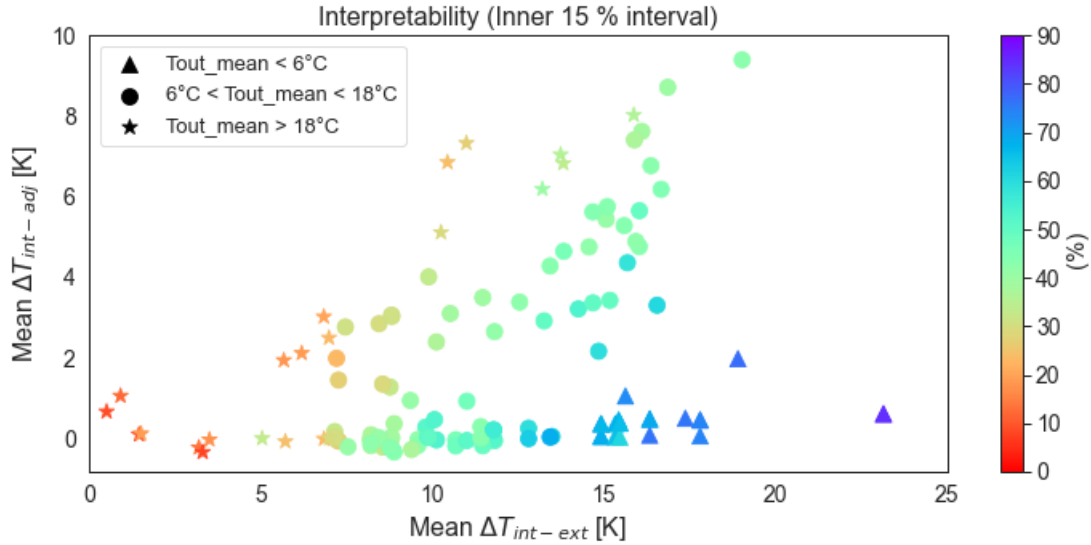


Figure 6.25 – Interpretability of results according to the mean $\Delta T_{int-ext}$ and $\Delta T_{int-adj}$ for 2 days of test in experimental plans A, B and C.

Besides the color describing the interpretability level, the shape indicates the ranges of outdoor temperatures during the test. The triangular points represent cold weather conditions, in which the mean outdoor temperature during test are below 6 °C. The circles and stars represent respectively mild and hot weather conditions.

The group of points sharing a same color have a general diagonal shape, showing that both difference of temperature influence the quality of the results. It can be seen that lower differences of temperature with the neighbours and higher differences with the outdoor environment provide higher levels of interpretability, which reinforces the importance of reaching elevated $\Gamma_{\phi_{ext-shar}}$ for better test results.

The uncertainty and bias of the same tests are presented in figure 6.24. It can be seen that a bias inferior to 15 % is often met when $\Delta T_{int-ext}$ is higher enough. At least 12 K of temperature difference would be desirable for achieving this criterion. The uncertainty criterion is more restrictive and it is mainly determining which results are acceptable. It presents a similar behavior to the interpretability, with better results for high $\Delta T_{int-ext}$ values. At least 15 K of temperature difference would be desirable to let the uncertainty inside the acceptable zone in addition with low temperature differences with the outdoor environment.

Increasing the test temperature is a strategy to consider in order to improve the results, however, it can also increase the ϕ_{shar} if the adjacent spaces are not heated similarly. Since usually the shared walls are less insulated than the exterior walls, a lower temperature difference could lead to important heat losses to the adjacent spaces and not to increase $\Gamma_{\phi_{ext-shar}}$. The effectiveness of the increment of the test temperature thus depend on the temperature of the adjacent spaces. During the heating season, it is less relevant since an important temperature

gradient with the outdoor environment can be reached with temperatures inside the thermal comfort range. If adjacent spaces are occupied, adjacent temperatures may be close to that of the tested area, leading to a low level of ϕ_{shar} .

In this case, there would be no need to control the adjacent spaces temperatures, which avoids the application of a more invasive protocol. However during mid-season, the $\Delta T_{int-adj}$ decreases and temperatures inside the thermal comfort zone might not be enough for testing the building envelope behavior. This gets critical during summer, when the level of indoor temperature demanded to have an important $\Delta T_{int-ext}$ can exceed the safety of materials in a dwelling.

For mid-season, a possibility would be the use of both strategies together: increasing the test temperature and controlling the adjacent spaces temperatures close to the test temperature. It can be seen in figure 6.25 that the down right zone of the graph, with higher interpretability, is only composed of tests performed with mean outdoor temperature below 6 °C. There are no points representing the mid-season months in this area. In experimental plan B, the test temperatures were limited to 25 °C. As a perspective of this work, it would be interesting to perform an experiment with higher temperatures and controlled neighbour temperatures to verify the improvement it could bring for mild temperature weather.

In the next section the work developed for the direct method is presented to compare the results quality with the indirect method.

6.4 Direct method for neighbours flow estimation

The direct method consists of placing several heat flow meters (HFM) per shared wall in order to directly assess the ϕ_{shar} . The estimate ϕ_{shar} would be then calculated by equation 6.10.

$$\phi_{shar} = \sum_{i=1}^m \sum_{j=1}^n \varphi_{shar_{m_n}} S_{m_n} \quad (6.10)$$

where:

- $\varphi_{shar_{m_n}}$ is the heat flow density measured by a sensor placed in one homogeneous part (j) of a shared wall (i) [W/m²];
- S_{m_n} is the area associated with one sensor in one homogeneous part (j) of a shared wall (i) [m²].

For simplification purposes, we initially considered each shared wall as a single homogeneous part and that each sensor placed on a same wall is associated with surfaces of equal parts if they are globally well distributed. The direct method has the potential to

increase the precision of the ϕ_{shar} estimation when comparing to the indirect method, since the data is based on direct measurements. However, an error can be committed due to the extra simplification on the inhomogeneity of the shared walls and of the flows passing through it. A hard point of this method consists in characterizing the level of uncertainty associated to these measurements.

In part 6.4.1.3, we presented an experimental work developed to define the level of uncertainty associated to the φ_{shar} . In part 6.4.2, the direct method is applied to the experimental plan C, from last section, to compare both methods and show their potentials.

6.4.1 Ranges of φ_{shar} uncertainty.

In order to have a magnitude of the uncertainty associated to these measurements, some experimental works using HFM were developed. The first experiment took place at Bordeaux IUT, in an educational building situated in the south of France. The second experiment was conducted by CEA, a SEREINE project partner, in a TSB office located in eastern France.

6.4.1.1 IUT experiment

The experiment was developed on a wall separating a heated area (cafeteria) and an unheated area (computer room). Four HFM were placed on a concrete shared wall to investigate the dispersion of the measurements. Figure 6.26 shows the disposition of these sensors on the wall. Also, a temperature sensor was also placed in each side.

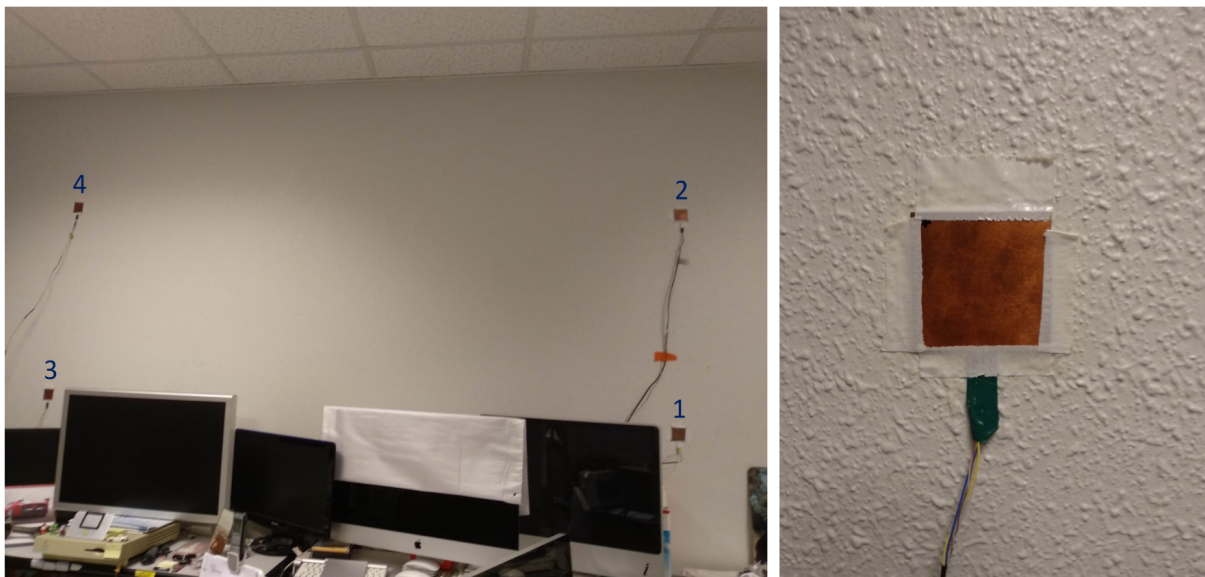


Figure 6.26 – Location of heat flow meters in the Bordeaux IUT experiment (left) and detail on the sensor (right).

The experiment did not interfere on the temperatures in the cafeteria side, the local heating

system was applied as usual. Although no heating device was used in the computer room, the many computers operating worked as a heating source and also the adjacent spaces were supplying heat to this area. Figure 6.27 shows the temperature profile in both areas and the HFM measurement of the four sensors. The difference of measurement between the HFM was also not high, with maximum differences mainly below 1 W/m².

Normally, the simple mean of all HFM on a same wall is used as the input heat flow of this shared wall. In order to determine the uncertainty associated to φ_{shar} in this experiment, the mean heat flow value was calculated for each time step, then it was subtracted from the measurement of each one of the HFM at this same time step. Table 6.11 shows the mean, minimum, maximum and the quartiles values for the mean φ_{shar} measurements from all HFM and for the $\Delta T_{int-adj}$. It can be seen that the temperature difference between both sides of the wall was below 2.2 K, but in the majority of the time it stay below 1 K.

The measurements of the four HFM at a determined time step were thus centered to zero and the dispersion of the points for the whole duration of the experiment could be combined. This allows to verify the dispersion of the values regarding the mean measurement value. The combination of the points for the whole experiment duration is presented in figure 6.28.

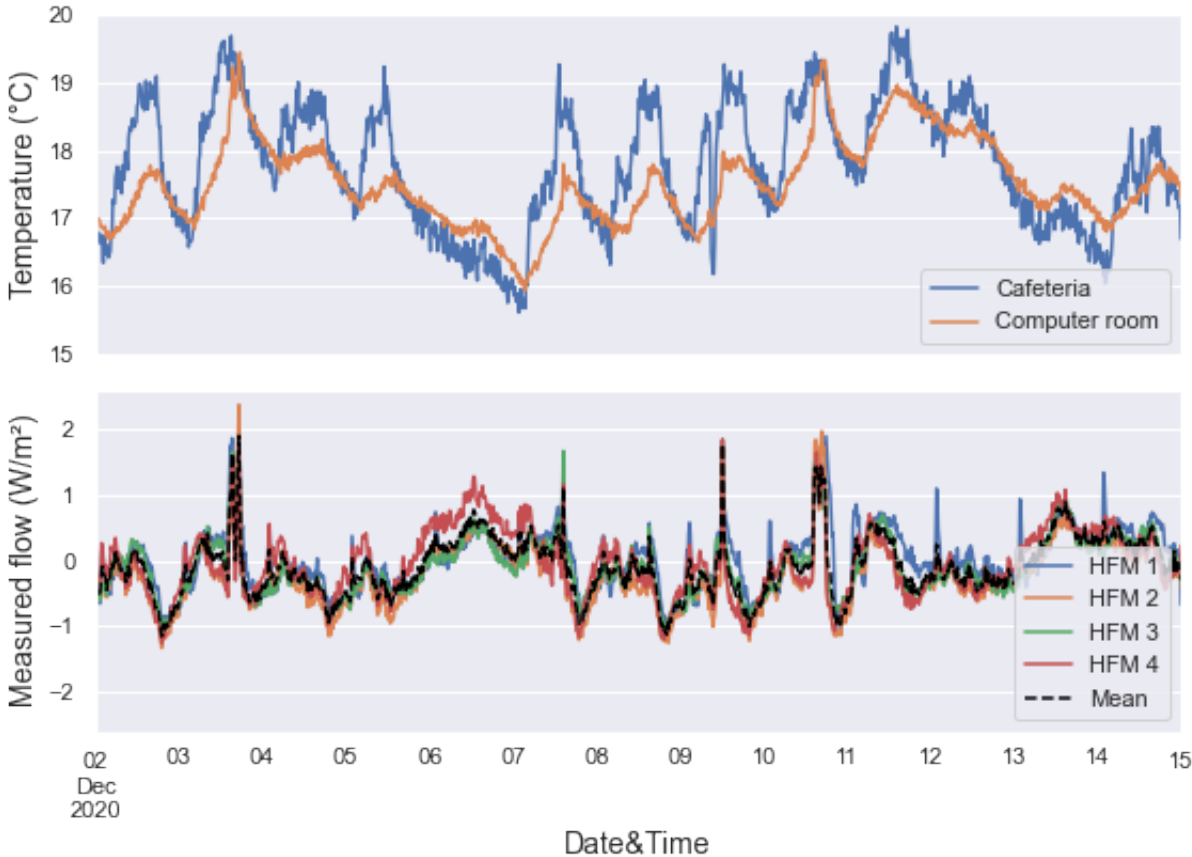


Figure 6.27 – Temperature and heat flow measurements during IUT Bordeaux experiment.

Table 6.11 – Statistics on the mean $\bar{\varphi}_{shar}$ and $\Delta T_{int-adj}$ over the time for the IUT experiment.

Time series	mean	min	max	Quartiles		
				1	2	3
$\bar{\varphi}_{shar}$ (W/m ²)	-0.1	-1.2	1.9	-0.4	-0.1	0.2
$\Delta T_{int-adj}$ (K)	-0.3	-2.2	0.9	-0.7	-0.1	0.2

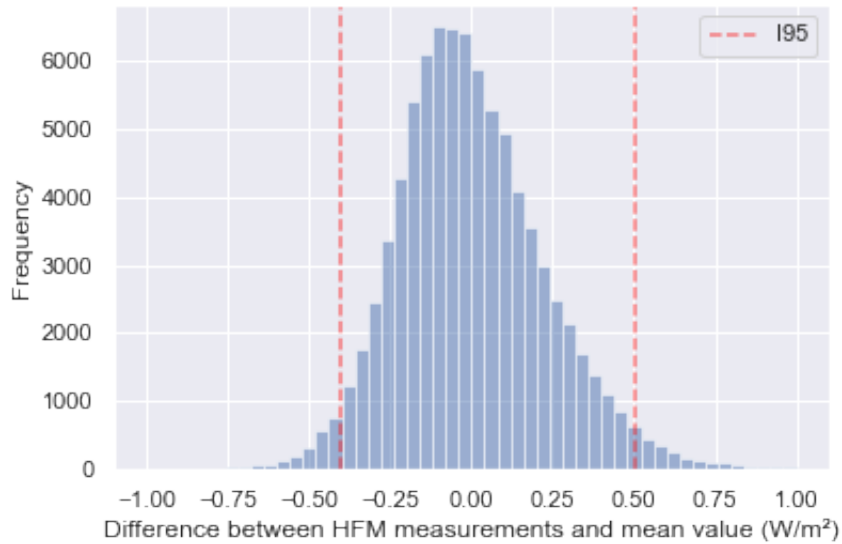


Figure 6.28 – Histogram of the difference between HFM measurements and mean value for each time step for IUT experiment.

The low and high borders of the I95 interval were respectively -0.4 W/m^2 and 0.5 W/m^2 . An uncertainty of $\pm 0.5 \text{ W/m}^2$ could be associated to the mean φ_{shar} of similar shared walls under similar conditions. This result is encouraging, but the HFM were placed in locations without furniture and far from the wall corners, where some thermal bridges could be present. Also the low temperature difference between both sides of the wall can be an optimum condition, which would not necessarily be the case during a SEREINE method application. This experiment gives a first feedback to define the uncertainty level of φ_{shar} . However, tests performed with different sensors, wall composition and temperature gradient might have other levels of uncertainty. An experiment developed by the CEA in the context of SEREINE project applied HFM in other wall composition. This experiment is described in the following part to give more basis to define the φ_{shar} input uncertainties.

6.4.1.2 CEA experiment

This experiment was performed in an office located at the first floor of the Hélios building at INES, in the Southeast of France, by Arnaud Jay from CEA. The objective of the experimental

campaign was to quantify the heterogeneity of HFM measurements through different walls [236]. The room is furnished and a SEREINE electrical heater is positioned on the table to avoid the direct heating impact on the floor. HFMs were placed on the concrete floor and on a wall with double concrete separated by an expansion joint. Some of the HFM are placed below the furniture, in order to test also this condition that could appear in real life experiments. Figure 6.29 shows the office with the experiment equipment. The nomenclature of the HFM represents the distance to the low right corner of the room.

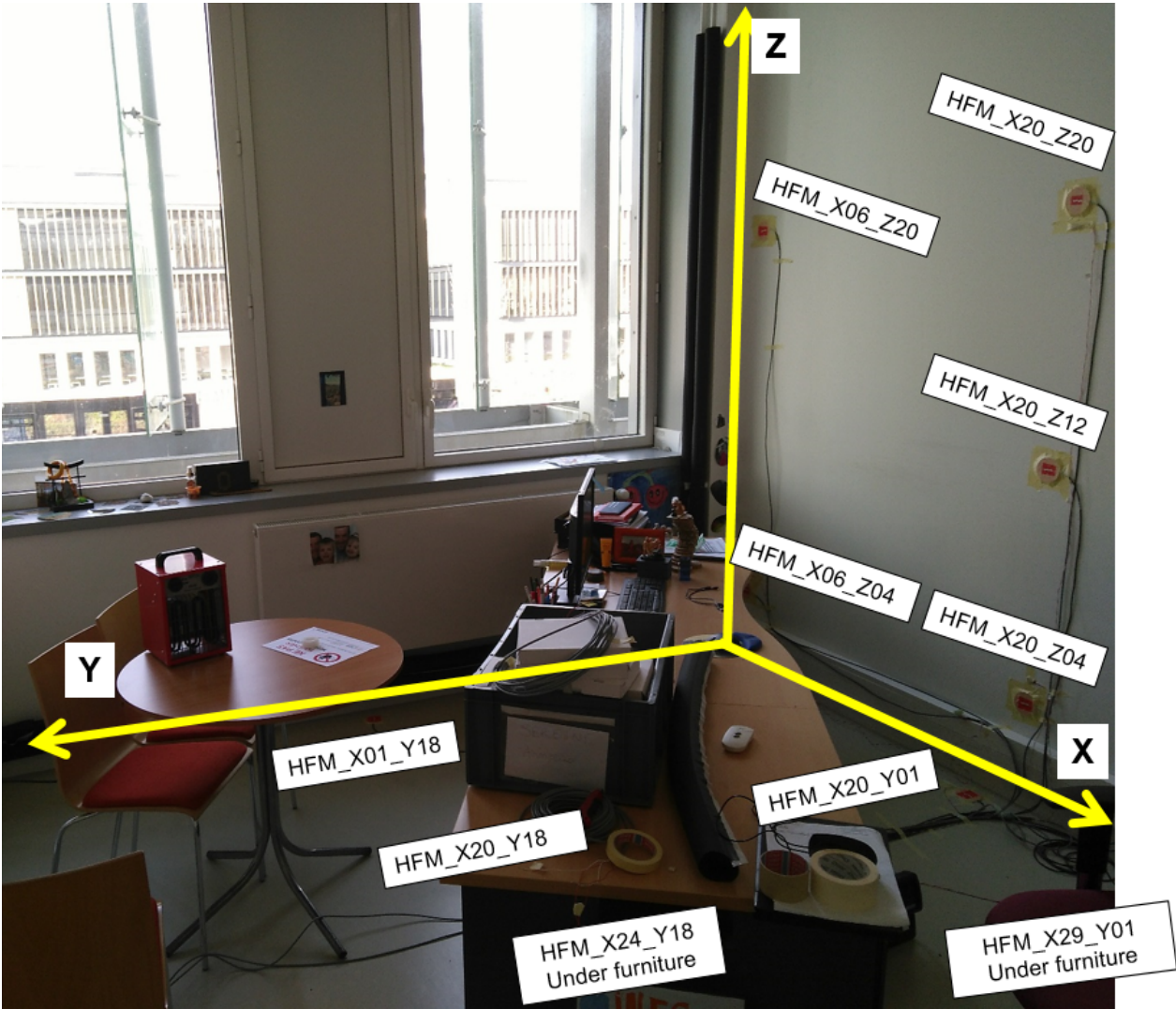


Figure 6.29 – Photo of the office with the equipment installed for CEA experiment Adapted from [246].

A fan is used in some scenarios to homogenize the temperature in the room. The experiment was performed with different heating scenarios, some with fast variation of indoor temperature and others with more stable temperatures over the time. Only part of the scenarios were analysed here to be closer to the heating scenarios applied in the sampling approach of MFH and TSB. Two scenarios were kept, one with high temperature difference with the adjacent spaces,

another with low differences.

6.4.1.2.1 Scenario with low $\Delta T_{int-adj}$

The temperatures and HFM measurements for the scenario with low temperature differences are presented in figure 6.30. The mean heat flow measurements were calculated for each time step and represented with dashed black lines.

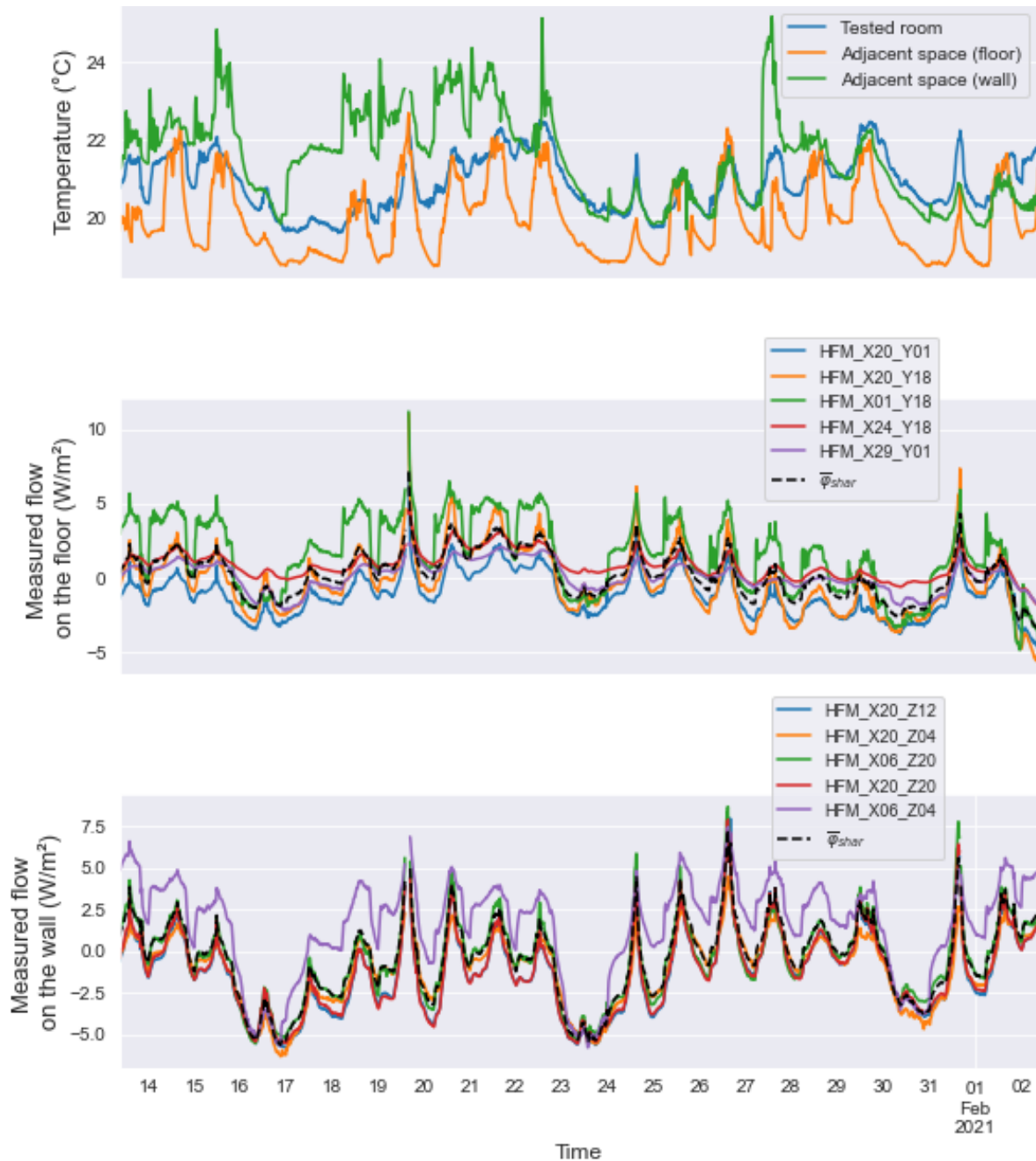


Figure 6.30 – Temperature and heat flow measurements on the wall and floor for the scenario of low $\Delta T_{int-adj}$ from CEA experiment.

Table 6.12 shows the main statistics about the $\Delta T_{int-adj}$ and the mean φ_{shar} from the HFM placed on each wall. The mean temperature difference with the adjacent space to the double

concrete wall is 0.6 K and with the adjacent space to floor is 1.0 K.

Table 6.12 – Statistics on the mean $\bar{\varphi}_{shar}$ and $\Delta T_{int-adj}$ over the time for the scenario with low temperature difference with adjacent spaces in CEA experiment.

Element	Time series	mean	min	max	Quartiles		
					1	2	3
Vertical shared wall	$\bar{\varphi}_{shar}$ (W/m ²)	-0.5	-5.6	7.3	-2.2	-0.2	1.2
	$\Delta T_{int-adj}$ (K)	-0.6	-4.0	1.4	-1.3	-0.4	0.1
Intermediate floor	$\bar{\varphi}_{shar}$ (W/m ²)	0.2	-3.6	7.2	-0.9	0.1	1.3
	$\Delta T_{int-adj}$ (K)	1.0	-1.0	2.5	0.7	1.0	1.4

The same treatment applied to the Bordeaux test was applied to this data. The values presented in the following histograms are the difference of measurement between each HFM and the mean value in a same time step and a same wall. Figures 6.31 and 6.32 show respectively the histogram of the data related to floor and wall for this scenario.

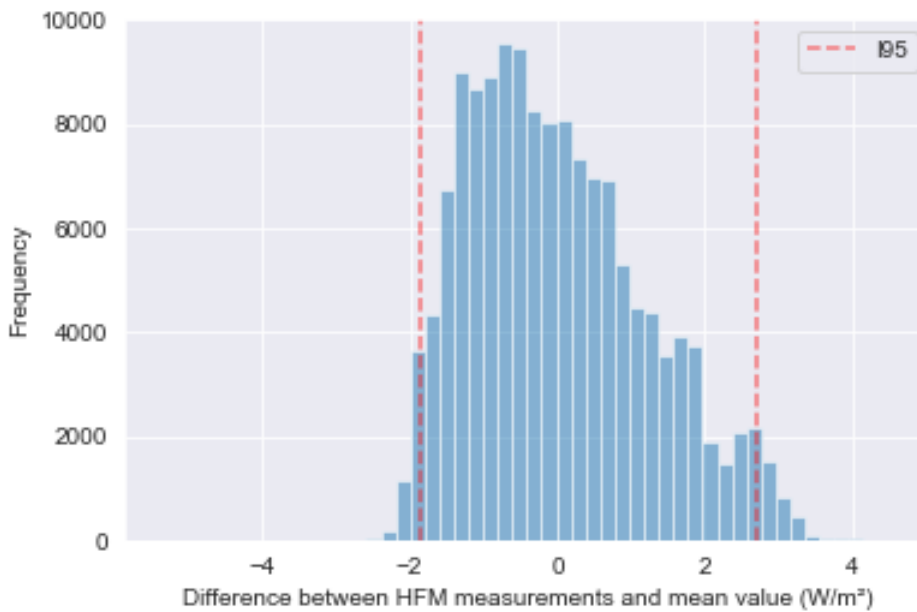


Figure 6.31 – Histogram of the difference between HFM measurements and mean value for each time step for the scenario of low $\Delta T_{int-adj}$ of the concrete floor from CEA experiment.

In this scenario of low temperatures and a concrete floor typology, an uncertainty of ± 2 to ± 3 W/m² could be considered for the measurements φ_{shar} . This uncertainty level is higher than that of IUT experiment. Although the mean $\bar{\varphi}_{shar}$ is close to zero, as that from the IUT experiments, the variations of $\bar{\varphi}_{shar}$ are much wider in the CEA experiment. The difference between the third and first quartiles of $\bar{\varphi}_{shar}$ of this experiment are 3.4 W/m² and 2.2 W/m²

respectively for the wall and floor, while this difference in the IUT experiment is of 0.6 W/m^2 . It seems that the uncertainties in the HFM measurements can decrease if the flow is more stable in time. The relative uncertainties, in regard to the mean φ_{shar} are much higher for this experiment.

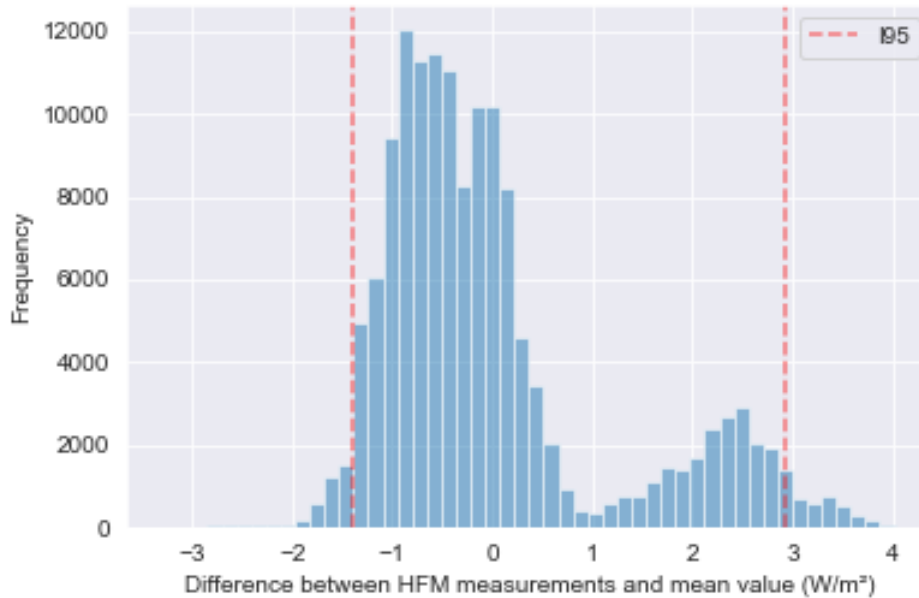


Figure 6.32 – Histogram of the difference between HFM measurements and mean value for each time step for the scenario of low $\Delta T_{int-adj}$ of the double concrete wall from CEA experiment.

In figure 6.32, a difference in behaviour concerning part of the data can be observed. This distribution looks as the sum of two normal distributions and might be describing two different states. In the part related to the wall flow measurements of figure 6.30 it can be perceived that the HFM_X06_Z04 consistently has higher measurements than the other. This HFM is also located close to a heating pipe. This pipe was mainly insulated during this experiment to reduce the impact on the measurements, however it was difficult to insulate properly the pipe fixing points to the wall (close to the location of this HFM). For this reason, the same procedure was applied to the data, excluding the measurements from this HFM and the results are shown in figure 6.33.

An uncertainty of $\pm 1 \text{ W/m}^2$ could be considered in this case. In a real case, the *in situ* test would not be feasible in presence of pipes with hot water passing through the tested area. In comparison with the IUT experiments, this presented higher levels of uncertainty. One difference from this experiment to the former one is the use of an electrical heater and fan inside the tested area, which can affect the measurements depending on the location of these devices and distance to the HFMs. In addition, the air gap between the double walls and the presence of furniture in this experiment might increase the dispersion of the measurements.

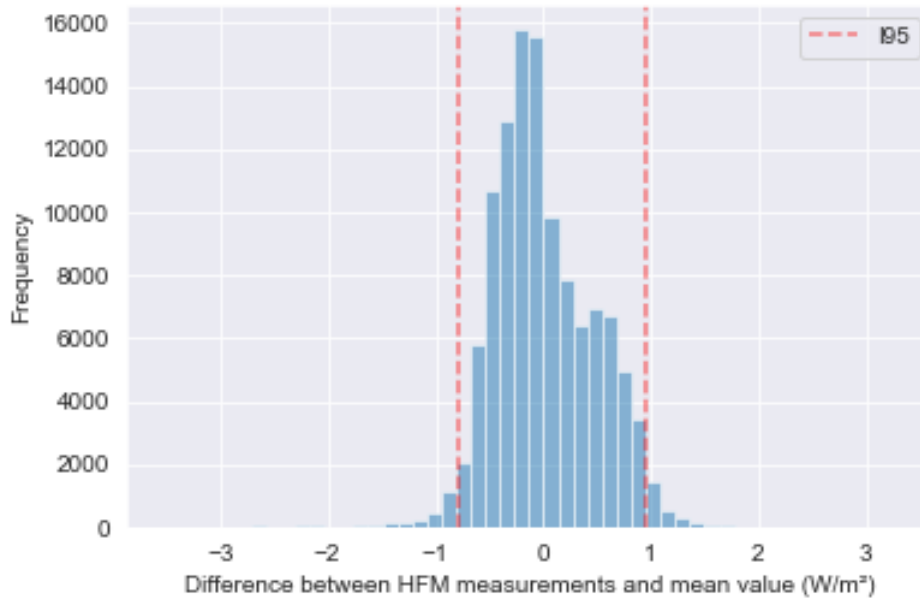


Figure 6.33 – Histogram of the difference between HFM measurements and mean value (without HFM_X06_Z04) for each time step for the scenario of low $\Delta T_{int-adj}$ of the double concrete wall from CEA experiment.

6.4.1.2.2 Scenario with high $\Delta T_{int-adj}$

The temperatures and HFM measurements for the scenario with high temperature differences is presented in figure 6.34. Table 6.13 shows the main statistics about the mean $\bar{\varphi}_{shar}$ and $\Delta T_{int-adj}$ in each wall for the scenario with high temperature difference with adjacent spaces. The mean temperature difference with the adjacent space to the double concrete wall is 9.4 K and with the adjacent space to floor is 9.8 K, much higher than the previous experiments. However, the difference between the maximum and minimum $\Delta T_{int-adj}$ were inferior than in the previous scenario.

Figure 6.35 shows the histogram of the data related to floor. In this scenario with high differences with the adjacent space, we can notice two groups in the histogram for the HFM on floor. Two HFMs were placed under the furniture in the room (HFM_X24_Y18 and HFM_X29_Y01). In figure 6.34, we can also see that these two HFMs present lower values than the other in the same wall. Figure 6.36 shows the histogram if these two HFM are not taken into account. The wall is probably further from a steady state when there is a greater temperature difference and the presence of furniture can have a bigger impact on the heat flow locally.

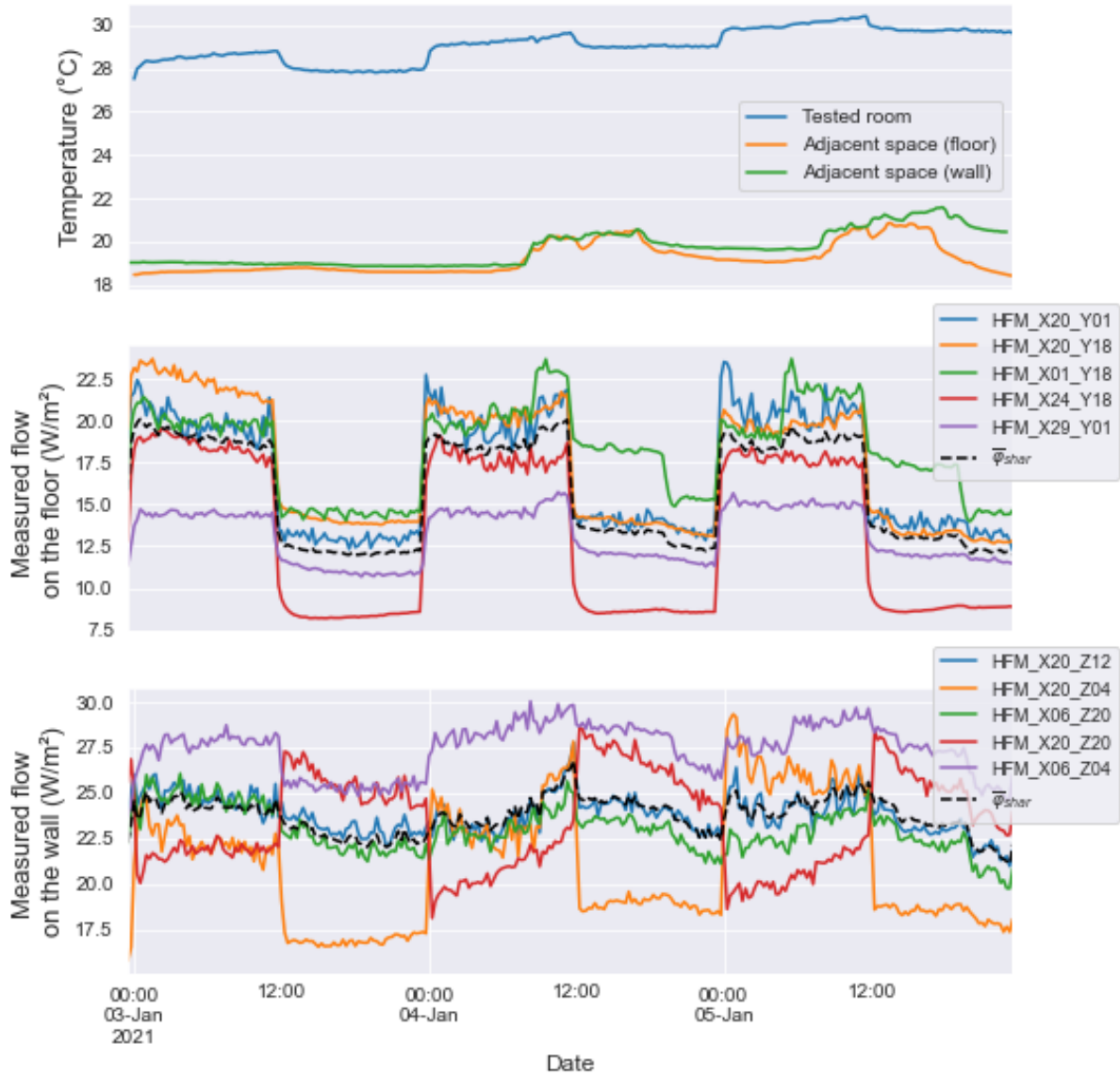


Figure 6.34 – Temperature and heat flow measurements on the wall and floor for the scenario of high $\Delta T_{int-adj}$ from CEA experiment.

Table 6.13 – Statistics on the mean $\bar{\varphi}_{shar}$ and $\Delta T_{int-adj}$ over the time for the scenario with high $\Delta T_{int-adj}$ from CEA experiment.

Element	Time series	mean	min	max	Quartiles		
					1	2	3
Vertical shared wall	$\bar{\varphi}_{shar}$ (W/m ²)	23.7	21.1	26.8	23.1	23.8	24.5
	$\Delta T_{int-adj}$ (K)	9.4	8.1	10.4	8.9	9.3	9.8
Intermediate floor	$\bar{\varphi}_{shar}$ (W/m ²)	15.8	12.0	20.1	12.5	15.7	18.8
	$\Delta T_{int-adj}$ (K)	9.8	8.5	11.2	9.2	9.8	10.5

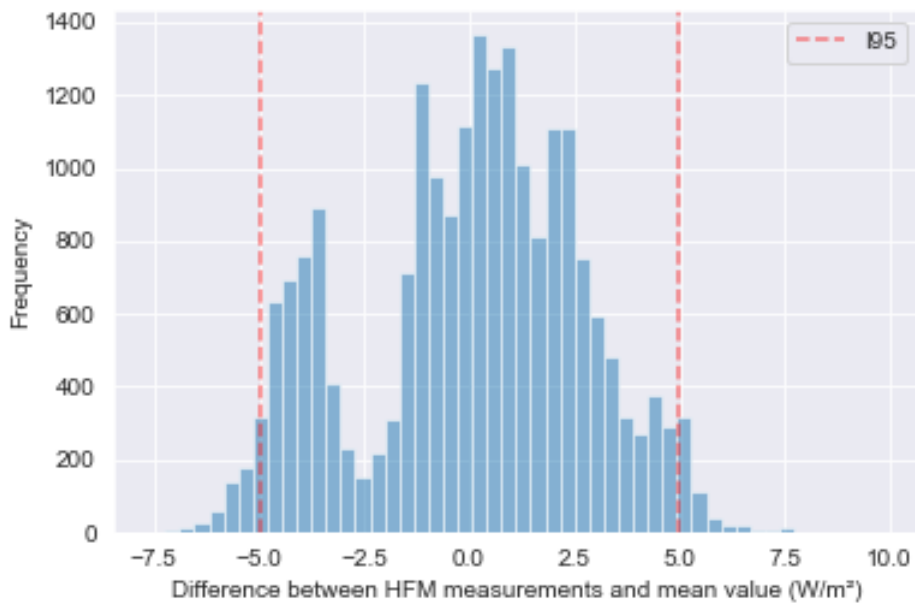


Figure 6.35 – Histogram of the difference between HFM measurements and mean value for each time step for the scenario of high $\Delta T_{int-adj}$ of the concrete floor from CEA experiment.

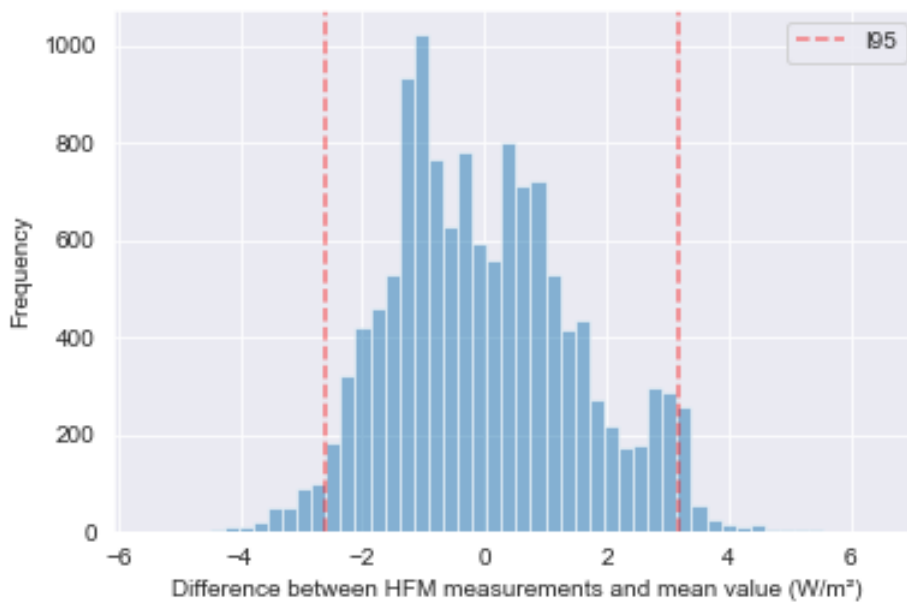


Figure 6.36 – Histogram of the difference between HFM measurements and mean value (without HFM_X24_Y18 and HFM_X29_Y01) for each time step for the scenario of high $\Delta T_{int-adj}$ of the concrete floor from CEA experiment.

This is presented mainly to understand the impact of the furniture on the heat flow dynamics, since in real cases of renovated buildings the tested area might be furnished. If it is not possible to take away the furniture, higher uncertainties could be considered to represent the

measurements or the surface might be divided in order to represent the parts with distinct behavior. However, it would be difficult in practice to define the boundaries between the surfaces.

Figure 6.37 shows the difference of measurement of each HFM to the mean value in a same time step for the wall.

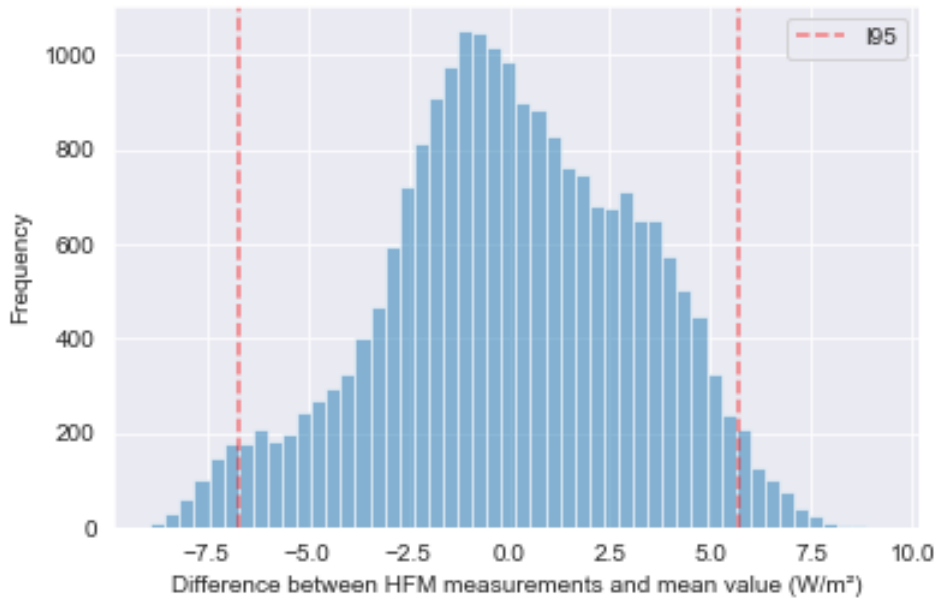


Figure 6.37 – Histogram of the difference between HFM measurements and mean value for each time step for the scenario of high $\Delta T_{int-adj}$ of the double concrete wall from CEA experiment.

In this case, the data from the HFM placed close to the hot water pipe is used, because it had low impact on the data dispersion. The difference of measurements from this HFM might have a relative lower impact, since higher heat flow is present in this scenario.

In contrast with the scenarios with low difference of temperature with the adjacent spaces, this experiment presented a higher dispersion of HFM on a same wall. In this case an uncertainty of ± 5 to ± 7 W/m^2 could be considered for the measurements. Although the absolute uncertainties are higher for this scenario, when compared with the mean value of φ_{shar} for each walls, the relative uncertainties are lower. Although the scenario with low temperatures difference has smaller values of φ_{shar} , it has also more variation in this measures, which can explain the higher relative uncertainties. The level of temperature difference is important to the φ_{shar} uncertainties, but the variation of φ_{shar} on time also seems to be relevant to the level of φ_{shar} uncertainties. More stable φ_{shar} seems to be related to lower uncertainties of φ_{shar} .

6.4.1.3 Discussion

Initially, we considered a homogeneous flow all over each shared wall, characterised by a one-dimensional behavior. However, with the experimental work, a considerable variation among the different sensors was noticed in some cases. This raises the hypothesis that the heat flow might have a more complex behavior than a one-dimension flow, with important variations on the plan of the wall. Variation in the temperature along the shared wall plan could be partially responsible for this dispersion. In addition, the walls might be composed of distinct parts and do not have the same thermal characteristics all along its dimensions. Another important aspect is the presence of furniture, that can locally affect the thermal behavior of the wall as a barrier to the heat flow.

It should be considered that the measurement is done at specific points on the wall and the location of these points influence the data. Two main alternatives can be envisaged to deal with walls presenting a heterogeneous behavior. The first alternative is to consider the variations of the measurements in the input uncertainty of φ_{shar} . This could be more practical in the experimental side, since the heat flow would be the arithmetic mean of the measurements in a same wall. However, depending on the wall heterogeneity, high levels of input uncertainty can be associated to the measurements. This can lead to results with high uncertainty and therefore non exploitable.

Another alternative consists in using infrared camera to study the shared wall previously to the test. If different patterns are identified, the location of the heat flow meters can be chosen accordingly, measuring at least one point in each different part. In this case, the areas associated to each sensor on a same wall equation 6.10 are thus different. A technique should be used to attribute the representative areas of each sensor. This alternative would be more precise, but it requires preparation with extra material and time for the analysis of the wall. However, more studies need to be done to investigate this option, since it might be difficult to define the boundaries between the surfaces.

Table 6.14 shows a summary of the experiments carried out to investigate the uncertainties ranges of φ_{shar} . When there are two values for $u_{\varphi_{shar}}$ is because hypothesis were made to withdraw the data of one or more HFM, those behaving differently of the other data. On the third line it corresponds to the HFM located close to a hot water pipe, in the last line it correspond to the HFM under the furniture in the office.

In these experiments, the level of φ_{shar} absolute uncertainty increased with the increment of $\Delta T_{int-adj}$ and it also seems to be related with the variation of φ_{shar} on time. However, the relative uncertainty of φ_{shar} ($u_{\varphi_{shar}}$ divided by $\bar{\varphi}_{shar}$) decreases for higher φ_{shar} levels. Still, the most important are the absolute uncertainties during a protocol application.

In order to decrease the $u_{\varphi_{shar}}$, lower levels of $\Delta T_{int-adj}$ and φ_{shar} variation are recommended. Although first conclusions can be made from these experiments, they are not enough to describe the relation among these parameters. For this purpose, it is necessary to develop a further study where various levels of temperature difference are kept constant between both sides of the wall. It would also be an asset to test other wall typologies with multiple HFM, to have a magnitude of the input uncertainties associated to the input φ_{shar} in an in-situ SEREINE test.

Table 6.14 – φ_{shar} uncertainty range according to the tested scenarios.

Wall	$\overline{\Delta T}_{int-adj}$ (K)	$\overline{\varphi}_{shar}$ (W/m ²)	φ_{shar} IQR (W/m ²)	$u_{\varphi_{shar}}$ (W/m ²)
Concrete vertical wall	-0.3	-0.1	0.6	0.5
Double concrete wall	-0.6	-0.5	3.4	3.0 / 1.0
	9.4	23.7	1.4	7.0
Concrete floor	1.0	0.2	2.2	3.0
	9.8	15.8	11.1	5.0 / 3.5

6.4.2 Virtual experimental plan

To assess the impact of directly measuring ϕ_{shar} on the quality of the results obtained, numerical simulations were performed in Pléiades Comfie. However, the heat flow through the walls is not directly provided by the software. In order to calculate ϕ_{shar} , each test case was simulated in two ways: first normally with the chosen scenarios, then with the shared walls removed from the model (which does not change the limits of the thermal zone). In the second simulation the scenarios are exactly the same from the first, but the shared walls are removed from the model, behaving then as adiabatic walls. Since the indoor temperature is fixed and the temperature scenarios and weather conditions are the same for each pair of simulation, the difference between both heating power from the tested area used to represent ϕ_{shar} .

This was applied to the experimental plan C, with identical conditions to those described in part 6.3.2.3. In the estimation process, three different levels of uncertainty input associated to the φ_{shar} were used: ± 0.5 W/m², ± 2 W/m² and ± 6 W/m². The first level is based on the IUT experiments. The second and the third levels are based on the CEA experiments, respectively for low and high temperature differences with the adjacent areas.

The results of the direct method, with these three levels of uncertainty, and of the indirect method are then compared. The mean interpretability values for each duration in each of these four groups are presented in figure 6.38.

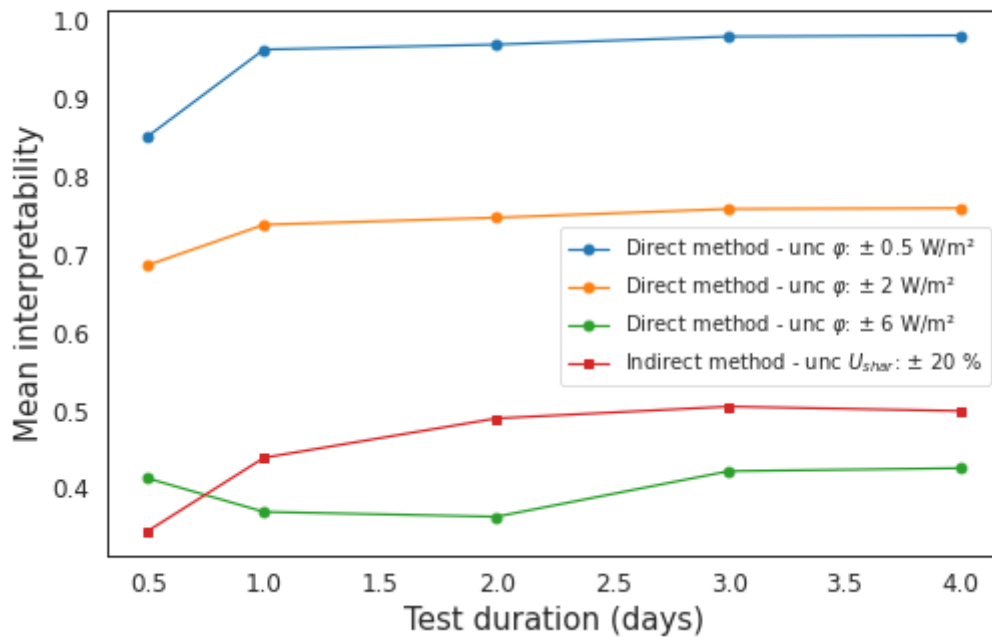


Figure 6.38 – Evolution of mean interpretability value with the test duration using the direct and indirect method with different input uncertainty levels.

Logically, the direct method presents higher interpretability levels when assuming low values of uncertainty input in φ_{shar} . The results of the direct method with the highest uncertainty input are worse than the results from the indirect method and seem to stabilize after three days of test. From one day of test duration, the results of the two groups with lower levels of uncertainty input of the direct method already stabilize. This can be considered an asset of the direct method in opposition to the indirect method, regarding the required vacancy time required by the protocol.

The following analysis are presented for two days of test duration to be consistent with the previous analysis in part 6.3.2.3. The results from these four groups according to the level of bias, uncertainty and interpretability are presented in figure 6.39. The dashed red line delimits the acceptable results, with uncertainty inferior to 35 % and bias within ± 15 %. We can notice that all the results of the direct method with ± 0.5 W/m² are acceptable. The maximum uncertainty in this group is 15 % and the results of this group are of excellent quality. The group using ± 2 W/m² of uncertainty has a majority of acceptable results, with two exceptions. The group using ± 6 W/m² of uncertainty input presents the exact opposite behavior.

It was previously shown that the indirect method (with ± 20 % of uncertainty input) only performed well for cold weather conditions. Figure 6.40 presented the performance of the direct method and indirect method for the different tested cases. The interpretability level of each city and month are shown for the four groups.

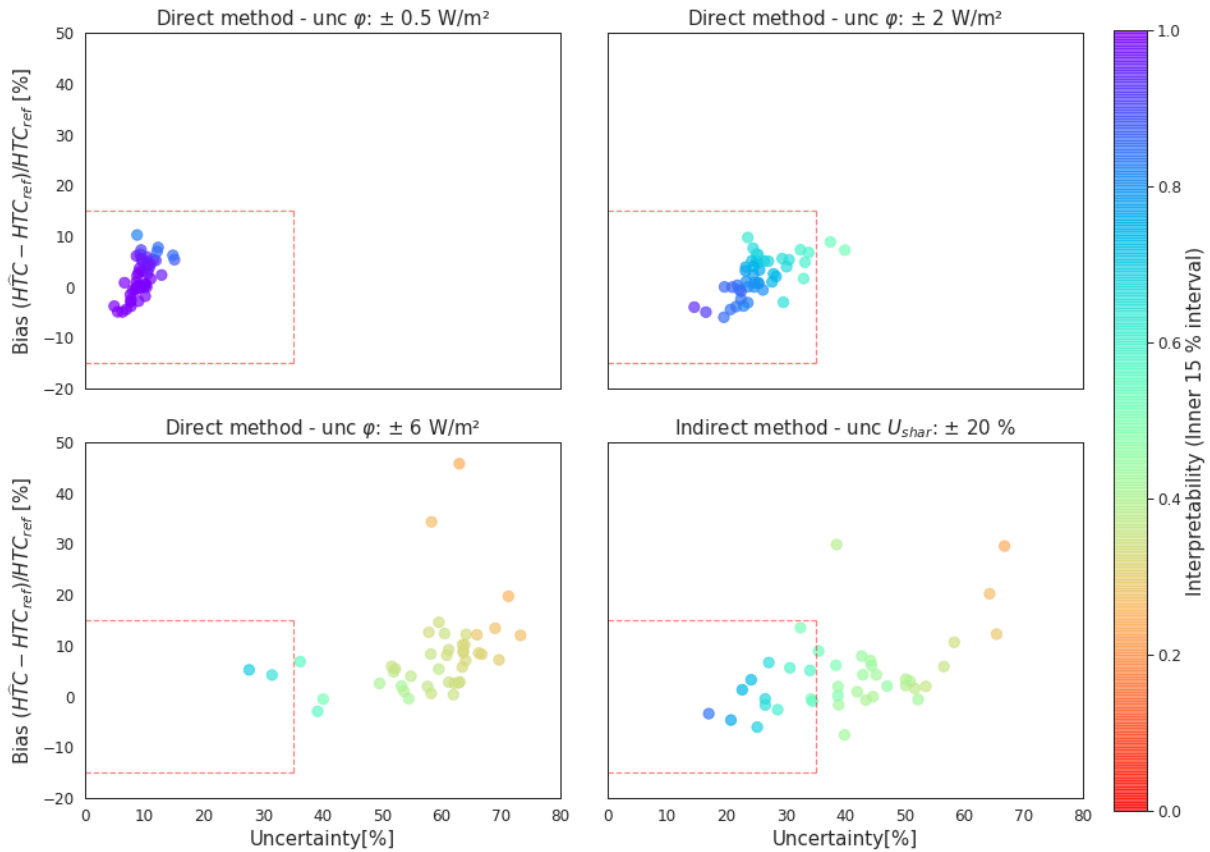


Figure 6.39 – Interpretability, bias and uncertainty of the results using the direct and indirect method with different input uncertainty levels.

There are less missing results for lower values of uncertainty in this parameter and even less than that of the indirect method. Also, the indirect method seems to be more influenced by the exterior conditions than the direct method, with higher interpretability variations over the year. This might be explained by the fact that in the indirect method, U_{shar} uncertainty is expressed in a percentage form and the $\Delta T_{int-adj}$ is taken into account to the ϕ_{shar} estimation. For this reason, in this method, a high $\Delta T_{int-adj}$ increases the impact of U_{shar} uncertainty input in the final results, while ϕ_{shar} uncertainty input is an absolute value of flow per meter square. Although it is an absolute value, in practice the level of ϕ_{shar} uncertainty should be chosen according to the test conditions, including $\Delta T_{int-adj}$ levels.

In this work, the uncertainty value associated to U_{shar} is related to the values of the uncertainties on wall thickness, materials conductivity and superficial heat transfer coefficients. One could consider narrower ranges on these parameters and decrease the 20% of uncertainty. However, it is hard to assume really low uncertainties to U_{shar} , because even with detailed information on the wall composition, variations in its performance related to workmanship, material degradation and others can occur. If no detailed information is given on the shared wall, this uncertainty input might be higher, which would intensify the results uncertainty.

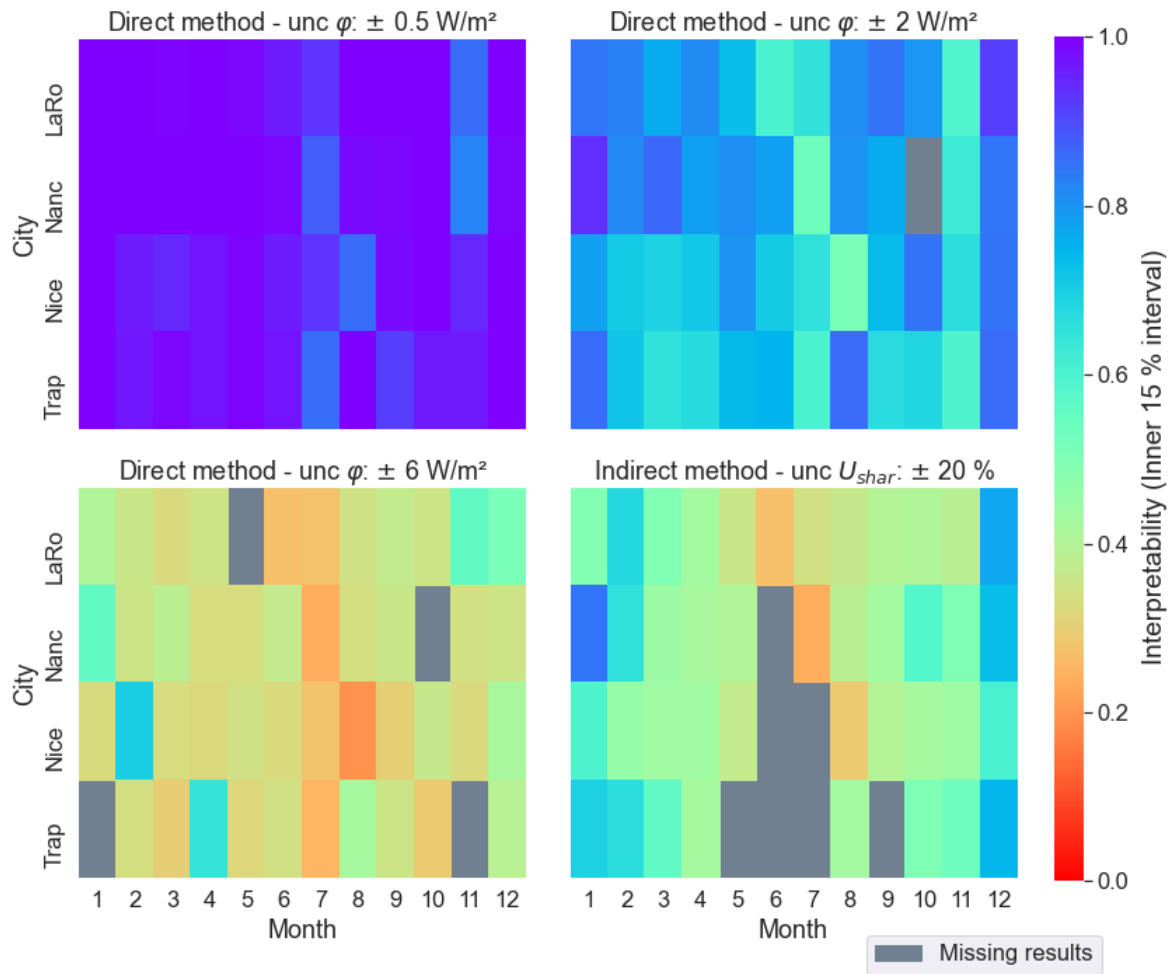


Figure 6.40 – Interpretability of the results using the direct and indirect method with different input uncertainty levels.

Regarding the uncertainties levels of the direct method, they are still to be further studied, according to the wall typology and the level of temperature difference with the adjacent spaces. With the preliminary results presented in part 6.4.1.3, a level of $\pm 2 \text{ W/m}^2$ uncertainty seems achievable when there is low $\Delta T_{int-adj}$. Considering the hypothesis of $\pm 2 \text{ W/m}^2$ of φ_{shar} uncertainty and 20 % of U_{shar} uncertainty, the indirect method would be beneficially replaced with the direct method.

In the experimental plan C the indoor temperature was defined to have 15 K of temperature difference with exterior, limited by 20 °C and 35 °C. Since in this experimental plan no interference was considered in the neighbours, T_{adj} was independent of the test and had the same scenario all year round. For these reason, the $\Delta T_{int-adj}$ value varies in the different tested months, reaching higher levels during the summer months and lower levels during the winter. In this experimental plan the colder months would follow the $\pm 0.5 \text{ W/m}^2$ or $\pm 2 \text{ W/m}^2$ graphs and the warmer months would follow the $\pm 6 \text{ W/m}^2$ graph. All results are presented with all tested φ_{shar} uncertainties to show how the direct method would perform if the same $\Delta T_{int-adj}$

were applied to the different months. Figure 6.41 shows an example of the results progression from one test applied during summer using $\pm 2 \text{ W/m}^2$ of φ_{shar} uncertainty. This represents one of the least optimal weather conditions for the indirect method and the result is still stable and acceptable with the direct method if a low level of φ_{shar} uncertainty is reached.

Low levels of $\Delta T_{int-adj}$ could be potentially reached during winter period without interference in the adjacent spaces, if they are occupied and heated. However, during mid-season and summer, controlling the T_{adj} to reach the temperature levels necessary for the test would probably be necessary. On one hand it implies a more invasive test, but on the other hand it expands the validity domain of the method. If low levels of φ_{shar} uncertainties inputs can be experimentally reached, the direct method opens opportunity to apply the sampling approach during mid-season and summer.

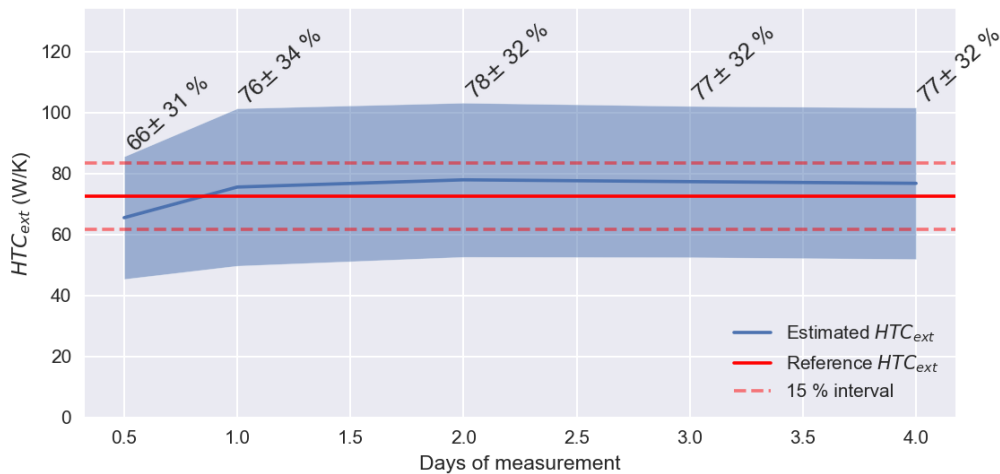


Figure 6.41 – Progression of results for the test applied in July in Trappes city using the direct method with $\pm 2 \text{ W/m}^2$ of uncertainty associated to φ_{shar} .

6.5 In-situ test application

In order to test both direct and indirect methods of the sampling approach, a SEREINE protocol of the sampling approach was applied in a real building.

6.5.1 Building description

The test was performed in the educational building A11 from Bordeaux University. Various works have been applied to this building, including a heavy retrofit of the West and North wings (4800 m²) and the demolition and reconstruction of the East wing (1000 m²). The renovated part of the building was under the standards of French Thermal Regulation for existent buildings

and the East wing followed the French Thermal Regulation 2012. The tested office is located at the corner of the last floor of the building East wing (figure 6.42). Figure 6.43 shows the position of the tested office in the building's blueprint.



Figure 6.42 – Google image of A11 building (left) and view of the tested office (in red) west facade from the central building area (right).

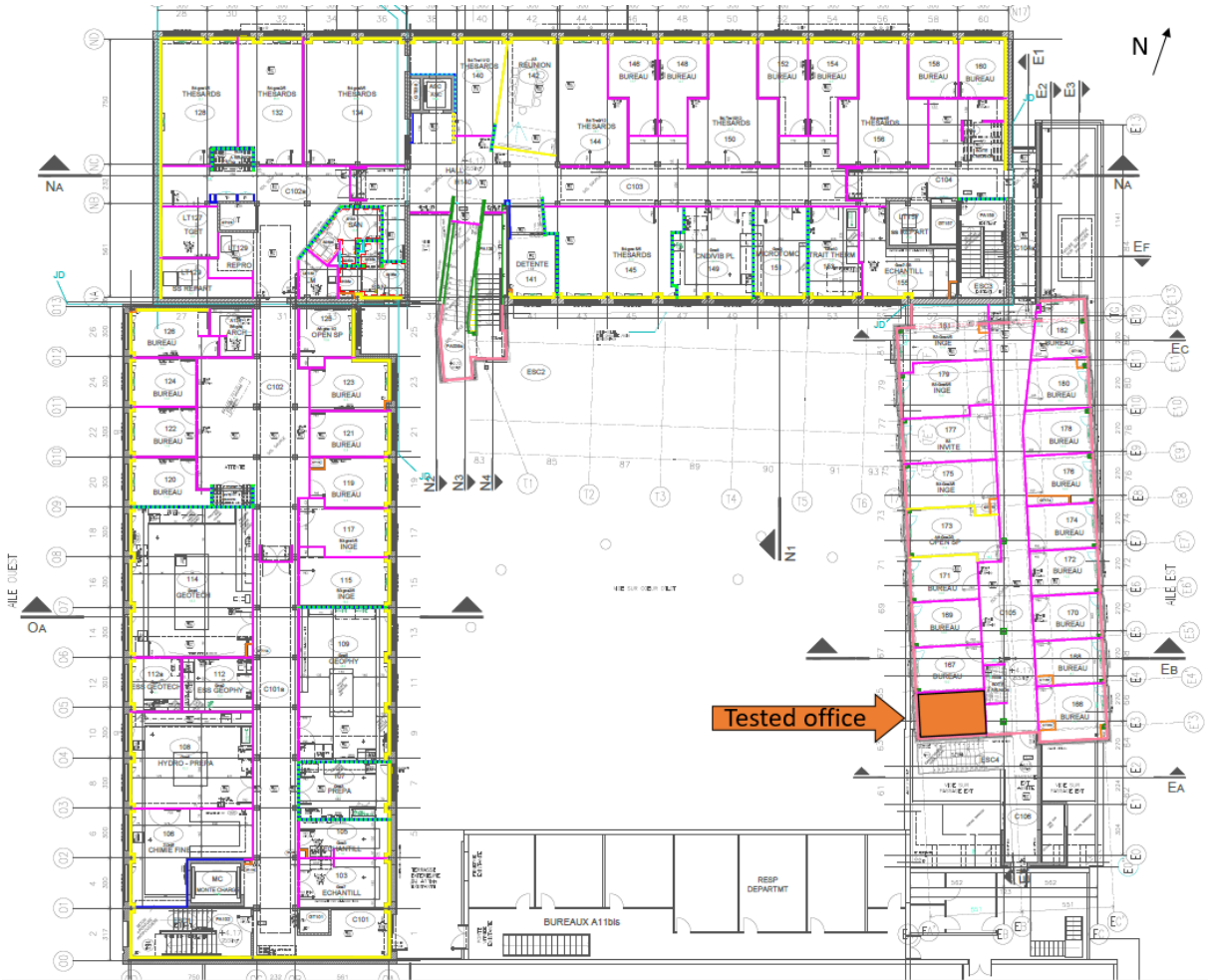


Figure 6.43 – Blueprint of A11 building first floor, with the tested office marked in orange.

Table 6.15 – Description of the composition and project U-values concerning the tested area of the A11 East wing.

Composition	Contact	Orientation	Area (m ²)	U-value (W/m ² /K)
High floor	Unheated space	-	6.5	2.27
Exterior wall	Exterior	South	7.6	0.20
Exterior wall		West	3.0	0.20
Window		West	4.0	1.45
Intermediate floor	Interior	-	6.5	2.27
Partition wall		North	7.6	0.74
Partition wall		East	4.9	0.74
Door		East	2.1	2.10

The exterior wall is composed of a 70 mm metal frame structure, to which plasterboards are screwed and filled with two layers of glass wool of 75 mm and 140 mm. The partition walls are made of a 62 mm metal frame with plasterboards and a 45 mm insulation layer, with a high acoustic performance (up to 48dB). The intermediate floor and the ceiling are composed of 20 cm of concrete slab. The description of the surfaces and the project U-values are presented in the table 6.15.

There is an unheated area between first and second floor of the East wing, where some technical equipment are located. In the thermal study, that area was considered isolated and without air transfer with exterior environment, The loss reduction coefficient, b , used in the project of the East wing first floor high floor was one percent. This b coefficient is multiplied by the U-value of the high floor to the consideration of an equivalent U of this wall.

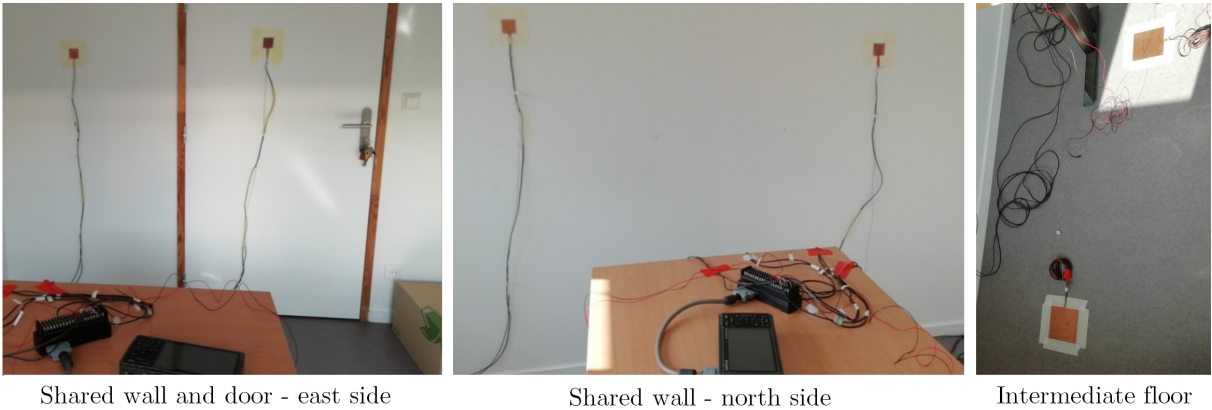
The office position is optimal for test, with a $\Gamma_{S_{ext-shar}}$ of 100 %. Even though the building has high thermal performance materials in the envelope, the fact that the shared walls have acoustic insulation makes this case less critical to test. The whole East wing was vacant and not heated before the test beginning and the tested area represents a small part of this building wing. For this reason, it is hard to assume the previous b coefficient during the experiment, since the ratio between the tested office high floor and the total area of unheated space in contact with the exterior is much lower than when the whole East wing is heated. Considering a b coefficient of 1, the calculated $HTC_{ext_{ref}}$ of the office is then of 22.7 W/K and the calculated $HTC_{shar_{ref}}$ is 28.5 W/K. The predict $\Gamma_{U_{ext-shar}}$ is thus 80 %, considering the thermal losses through plan elements. The range of $\Gamma_{S_{ext-shar}}$ and $\Gamma_{U_{ext-shar}}$ are considered adequate for a quality test with the direct and indirect methods.

6.5.2 Experimental description test

The SEREINE equipment kit from Nobatek/Inef4 Bordeaux was lent to perform the test. The tested office and the adjacent spaces were each equipped with one heating module composed of an electrical heater, a temperature sensor and a fan. SENS sensors were placed on a footbridge in front of the unheated area access. An exterior temperature sensor was placed in the attic floor. Part of the SEREINE equipment used during the test are shown in figure 6.44. Besides the usual SEREINE equipment, HFM were placed on each shared wall, as presented in figure and 6.45. In this way, both direct and indirect method can be used to estimate the tested office thermal performance.



Figure 6.44 – SEREINE Heating module placed in the tested office (left), SENS sensors placed outside the building in the footbridge in front of the entrance of the unheated space (right).



Shared wall and door - east side Shared wall - north side Intermediate floor

Figure 6.45 – HFM location for each shared wall of the tested office in A11 building.

The SEREINE test was applied just before the East wing of the building was occupied after the end of the construction. It started on April 28th 2021 and lasted one week. No preheating was applied neither in the tested room nor in the adjacent areas, although the electrical heaters were on during the equipment assembly. For this reason, a longer test duration than that prescribed

by the numerical experiments is expected to converge to stable results. The vacancy of the East wing of the building also allowed to control the temperature of the spaces adjacent to the tested office. In order to assure a low $\Delta T_{int-adj}$ and good results for both methods, the same heating scenario of the tested office was applied to the adjacent spaces. All these areas had a fixed setpoint temperature of 27 °C all along the test duration. As usual for SEREINE/ISABELE methods, the shutter of the window were closed and the inlet vents were obstructed during the test.

The experimental data related to ϕ_{shar} is presented in figure 6.46. The main part of the ϕ_{shar} passes through the concrete floor, which is expected since this wall has a higher thermal capacity than the partition walls. The concrete floor thermal charging is noticeable during the first days of test. In addition to this wall property, the heating module was placed on the floor of the space beneath the tested office, that has a suspended ceiling. Regarding the adjacent temperatures, the variations measured by the sensor placed in the corridor close to the office door are due to the opening of an entrance of the building besides this sensor. Even so, the adjacent temperatures were close to that of test all along of the experience, with variations inferior to 1.2 K.

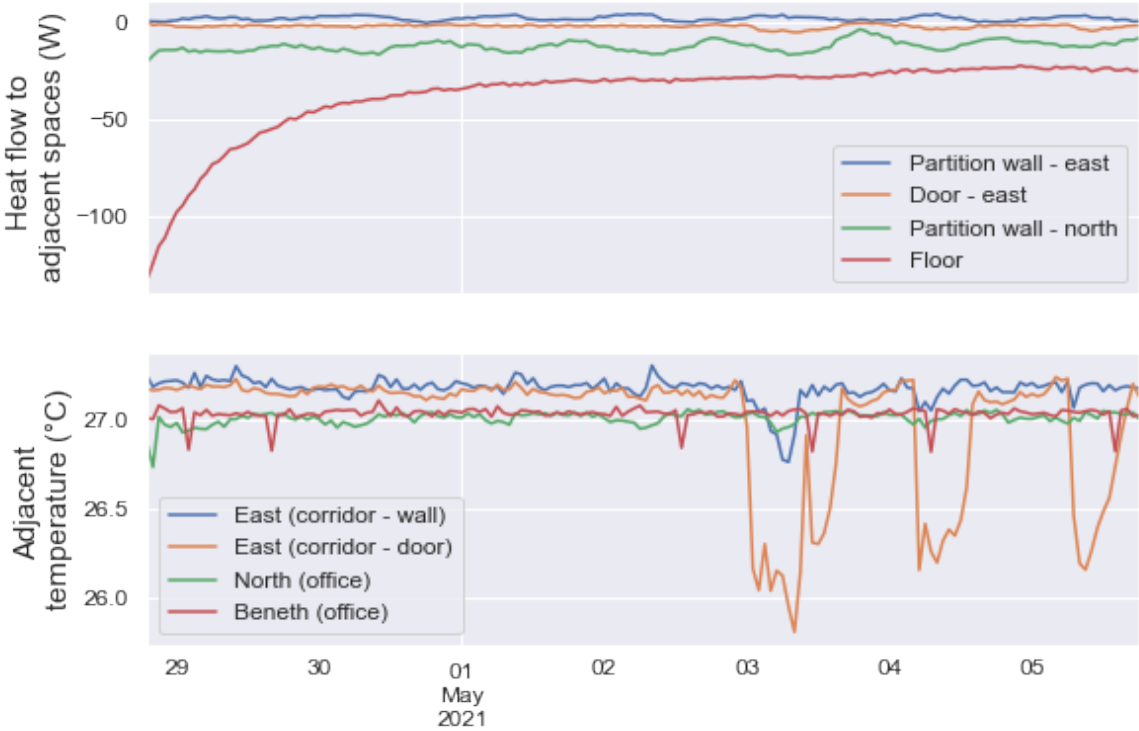


Figure 6.46 – Heat flow passing through the shared walls (HFM measurements) and adjacent spaces temperature during the experiment in A11 building.

Figure 6.47 shows other power and temperature data. The mean outdoor temperature during test was 12 °C, with thus a mean $\Delta T_{int-ext}$ of 15 K, which is considered enough heat signal towards the exterior. The mean heat power delivered during the test was 363 W, subtracting the

ϕ_{shar} it was 312 W. Applying the average method in the data collected during the experiment, an HTC_{ext} of 25.7 W/K is expected. The average method does not take into account the dynamic effects of the building thermal mass, that can have an important contribution during the test.

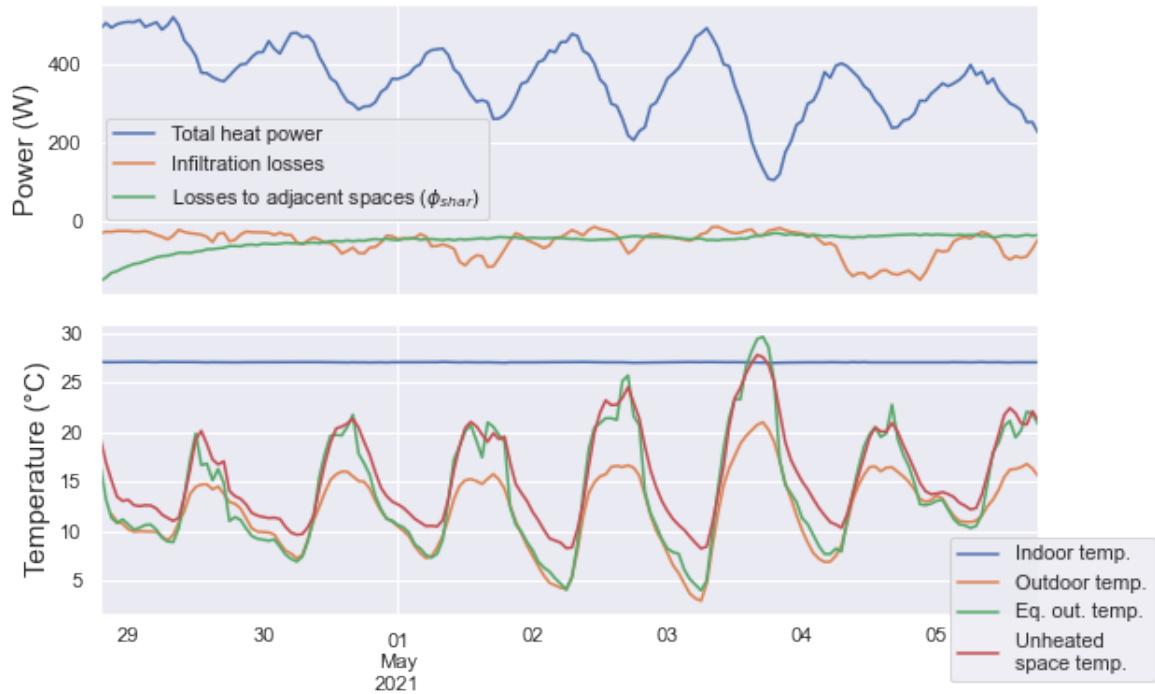


Figure 6.47 – Heat power and temperatures during the experiment in A11 building.

To enable the HTC estimation, a blower door test was conducted in the tested office (figure 6.48).

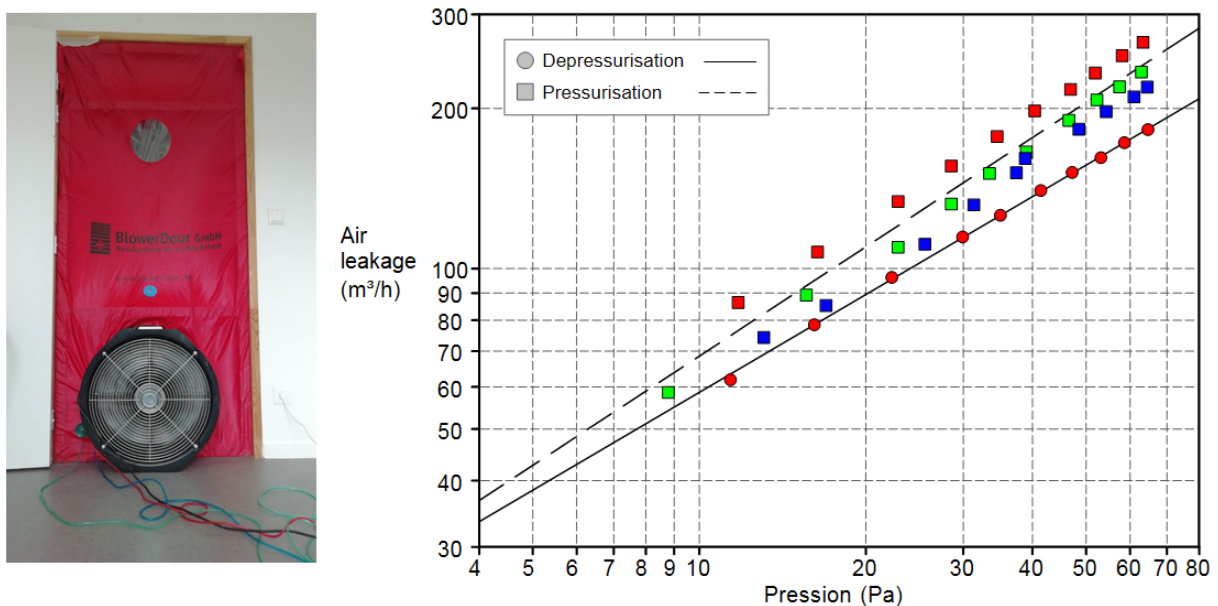


Figure 6.48 – Blower door setup in the office doorway (left) and the result of the four tests in the graph of air leakage versus pressure (right).

The blower door test was performed three times in pressurization and once in depressurization, with the collaboration of the post-doc Ryad BOUZOUIDJA. The air leakage coefficient (CL) was of $14.4 \text{ m}^3\text{h}^{-1}\text{Pa}^{-n} \pm 4 \%$, the exponent n was of $0.61 \pm 1.64 \%$ and the Q_4 was of $1,6 \text{ m}^3/\text{h}/\text{m}^2$.

6.5.3 Results and discussion

Since the detailed description of the shared walls is provided in the building technical documents, an uncertainty of 20 % associated to U_{shar} was considered in the indirect method, based on the study from part 6.3.1. The adjacent spaces were heated and there was low levels of $\Delta_{T_{int-adj}}$ during the test. Therefore, an uncertainty related to φ_{shar} of $3 \text{ W}/\text{m}^2$ was used, based on the experimental results from part 6.4.1.2.

The results of HTC_{ext} for the direct and indirect method are respectively presented in figures 6.50 and 6.49. Both cases seem to converge to a similar HTC_{ext} of 21 to 22 W/K inside the available test duration. The $HTC_{ext_{ref}}$ of 22.7 W/K is inside the range of uncertainty of both methods in the end of the test duration.

The direct method converges faster to this value than the indirect method. Considering the uncertainty range, the direct method already presents acceptable results from the beginning of the test, while the indirect method needs at least two days of test. This difference in behavior is expected, once there was no preheating of the building before the protocol application. In the beginning of the test, part of the delivered energy is consumed to thermally charge the shared walls. In the direct method, the flow passing through these walls is directly measured and then subtracted from the total heating power. In the indirect method, the thermal dynamic effects happening in the shared walls are neglected. For this reason, the energy used to heat these walls in the beginning of the test is included in the total heating power, which leads to the impression of a thermally poorer envelope.

For this study case, both methods presented equivalent low levels of uncertainty. This is probably due to the fact that the shared walls are partially insulated and that there is a high heat flow passing through the envelope. Also, the adjacent spaces are heated, $\Delta_{T_{ext-adj}}$ is small and therefore there is a low level of ϕ_{shar} , so its uncertainty inputs have less impact in the final result uncertainty.

This experimental work shows the applicability of both direct and indirect method on a real case. Although the outdoor temperature was not very cold, the combined strategy of a higher indoor temperature (15 K of mean $\Delta_{T_{int-ext}}$) and of heating the adjacent spaces was successful. Both results converged to a similar value, which is coherent with the calculated HTC, and had acceptable uncertainties. It should be considered that the test conditions were optimal, with

a high $\Gamma_{S_{ext-shar}}$ and $\Gamma_{U_{ext-shar}}$ and a low $\Delta_{T_{int-adj}}$, which might be difficult to achieve in every *in-situ* protocol application. Although the indirect method is more practical in a technical point of view, the direct method allows to reduce the duration of building vacancy, with faster convergence to the final result. This effect is more relevant for unoccupied and/or unheated buildings.

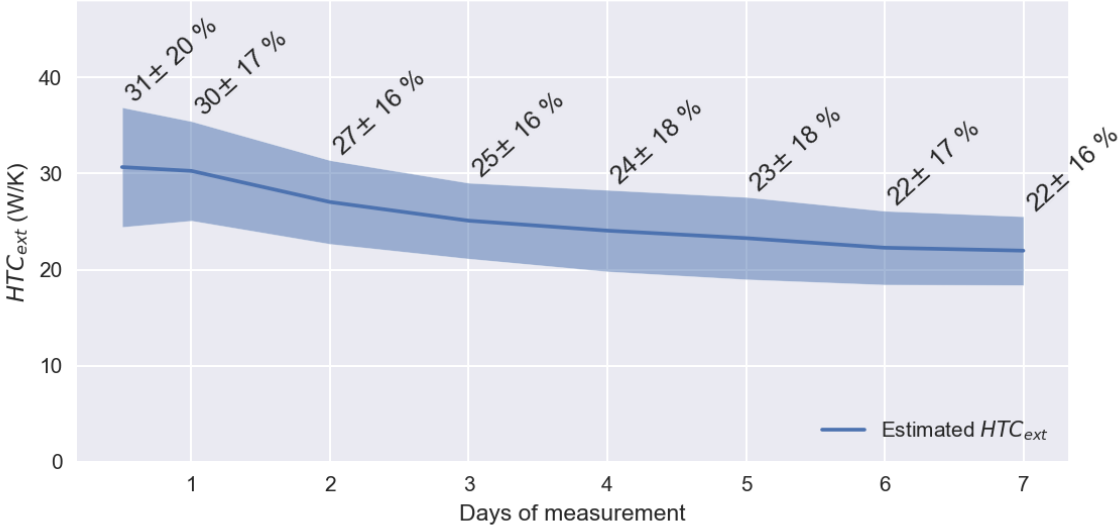


Figure 6.49 – Progression of results for the test in the A11 building using the indirect method with $\pm 20\%$ of uncertainty input in the U_{shar} .

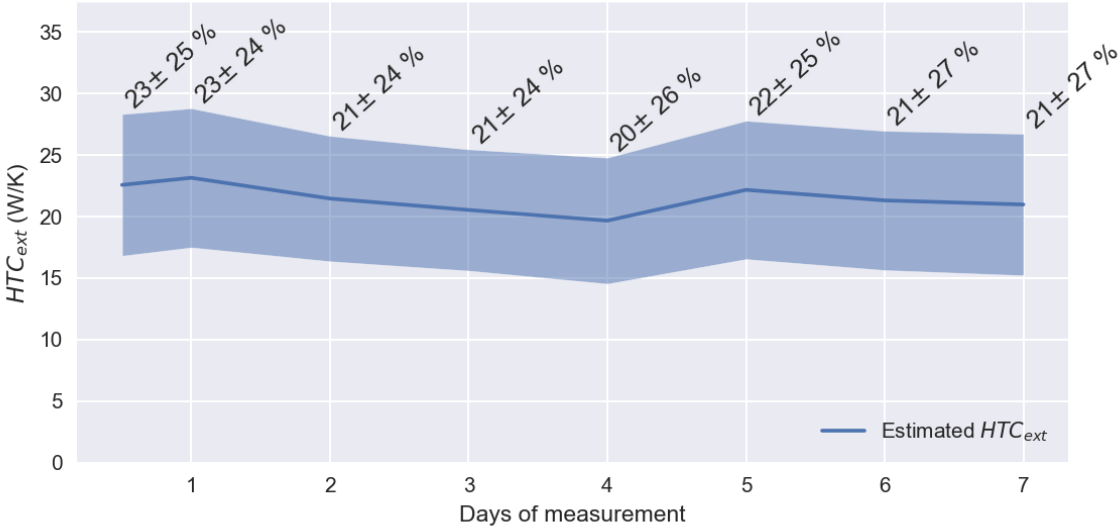


Figure 6.50 – Progression of results for the test in the A11 building using the direct method with $\pm 3\text{ W/m}^2$ of uncertainty input in the φ_{shar} .

6.6 Chapter conclusion

In order to investigate the behavior of the sampling approach, a simplified model was developed, for which the uncertainty of the results can be calculated with a mathematical formula. The variation of the input parameters and uncertainties highlighted the importance of increasing the $\Gamma_{\phi_{ext-shar}}$ during the protocol application. To increase this ratio, the choice of a sampled area at the corner of last the floor, which optimizes the $\Gamma_{S_{ext-shar}}$ of a single tested apartment, should be considered. Adjacent apartments or offices can also be aggregated for increasing $\Gamma_{S_{ext-shar}}$, with the limitation of the available equipment kits to cover the tested area. Another important parameter is $\Gamma_{U_{eq_{ext-shar}}}$, which is critical for buildings with thermally efficient envelope and non insulated shared walls. This means that the results uncertainties are likely to be higher for new and renovated buildings than for poorly insulated buildings with the same experimental protocol. Another influential parameter is the $\Delta T_{int-adj}$ and reducing this temperature difference could be a strategy for the indirect method.

For the sampling approach, the uncertainties related to ϕ_{shar} estimation must be considered in the uncertainty propagation of the SEREINE estimation process. The simplified model investigation shows that the ϕ_{shar} estimation input uncertainty has a significant impact on the final result uncertainty for both methods. The reachable level of input uncertainty being used for this new variable estimation is a major lever in the feasibility of the sampling approach. A Monte Carlo uncertainty propagation technique was used to define a first level of U_{shar} uncertainty, considering the detailed description of the shared walls were available for the indirect method. This allowed to give a reference to be used later in the numerical simulations, however this value needs to be further investigated if the hypothesis and conditions change. In the direct method, experimental work with HFM was developed to define the levels of φ_{shar} input uncertainty. This work showed that in reality higher levels of uncertainty are related to higher $\Delta T_{int-adj}$, which was not expected prior to the experiment. To better define the φ_{shar} uncertainties to be used for *in situ* tests, this experimental work needs to be extended for walls with different characteristics and using various levels of $\Delta T_{int-adj}$ with a stable temperature scenario.

Numerical simulations were used to investigate the methods behavior and their validity domain. The variation of the insulation location showed that the results stabilize faster for building with internal wall insulation than for those with external wall insulation. The variations of indoor and preheating temperatures showed that a protocol with zero $\Delta T_{beg-end}$ reaches stable results faster for the indirect method. Forty-eight different weather conditions were used with three variations in the protocol conditions related to $\Delta T_{int-ext}$ and $\Delta T_{int-adj}$. As expected, high $\Delta T_{int-ext}$ levels were associated with higher quality results, better conditions

were reached during colder months of the year. Although low $\Delta T_{int-adj}$ slightly improved the results for some cases, it did not yield acceptable results for the indirect method applied in mild and hot weather. The combination of higher test temperatures and lower temperatures differences with the adjacent spaces should be studied for the application of the indirect method in mid-season. The direct method was tested only for one experimental plan with a total of forty-eight estimations per test duration. The comparison of the results of the direct and indirect method showed that the first has the potential to significantly improve the sampling approach if low input uncertainties can be reached in-situ. Using the level of φ_{shar} uncertainty input from the experimental results, this method could be applied all year round, if the adjacent spaces temperatures are kept close to that of test.

Although first conclusions can be made from these numerical simulations, it is necessary to test the methods in-situ. Both methods were applied in a building located at Bordeaux university. The tested area presented favorable test conditions, with high $\Gamma_{S_{ext-shar}}$ and $\Gamma_{U_{eq_{ext-shar}}}$. The building wing was vacant before test and no preheating was applied previously to the equipment assembly. The test had a total duration of one week and both methods converged to similar values within this time, which is consistent with the expected HTC_{ext} . Since a high $\Gamma_{\phi_{ext-shar}}$ was reached during the test, the uncertainty levels were within the acceptable range. The floor of the tested area was made of a heavy material and the direct method presented the advantage of measuring the dynamic behavior of this wall. Because the building was not preheated and the indirect method neglects the shared walls dynamics, it took two days for the results to converge, while the direct method presented acceptable results from the first half day.

Both methods have their advantages and drawbacks. The indirect method is more practical from a technical point of view, without the need of extra measurement equipment to be added to the current SEREINE/ISABELE kit. However, it has strong limitations regarding its pertinency domain. It should be applied to buildings with detailed information on the shared walls composition and during the colder months of the year. The direct method does not present these limitations, but to reach low uncertainty, the adjacent temperatures need to be kept close to that of the tested area. This can be a strong constraint in the method application if the adjacent spaces are occupied, for example in the case of the renovated buildings. This is less important in the context of new buildings, which might not be occupied yet. Another drawback of this method is related to the extra necessary equipment, which requires time for assembly and can damage the wall surface depending on the installation technique. If the conditions necessary for the direct method are reached, the sampling approach can be applied in different months of the year, even during mid-season and summer.

Chapter 7

Conclusion and perspectives

Building energy efficiency is a key factor in reducing CO₂ emissions and in-situ methods can be applied to estimate building envelope thermal performance. Different methods are nowadays available, but those relying on fast duration protocols are mainly applicable in the context of single-family houses. Multi-family housings and tertiary sector building account for an important part of the building stock, presenting them a relevant potential for energy savings. It is thus important to have reliable methods to assess the building envelope thermal performance in those building typologies. The current work investigate the adaptation and applicability of a short duration method for identifying the HTC and HLC in large buildings.

As an outcome of the literature review on the existing methods for building envelope thermal performance assessment, ISABELE/SEREINE methods were chosen to be adapted to the context of large buildings. These methods, initially defined for single-family houses, have the asset of a methodology to estimate the results uncertainty. Although, the change on building size implies new challenges in a scientific, technical and operational aspect to have an applicable and valid method. After a detailed study, two main approaches were considered to face these challenges:

- Global approach: the protocol is applied to the whole building and the tested volume perimeter coincides with the building envelope.
- Sampling approach: the protocol is applied to parts of the building and the tested volume perimeter includes samples of the building envelope and shared walls.

Both approaches present advantages and drawbacks. For this reason, the work was conducted to adapt the protocol and estimation process to each one. Their applicability in the building stock was studied, considering their limits and possibilities. The approaches were developed with numerical simulations, having the advantages of multiple test scenarios and of reliable reference values. The latter allows the use of quality criteria, as the acceptability and interpretability indicators, which enables the analysis of the method validity domain. Both

approaches were finally applied in a real building to verify their quality and applicability in *in situ*.

The main limitations of the global approach are related to the protocol applicability, regarding the instrumentation and vacancy of the whole building. A possible strategy to decrease the volume of equipment for a test is the use of the local heating system during the test. This approach is however limited to the conditions of the local system and impacts the building's normal usage on a global scale. It was considered possible in buildings with a centralized heating system with hot water distribution, in which a calorimeter can be used to measure the power delivered during the test. This would be the case of half of the French multi-family housing stock, according to the 2013 National Housing Survey database. The approach would be more difficult to apply to buildings with individual electric heating systems, which accounts for a quarter of multi-family buildings according to the same source.

The global approach was applied to a four-storey building model with variations in the protocol temperatures. The protocol with low temperature difference between the beginning and the end of the test presented less temperature dispersion among the thermal zones and better results. The global approach was successfully applied to a low-rise real building with the use of multiple SEREINE kits, achieving stable results after two days and a half of test duration. The blower door test was performed in each apartment to estimate the HTC, which was possible due to the building size. If the HTC is aimed to be estimated in larger buildings, the development of another infiltration losses model should be considered. More building configurations and weather scenarios could be further studied with virtual and real test applications to define the method pertinency domain.

The sampling approach is an alternative to the global approach, in which the envelope thermal performance is verified locally. The main challenge in this approach concerns the thermal losses through the shared walls, since they are not commonly insulated. Two methods are proposed in order to estimate the flow towards the adjacent spaces: the indirect and direct methods. In the indirect method, the flow is estimated based on the wall U-value, surface and the temperature difference between the two sides of the wall. The direct method is based on the measurement of the heat flow on the wall with the use of heat flow meters. The input uncertainties related to the ϕ_{shar} estimation in each method have major influence in the final results and they could be further studied for different wall typologies and heating scenarios.

Numerical studies concluded that the indirect method reaches faster stable results in buildings with internal wall insulation and when the building is preheated before the protocol application. The indirect method performed better for tests with higher levels of temperature difference with the exterior and lower with the adjacent spaces, which was commonly reached

during the colder months. In the tested condition, heating the neighbours only slightly improved the results of the indirect method and it was not a sufficient condition to guarantee acceptable results. However, protocols with higher indoor temperatures and heated neighbours could be further investigated to verify if both strategies together enable the application of the indirect method on mild and hot weather conditions. In general, the uncertainty level was the most challenging aspect for reaching acceptable results with the indirect method. The bias criterion was commonly reached during winter and mid season and also in some tests applied during summer. The indirect method is viable during the colder months of the year and two days of test are enough to reach stable results if the building is preheated.

The direct method presented high levels of convergence and interpretability for low levels of φ_{shar} input uncertainties. However, if this input uncertainty is high, the method does not present advantages in comparison to the indirect method. The φ_{shar} input uncertainties presented relation with the temperature difference between both sides of the shared walls. It seems to be sensible not only to the $\Delta T_{int-adj}$ levels, but also to its variations on time. Lower levels of $\Delta T_{int-adj}$, that are stable on time, are associated to lower φ_{shar} input uncertainties. The control of the adjacent areas temperatures can therefore be a strategy to enlarge the validity domain of the sampling approach. This input uncertainty level is a key factor on the direct method quality and more research should be developed to continue to investigate the appropriated levels to be used under different test conditions. If the adjacent spaces temperatures can be controlled close to the indoor temperature, the direct method presents acceptable results from half a day of test duration and is valid all year round.

The indirect and the direct methods were applied *in situ* to verify their behavior in a real case scenario. The strategy of heating the adjacent spaces and choosing an indoor temperature 15 K above the mean outdoor temperature was effective. The results of both methods converged to a similar value, coherent with the calculated HTC_{ext} , and presented acceptable levels of uncertainty, under the threshold of $\pm 15\%$. Also in a real application, the direct method presents stable results faster, with half a day of test duration, against two days for the indirect method. For further *in situ* tests, it is recommended to calculate the theoretical ratios ($\Gamma_{U_{eq_{ext-shar}}}$, $\Gamma_{S_{ext-shar}}$ and $\Gamma_{\Delta T_{ext-adj}}$) prior to the protocol application. The uncertainty level correspondent to the calculated ratios in the static method graphs, can be used to indicate if the conditions for test are enough for achieving a reliable result.

This thesis consists in the exploration of possibilities to find solutions for the application of a fast BETPA method into large buildings. The results presented are a product of the choices made on the suggested approaches. Since there is a wide range of possibilities to be tested regarding methods, building characteristics and weather conditions, many of them have not been studied

and are part of the perspectives. The research developed in this thesis could also be applied to other building typologies, with variations in building architectural characteristics and envelope composition. In this work, a mid-rise MFH model was studied numerically, but other building typologies could be further studied, such as TSB and high-rise MFH. Although the conclusions are limited to the tested cases, a similar reasoning could be applied to other case studies to investigate the method possibilities and limits. Testing different apartments in the sampling approach could also be verified, in an attempt to better describe the performance indicators of the whole building envelope. In addition, other methods could be adapted for application in large buildings, including those with occupied buildings, for which protocol duration is not a major concern.

Bibliography

- [1] European Commission. Final communication from the commission to the council, the european parliament, the european economic and social committee and the committee of the regions - limiting global climate change to 2 degrees celsius the way ahead for 2020 and beyond, 2007.
- [2] European Environment Agency. Eu on track to meet greenhouse gas emissions and renewable energy 2020 targets, progress in 2019 shows more ambitious long-term objectives are reachable. <https://www.eea.europa.eu/highlights/eu-on-track-to-meet>, 2020. Online; accessed on 2021-09-12.
- [3] European Commission. 2030 climate & energy framework. https://ec.europa.eu/clima/policies/strategies/2030_en#tab-0-0, 2018. Online; accessed on 2021-09-12.
- [4] International Energy Agency. Multiple benefits of energy efficiency. <https://www.iea.org/reports/multiple-benefits-of-energy-efficiency/emissions-savings>, 2019. Online; accessed on 2021-09-12.
- [5] European Commission. Eu buildings factsheets. https://ec.europa.eu/commission/presscorner/detail/en/fs_19_6725, 2020. Online; accessed on 2021-09-07.
- [6] University of Siegen. Directive 2010/31/eu of the european parliament and of the council on the energy performance of buildings. <http://data.europa.eu/eli/dir/2010/31/oj>, 2018. Online; accessed on 2021-11-10.
- [7] Ulrich Rochard. Etude comparative des réglementations thermiques des batiments et labels à l'échelle européenne, 2013.
- [8] Patrick X.W. Zou, Xiaoxiao Xu, Jay Sanjayan, and Jiayuan Wang. Review of 10 years research on building energy performance gap: Life-cycle and stakeholder perspectives. *Energy and Buildings*, 178:165–181, 2018.

- [9] Patrick X.W. Zou and Morshed Alam. Closing the building energy performance gap through component level analysis and stakeholder collaborations. *Energy and Buildings*, 224:110276, 2020.
- [10] Marta Pappalardo and Thomas Reverdy. Explaining the performance gap in a french energy efficient building: Persistent misalignment between building design, space occupancy and operation practices. *Energy Research & Social Science*, 70:101809, 2020.
- [11] Jing Liang, Yueming Qiu, and Ming Hu. Mind the energy performance gap: Evidence from green commercial buildings. *Resources, Conservation and Recycling*, 141:364–377, 2019.
- [12] Henrik Madsen, Peder Bacher, Geert Bauwens, An-Heleen Deconinck, Glenn Reynders, Staf Roels, Eline Himpe, and Guillaume Lethé. Annex 58 report of subtask 3, part 2: Thermal performance characterisation using time series data – statistical guidelines, 2021.
- [13] International Energy Agency. Annex 58 -reliable building energy performance characterisation based on full scale dynamic measurements. <https://iea-ebc.org/projects/project?AnnexID=58>, 2016. Online; accessed on 2021-10-12.
- [14] Geert Bauwens, Katia Ritosa, and Staf Roels. Annex 71 final report - building energy performance assessment based on in-situ measurements: Physical parameter identification, 2021.
- [15] Christoffer Rasmussen. *Data-driven Methods for Reliable Energy Performance Characterisation of Occupied Buildings*. phdthesis, DTU Compute Department of Applied Mathematics and Computer Science, May 2020.
- [16] State of Connecticut Department of Environmental Protection. Hearing report prepared pursuant to section 4-168(d) of the connecticut general statutes and section 22a-3a-3(d)(5) of the department of environmental protection rules of practice regarding regulations for the abatement of air pollution: Proposed adoption of section 22a-174-31 and proposed adoption of section 22a-174-31(a) of the regulations of connecticut state agencies, 2008.
- [17] Directive Parliament. Directive 2002/91/ce du parlement européen et du conseil du 16 décembre 2002 sur la performance énergétique des bâtiments. <https://eur-lex.europa.eu/legal-content/FR/ALL/?uri=celex:32002L0091>, 2002. Online; accessed on 2021-09-05.

- [18] L. Pérez-Lombard, J. Ortiz, and D.a Velázquez. Revisiting energy efficiency fundamentals. *Energy Efficiency*, 6:239–254, 2013.
- [19] UNIDO. Energy efficiency in buildings - module 18 - sustainable energy regulation and policymaking for africa, 2006.
- [20] Ministère de la transition Ecologique. Le nouveau diagnostic de performance énergétique (dpe), 2021.
- [21] Nicolas Bourbon, Thomas Recht, Rofaïda Lahrech, and Laurent Mora. A framework to evaluate the reliability of energy performance assessment methods using buildings databases, application to the french residential energy performance certificate. In *Building Simulation 2021 Conference*. BS2021, 2021.
- [22] Xiaoshan Yang, Lihua Zhao, Michael Bruse, and Qinglin Meng. An integrated simulation method for building energy performance assessment in urban environments. *Energy and Buildings*, 54:243–251, 2012.
- [23] Carolina Abrahão Alves, Fábio Luiz Teixeira Gonçalves, and Denise Helena Silva Duarte. The recent residential apartment buildings’ thermal performance under the combined effect of the global and the local warming. *Energy and Buildings*, 238:110828, 2021.
- [24] I. Andrić, J. Fournier, B. Lacarrière, O. Le Corre, and P. Ferrão. The impact of global warming and building renovation measures on district heating system techno-economic parameters. *Energy*, 150:926–937, 2018.
- [25] Lisa Guan. Energy use, indoor temperature and possible adaptation strategies for air-conditioned office buildings in face of global warming. *Building and Environment*, 55:8–19, 2012. Implications of a Changing Climate for Buildings.
- [26] Hassan Radhi. Evaluating the potential impact of global warming on the uae residential buildings – a contribution to reduce the co2 emissions. *Building and Environment*, 44(12):2451–2462, 2009.
- [27] M. Santamouris. On the energy impact of urban heat island and global warming on buildings. *Energy and Buildings*, 82:100–113, 2014.
- [28] D.P. Jenkins, A.D. Peacock, and P.F.G. Banfill. Will future low-carbon schools in the uk have an overheating problem? *Building and Environment*, 44(3):490–501, 2009. cited By 44.

- [29] Alain Liébard and André De Herde. *Traité d'architecture et d'urbanisme bioclimatiques : concevoir, édifier et aménager avec le développement durable*. Observ'ER, September 2005. 1 vol. (XV-[736] p., pagination double).
- [30] ICF International. Energy performance of buildings directive (epbd) compliance study, 2015.
- [31] María Teresa Baquero Larriva and Ester Higuera García. Confort térmico de adultos mayores: una revisión sistemática de la literatura científica. *Revista Española de Geriátria y Gerontología*, 54(5):280–295, 2019.
- [32] David Annebicque, Bruno Robert, Jean-Francois Henry, Jaona Randrianalisoa, and Catalin Popa. A multidisciplinary approach to improve energetic performance in smart buildings. *IFAC-PapersOnLine*, 49(27):313–317, 2016. IFAC Workshop on Control of Transmission and Distribution Smart Grids CTDSG 2016.
- [33] Ioana Udrea, Cristiana Croitoru, Ilinca Nastase, Ruxandra Crutescu, and Viorel Badescu. Thermal comfort in a romanian passive house. preliminary results. *Energy Procedia*, 85:575–583, 2016. EENVIRO-YRC 2015 - Bucharest.
- [34] Pamela Smith and Cristián Henríquez. Perception of thermal comfort in outdoor public spaces in the medium-sized city of Chillán, Chile, during a warm summer. *Urban Climate*, 30:100525, 2019.
- [35] M'sellem Houda, Alkama Djamel, and Labidi Fayçal. An assessment of thermal comfort and users' "perceptions" in office buildings - case of arid areas with hot and dry climate -. *Energy Procedia*, 74:243–250, 2015. The International Conference on Technologies and Materials for Renewable Energy, Environment and Sustainability –TMREES15.
- [36] Liping Wang, Paul Mathew, and Xiufeng Pang. Uncertainties in energy consumption introduced by building operations and weather for a medium-size office building. *Energy and Buildings*, 53:152–158, 10 2012.
- [37] Hugo Hens, Arnold Janssens, W. Depraetere, Jan Carmeliet, and J. Lecompte. Brick cavity walls: A performance analysis based on measurements and simulations. *Journal of Building Physics - J BUILD PHYS*, 31:95–124, 10 2007.
- [38] David Johnston, Dominic Miles-Shenton, and David Farmer. Quantifying the domestic building fabric 'performance gap'. *Building Services Engineering Research and Technology*, 36, 02 2015.

- [39] Lina La Fleur, Bahram Moshfegh, and Patrik Rohdin. Measured and predicted energy use and indoor climate before and after a major renovation of an apartment building in sweden. *Energy and Buildings*, 146, 04 2017.
- [40] Pieter de Wilde. The gap between predicted and measured energy performance of buildings: A framework for investigation. *Automation in Construction*, 41:40–49, 2014.
- [41] Davide Calì, Tanja Osterhage, Rita Streblow, and Dirk Müller. Energy performance gap in refurbished german dwellings: Lesson learned from a field test. *Energy and Buildings*, 127:1146–1158, 2016.
- [42] D. Majcen, L.C.M. Itard, and H. Visscher. Theoretical vs. actual energy consumption of labelled dwellings in the netherlands: Discrepancies and policy implications. *Energy Policy*, 54:125–136, 2013. Decades of Diesel.
- [43] IPEEC. Building energy performance gap issues - an international review, 2019.
- [44] Dorothée Charlier. Explaining the energy performance gap in buildings with a latent profile analysis. *Energy Policy*, 156:112480, 2021.
- [45] Wei Tian, Yeonsook Heo, Pieter de Wilde, Zhanyong Li, Da Yan, Cheol Soo Park, Xiaohang Feng, and Godfried Augenbroe. A review of uncertainty analysis in building energy assessment. *Renewable and Sustainable Energy Reviews*, 93:285–301, 2018.
- [46] Stefano Cozza, Jonathan Chambers, Arianna Brambilla, and Martin K. Patel. In search of optimal consumption: A review of causes and solutions to the energy performance gap in residential buildings. *Energy and Buildings*, 249:111253, 2021.
- [47] Stefano Cozza, Jonathan Chambers, Arianna Brambilla, and Martin K. Patel. In search of optimal consumption: A review of causes and solutions to the energy performance gap in residential buildings. *Energy and Buildings*, 249:111253, 2021.
- [48] Michaël Cohen. Epilog livrable n°2 rapport de synthèse sur la méthodologie employée avec tests sur cas d'étude théoriques par simulation, 2017.
- [49] Patrick Zou, Dipika Wagle, and Morshed Alam. Strategies for minimizing building energy performance gaps between the design intend and the reality. *Energy and Buildings*, 191, 03 2019.
- [50] Riad Ziour and Paul Calberg-Ellen. Mpeb: Les différentes configurations de mpeb, 2020.
- [51] ZeroCarbonHub. Closing the gap between design as-built performance - evidence review report, 2014.

- [52] Olivia Guerra Santin. Behavioural patterns and user profiles related to energy consumption for heating. *Energy and Buildings*, 43(10):2662–2672, 2011.
- [53] Fateh Bélaïd and Thomas Garcia. Understanding the spectrum of residential energy-saving behaviours: French evidence using disaggregated data. *Energy Economics*, 57, 05 2016.
- [54] Ian G. Hamilton, Philip J. Steadman, Harry Bruhns, Alex J. Summerfield, and Robert Lowe. Energy efficiency in the british housing stock: Energy demand and the homes energy efficiency database. *Energy Policy*, 60:462–480, 2013.
- [55] Salome Bakaloglou and Dorothée Charlier. Energy consumption in the french residential sector: How much do individual preferences matter? *The Energy Journal*, 40, 03 2018.
- [56] Adrienne Schmitz. *Multifamily Housing Development Handbook*. September 2000. Urban Land Institute.
- [57] European Commission. Eu buildings factsheets. https://ec.europa.eu/energy/eu-buildings-factsheets_en, 2018. Online; accessed on 2021-09-10.
- [58] ADEME. Chiffres clés, 2013.
- [59] PACTE. Analyse détaillée du parc résidentiel existant, 2017.
- [60] Huu Tam Nguyen, Fabrice Decellas, Bruno Duplessis, Philippe Rivière, and Dominique Marchio. Tertiary building stock modeling: Area determination by fusion of different datasets. *Journal of Physics: Conference Serie*, November 2019.
- [61] CEREMA. Consommation d'énergie dans les bâtiments – chiffres clés 2013. <http://reseaux-chaleur.cerema.fr/consommation-denergie-dans-les-batiments-chiffres-cles-2013>, 2014. Online; accessed on 2021-09-07.
- [62] Ministère de la Transition Ecologique. Bilan énergétique de la france pour 2019 - janvier 2021. <https://www.statistiques.developpement-durable.gouv.fr/edition-numerique/bilan-energetique-2019/pdf/document.pdf>, 2014. Online; accessed on 2021-09-12.
- [63] Republique Francaise. Diagnostic immobilier : diagnostic de performance énergétique (dpe). <https://www.service-public.fr/particuliers/vosdroits/F16096>, 2014. Online; accessed on 2021-09-07.
- [64] Aras Khazal and Ole Jakob Sønstebø. Valuation of energy performance certificates in the rental market – professionals vs. nonprofessionals. *Energy Policy*, 147:111830, 2020.

- [65] Franz Fuerst, Pat McAllister, Anupam Nanda, and Pete Wyatt. Energy performance ratings and house prices in wales: An empirical study. *Energy Policy*, 92:20–33, 2016.
- [66] Jenny von Platten, Carolina Holmberg, Mikael Mangold, Tim Johansson, and Kristina Mjörnell. The renewing of energy performance certificates—reaching comparability between decade-apart energy records. *Applied Energy*, 255:113902, 2019.
- [67] Stefano Cozza, Jonathan Chambers, Chirag Deb, Jean-Louis Scartezzini, Arno Schlüter, and Martin K. Patel. Do energy performance certificates allow reliable predictions of actual energy consumption and savings? learning from the swiss national database. *Energy and Buildings*, 224:110235, 2020.
- [68] Ciara Ahern and Brian Norton. Energy performance certification: Misassessment due to assuming default heat losses. *Energy and Buildings*, 224:110229, 2020.
- [69] Emmanuelle Cayrea, Benoit Allibea, Marie-Hélène Laurenta, and Dominique Ossoa. There are people in the house! how the results of purely technical analysis of residential energy consumption are misleading for energy policies, 2011.
- [70] Joana André Reis and Patrícia Escórcio. Energy certification in st. antónio (funchal) – statistical analysis. *Energy and Buildings*, 49:126–131, 2012.
- [71] Patrik Thollander, Magnus Karlsson, Patrik Rohdin, Johan Wollin, and Jakob Rosenqvist. Energy auditing 11. In Patrik Thollander, Magnus Karlsson, Patrik Rohdin, Johan Wollin, and Jakob Rosenqvist, editors, *Introduction to Industrial Energy Efficiency*, pages 61–87. Academic Press, 2020.
- [72] Amine Allouhi, Ali Boharb, Rahman Saidur, Tarik Kousksou, and Abdelmajid Jamil. 5.1 energy auditing. In Ibrahim Dincer, editor, *Comprehensive Energy Systems*, pages 1–44. Elsevier, Oxford, 2018.
- [73] Ana Rodriguez, Stefán Thor Smith, and Ben Potter. Sensitivity analysis for building energy audit calculation methods: Handling the uncertainties in small power load estimation. *Energy*, 238:121511, 2022.
- [74] Nicholas Long, Katherine Fleming, Christopher CaraDonna, and Cory Mosiman. Buildingsync: A schema for commercial building energy audit data exchange. *Developments in the Built Environment*, 7:100054, 2021.
- [75] Manexi and Ibtech. Garantie de performance énergétique principaux éléments de définition d’un protocole de mesure et vérification - tâche n°6.4, 2014.

- [76] Guarantee optimization in energy performance contracting with real option analysis. *Journal of Cleaner Production*, 258:120908, 2020.
- [77] Cx associates. Building measurement & verification. <https://www.cx-associates.com/building-mv>, 2020. Online; accessed on 2021-10-05.
- [78] Anne De Geeter and Anatole Boute. Directive 2006/32/ec on energy end-use efficiency and energy services: Realising the transition to sustainable energy markets? *Journal for European Environmental & Planning Law*, 3(5):414–431, 2006.
- [79] Efficiency Valuation Organization. *Protocole International de Mesure et de Vérification de la Performance énergétique*. September 2010.
- [80] Marc Agenis-Nevers, Yuqi Wang, Muriel Dugachard, Raphael Salvazet, Gwenaëlle Becker, and Damien Chenu. Measurement and verification for multiple buildings: An innovative baseline model selection framework applied to real energy performance contracts. *Energy and Buildings*, 249:111183, 2021.
- [81] Mingshun Zhang, Mujie Wang, Wei Jin, and Chun Xia-Bauer. Managing energy efficiency of buildings in china: A survey of energy performance contracting (epc) in building sector. *Energy Policy*, 114:13–21, 2018.
- [82] E.H. Borgstein, R. Lamberts, and J.L.M. Hensen. Evaluating energy performance in non-domestic buildings: A review. *Energy and Buildings*, 128:734–755, 2016.
- [83] Sullivan Royer, Stéphane Thil, Thierry Talbert, and Monique Polit. Black-box modeling of buildings thermal behavior using system identification. *IFAC Proceedings Volumes*, 47(3):10850–10855, 2014. 19th IFAC World Congress.
- [84] Harijaona Lalao Rakotoarison. *Méthode et outil de génération automatique de modèle pour l'optimisation fortement contrainte des microsystemes magnétiques.. Energie électrique*. phdthesis, Université Joseph-Fourier - Grenoble I, 2007.
- [85] Yanfei Li, Zheng O'Neill, Liang Zhang, Jianli Chen, Piljae Im, and Jason DeGraw. Grey-box modeling and application for building energy simulations - a critical review. *Renewable and Sustainable Energy Reviews*, 146:111174, 2021.
- [86] Gaby Baasch, Paul Westermann, and Ralph Evins. Identifying whole-building heat loss coefficient from heterogeneous sensor data: An empirical survey of gray and black box approaches. *Energy and Buildings*, 241:110889, 2021.

- [87] Christian Ankerstjerne Thilker, Peder Bacher, Hjörleifur G. Bergsteinsson, Rune Grønborg Junker, Davide Cali, and Henrik Madsen. Non-linear grey-box modelling for heat dynamics of buildings. *Energy and Buildings*, 252:111457, 2021.
- [88] Nelson Fumo. A review on the basics of building energy estimation. *Renewable and Sustainable Energy Reviews*, 31:53–60, 2014.
- [89] Daniel Coakley, Paul Raftery, and Marcus Keane. A review of methods to match building energy simulation models to measured data. *Renewable and Sustainable Energy Reviews*, 37:123–141, 09 2014.
- [90] Clara Spitz. *Analyse de la fiabilité des outils de simulation et des incertitudes de métrologie appliquée à l'efficacité énergétique des bâtiments*. phdthesis, Université de Grenoble, 2012.
- [91] Sandra Martínez, Aitor Erkoreka, Pablo Eguía, Enrique Granada, and Lara Febrero. Energy characterization of a paslink test cell with a gravel covered roof using a novel methodology: Sensitivity analysis and bayesian calibration. *Journal of Building Engineering*, 22:1–11, 2019.
- [92] G. Allesina, E. Mussatti, F. Ferrari, and A. Muscio. A calibration methodology for building dynamic models based on data collected through survey and billings. *Energy and Buildings*, 158:406–416, 2018.
- [93] Xin Liang, Tianzhen Hong, and Geoffrey Qiping Shen. Improving the accuracy of energy baseline models for commercial buildings with occupancy data. *Applied Energy*, 179:247–260, 2016.
- [94] Hai xiang Zhao and Frédéric Magoulès. A review on the prediction of building energy consumption. *Renewable and Sustainable Energy Reviews*, 16(6):3586–3592, 2012.
- [95] Liang Zhang, Jin Wen, Yanfei Li, Jianli Chen, Yunyang Ye, Yangyang Fu, and William Livingood. A review of machine learning in building load prediction. *Applied Energy*, 285:116452, 2021.
- [96] Yong Zhou, Yanfeng Liu, Dengjia Wang, and Xiaojun Liu. Comparison of machine-learning models for predicting short-term building heating load using operational parameters. *Energy and Buildings*, 253:111505, 2021.
- [97] R.K. Veiga, A.C. Veloso, A.P. Melo, and R. Lamberts. Application of machine learning to estimate building energy use intensities. *Energy and Buildings*, 249:111219, 2021.

- [98] H. Han, B. Gu, T. Wang, and Z.R. Li. Important sensors for chiller fault detection and diagnosis (fdd) from the perspective of feature selection and machine learning. *International Journal of Refrigeration*, 34(2):586–599, 2011.
- [99] Baojie Li, Claude Delpha, Anne Migan-Dubois, and Demba Diallo. Fault diagnosis of photovoltaic panels using full i–v characteristics and machine learning techniques. *Energy Conversion and Management*, 248:114785, 2021.
- [100] Saman Taheri, Amirhossein Ahmadi, Behnam Mohammadi-Ivatloo, and Somayeh Asadi. Fault detection diagnostic for hvac systems via deep learning algorithms. *Energy and Buildings*, 250:111275, 2021.
- [101] Zhe Wang, Tianzhen Hong, Mary Ann Piette, and Marco Pritoni. Inferring occupant counts from wi-fi data in buildings through machine learning. *Building and Environment*, 158:281–294, 2019.
- [102] Yuan Jin, Da Yan, Xuyuan Kang, Adrian Chong, Hongsan-Sun, and Sicheng Zhan. Forecasting building occupancy: A temporal-sequential analysis and machine learning integrated approach. *Energy and Buildings*, 252:111362, 2021.
- [103] Huynh Phan, Thomas Recht, Laurent Mora, and Stéphane Ploix. Consequences-based graphical model for contextualized occupant activities estimation in connected buildings. In *Building Simulation 2021 Conference*. BS2021, 2021.
- [104] Shiyu Yang, Man Pun Wan, Wanyu Chen, Bing Feng Ng, and Swapnil Dubey. Experiment study of machine-learning-based approximate model predictive control for energy-efficient building control. *Applied Energy*, 288:116648, 2021.
- [105] Zachary E. Lee and K. Max Zhang. Generalized reinforcement learning for building control using behavioral cloning. *Applied Energy*, 304:117602, 2021.
- [106] Razak Olu-Ajayi, Hafiz Alaka, Ismail Sulaimon, Funlade Sunmola, and Saheed Ajayi. Building energy consumption prediction for residential buildings using deep learning and other machine learning techniques. *Journal of Building Engineering*, page 103406, 2021.
- [107] Zhengwei Li, Yanmin Han, and Peng Xu. Methods for benchmarking building energy consumption against its past or intended performance: An overview. *Applied Energy*, 124:325–334, 2014.
- [108] Benedetto Grillone, Stoyan Danov, Andreas Sumper, Jordi Cipriano, and Gerard Mor. A review of deterministic and data-driven methods to quantify energy efficiency savings and

- to predict retrofitting scenarios in buildings. *Renewable and Sustainable Energy Reviews*, 131:110027, 2020.
- [109] Edward Borgstein, Roberto Lamberts, and Jan Hensen. Evaluating energy performance in non-domestic buildings: A review. *Energy and Buildings*, 128, 07 2016.
- [110] Staf Roels. Ebc annex 58 project summary report, 2017.
- [111] Phillip Biddulph, Virginia Gori, Clifford A. Elwell, Cameron Scott, Caroline Rye, Robert Lowe, and Tadj Oreszczyn. Inferring the thermal resistance and effective thermal mass of a wall using frequent temperature and heat flux measurements. *Energy and Buildings*, 78:10–16, 2014.
- [112] Thanh-Tung Ha, Vincent Feuillet, Julien Waeytens, Kamel Zibouche, Simon Thébault, Rémi Bouchie, Véronique Le Sant, and Laurent Ibos. Benchmark of identification methods for the estimation of building wall thermal resistance using active method: Numerical study for iwi and single-wall structures. *Energy and Buildings*, 224:110130, 2020.
- [113] Aimee Byrne, Gerard Byrne, Anna Davies, and Anthony James Robinson. Transient and quasi-steady thermal behaviour of a building envelope due to retrofitted cavity wall and ceiling insulation. *Energy and Buildings*, 61:356–365, 2013.
- [114] Lia De Simon, Marco Iglesias, Benjamin Jones, and Christopher Wood. Quantifying uncertainty in thermophysical properties of walls by means of bayesian inversion. *Energy and Buildings*, 177:220–245, 2018.
- [115] Emilio Sassine. A practical method for in-situ thermal characterization of walls. *Case Studies in Thermal Engineering*, 8:84–93, 2016.
- [116] David Farmer, Chris Gorse, William Swan, Richard Fitton, Matthew Brooke-Peat, Dominic Miles-Shenton, and David Johnston. Measuring thermal performance in steady-state conditions at each stage of a full fabric retrofit to a solid wall dwelling. *Energy and Buildings*, 156:404–414, 2017.
- [117] C. Deb, L.V. Gelder, M. Spiekman, Guillaume Pandraud, R. Jack, and R. Fitton. Measuring the heat transfer coefficient (htc) in buildings: A stakeholder’s survey. *Renewable and Sustainable Energy Reviews*, 144:111008, 2021.
- [118] C.A. Balaras and A.A. Argiriou. Infrared thermography for building diagnostics. *Energy and Buildings*, 34(2):171–183, 2002. TOBUS - a European method and software for office building refurbishment.

- [119] Itai Danielski and Morgan Fröling. Diagnosis of buildings' thermal performance - a quantitative method using thermography under non-steady state heat flow. *Energy Procedia*, 83:320–329, 2015. Sustainability in Energy and Buildings: Proceedings of the 7th International Conference SEB-15.
- [120] Xiaofeng Zheng, Joe Mazzon, Ian Wallis, and Christopher J. Wood. Airtightness measurement of an outdoor chamber using the pulse and blower door methods under various wind and leakage scenarios. *Building and Environment*, 179:106950, 2020.
- [121] BOUCHIE Rémi and IBOS Laurent. Mpeb: Inventaire des méthodes applicables à la caractérisation de la performance énergétique de l'enveloppe, 2020.
- [122] Simon Romain Thébault. *Contribution à l'évaluation in situ des performances d'isolation thermique de l'enveloppe des bâtiments*. Theses, Université de Lyon, January 2017.
- [123] Rémi Bouchié, Florent Alzetto, Adrien Brun, caroline weeks, Mathew Preece, Muhammad Ahmad, and Mario Sisinni. Methodologies for the assessment of intrinsic energy performance of buildings' envelop. 03 2015.
- [124] Simon Rouchier, Maria José Jiménez, and Sergio Castaño. Sequential monte carlo for on-line parameter estimation of a lumped building energy model. *Energy and Buildings*, 187:86–94, 2019.
- [125] María José Jiménez. Reliable building energy performance characterisation based on full scale dynamic measurements - report of subtask 3, part 1: Thermal performance characterization based on full scale testing - description of the common exercises and physical guidelines, 2016.
- [126] Díaz-Hernández, Torres-Hernández, Karla Maria Castro, Macias-Melo, and María José Jiménez. Data-based rc dynamic modelling incorporating physical criteria to obtain the hlc of in-use buildings: Application to a case study. *Energies*, 13:313, 01 2020.
- [127] Simon Rouchier, Mickaël Rabouille, and Pierre Oberlé. Calibration of simplified building energy models for parameter estimation and forecasting: Stochastic versus deterministic modelling. *Building and Environment*, 134:181–190, 2018.
- [128] Marieline Senave, Staf Roels, Stijn Verbeke, Evi Lambie, and Dirk Saelens. Sensitivity of characterizing the heat loss coefficient through on-board monitoring: A case study analysis. *Energies*, 12:3322, 08 2019.

- [129] International Energy Agency. Annex 71 - building energy performance assessment based on in-situ measurements. <https://iea-ebc.org/projects/project?AnnexID=71>, 2021. Online; accessed on 2021-10-12.
- [130] Richard Klosterman. Simple and complex models. *Environment and Planning B: Planning and Design*, 39, 01 2012.
- [131] Sophia Krause and Kai-Uwe Goss. Comparison of a simple and a complex model for bcf prediction using in vitro biotransformation data. *Chemosphere*, 256:127048, 2020.
- [132] F. Reventos. 3 - parameters and concepts. In Francesco D’Auria, editor, *Thermal-Hydraulics of Water Cooled Nuclear Reactors*, pages 89–141. Woodhead Publishing, 2017.
- [133] Kailai Xu and Eric Darve. Solving inverse problems in stochastic models using deep neural networks and adversarial training. *Computer Methods in Applied Mechanics and Engineering*, 384:113976, 2021.
- [134] J.L. Fernández-Martínez, Z. Fernández-Muñiz, J.L.G. Pallero, and L.M. Pedruelo-González. From bayes to tarantola: New insights to understand uncertainty in inverse problems. *Journal of Applied Geophysics*, 98:62–72, 2013.
- [135] Simon Rouchier. Solving inverse problems in building physics: An overview of guidelines for a careful and optimal use of data. *Energy and Buildings*, 166:178–195, 2018.
- [136] Henrik Madsen, Peder Bacher, Geert Bauwens, An-Heleen Deconinck, Glenn Reynders, Staf Roels, Eline Himpe, and Guillaume Lethé. Thermal performance characterization using time series data; IEA EBC Annex 58 guidelines, 12 2015.
- [137] Staf Roels, Peder Bacher, Geert Bauwens, Sergio Castaño, María José Jiménez, and Henrik Madsen. On site characterisation of the overall heat loss coefficient: Comparison of different assessment methods by a blind validation exercise on a round robin test box. *Energy and Buildings*, 153, 08 2017.
- [138] Staf Roels, Peder Bacher, Geert Bauwens, Henrik Madsen, and María José Jiménez. Characterising the actual thermal performance of buildings: Current results of common exercises performed in the framework of the IEA EBC Annex 58-project. *Energy Procedia*, 78:3282–3287, 2015. 6th International Building Physics Conference, IBPC 2015.
- [139] Irati Uriarte, Aitor Erkoreka, Catalina Giraldo-Soto, Koldo Martín, Amaia Uriarte, and Pablo Eguía. Mathematical development of an average method for estimating the

- reduction of the heat loss coefficient of an energetically retrofitted occupied office building. *Energy and Buildings*, 192:101–122, 2019.
- [140] Irati Uriarte, Aitor Erkoreka, Asier Legorburu, Koldo Martin-Escudero, Catalina Giraldo-Soto, and Moises Odriozola-Maritorena. Decoupling the heat loss coefficient of an in-use office building into its transmission and infiltration heat loss coefficients. *Journal of Building Engineering*, 43:102591, 2021.
- [141] Catalina Giraldo Soto. *Optimized monitoring techniques and data analysis development for in-situ characterization of the building envelope’s real energetic behaviour*. phdthesis, Université de Bordeaux and Universidad del País Vasco, 2021.
- [142] Geert Bauwens and Staf Roels. Co-heating test: A state-of-the-art. *Energy and Buildings*, 82:163–172, 2014.
- [143] Jez Wingfield. Whole house heat loss test method (coheating), 2010.
- [144] R. J. Lowe, J. Wingfield, M. Bell, , and J. M. Bell. Evidence for heat losses via party wall cavities in masonry construction. *Building Services Engineering Research and Technology*, 28:161–181, 2007.
- [145] M. Bell, J. Wingfield, and D. Miles-Shenton. Low carbon housing: Lessons from elm tree mews technical report, 2010.
- [146] G. Bauwens, P. Standaert, F. Delcuve, and S. Roels. Reliability of co-heating measurements first building simulation and optimization conference, ibpsa. In *Building Simulation 2021 Conference*. First Building Simulation and Optimization Conference, IBPSA, 2012.
- [147] Chadia Zayane. *Identification d’un modèle de comportement thermique de bâtiment à partir de sa courbe de charge*. Theses, École Nationale Supérieure des Mines de Paris, January 2011. Co-encadrement de la thèse : Laurent Praly.
- [148] Gustav Nordström, Helena Johnsson, and Sofia Lidelöw. *Using the Energy Signature Method to Estimate the Effective U-Value of Buildings*, volume 22, pages 35–44. 01 2013.
- [149] Guiavarch A., Peuportier B., and Lokhat I. Epilog livrable n°2 rapport de synthèse sur le retour d’expérience, l’état de l’art et étude de marché, 2017.
- [150] Cristian Ghiaus. Experimental estimation of building energy performance by robust regression. *Energy and Buildings*, 38(6):582–587, 2006.
- [151] Moving-average model. https://en.wikipedia.org/wiki/Moving-average_model, 2020. Online; accessed on 2021-10-27.

- [152] Neil J. Salkind. Covariate - encyclopedia of research design. <https://methods.sagepub.com/reference/encyc-of-research-design/n85.xml>, 2010. Online; accessed on 2021-10-27.
- [153] The arimax model muddle. <https://robjhyndman.com/hyndsight/arimax/>, 2010. Online; accessed on 2021-10-27.
- [154] Jonathan R. Partington. *Linear Operators and Linear Systems: An Analytical Approach to Control Theory*. London Mathematical Society Student Texts. Cambridge University Press, 2004.
- [155] M.J. Jiménez and M.R. Heras. Application of multi-output arx models for estimation of the u and g values of building components in outdoor testing. *Solar Energy*, 79(3):302–310, 2005.
- [156] M.J. Jiménez, H. Madsen, and K.K. Andersen. Identification of the main thermal characteristics of building components using matlab. *Building and Environment*, 43(2):170–180, 2008. Outdoor Testing, Analysis and Modelling of Building Components.
- [157] D. Rowell. 2 . 14 analysis and design of feedback control systems state-space representation of lti systems. 2002.
- [158] B. Peuportier and I. Blanc Sommereux. *Comfie, Passive solar design tool for multizone buildings*. 1994. Centre énergétique, Ecole des Mines de Paris, Version 3.
- [159] Shengwei Wang and Xinhua Xu. Parameter estimation of internal thermal mass of building dynamic models using genetic algorithm. *Energy Conversion and Management*, 47(13):1927–1941, 2006.
- [160] Zequn Wang, Yuxiang Chen, and Yong Li. Development of rc model for thermal dynamic analysis of buildings through model structure simplification. *Energy and Buildings*, 195, 05 2019.
- [161] Hugo Viot. *Modélisation et instrumentation d'un bâtiment et de ses systèmes pour optimiser sa gestion énergétique*. phdthesis, Université de Bordeaux, November 2016.
- [162] H. Madsen and J. Holst. Estimation of continuous-time models for the heat dynamics of a building. *Energy and Buildings*, 22(1):67–79, 1995.
- [163] Andreas Raue, Clemens Kreutz, Thomas Maiwald, J. Bachmann, Marcel Schilling, Ursula Klingmüller, and Jens Timmer. Structural and practical identifiability analysis of

- partially observed dynamical models by exploiting the profile likelihood. *Bioinformatics*, 25:1923–1929, 06 2013.
- [164] Peder Bacher and Henrik Madsen. Identifying suitable models for the heat dynamics of buildings. *Energy and Buildings*, 43(7):1511–1522, 2011.
- [165] Zequn Wang, Yuxiang Chen, and Yong Li. Development of rc model for thermal dynamic analysis of buildings through model structure simplification. *Energy and Buildings*, 195:51–67, 2019.
- [166] Klaus Kaae Andersen, Henrik Madsen, and Lars H. Hansen. Modelling the heat dynamics of a building using stochastic differential equations. *Energy and Buildings*, 31(1):13–24, 2000.
- [167] Niels Rode Kristensen, Henrik Madsen, and Sten Bay Jørgensen. Parameter estimation in stochastic grey-box models. *Automatica*, 40(2):225–237, 2004.
- [168] Florent Alzetto, Guillaume Pandraud, Richard Fitton, Ingo Heusler, and Herbert Sinnesbichler. Qub: A fast dynamic method for in-situ measurement of the whole building heat loss. *Energy and Buildings*, 174:124–133, 09 2018.
- [169] Wu Xining. Evaluation de la performance intrinsèque de logements." département génie énergétique et environnement, 2017.
- [170] Florent Alzetto, Johann Meulemans, Guillaume Pandraud, and Didier Roux. A perturbation method to estimate building thermal performance. *Comptes Rendus Chimie*, 21(10):938–942, 2018. The power of synthesis towards new materials. Joint Symposium of the National Academy of Sciences Leopoldina and the “Académie des Sciences”, Paris Halle (Saale), Germany, 23 & 24 November 2017.
- [171] Eric Mangematin, Guillaume Pandraud, and Didier Roux. Quick measurements of energy efficiency of buildings. *Comptes Rendus Physique*, 13:383–390, 05 2012.
- [172] Agence Qualite Construction PACTE. Epilog - evaluation de la performance intrinsèque de logements. <http://www.programmepacte.fr/epilog-evaluation-de-la-performance-intrinseque-de-logements>, 2017. Online; accessed on 2018-09-23.
- [173] Lorena de Carvalho Araujo. Study of a methodology for measuring the energy performance of building. master’s thesis in the master’s program energy - psl research university, 2018.

- [174] Rémi Bouchié, Florent Alzetto, Adrien Brun, Pierre Boisson, and Simon Thébault. Short methodologies for in-situ assessment of the intrinsic thermal performance of the building envelope. 10 2014.
- [175] P. Schetelat et R. Bouchié. Isabelle : a method for performance assessment at acceptance stage using bayesian calibration. *System Simulation in Buildings*, pages 594–608 (P34), 2014. 9th International Conference on System Simulation in Buildings - SSB2014.
- [176] Rémi Bouchie, Arnaud Challansonnex, Fadi Lahlou, Pierre Oberlé, Mickael Rabouille, and Patrick Schalbart. Livrable serene n°1.1.a. méthode combinée epilog/isabele v0 de mesure de la performance énergétique intrinsèque de l'enveloppe - cas des maisons individuelles rénovées, 2019.
- [177] Simon Thébault and Rémi Bouchié. Estimating infiltration losses for in-situ measurements of the building envelope thermal performance. *Energy Procedia*, 78:1756–1761, 2015. 6th International Building Physics Conference, IBPC 2015.
- [178] Simon Thébault. and Rémi Bouchié. Refinement of the isabele method regarding uncertainty quantification and thermal dynamics modelling. *Energy and Buildings*, 178:182–205, 2018.
- [179] Rune Juhl, Jan Møller, and Henrik Madsen. ctsmr - continuous time stochastic modeling in r. 06 2016.
- [180] Beñat Arregi and Roberto Garay. Regression analysis of the energy consumption of tertiary buildings. *Energy Procedia*, 122:9–14, 2017. CISBAT 2017 International Conference Future Buildings & Districts – Energy Efficiency from Nano to Urban Scale.
- [181] Myriam Humbert, Constance Lancelle, Jean-Alain Bouchet, and Bassam Moujalled. Bâtiments démonstrateurs prebat : retour d'expérience et premiers enseignements sur la performance réelle et sur les écarts calcul/mesure. 05 2018.
- [182] Julien Berger, Sihem Guernouti, and Myriam Humbert. Experimental method to determine the energy envelope performance of buildings. 01 2010.
- [183] Emma Brycke and Nilssen Jannicke. Assessment of co-heating test: A practical method to evaluate the in-situ heat transfer coefficient in dwellings. master's thesis in the master's program structural engineering and building technology, 2015.
- [184] Johann Meulemans. An assessment of the qub/e method for fast in situ measurements of the thermal performance of building fabrics in cold climates. 03 2018.

- [185] Simon Thébault, Alexis Puysilloux, and Rémi Bouchié. Merlin: Livrable n°3: Etude de faisabilité: Méthode et protocole de mesure de l'isolation thermique de l'enveloppe à réception des travaux en logement collectif, 2019.
- [186] Khee Lam, Michael Hoeynck, Bing Dong, Burton Andrews, Yun-Shang Chiou, Rui Zhang, Diego Benitez, and Joon-Ho Choi. Occupancy detection through an extensive environmental sensor network in an open-plan office building. *IBPSA 2009 - International Building Performance Simulation Association 2009*, January 2009.
- [187] Jinwoo Kim, Kyungjun Min, Minhyuk Jung, and Seokho Chi. Occupant behavior monitoring and emergency event detection in single-person households using deep learning-based sound recognition. *Building and Environment*, 181:107092, August 2020.
- [188] Sajad M. R. Khani, Fariborz Haghighat, Karthik Panchabikesan, and Milad Ashouri. Extracting energy-related knowledge from mining occupants' behavioral data in residential buildings. *Journal of Building Engineering*, 39:102319, July 2021.
- [189] Shuo Chen, Guomin Zhang, Xiaobo Xia, Yixing Chen, Sujeeva Setunge, and Long Shi. The impacts of occupant behavior on building energy consumption: A review. *Sustainable Energy Technologies and Assessments*, 45:101212, June 2021.
- [190] Saba Akbari and Fariborz Haghighat. Occupancy and occupant activity drivers of energy consumption in residential buildings. *Energy and Buildings*, 250:111303, November 2021.
- [191] H.P. Díaz-Hernández, M.N. Sánchez, R. Olmedo, M.M. Villar-Ramos, E.V. Macias-Melo, K.M. Aguilar-Castro, and M.J. Jiménez. Performance assessment of different measured variables from onboard monitoring system to obtain the occupancy patterns of rooms in an office building. *Journal of Building Engineering*, 40:102676, 2021.
- [192] Ron Gagnier. Follow the recipe. <https://www.uxmatters.com/mt/archives/2009/05/follow-the-recipe.php>, 2009. Online; accessed on 2021-10-05.
- [193] Technopedia. Protocol. <https://www.techopedia.com/definition/4528/protocol>, 2020. Online; accessed on 2021-10-10.
- [194] Medicine Libretexts. 3.3: The digestion and absorption process. [https://med.libretexts.org/Courses/American_Public_University/APU%3A_Basic_Foundation_of_Nutrition_for_Sports_Performance_\(Byerley\)/03%3A_Digestion_and_Absorption/3.3%3A_The_Digestion_and_Absorption_Process](https://med.libretexts.org/Courses/American_Public_University/APU%3A_Basic_Foundation_of_Nutrition_for_Sports_Performance_(Byerley)/03%3A_Digestion_and_Absorption/3.3%3A_The_Digestion_and_Absorption_Process), 2020. Online; accessed on 2021-10-12.

- [195] Richard Fitton. Annex 71 - building energy performance assessment based on in-situ measurements: Challenges and general framework, 2021.
- [196] Data pre-processing. https://en.wikipedia.org/wiki/Data_pre-processing, 2021. Online; accessed on 2021-10-27.
- [197] David Hestenes. Modeling methodology for physics teachers. 399, 03 1997.
- [198] Andrew Ford. *Modeling the Environment*. Island Press, Washington D.C, 2009. (2nd edition).
- [199] Morgane Pouzet, Pauline Perdrix, Frédéric Bougrain, Myriam Humbert, and Sihame Hini. Livrable sereine - analyse technico-économique du dispositif sereine orientations souhaitables suite à la filière mesure du niveau d'isolation thermique, 2021.
- [200] Conseils thermiques. Les radiateurs électriques. https://conseils-thermiques.org/contenu/chauffage_electrique.php, 2020. Online; accessed on 2021-10-12.
- [201] Rémi Bouchié, Stéphanie Derouineau, Charlotte Abele, and Jean-Robert Millet. Conception et validation d'un capteur de mesurage de la température extérieure équivalente d'une paroi opaque d'un bâtiment. *Sartori*, pages 1–8, 2014. Conférence IBPSA France-Arras.
- [202] CSTB. Sereine - solution d'évaluation de la performance énergétique intrinsèque - formation à l'outil numérique, 7 2020.
- [203] Continuous time stochastic modelling - ctsm 2.3 - mathematics guide. Technical report, Technical University of Denmark, December 2003.
- [204] loïc Raillon, Simon Rouchier, and Sarah Juricic. pysip: an open-source tool for bayesian inference and prediction of heat transfer in buildings. 01 2020.
- [205] Loïc Raillon and Maxime Janvier. locie/pysip. <https://github.com/locie/pySIP>, 2020. Online; accessed on 2021-10-15.
- [206] JCGM. Evaluation of measurement data — guide to the expression of uncertainty in measurement, 2008.
- [207] SALib. Source code for salib.sample.sobol_sequence. https://salib.readthedocs.io/en/latest/_modules/SALib/sample/sobol_sequence.html, 2021. Online; accessed on 2021-11-22.

- [208] Simon Thébault, Lorena de Carvalho Araujo, Arnaud Challansonnex, and Fadi Lahlou. Sereine livrable n°1.2.a: Spécification des travaux pour la conception de la méthode sereine de mesure de la performance énergétique intrinsèque de l'enveloppe - cas des logements collectifs rénovés, 2020.
- [209] Performance thermique des bâtiments - Détermination de la perméabilité à l'air des bâtiments - Méthode de pressurisation par ventilateur. Standard, Normes Francaises et Européennes, France, October 2015.
- [210] Min-Hwi Kim, Jae-Hun Jo, and Jae-Weon Jeong. Feasibility of building envelope air leakage measurement using combination of air-handler and blower door. *Energy and Buildings*, 62:436–441, 2013.
- [211] Catalina Giraldo Soto, Irati Uriarte, A. Erkoreka, J.M. Sala, and Pablo Eguía. Applying the decay method to the co₂ produced by occupants for decoupling the heat loss coefficient of an in-use office building. 07 2017.
- [212] Andrade Morettin Arquitetos. Edifício marcos lopes. <https://www.andrademorettin.com.br/projetos/edificio-rua-marcos-lopes/>, 2010. Online; accessed on 2021-11-2.
- [213] Eline Himpea and Arnold Janssens. Characterisation of the thermal performance of a test house based on dynamic measurements. *Energy Procedia*, 78:3294–3299, 2015. 6th International Building Physics Conference, IBPC 2015.
- [214] Simon Moeller, Ines Weber, Franz Schröder, Amelie Bauer, and Hannes Harter. Apartment related energy performance gap – how to address internal heat transfers in multi-apartment buildings. *Energy and Buildings*, 215:109887, 2020.
- [215] Matthieu Cavallo. Thèse professionnelle - quel est l'impact des transferts thermiques sur la performance énergétique entre zone de jour et zone de nuit d'un même logement ou entre logements d'un bâtiment collectif?, 2020.
- [216] Marieline Senave, Staf Roels, Glenn Reynders, Stijn Verbeke, and Dirk Saelens. Assessment of data analysis methods to identify the heat loss coefficient from on-board monitoring data. *Energy and Buildings*, 209:109706, 12 2019.
- [217] République Française. Journal officiel électronique authentifié n° 0087 du 13/04/2021. <https://www.legifrance.gouv.fr/download/pdf?id=doxMrRrOwbfJVvtWjfdP4qE7zNsiFZL-4wqNyqoY-CA=>, 2021. Online; accessed on 2021-11-22.

- [218] AFOC du groupe Arcade. Chauffage collectif : les compteurs individuels, c'est pour quand ? vraiment une économie ? <http://afoc-locataires-arcade.eklablog.fr/chauffage-collectif-les-compteurs-individuels-c-est-pour-quand-vraimen-a129575726>, 2020. Online; accessed on 2021-11-2.
- [219] Simon Thébault, Lorena de Carvalho Araujo, and Arnaud Jay. Livrable n°1.2.b - méthode et protocole serene v1.0 de mesure de la performance énergétique intrinsèque de l'enveloppe - cas des logements collectifs rénovés, 2020.
- [220] Soukayna Berrabah, Zineb Bouhssine, Anas El Maakoul, Alain Degiovanni, and Mohamed Bakhouya. Towards a quadrupole-based method for buildings simulation: Validation with ashrae 140 standard. *Thermal Science and Engineering Progress*, page 101069, 2021.
- [221] T. Soubdhan, T.A. Mara, H. Boyer, and A. Younes. Chapter 376 - use of bestest procedure to improve a building thermal simulation program. In A.A.M. Sayigh, editor, *World Renewable Energy Congress VI*, pages 1800–1803. Pergamon, Oxford, 2000.
- [222] 96/04289 using the building energy simulation test (bestest) to evaluate chenath, the national house energy rating scheme simulation engine. *Fuel and Energy Abstracts*, 37(4):297, 1996.
- [223] Søren Østergaard Jensen. Validation of building energy simulation programs: a methodology. *Energy and Buildings*, 22(2):133–144, 1995.
- [224] Bruno Peuportier and Isabelle Blanc Sommereux. Simulation tool with its expert interface for the thermal design of multizone buildings. *International Journal of Solar Energy*, 8:109–120, 01 1990.
- [225] ARMINES. Les centres de recherche énergétique et génie des procédés. <https://armines.net/fr/centres-de-recherche-departements-thematiques/%C3%A9nerg%C3%A9tique-et-g%C3%A9nie-des-proc%C3%A9d%C3%A9s>. Online; accessed on 2021-10-28.
- [226] IZUBA énergies. Optimisation énergétique et environnementale dans le secteur du bâtiment. <https://www.izuba.fr/>, 2020. Online; accessed on 2021-10-28.
- [227] Thomas Recht, Jeanne Goffart, Laurent Mora, Monika Woloszyn, and Buhe Catherine. Méthodologie pour la comparaison des performances simulées et mesurées de maisons « à énergie positive ». 05 2018.
- [228] François Leconte. Validation empirique du logiciel pleiades+comfie dans le cas de bâtiments passifs – étude préliminaire : Analyses d'incertitudes et de sensibilité, 2010.

- [229] Adrien Brun, Clara Spitz, Etienne Wurtz, and Laurent Mora. Behavioural comparison of some predictive tools used in a low-energy building. 07 2009.
- [230] PACTE. Analyse détaillée du parc résidentiel existant, 2017.
- [231] La cartographie des actions et des réalisations remarquables. Résidence vignette figuière - feyzin. <https://carto.infoenergie69-grandlyon.org/projet/residence-vignette-figuiere/>, 2020. Online; accessed on 2021-10-27.
- [232] ADEME. Enquête tremi – travaux de rénovation énergétique des maisons individuelles - campagne 2017., 2018.
- [233] CSTB. Règles th-u – fascicule 5/5 – ponts thermiques. réglementation thermique des bâtiments existants, 2007.
- [234] Cahier d’algorithmes de comfie. Technical report, IZUBA, 2014.
- [235] Sarah Juricic, Jeanne Goffart, Simon Rouchier, Aurélie Fouquier, Nicolas Cellier, and Gilles Fraisse. Influence of natural weather variability on the thermal characterisation of a building envelope. *Applied Energy*, 288:116582, 2021.
- [236] Simon Thébault, Arnaud Jay, Mickael Cohen, Hugo Coulandreau, Simon Rouchier, Auline Rodler, and Sihem Guernouti. Annexe au livrable n°1.2.c travaux d’avancements sur la méthode et protocole sereine optimisés de mesure de la performance énergétique intrinsèque de l’enveloppe cas des logements collectifs rénovés, 2021.
- [237] University of Siegen. Heating systems. <http://nesa1.uni-siegen.de/wwwextern/idea/keytopic/10.htm>, 2002. Online; accessed on 2021-11-9.
- [238] Sarah Olei Cerema. L’enquête nationale logement (enl). <http://outil2amenagement.cerema.fr/1-enquete-nationale-logement-enl-r789.html>, 2020. Online; accessed on 2021-12-22.
- [239] Institut National de la Statistique et des Etudes Economiques. Enquête logement. <https://www.insee.fr/fr/metadonnees/source/serie/s1004>, 2021. Online; accessed on 2021-11-15.
- [240] Ministère de la Transition Ecologique. Enquête performance de l’habitat, Équipements, besoins et usages de l’énergie (phébus). <https://www.statistiques.developpement-durable.gouv.fr/enquete-performance-de-lhabitat-equipements-besoins-et-usages-de-lenergie-phebus>, 2018. Online; accessed on 2021-11-15.

- [241] Fireplace universe. Can a wood stove heat a whole house? <https://fireplaceuniverse.com/can-a-wood-stove-heat-a-whole-house/>, 2020. Online; accessed on 2021-11-15.
- [242] Mirco Andreotti, Dario Bottino-Leone, Marta Calzolari, Pietromaria Davoli, Luisa Dias Pereira, Elena Lucchi, and Alexandra Troi. Applied research of the hygrothermal behaviour of an internally insulated historic wall without vapour barrier: In situ measurements and dynamic simulations. *Energies*, 13(13), 2020.
- [243] Ghjuvan Faggianelli, Laurent Mora, and Rania Merheb. Uncertainty quantification for energy savings performance contracting: Application to an office building. *Energy and Buildings*, 152, 07 2017.
- [244] Clara Spitz, Monika Woloszyn, Catherine Buhé, and Mathieu Labat. Simulating combined heat and moisture transfer with energyplus: an uncertainty study and comparison with experimental data. In *Building Simulation 2013 Conference*. BS2013, 2013.
- [245] Clara Spitz, Laurent Mora, Etienne Wurtz, and Arnaud Jay. Practical application of uncertainty analysis and sensitivity analysis on an experimental house. *Energy and Buildings*, 55:459–470, 2012.
- [246] Arnaud JAY. Mesure fluxmétrique : homogénéité - essais héios 2086. Réunion d’avancement SEREINE, 3 2021.

Annexes

Contents

A.	Input files from SEREINE method	223
B.	Building components of Pléiades Comfie model	228

A. Input files from SEREINE method

An example of the input files used in the SEREINE method are presented in this annex. The files formats and configurations are under modification inside the SEREINE project and here there are the version applied in 2021. Figures A.1 to A.4 are part of the same excel file describing the building characteristics. The json file describing the experiment is presented in figure A.5. The yml file with the configuration of the estimation process is presented in figure A.6. The time series data from the weather station and the sensor is presented in figures A.7 and A.8.

No	Name	Surface (m ²)	Inclination	If other inclination in ° (0 = horizontal, 90 = vertical)	Orientation	U- value (W/m ² /K), if known	Insulation thickness (cm), if known	Associated sensor	Sensor number	Kit number
1	Ceiling	23.64	horizontal		Any (horizontal)	4.0		SENS sensor	5	13
2	West facade	9.27	vertical		West	3.3		SENS sensor	2	13
3	Sud facade	18.03	vertical		South	2.9		SENS sensor	6	13

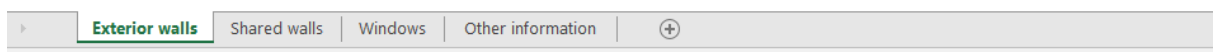


Figure A.1 – Description of the building: excel sheet tab of exterior walls.

No	Name	Surface (m ²)	Inclination	Orientation	U- value (W/m ² /K), if known	Insulation thickness (cm), if known	Associated sensor	Sensor number	Kit number
1	Intermediate floor - office	13.98	horizontal	Any (horizontal)	2.63		Text sensor	1	13
2	Intermediate floor - hall	9.66	horizontal	Any (horizontal)	2.63		SENS sensor	4	13
3	Plaster wall - corridor	5.34	vertical	East	0.72		SENS sensor	8	13
4	Glass wall	2.23	vertical	East	3.54		Text sensor	2	13
5	Plaster wall - office	18.03	vertical	North	0.72		SENS sensor	3	13
6	Door	1.69	vertical	West	5.00				

Exterior walls	Shared walls	Windows	Other information	+
----------------	---------------------	---------	-------------------	---

Figure A.2 – Description of the building: excel sheet tab of shared walls.

No	Name	Surface (m ²)	Inclination	if other inclination in ° (0 = horizontal, 90 = vertical)	Orientation	U- value (W/m ² /K), if known	Number of glazings, if known	Associated sensor	Sensor number	Kit number
1	Sud_1	2.5	vertical		West		1	SENS sensor	2	13
2	Sud_2	2.5	vertical		West		1	SENS sensor	2	13

Exterior walls	Shared walls	Windows	Other information	+
----------------	--------------	----------------	-------------------	---

Figure A.3 – Description of the building: excel sheet tab of windows

Name	IUT
N° Chrono operation	OP-aa.xxx
N° Chrono report	RE-aa.xxx
Volume (m ³)	188.42
Floor space (m ²)	23.64
Height of the area (m)	2.5
Floor height (m)	7.5
Altitude (m)	123
Average annual temperature (°C) (if a median is present)	11.8

Exterior walls	Shared walls	Windows	Other information	+
----------------	--------------	---------	--------------------------	---

Figure A.4 – Description of the building: excel sheet tab of other information



Figure A.5 – Description of the experiment: json file.


```

1  global_config :
2    result_path : 'result.json'
3    indicators: ['HLC'] # ['HLC', 'Htr']
4    weather_data_source : csv # weather_station, mereen or csv
5    language : Fr
6    Sens_usage : full_sens #full_sens or no_sens or mixt
7    Teq_calculation : solar # solar or Ta
8    roof_treatment : sens # other or sens
9    time_step : 5min # 5min , 1h
10   distinct_boundaries_order : {'atticFloor':1, 'basementCeiling':2, 'terreplein':3, 'garage
11
12  numerical_settings :
13    infiltration:
14      Qin_optim_xtol : 1e-3 # relative convergence criteria on the pressure
15      Qin_optim_fatol : 1e-3 # relative convergence criteria on the residual
16
17  stages:
18    - model_selection
19    - uncertainty_propagation
20    - result_progression
21    - report
22    - save
23
24  user_best_model : tw
25  model_selection :
26    max_order : 1
27
28
29  uncertainty_propagation :
30    bias :
31      yTi : [-0.5, 0.5] # [°C]
32      Ta : [-1.0, 1.0] # [°C]
33      wall_single_air_temp : [-1.0, 1.0] # [°C]
34      wall_no_temp : [-5.0, 5.0] # [°C]
35      wall_terreplein : [-5.0, 5.0] # [°C]
36      T_white : [-0.5, 0.5] # [°C]
37      T_black : [-0.5, 0.5] # [°C]
38      Ph_p : [-2.0, 2.0] # [%]
39      V_p : [-30, 30] # [%]
40      absorpt_white : [-0.05, 0.05] # [-]
41      absorpt_black : [-0.05, 0.05] # [-]
42      absorpt_walls : [-0.2, 0.2] # [-]
43      Umit : [-20, 20] # [%]
44      Tmit : [-0.5, 0.5] # [°C]
45      #hci : [-1.5, 1.5] # [W.m-2.K-1]
46      Pmit_mes : [-0.5, 0.5] # [W/m2]
47    do_sensitivity_analysis : True
48    N_sample_max : 300 # maximum number of evaluation | (preferably 300)
49
50  result_progression :
51    model_selection: True
52    day_range : [0.5,1,1.5,2,2.5,3,]
53
54
55  report :
56    type: debug # simple #| detailed
57    path : report.pdf
58    figures :
59      #- figure_CDF
60      - figure_PDF
61
62  save :
63    backend : filesystem
64    timeserie_format : hdf # csv | json
65    to_save :
66      - setup
67      - rset
68      - conf
69      - timeseries
70      - figures
71      - html
72      - pdf

```

Figure A.6 – Description of the estimation process: yml configuration file

date	temperature [C]	relative humidity [%]	wind speed [m/s]
15/04/2021 00:00	7.57	47.23	4.28
15/04/2021 01:00	7.00	48.96	5.32
15/04/2021 02:00	6.02	52.45	4.70
15/04/2021 03:00	5.50	54.56	4.22
15/04/2021 04:00	5.02	56.22	4.91
15/04/2021 05:00	4.04	60.29	3.28
15/04/2021 06:00	4.83	57.15	3.82
15/04/2021 07:00	6.40	50.71	4.91
15/04/2021 08:00	8.38	47.63	6.14
15/04/2021 09:00	10.43	39.11	6.66
15/04/2021 10:00	11.96	30.11	7.57
15/04/2021 11:00	12.96	29.30	7.57
15/04/2021 12:00	13.37	31.08	6.23
15/04/2021 13:00	14.00	27.45	6.14
15/04/2021 14:00	14.92	25.73	5.93
15/04/2021 15:00	14.93	24.84	6.59
15/04/2021 16:00	14.96	24.76	6.96

weather_IUT15_25_04_2021_modifi (+)

Figure A.7 – Weather time series measurements: csv file.

	16225	16226	16238	16243	16248	16253	16258	16268	16239	16244	16249	16254	16259	16269	16273	16277
15/04/2021 19:10	23,4	0	32,6	21,9	22,4	19,7	15,2	22,4	18	21,9	22,4	15,4	14,8	22,4	23,2	21,4
15/04/2021 19:11	23,4	19	31,7	22	22,3	19,4	15,1	22,4	17,7	21,9	22,3	15,3	14,6	22,4	23,2	21,4
15/04/2021 19:12	23,4	30	32,1	22	22,3	19,3	15	22,4	17,8	22	22,3	15,2	14,6	22,4	23,2	21,5
15/04/2021 19:13	23,4	31	32,1	22,1	22,3	19,5	15	22,5	17,8	22,1	22,3	15,2	14,6	22,5	23,3	21,7
15/04/2021 19:14	23,6	34	32,8	22,2	22,4	19,4	15,1	22,6	17,9	22,2	22,3	15,3	14,7	22,6	23,5	21,9
15/04/2021 19:15	23,8	32	31,2	22,3	22,4	19,2	15	22,8	17,4	22,3	22,4	15,2	14,6	22,7	23,6	22,3
15/04/2021 19:16	24	31	30,2	22,4	22,4	18,8	14,9	22,9	17,2	22,3	22,4	15,2	14,5	22,9	23,9	22,7
15/04/2021 19:17	24,3	33	29,6	22,5	22,5	18,8	14,9	23	17,1	22,4	22,5	15,1	14,5	23	24	22,9
15/04/2021 19:18	24,5	34	29,4	22,6	22,6	18,8	14,9	23,2	17,1	22,5	22,5	15	14,5	23,2	24,1	23,2
15/04/2021 19:19	24,7	30	29,7	22,7	22,6	18,6	14,8	23,2	17,2	22,6	22,6	14,9	14,4	23,3	24,3	23,3
15/04/2021 19:20	24,9	31	29,7	22,8	22,7	18,4	14,7	23,3	17,1	22,6	22,7	14,8	14,3	23,4	24,4	23,5
15/04/2021 19:21	25,1	34	30	22,9	22,8	18,4	14,7	23,4	17,1	22,7	22,8	14,7	14,3	23,4	24,5	23,5
15/04/2021 19:22	25,2	31	30,2	22,9	22,9	18,3	14,6	23,4	17,1	22,8	22,8	14,6	14,2	23,5	24,6	23,6
15/04/2021 19:23	25,4	31	29,7	23	22,9	18,1	14,5	23,5	16,9	22,9	22,9	14,6	14,2	23,6	24,7	23,7

sensors (+)

Figure A.8 – Sensors time series measurements: csv file.

B. Building components of Pléiades Comfie model

The compositions of the walls and floors with the thickness of their components and thermal characteristics are presented in table B.1 and B.2. The types of thermal bridges with their thermal characteristics are presented in table B.3, the figures come from P+C software. The thermal characteristics of the openings are shown in table B.4.

Table B.1 – Thermal resistance of walls of the building model in Pleiades Modeller

<i>Component</i>	<i>Material (ext → int)</i>	<i>thickness [cm]</i>	λ <i>[W/(m.K)]</i>	<i>R</i> <i>[K.m²/W]</i>	<i>U-value</i> <i>[W/K.m²]</i>
Low floor	Concrete	16	1.600	0.10	0.314
	Expanded polystyrene	12	0.039	3.08	
Intermediate Floor	Heavy concrete	20	1.750	0.11	2.778
High floor	Heavy concrete	20	1.750	0.11	0.209
	Polyurethane	14	0.030	4.67	
Exterior wall	Heavy concrete	15	1.750	0.09	0.254
	Expanded polystyrene	15	0.039	3.85	
Shared wall	Plaster	1	0.350	0.03	2.525
	Concrete	15	1.750	0.09	
	Plaster	1	0.350	0.03	

Table B.2 – Heat capacity of the building model per component material in Pleiades Modeller

<i>Material (order) - Component</i>	<i>Density kg/m³</i>	<i>Specific heat J/kg K</i>	<i>Volume m³</i>	<i>Heat capacity J/K</i>
Plaster (1) - Shared wall	1000	800	4.94	3.95E+06
Concrete (2) - Shared wall	2300	920	74.05	1.57E+08
Plaster (3) - Shared wall	1000	800	4.94	3.95E+06
Concrete (1) - Exterior wall	2300	920	96.72	2.05E+08
Expanded polystyrene (2) - Exterior wall	25	1380	96.72	3.34E+06
Concrete (1) - Low floor	2300	920	55.11	1.17E+08
Expanded polystyrene (2) - Low floor	25	1380	41.33	1.43E+06
Concrete (1) - High floor	2300	920	68.59	1.45E+08
Polyurethane (2) - High floor	35	837	48.01	1.41E+06
Concrete (2) - Intermediate Floor	2300	920	202.78	4.29E+08
Total				1.07E+09

Table B.3 – Thermal properties of thermal bridges of the building model in Pleiades Modeller

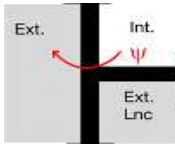
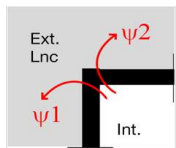
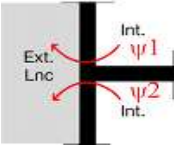
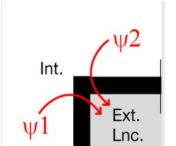
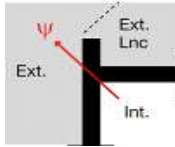
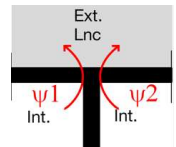
Wall connection	ψ [W/m.K]		Wall connection	ψ [W/m.K]	
	Retrofitted	New		Retrofitted	New
Exterior wall / low floors 	0,06	0,05	Outward angles 	0,03	0,03
Exterior wall / intermediate floors 	1,1	0,77	Inward angles 	0,03	0,03
Exterior wall / high floor 	0,97	0,05	Shared wall / high floor 	0,95	0,68

Table B.4 – Thermal properties of openings of the building model in Pleiades Modeller

Coefficient	Windows	Doors
U_w [W/(m ² .K)]	1,9	3,5
Solar factor [-]	0,5	0,14